UNIVERSITY OF OKLAHOMA

GRADUATE COLLEGE

DEVELOPMENT OF A NEW SYNTHETIC SCHEME FOR VINYL DIETHERS AND SYNTHESIS OF PRODRUGS FOR TARGETED DELIVERY AND VISIBLE/NIR LIGHT-TRIGGERED RELEASE

A DISSERTATION

SUBMITTED TO THE GRADUATE FACULTY

in partial fulfillment of the requirement for the

Degree of

DOCTOR OF PHILOSOPHY

By

GREGORY N. NKEPANG
Norman, Oklahoma
2014

DEVELOPING NEW SYNTHETIC SCHEME FOR VINYL DIETHER AND SYNTHESIS OF PRODRUGS FOR TARGETED DELIVERY AND VISIBLE/NIR LIGHT-TRIGGERED RELEASE

A DISSERTATION APPROVED FOR THE
DEPARTMENT OF CHEMISTRY AND BIOCHEMISTRY

BY

_____
Dr. Kenneth Nicholas, Chair

_____
Dr. Youngjae You

_____
Dr. Daniel Glatzhofer

_____
Dr. Wai Tak Yip

_____

Dr. Elisens Wayne

Acknowledgments

I would like to express my sincere gratitude to: my advisor, Dr. Youngjae You, for his direction, criticism and encouragement which has seen me through the project, the chair of my graduate committee Dr. Kenneth Nicholas for his patience and advice, my graduate committee members: Dr Elisens Wayne, Dr. Wai Tak Yip, Dr. Daniel Glatzhofer for the kind encouragement and understanding throughout the program.

Members of medicinal chemistry laboratory both past and present are not also forgotten especially Dr. Praveen Kumar Pogula and Dr. Bio Moses that I worked with in developing the synthetic scheme for the vinyl diethers and analogs, and Dr. Pallavi Rajaputra, Dr. Samuel Awuah, Dr. Abugafar Hossion for their contributions to the project in one way or another.

I also thank my family especially my kids that are not with me now and to friends for their support and encouragement. I would like to dedicate this work in memory of my late father who passed away while I was here in the US to pursue my PhD degree.

Table of Contents **Page**

List of Abbreviations

$^1O_2$: Singlet oxygen

^{1}PS: Singlet state photosensitizer

$^3O_2$: Molecular oxygen or triplet oxygen

^{3}PS: Triplet state photosensitizer

CA-4: Combretastatin A-4

CMPLCA4: Dithiaporphyrin-linker- Combretastatin A-4

CMP: Core-modified porphyrin (Dithiaporphyrin)

DIEA: Diisopropylethylamine

DMSO: Dimethyl sulfoxide

DNA: Deoxyribonucleic acid

FRET: Fluorescence resonance energy transfer

HBTU: *O*-(benzotriazol-yl)-*N,N,N',N'*-tetramethyluronium hexafluorophosphate

IP: Intraperitoneal

ISC: Inter-system crossing

MCF-7: Michigan cancer foundation-7(human breast adenocarcinoma cell line)

MTT: 3-(4,5-Dimethylthiazol-2-yl)-2,5-diphenyltetrazolium bromide

NMR: Nuclear magnetic resonance

PAMAM: Polyamidoamine

PMDETA: *N,N,N',N'',N''*-pentamethyldiethylenetriamine

POPAM	Modified poly (propyleneimine)
PTPC:	Permeability transition pore complex
PDT:	Photodynamic therapy
PEG:	Polyethylene glycol
PGA:	Polylactide-co-glycolide
PLA:	Polylactic acid
PLGA:	Polylactide-co-glycolide
PS:	Photosensitizer
PCD:	Programmed cell death
Rh-123:	Rhodamine-123
Rh B:	Rhodamine B
SO:	Singlet oxygen
TFA	Trifluoroacetic acid
TPP:	Tetraphenyl porphyrin
TPP-OH:	*5,10,15*-triphenyl-20-(4-hydroxyphenyl)-21*H*,23*H*-porphyrin

List of Tables

List of Reaction Schemes

Scheme

Page

List of Figures

Abstract

Tumor specific drug delivery has become increasingly interesting in cancer therapy, as the use of chemotherapeutics is often limited due to severe side effects. Targeted chemotherapy for cancer treatment offers a great potential advantage in tumor treatment due to greater specificity of delivery, which leads to an increased dose of the cytotoxin delivered to the malignant cells relative to healthy cells in the rest of the body. There are two general directions in anticancer drug delivery that focus on achieving a high local drug concentration specifically in the cancerous tissue while reducing its uptake in healthy cells. i) Site-specific delivery can be achieved by conjugating the drug or coating the delivery vehicle (liposomes, micelles, etc.) with ligands or antibodies that target overexpressed receptors in the tumor tissue. This could also possibly be used to direct a drug away from the body sites that are sensitive to the toxic action of the carried drug (site avoidance). ii) By incorporating an active and site-specific release mechanism within the prodrug or delivery vehicle, it is possible to increase the release and therapeutic efficacy of the cytotoxic agent. A chemotherapeutic drug delivery system designed to combine these two principles (site–specific targeting and site-specific triggering) will fulfill Paul Ehrich's vision of a magic bullet in the treatment of diseases there by overcoming the selectivity problems of conventional chemotherapy.

The folate receptor (FR) is a potentially useful biological target for the management of human cancers. Owing to the overexpression of the FRs on the surface of malignant cells, conjugation of the cytotoxic agent to folic acid (FA) via

suitable spacers has demonstrated the enhanced selective drug delivery to the tumor site. Furthermore the degree of over-expression has been found to correlate with the stage of tumor growth. Various FA-conjugated prodrugs and folate targeted delivery vehicles have been synthesized and are currently in preclinical and clinical trials. Biotin (vitamin B7) is also an essential cellular micronutrient responsible for various normal cellular functions, and its receptors are overexpressed in various cancer cell lines. It has been suggested that the sodium dependent multivitamin transporter (SMVT) is responsible for the uptake of biotin. It has also been indicated that there has been a higher expression of SMVT in several lung, renal, colon and breast cancer cell lines than FR. Several biotinylated anticancer agents have also been used in the selective delivery to cell lines overexpressing the SMVTs. Most of the folate and biotinylated conjugates are equipped with release mechanisms that rely on intrinsic activating agents such as small changes in temperature, pH differences, enzyme and an external activating tool such as light triggered release (light of shorter wavelengths). The use of light of longer wavelengths with better tissue penetration to active release of the drugs is warranted, which then will lead to the search for novel singlet oxygen photocleavable linkers.

To address this issue, our lab has screened various olefins and identified vinyl diether linker as a potential singlet oxygen-mediated photocleavable linker that can be cleaved with a fast rate and in the presence of a photosensitizer (core-modified porphyrin). The reported synthetic schemes were for symmetric molecules with lengthy reaction steps and some reaction conditions not being

functional group tolerant. Herein, the chemical synthesis (synthetic scheme) and kinetic studies of vinyl diether and some nitrogen and sulphur analogs will be described. The potential application of the vinyl diether linker to the synthesis of the biological active molecule was not achieved due to high instability of the linker in the presence of light. Hence we turned our attention to the alternative linker, the aminoacrylate linker, which could be synthesized with high yields and was functional group tolerant.

A multifunctional drug delivery system constituted of the folate (or biotin) linked to the photosensitizer (phthalocyanine) by PEG and combretastatin A-4 linked to the photosensitizer by a photolabile linker (aminoacrylate) was designed and synthesized, and biological activity of six conjugates were determined. The conjugates were prepared through straightforward and versatile synthetic routes. The evaluation of cell specificity was examined using colon 26 cells that overexpress both the folate receptors and biotin receptors. Three of the conjugates (FA-PEG2K-PC-CA4, Biotin-PEG897-PC-CA4 and FA-PEG897-PC-CA4) exhibited high specificity in the *in vitro* test conducted and *in vivo* imaging using the colon 26 cells. Preliminary *in vivo* PDT indicated tumor shrinkage after the irradiation with two of these conjugates: FA-PEG2K-PC-CA4 and Biotin-PEG897-PC-CA4. (Data not included in the thesis)

The ability of the multifunctional prodrugs of optical imaging and treatment by a combination of PDT and local chemotherapy could possibly lay the foundations for further development for the clinical management of FR and biotin receptor overexpressing tumors.

Chapter 1: Introduction

Cancer is one of the most devastating diseases in America and worldwide with an estimated 16 million new cases expected per year globally by 2020.[1,2] Cancer remains a challenging disease to combat because cancer cells share many common characteristics with the normal cells from which they originate.[3] Despite significant progress in the development of anticancer technologies (involving tumor detection, prevention, surgery and chemotherapeutic treatments) there is no efficient cure for patients with malignant diseases. Thus, current methods for diagnosis of cancer often reveal the malignant tissue only after it has already metastasized to other parts of the body.[4] The main treatment at this stage is chemotherapy, which usually can have marginal efficacy due to dose-limiting toxicities, inadequate potency, rapid clearance from the body, poor aqueous solubility and compromised in vivo stability.[5] To limit the onset of severe side effects, anticancer chemotherapeutics are often given at suboptimal doses which hamper their ability to reach tumor-destroying drug concentrations while prompting after prolonged treatments, prompting the development of resistance phenomena. Moreover, chemotherapeutic drugs also display a high degree of toxicity against normal tissues that show enhanced proliferation rates such as the bone marrow, gastrointestinal tract, and hair follicles.[6,7] Thus, minimally invasive novel cancer treatment modalities that can have selective therapeutic action at the malignant tissue are needed.

1.1. Photodynamic Therapy (PDT)

Photodynamic therapy (PDT) is a clinically approved, minimally invasive treatment modality that can induce cytotoxic effects in tumor tissues with some selectivity.[8] Selectivity can be achieved by focused irradiation to tumors and by using photosensitizers that preferentially accumulate in tumors.[9-11] Currently, PDT is applied for the treatment of different types of solid tumors as well as some non-cancerous diseases such as age-related macular degeneration, endometriosis[12] and microbial infection.[8,13]

1.1.1. Mechanism of PDT

Unlike conventional cancer treatments, PDT does not cause major systemic toxicity. It enables the selective destruction of malignant tissues due to specific interaction of three individual non-toxic components a photosensitizer (PS), light (600-800 nm) and molecular oxygen.[14] Clinically the PS is administered into patients intravenously, intraperitoneally or topically. At some time interval after the PS administration, the majority of it is cleared from most body tissues but retained mainly in tumor, skin and organs of the reticuloendothelial system.[15,16] Upon the irradiation by light of appropriate wavelength mostly from laser source or light emitting diode, photosensitizers are excited to the first singlet state (S_1) (Figure 1). The absorbed energy can be released as heat, emitted as fluorescence (utilized for cancer diagnosis) or may undergo an intersystem crossing (ISC) into a long-lived triplet state (T_1). The energy of the triplet state

may also be released as heat and/or light (phosphorescence) or be used in photochemical or photophysical reactions to form reactive oxygen species (ROS).

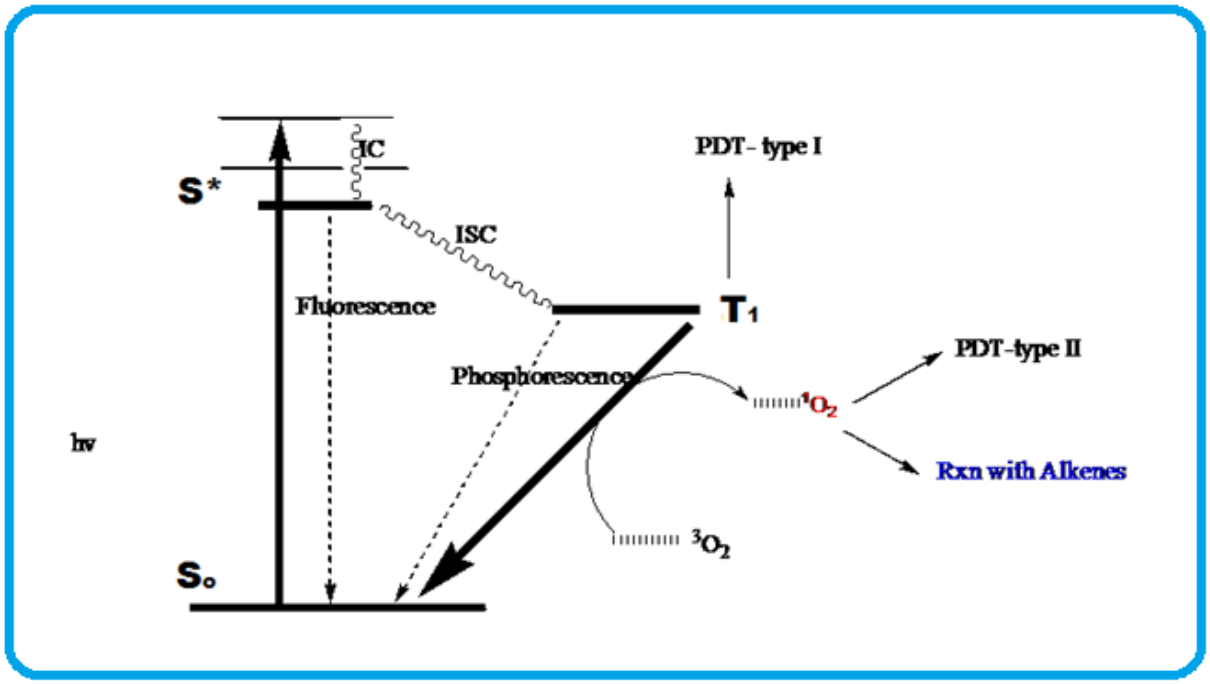

Figure 1. Modified Jablonski diagram.[17]

The triplet state may react in two ways. In what is known as type I mechanism, the excited photosensitizer reacts with substrate molecule through a hydrogen-atom abstraction or electron transfer reactions to yield free radicals and radical ions that react with molecular oxygen, and produce reactive oxygen species (ROS) such as superoxide, hydrogen peroxide and hydroxyl radicals. ROS are thought to play an important role in an increasing number of physiological and pathological processes in living organisms. A type II mechanism involves the

direct transfer of the energy of the excited triplet photosensitizer to molecular oxygen to generate singlet oxygen another ROS. Generally type I reactions occur at low oxygen (hypoxia) and high substrate concentrations while type II reactions occur in oxygenated environments.[18] The photodynamic generation of reactive oxygen species, especially singlet oxygen, to damage the target disease is the base of cancer treatment known as photodynamic therapy (PDT).[19-22] Singlet oxygen is known as a main ROS in photoinduced processes of PDT.[23,24] The ROS then oxidizes amino acids (tryptophan, phenylalanine histidine, and methionine), unsaturated fatty acids and cholesterol found in membranes as well as nucleic acid (guanine), which leads to cell death.[25,26]

1.1.2. Singlet Oxygen ($^1O_2$)

Singlet oxygen is the main cytotoxic agent in PDT. Although molecular oxygen has a double bond, its outermost pair of electrons are in different (π^*_x and π^*_y antibonding) orbitals and have their spins parallel, which makes the ground state a triplet ($^3\sum_g$). Furthermore, two other arrangements of these two electrons are possible and result in the presence of two low-lying singlet states ($^1\sum_g$ and $^1\Delta_g$ states). The $^1\Delta_g$ lies only 22.5 kcal above the ground state and has a remarkable life time of 1 h in the absence collisions with other molecules,[27] while $^1\sum_g$ is 37.51 kcal[28] above the $^3\sum_g$ ground state and has a very short lifetime. It is $^1\Delta_g$ that has come to be called singlet oxygen ($^1O_2$): it is the only species that lives long enough to take part in chemical reactions.

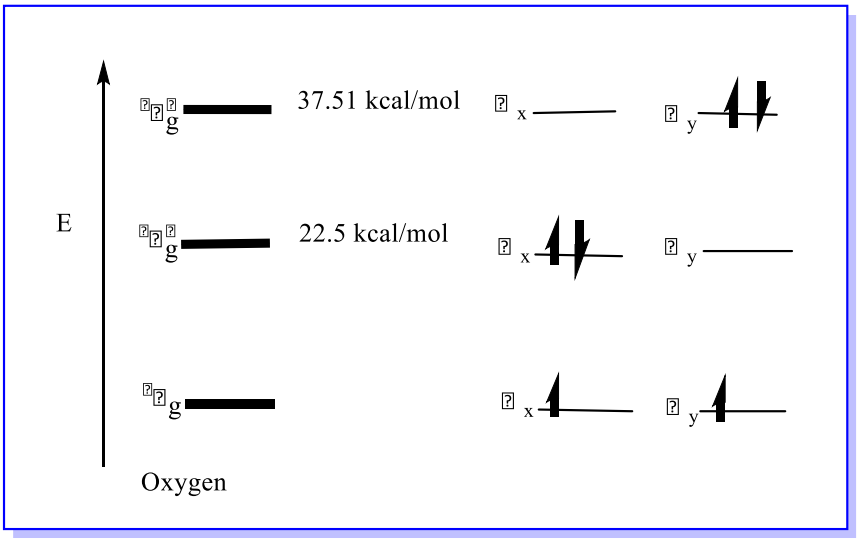

Figure 2. Singlet oxygen MO energy levels [29,30]

1.1.2.1. Generation of Singlet Oxygen

Singlet Oxygen can be generated in many ways. Although $^1O_2$ is formed in the earth's biosphere by the absorption of visible and ultraviolet light from the sun,[31] which usually leads to the electronic excitation of the molecules (direct photoexcitation), this is not practical since the transition is spin-forbidden. Since $^1O_2$ permeates most organic matter, oxygen is a common quencher of electronic excitation of organic matter.[30,32,33] The quenching of the triplet sensitizer by triplet molecular oxygen to afford ground sensitizer and singlet oxygen is the most

common and practical method of generating the $^1O_2$ (eq 1).[30,34] When the molecular oxygen in its ground triplet state interact with an excited photosensitizer in its triplet state, an energy transfer by triplet-triplet annilation[35] occurs, which proceeds an electron exchange mechanism and result in the inversion of the outermost electronic spin and pairing in one π*-antibonding orbital. Singlet oxygen has also been generated the quenching of a singlet sensitizer with molecular oxygen to afford triplet excited sensitizer (eq 2).[36,37]

$$^3\text{sens}^* + {}^3O_2 \longrightarrow {}^1\text{sens} + {}^1O_2 \qquad (1)$$

$$^1\text{sens}^* + {}^3O_2 \longrightarrow {}^3\text{sens}^* + {}^1O_2 \qquad (2)$$

Figure 3. Equations for the formation of the singlet oxygen

The singlet oxygen state is difficult to be represented in a conventional orbital diagram in which the electrons are in two antibonding orbitals because it is a two-fold degenerate compared to the triplet ground state molecular oxygen. One component has two electrons in different orbitals. This is a stable arrangement and cannot account for the observed reactivity of the singlet oxygen.

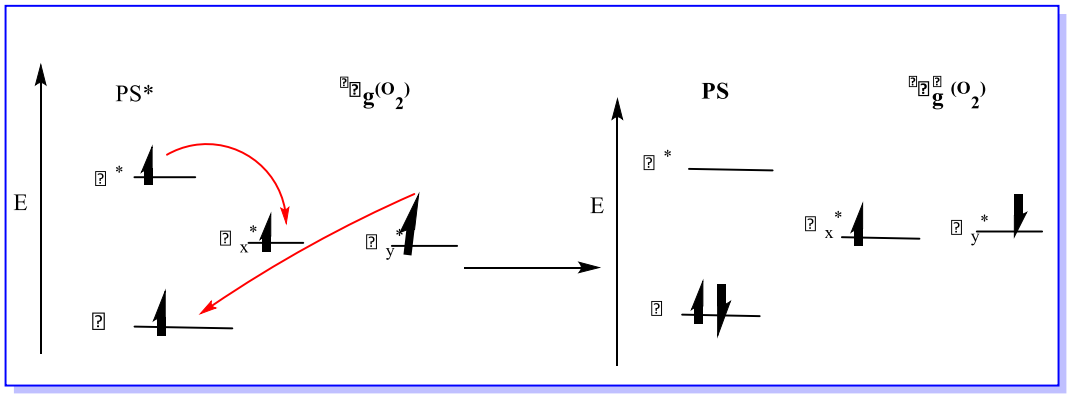

Figure 4 A. $^1\Delta_g$ ($^1O_2$) formation via triplet-triplet annihilation

The other component with both electrons in the same orbital as indicated by the wave function is the most unstable species because this destabilizes the molecule and may account for the high reactivity of this singlet oxygen species ($^1\Delta_g^+$).[29]

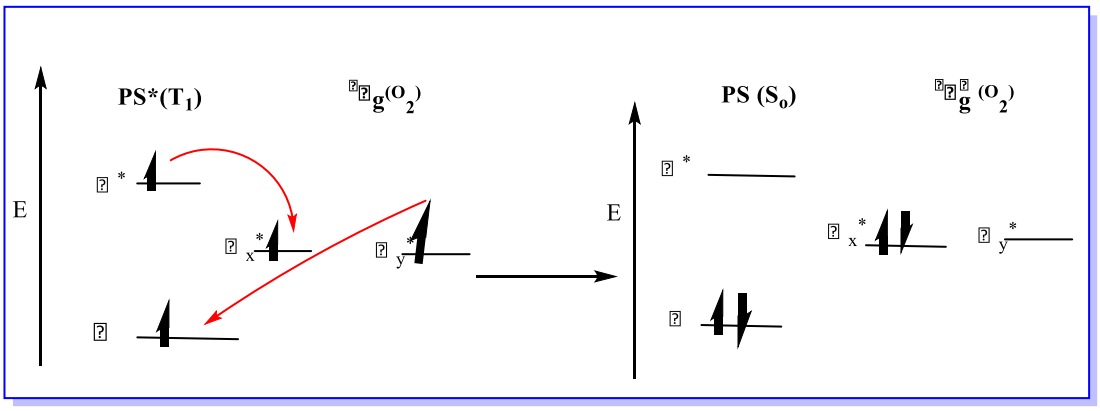

Figure 4 B. $^1\Delta_g$ ($^1O_2$) formation via triplet-triplet annihilation. [29,35,37,38]

The orbital wave function also indicates that both electrons are in the same orbital for the $^1\sum_g^+$ state.[29]

1.1.2.2. Photochemical Reactions of $^1O_2$

The two principal reactions characteristic of $^1O_2$ are cycloaddition ([2+2] and [2+4]) and the 'ene' reactions.

Ene- Reactions: $^1O_2$ reacts rapidly with allylic alkenes to give allylic hydroperoxides.[39,40] It has been shown that the attack of the singlet oxygen and the subsequent removal of the hydrogen occur in a *cis*-manner.[41]

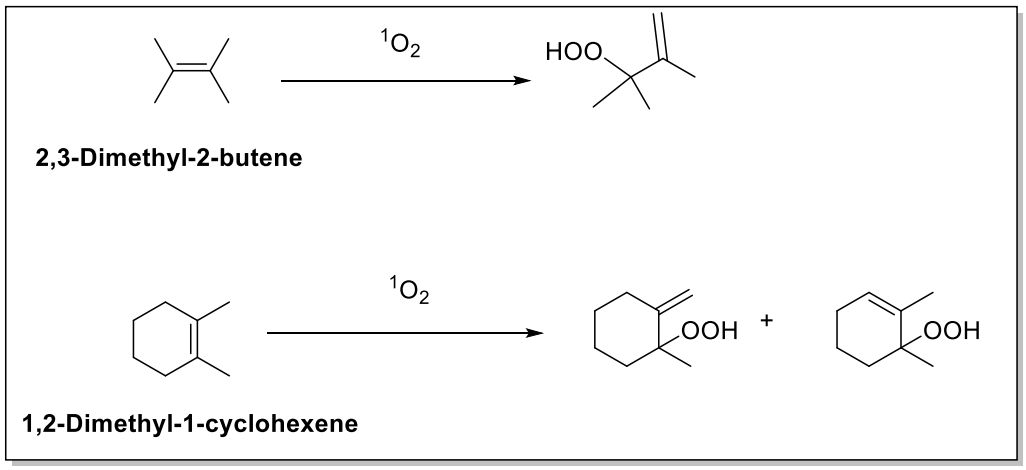

Figure 5. 'Ene' reactions of singlet oxygen. [42-44]

[2+4]-Cycloaddition Reactions: Singlet oxygenation of arenes and conjugated or 1,3-diene compounds leads to the formation six-membered ring peroxides called

endoperoxides.[45,46] These reactions are examples of the 1,4-cycloaddition of singlet oxygen to cisoid conjugated dienes.

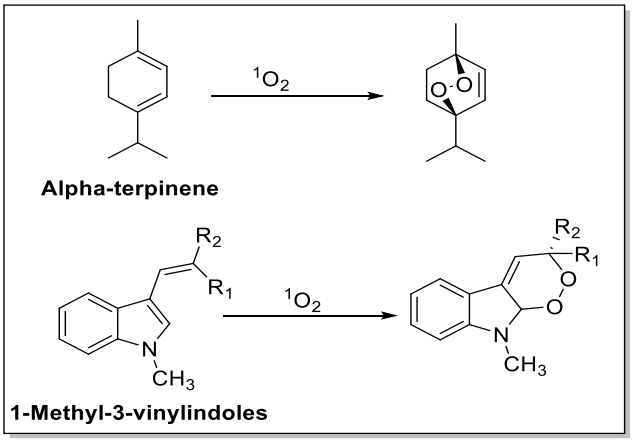

Figure 6. [2+4] reactions of singlet oxygen. [47-49]

[2+2]-Cycloaddition Reactions: $^1O_2$ reacts with electron-rich olefins, alkenes without allylic protons or with sterically hindered alkenes to give four-membered ring peroxides called 1,2-dioxetanes.[50,51] The photooxidation of the alkenes proceeds rapidly with visible light, but stops after the consumption of one equivalent of oxygen.

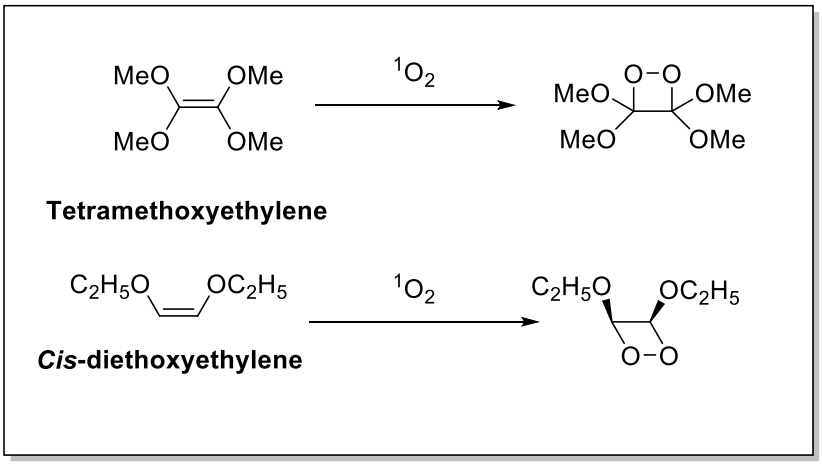

Figure 7. [2+2] Reactions of singlet oxygen. [52,53]

Dioxetanes tend to unstable and decompose spontaneously two carbonyls.

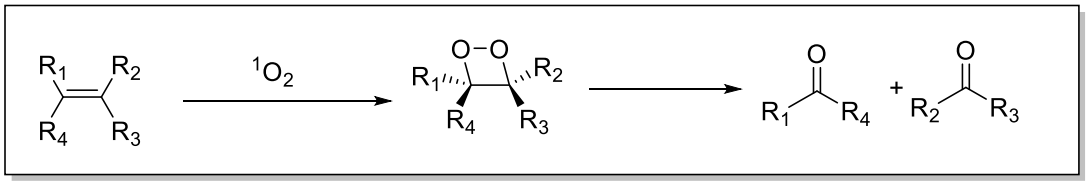

Figure 8. Decomposition of dioxetanes.[54,55]

Biologically, $^1O_2$ tend oxidize amino acids in proteins and peptides (tryptophan, cysteine, histidine, methionine and phenylalanine), unsaturated fatty acids, cholesterol and nucleic acid bases (such as guanine).

1.1.2.3. Lifetime of singlet oxygen

The lifetime of $^1O_2$ varies from one solvent to another. In particular in halogenated solvents $^1O_2$ has a longer lifetime than in non-halogenated solvents or in aqueous solvents. For example, $^1O_2$ lifetime in CCl_4 is 700 us while that in non-halogenated solvents is between 10 -100 us, water 2 us and biological systems < 0.04 us. An explanation of the variation of lifetimes with solvent has been presented by Kearns.[56] He has shown that there is correlation between the lifetime of singlet oxygen and the infrared spectral properties of solvent. Solvents such as water, biological media, alcohols and hydrocarbons with overtones and combination bands that absorb strongly near 8000 $cm^{-1}$of IR spectra region have been shown to have a short oxygen lifetime. This suggests the direct conversion of the electronic energy from singlet oxygen into the vibrational energy of the solvent is predominant in determining the decay of singlet oxygen. There is little indication of heavy–atom effect on the lifetime of singlet oxygen.[57]

Since the lifetime of $^1O_2$ in cells is short and it has a limited diffusion distance (10-300 nm) [21,58,59], the $^1O_2$ generated in the irradiated part of the body cannot directly damage cells in the unirradiated part. In PDT, it means the source and the concentration of oxygen may have a major impact on the $^1O_2$ generating capacity and hence the biological activity. The concentration of $^1O_2$ varies from one medium to another and from one compartment to another. For example, the oxygen concentration at atmospheric pressure in water is 270 μM while that in the blood is 68-171 μM and in tissue is 7-34 μM.[60] Solid tumors are known to exist under hypoxic conditions.[61] The biological implications are that we can

selectively generate $^1O_2$ only in particular locations to damage the diseased cells while sparing the healthy ones when the light is focused only on those cells. Therefore, PDT-induced oxidative damage is highly localized to regions around the photosensitizer.[62] This specific damage to the targets can also be improved by using a targeted delivery system for the photosensitizer to selectively accumulate only in the diseased cells.

1.1.3. Photosensitizers

Porphyrin or porphyrin-related compounds form the bulk of the PSs used in PDT in clinical settings. (Figure 9) Photofrin was the first generation photosensitizer approved in 1993 for the treatment of bladder cancer and as prophylactic treatment of several others, such as the treatment of early stage esophageal, gastric, cervical and lung cancers.[10,63]. However, this first generation photosensitizer had several limitations with respect to its clinical use such as [38,63-65] composition of undefined mixture of hematoporphyrin derivatives (HpD), induction of long-lasting skin photosensitization, a low extinction coefficient at wavelengths for optimal tissue penetration and limited selectivity for target tissue. Other first generation photosensitizers were chlorine, bacteriochlorin and other porphyrins (Figure 9).[66]

Second generation PSs were then developed with better features or characteristics such as[67] single and chemically pure compound, low tendency to aggregate, high singlet oxygen quantum yield, low phototoxicity towards healthy

tissue, no dark toxicity, fast clearance from the healthy parts of the body and specific retention in diseased tissues, stability and good solubility in pharmaceutically acceptable formulations and in biological media, high photostability and fluorescence, strong absorbance in near infrared (NIR) region and a minimum absorbance between 400 to 600 nm. PSs with lowest absorbance in the range (400 to 600 nm) where daylight intensity is the highest will tend to avoid skin photosensitization when used clinically. Furthermore, optimal light penetration into the tissue is favored by strong absorbance in the NIR region between 600 to 800 nm (since wavelengths above 800 nm are absorbed by water molecules and singlet oxygen generation is suboptimal), which thereby results in more efficient PDT when treating deeper seated lesions.[62,68,69]

Selective accumulation of PS in tumor combined with it controlled light activation enables selective destruction of tumor, sparing the neighboring healthy tissue. Selectivity of PS for tumor tissues over healthy tissues is thought to be a multifactorial process including physico-chemical properties and binding to plasma proteins as well as the particular characteristics of tumors such as leaky vasculature, low lymphatic drainage, expression of specific enzymes and receptors and pH variation. PSs exhibit direct or indirect cell killing, vascular occlusion, release of cytokines and the response of the immune system depending on their cellular or intracellular localization or relocalization.

Figure 9 gives the chemical structures of some PSs investigated in clinical trials, while Table 1 summarizes the same PSs with their potential therapeutic application in oncology.

References [10,12,63,70-81]

Trade Name	**Absorption wavelength**	**Potential Indications**
Photofrin, Photogem, Photosan, Hemporfin	630 nm	Cervical, brain, Oesophagus, breast, head and neck, lung, bladder, superficial gastric cancers, Bowen's disease, cutaneous Kaposi's sarcoma
Foscan	652 nm	Oesophageal, prostate and pancreatic cancer, advanced head and neck tumors
Visudyne	689 nm	Basal and squamous cell carcinomas
Photochlor	665 nm	Basal cell carcinoma, Oesophageal cancers, head and neck tumors
Tookad	763 nm	Prostate cancer

BOPP	630 nm	Malignant gliomas
Pc 4	675 nm	Cutaneous and Subcutaneous lesions from diverse solid tumor origins
CGP55847	670 nm	Squamous cell carcinoma of upper aerodigestive tract
Photosens	675 nm	Skin, breast, lung, oropharingeal, breast, larynx, head and neck cancers, Sarcoma M1, epibulbal and choroidal tumors, eyes and eyelis tumors, cervical cancer
Purlytin, Photrex	659 nm	Kaposi's sarcoma, cutaneous metastatic adenocarcinomas, prostate, brain, lung cancers, basal cell carcinomas
NA	515 nm	Breast, myeloma, non-melanoma skin cancer
Levulan	630 nm	Skin tumors, head and neck, gynaecological tumors and basal cell carcinomas

	375- 400 nm	Brain, head and neck and bladder cancer photodetection
Talaporfin, laserphyrin	664 nm	Solid tumor, lung cancer, cutaneous malignancies
Lutex	732	Prostate, cervical, breast, brain cancer, melanoma

Table 1. Summary of PSs and potential therapeutic applications in oncology

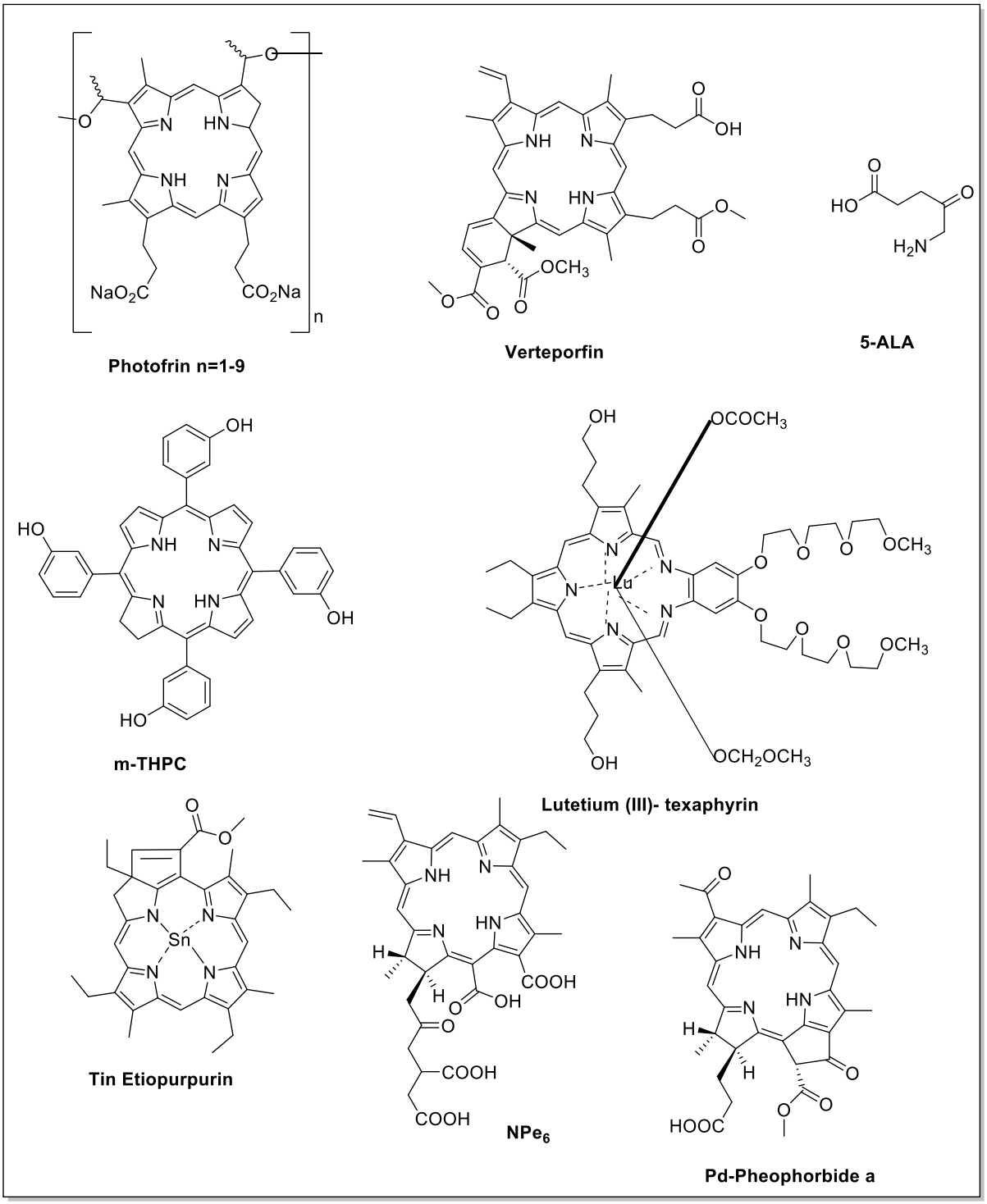

Figure 9: Structures of PSs in clinics

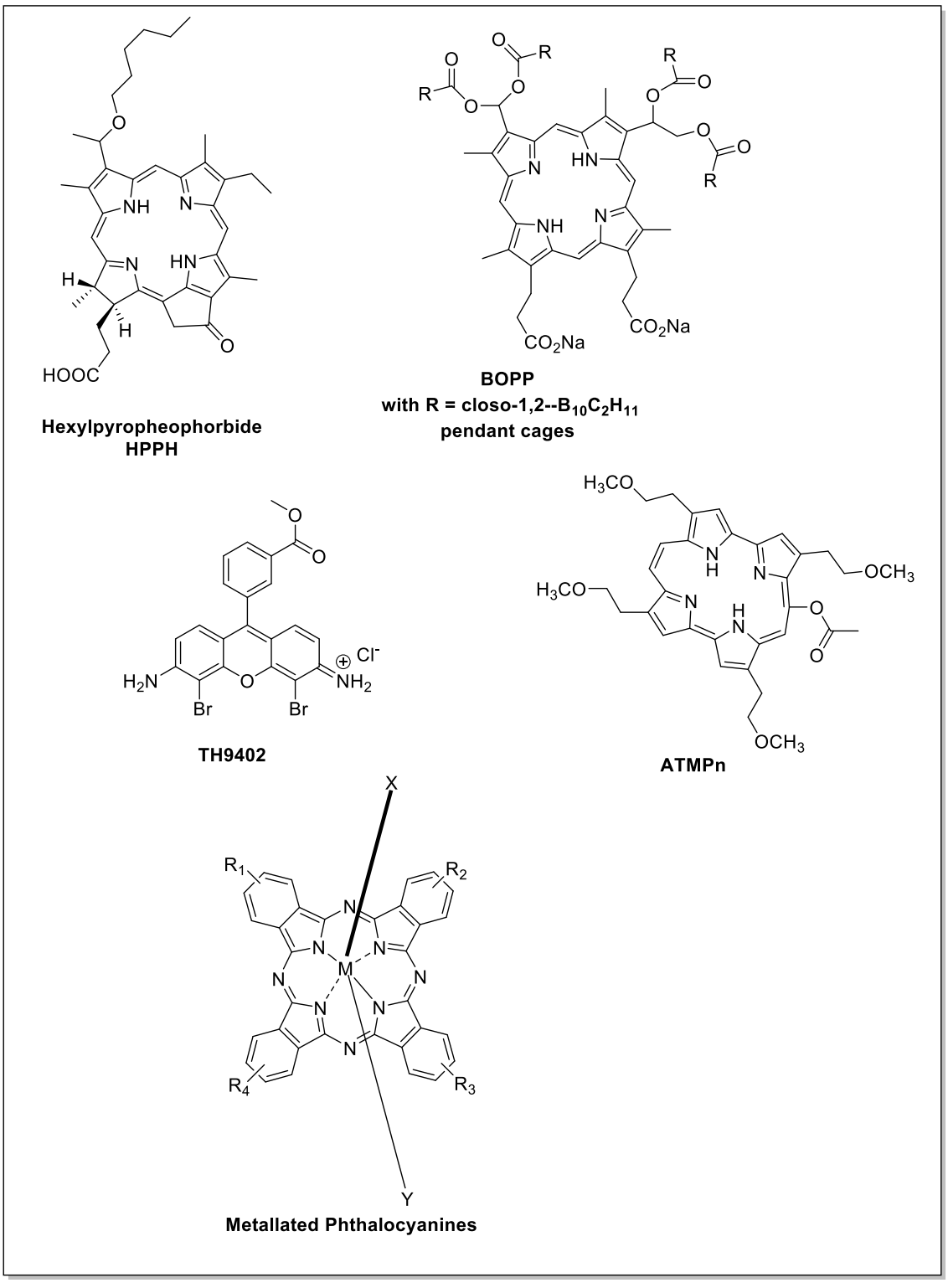

Figure 9: Structures of PSs in clinics

1.2. Receptor-Targeted Drug Delivery

Receptor-mediated drug delivery has two advantages over conventional nontargeted therapies. 1) It can enhance net drug up-take by pathologic or diseased cells. 2) It reduces drug deposition into nonmalignant cells, which therefore reduces the collateral toxicity to normal cells. Differences in the structure and behavior of normal and tumor tissue could be used for designing drug delivery system facilitating tumor-specific delivery of drug or prodrug and specific activation. Generally three targets for the delivery of anticancer drugs in drug delivery research have been identified–tumor vasculature, extracellular space in the tumor tissue and tumor cells.

Targeting techniques are classified into passive targeting and active targeting. Tumor vasculature continuously undergoes angiogenesis to provide the blood supply that feeds the growing tumor.[82] High molecular weight molecules and other nanoparticles will accumulate in solid tumors at much higher concentrations than in normal tissues or organs due to enhanced permeability and retention (EPR) effect. Passive targeting is achieved in this case by EPR effect as a result of leaky vasculature and limited lymphatic drainage, which is found in tumor tissues but absent in normal tissues.[83-85] An example of such a targeting technique is Doxil. This is a polyethylene glycol (PEG)-modified liposome containing doxorubicin (DOX).[86,87]. Although this technique is useful in cancer therapy, it is difficult to completely eliminate the adverse effects of antitumor

drugs.[88] Hence, there is need for the development of drug delivery systems with both passive and active targeting capabilities.

Certain antigens and receptors are known to be aberrantly up-regulated on the surfaces of cancer cells compared to those of normal cells. The tumor antigen- or receptor-mediated approach has been largely exploited to enhance the selective delivery of cytotoxic agents or imaging probes to target tumors. Therefore, to actively target such receptors or antigens, chemical modification of drug carriers with tumor targeting ligands such as sugars,[89] transferrin,[90] antibodies,[91] peptides[92,93] and folic acid[94] is used. The other receptors devoted to the transport of vitamin B12,[95] biotin,[96,97] and riboflavin[98] have been quite recently introduced as methods for targeted drug delivery. Of these ligands, FA is one of the most widely used because of the advantages. The concept of active targeting consists in grafting a molecule (termed 'promoiety') onto an active drug molecule that will help it in reaching the pharmacological target, while ensuring that the promoiety can afterwards be removed to regenerate the biologically active compound.[99]

1.2.1. Folate Receptor-mediated drug Targeting

Folic acid (FA) is natural vitamin B9 with molecular weight of 441 g/mol that plays an essential role in cell survival. It is a vitamin required for a one carbon transfer reaction in several metabolic pathways. Rapidly proliferating cells consume the vitamin in elevated levels because it is essential for the biosynthesis of the nucleotide bases for the nucleic acids (DNA and RNA). There are two routes of

transportation of the folate across the plasma membrane in normal cell cells under physiological conditions using membrane associated-proteins viz, the reduced folate carrier or the folate receptor. The reduced-folate carrier[100] is the major route of reduced form of vitamin (5-methyl-tetrahydrofolate) entry into nonmalignant (normal) cells and will not transport folate conjugates of any type under physiological conditions.

The folate receptor (FR), a 38 kDa glycosylphosphatidylinositol (GP1) anchor glycoprotein[101], exists in three isoforms[102] namely FR-α, FR-β, and FR-γ. Among them, the FR-α is often up regulated on cell surface of a wide variety of human carcinomas, which include ovary, brain, kidney, breast, colon, myeloid cells and lung malignancies, but it is rarely expressed on most normal cells. FR- β is expressed on activated macrophages and on the surface of malignant cells of hematopoietic origin. The over expression of the folate receptor on the cancer cells perhaps enable the malignant cells to compete successfully for the vitamin when supplies are limited.[103,104] The inability of folate conjugates to penetrate the reduced–folate carrier greatly contributes the low toxicity of folate-linked therapeutic agents to normal cells. The FR is significantly upregulated on many cancer cells compared to their non-transformed counterparts, and the FR-α density also appears to increase as the stage of the cancer increases.[104] Taken together, it is conceivable that the more advanced stage, the higher grade, and chemotherapy-resistant cancers, i.e. the tumors that are most difficult to treat by standard procedures, comprise the population of cancers most readily targeted

by folate-linked drugs. An additional correlation has been reported between the degree of expression and resistance to standard chemotherapy.[105] Since the folate receptors bind folic acid with nanomolar affinity [106] (K_d ~ 0.1- 1.0 nmol/L) and transport the captured vitamin into the cell by receptor-mediated endocytosis,[107] the striking consequence is that those FRs over expressed by cancer cells can be selectively be exploited for specific delivery of folate-linked drugs into the cancer cells.[98] Further reasons for the attractiveness of FA as a ligand for FRs are that it is stable and compatible with a variety of organic and aqueous solvents, inexpensive, a generally poor immunogenic chemical endowed with high affinity for FRs that enhances the differential specificity of therapeutic and imaging compounds/particles by targeting folate receptor positive cells and can easily be linked to a variety of molecules.[108]

FA conjugates covalently linked via folate's γ-carboxyl moiety to target tumor cells maintain a high affinity for the FRs, and their cellular uptake mechanism by FRs is as effective as that displayed by FA in its free form.[109] Folate conjugates enter cells by FR-mediated endocytosis and move through the organelles, and deliver their carried cargo to the cell cytoplasm (cytosol) or deposit them in a nondegradative compartment. The drug is then released in the endosomes/lysosomes mainly by enzymatic cleavage (owing to the acidic environment occurring in lysosomes, pH-dependent drug release has also been extensively considered).[110] Because of the recycling of the unlitigated FR back to

cell surface, the cellular uptake process of these conjugates can be repeated and allow a continuous supply into the cell.

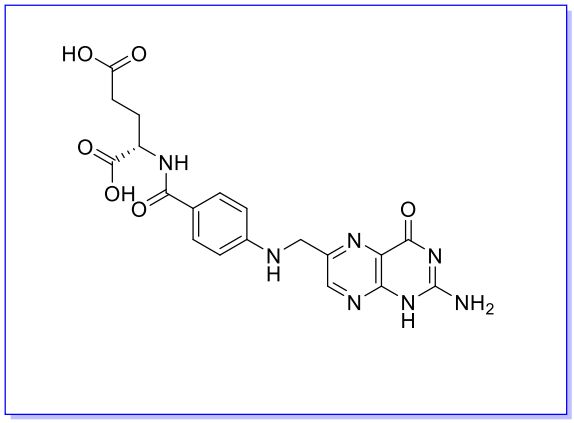

Figure 10. Structure of folic acid (FA)

The success of FR targeting is in the enhancement of the intracellular delivery of attached macromolecules such as a large number of folate appended polymeric drug carriers (liposomes,[111-114], dendrimers,[115], polysaccharides,[116,117], and micelles,[118], protein toxins,[119,120], viruses,[121], antisense oligosaccharides,[122-124], gene therapy vectors,[125-127], imaging compounds and neutron activation agents.[128-131]

1.2.2. Limitations of Folate-targeted drug delivery

Folate-mediated targeted delivery of drugs/carriers towards solid tumors seems very attractive in solid tumor chemotherapy. Unfortunately, not all cancers over-express a FR. In this light, prostate, pancreatic, bladder and lymphoid cancers

that do not have folate receptors will have to use alternative tumor-specific ligands if drug therapies were to be used.

The second and major concern is that not all FR targeting trials were successful. Because of the high affinity of folate for its receptor, some conjugates may release slowly from the receptor to permit accumulation of the therapeutic dose. This problem has been solved by the use of hydrolysable linkers to discharge the payload or use of therapeutic agents that are effective in the attached form constituted the two possible solutions for this potential problem. *The most critical issue is how to control the release of free drugs (active forms) from the delivery system (inactive drug forms) after cellular uptake (need for extrinsic stimulus) since the two possible solutions enumerated above relied on intrinsic stimuli (physiological conditions within the tumor microenvironment).*

1.3. Current Drug Delivery Systems

1.3.1. Dendrimers

These are uniform spherical (globular) nanostructures (macromolecules) ranging from 5-10 nm in diameter. Each dendrimer carrier has an initiator core and arms made of repeated monomer subunits that act as branching points. Generation or layers are synthesized in multiple reaction steps to add layers of monomers until the overall structure reaches the desired size.[132] Dendrimers synthesized in this way create a structure with multiple functionalities for conjugation of functional groups or drugs.[133] As the generation increases, the repetitive synthetic steps

produce a highly branched macromolecule with a three-dimensional structure characterized by interior cavities capable of encasing therapeutic drugs or imaging units and reactive terminal groups capable of attaching drugs, dyes, and/or a variety of sensors.[134] Drug release kinetics controlled through the properties of the polymer chains that have been designed to be degraded for release of a payload.[135] Dendrimeric structures including polyamidoamine (PAMAM), [135-137] modified poly(propyleneimine) [POPAM] and aromatic ether-type dendrimers have been developed for drug delivery.[138]

1.3.2. Liposomes Drug Delivery

These are spherical vesicles formed by the self-assembly of amphiphilic lipids and excipients. Lipids form a bilayer based on hydrophobic interactions in continuous parallel packing with the hydrophilic head groups positioned towards the aqueous environment. Hydrophilic molecules can be encapsulated in the inner aqueous phase while hydrophobic molecules can be carried in the hydrophobic domains of the lipid bilayer. The membrane is composed of a phospholipid and cholesterol bilayer with an aqueous solution at the core. They represent one of the first “nanotechnologies” to enter clinical medicine.[139] They have been utilized for drug delivery due to their ability to encapsulate or sequester DNA or drugs that would normally not enter the intercellular compartment. When these molecules are encased in a liposome, they can be delivered to cells through diffusion as well as receptor-mediated events. They have already been used to deliver a wide variety of therapeutics and imaging

agents, which include small molecule drugs, gene therapies and antisense oligonucleotides.[140] [141] Another example is Doxil, which is a PEGylated liposome clinically used to treat multiple types cancer, and is one of the most important liposomal drug delivery systems. It consists of a packed PEGylated surface loaded with doxorubicin through drug diffusion based on ammonium salt gradient.[142] The liposomal formulations are able to change surface charge (zeta potential) with a change in solution pH. The charge switch at acidic pH results in the fusion with the cell membrane during endocytosis uptake and allows escape of nanocarriers into the cytoplasm to deliver the therapeutic load.[143] *Some of the challenges posed by the liposomal formulations are instability in the blood stream, poor solubility of many drugs in the lipid/ surfactant solution, rapid burst release of drug and the severe side effects due to their accumulation in skin tissue. Another challenge posed in this formulation system is the difficulty to control prolonged drug release kinetics*

1.3.3. Polymeric Micelles

Micelles are composed of spherical vesicles of lipids or other amphiphilic molecules, such as polymers or polyamino-acids that self-assemble into small nanoparticles with a hydrophobic core. They have been developed as drug delivery carriers for hydrophobic drugs.[144,145]. Genexol-PM is the first non-targeted polymeric micellar formulation approved for cancer therapy or metastatic cancer breast cancer and NSCL cancer, and in the USA it is in a clinical phase II trial for metastatic pancreatic cancer therapy.[146] Genexol is composed of a block

copolymer PDLLA (1.75 kDa)-mPEG (2 kDa) forming micelles with size of ~ 60 nm and taxol loading of ~ 15%(w/w).[146,147] Micellar drug delivery systems are also being developed for myriad of anticancer agents using formulations with sizes ranging from 10-200 nm using polyamino acids and synthetic polymers.[148,149]

1.3.4. Polymeric Nanoparticles

Polymeric nanoparticles represent the most effective nanocarriers for prolonged delivery. They provide significant flexibility in design because polymers can be biodegradable or nonbiodegradable and made synthetically or derived from natural sources. Common polymers used include poly (lactic acid)(PLA), dextran, and chitosan.[150] The polymers are degraded into individual monomers, which are metabolized and removed from the body via metabolic pathways. Degradation and drug release kinetics can be precisely controlled by physicochemical properties of the polymer such as molecular weight, dispersity index, hydrophobicity, and crystallinity. Hydrophilic polymer such as PEG is usually grafted, conjugated or adsorbed unto the surface of the nanoparticle to stabilize it, reduce hepatic uptake and improve circulation half-life. The polymeric nanoparticles are now in several stages of preclinical and clinical development e.g. drug–loaded polymethacrylate encapsulated nanocapsules have been developed. These are most commonly approved drug delivery systems in late

stage of clinical trials. Multiple factors affect the pharmacokinetic behavior, but the surface charge, size, shape and stealth properties are the most critical,[151].

1.4. Visible/ near IR light as an external stimulus for controlling the release of drugs

Being an external stimulus with unique properties such as external applicability, tenability of intensity, flexibility of wavelength and deliverability via various methods, light has been considered as a very important tool for a spatiotemporal control of drug release/ activation.[152] Its success has been seen the release of drugs and bioactive compounds (caged compounds-deactivated forms of drugs from bioactive compounds).[153] UV and short visible (< 400 nm) light have been used for the controlled release of drugs to cultured monolayer cells and skin surface or the mucosa.[154-156] The major limitation of using light of wavelength below 700 is due to limited tissue penetration ability because of scattering and high level of endogenous absorbers such as oxy and deoxy-haemoglobin, lipid and water.[157] Visible/NIR light (650-900 nm) is desired due to its ability to reach deeper tissues for the treatment of deep residing (solid) tumor. However, due to the low energy light, its direct application in drug release is impossible since the light energy cannot directly trigger the chemical bond (linker) cleavage often required for releasing the drugs.[158-162] (This section is an invited book chapter in press by G. Nkepang and Dr. You Y. in: The Chemistry of Peroxides Volume 3 (Patai series)).[163]

1.5. Specific aims and scope

The chemical principle underlying PDT is the activation of photosensitizer by light to convert triplet state oxygen to singlet state oxygen, which can then react with biomolecules to cause cell modification or death. Reactions of singlet oxygen with double bonds in biological molecules are either through the 1,4- or 1,2-cycloaddition reactions or through the 'ene'-reactions. 1,2-Cycloaddition reactions generate two carbonyl fragments through the dioxetane intermediate. It is from this basis that singlet oxygen photocleavable prodrug release systems have been developed. Following the same idea, we have proposed that a photodynamic multifunctional drug delivery platform could be developed to release drug molecules bearing either –OH, -NH or –SH functional groups.

1.5.1 Hypothesis:

A multifunctional prodrug system made up of a drug molecule covalently conjugated via a photocleavable linker could be designed. The active drug can be released by cleavage of the linker using singlet oxygen generated by PS upon activation by near infrared (NIR) light. This could serve as a new strategy for controlling drug-release by NIR that is biocompatible and penetrate deeper tissue than UV and Visible light.

1.5.2. Specific aims.

To test our hypothesis, the following specific aims were established.

- Develop a facile synthetic scheme to model conjugates constituting of two different molecules containing -OH, -NH and /or –SH as a common functional groups readily encountered in drug molecules that were linked via vinyl diether bond or analogs [electron rich-double bonds] based on previous screening in our lab.
- Synthesize a prototype prodrug constituting of a drug and photosensitizer using the above chemistry and conduct photophysical and biological studies (*in vitro* and *in vivo* studies) with the prototype prodrug.
- Synthesize a multifunctional drug delivery platform constituting of a photosensitizer and drug molecule(s), covalently attached using the photolabile linker and targeting moiety (folic acid or biotin) on a common platform and carry out both *in vitro* and *in vivo* studies.

CHAPTER 2: FACILE SYNTHESIS OF VINYL DIETHER AND ANALOGS, AND PHOTOOXIDATION BY SINGLET OXYGEN

2.1. Introduction

Although vinyl diether looks as simple as it is, synthesis of this functional group was not easy. Very little work has been done in the past for the development of the vinyl diether linker since it had very little importance until recent developments in drug delivery systems that require it. Previous methods are limited to symmetric molecules, lengthy steps, low yields, harsh reaction conditions and non-stereospecficity (mixture of *E* and *Z*-isomers). I will cite only the most recent references used for the synthesis of vinyl diether linker and monoether monothioether linkers.(This chapter is an already published work by G. Nkepang)[164]

1,2-Diphenoxyethene was synthesized from ethylene chlorohydrins in a 7-step sequence involving high pressure and temperature by Baganz et al. (1959).[165] The other method for the same compound involved chlorination and dehydrochlorination of *1,2*–diphenoxyethane was used by Serratosa et al. (1979).[166] This method is limited for the synthesis of symmetric molecules and yields a mixture of *E* and *Z*-products in low yields. Bauld et al. (1999) developed the most recent method for the preparation of *1,2*-diphenoxyethene and derivatives involving bromination, followed by stereospecific debromination to give either the *E*- or *Z*-intermediates. Treatment of the *cis*- or *trans*- intermediates with *n*-BuLi, followed by either protonation or methylation, then afforded pure *cis* or *trans*- *1,2*-diphenoxyethene or the corresponding *4,4'*-dimethyl derivative. This method has a number of problems such as limitation only to symmetric vinyl diether molecules, facile electrophilic ring bromination on the phenyl or benzene ring para to the ether functionality, lengthy steps, and finally low yields.[167] These are the methods developed so far for the synthesis of vinyl diether bonds with phenolic of aryl alcohols. Methods involving aliphatic alcohols are quite different and requires a different approach as shown by Dolphin et al.(2008).[168] The only synthetic scheme of compounds with unsymmetrical molecules (*2*-aryloxyvinyl)phenylsulfanes involving the reaction of phenyl hypchlorothioite with vinylaryl ethers was developed by Bychkova et al. (1984).[169] This method required harsh reaction conditions.

Many reaction schemes have been tried to establish the vinyl diether linker, however, the limited available synthetic methods for *1,2*-diheteroatom-substituted

olefins have been one of the major hurdles. Here, we describe the first facile synthetic approach for the *1,2*-diheteroatom substituted olefins (scheme 1). It is a versatile, efficient, and stereospecific method in as few as four steps from starting materials. We have been able to demonstrate that the chemistry can be used for the preparation of both symmetrically and asymmetrically diheteroatom-substituted olefins from a variety of functional groups such as –OH, -NH, and –SH (Table2). The photooxidation of those olefins that were not tested in the previous paper is also reported (Figure 11).

2.2. Materials and Methods

All solvents and reagents were used as obtained from Sigma Aldrich and Thermo Fisher Scientific unless otherwise stated. All reactions were monitored by TLC using 5-17 μm silica gel plates with fluorescent indicators from Sigma-Aldrich. All column chromatography was done using 40-63 μm silica gel from Sorbent Technologies. NMR spectra were recorded at 25 ºC using a 300 MHz Spectrometer (NMR data of *E*/*Z*-**4** and *E*/*Z*-**8** were recorded with a 400 MHz Spectrometer). NMR solvents with residual solvent signals were used as internal

standards. ESI mass spectrometry was done at Mass Spectroscopy South Dakota State University, University of Oklahoma, or University of Buffalo. IR spectra were recorded on a BioRad FT-155FT-IR spectrometer (using dichloromthane as solvent). Melting points were determined by using a Mel-temp® Electrothermal instrument.

2.3. Experimental Section

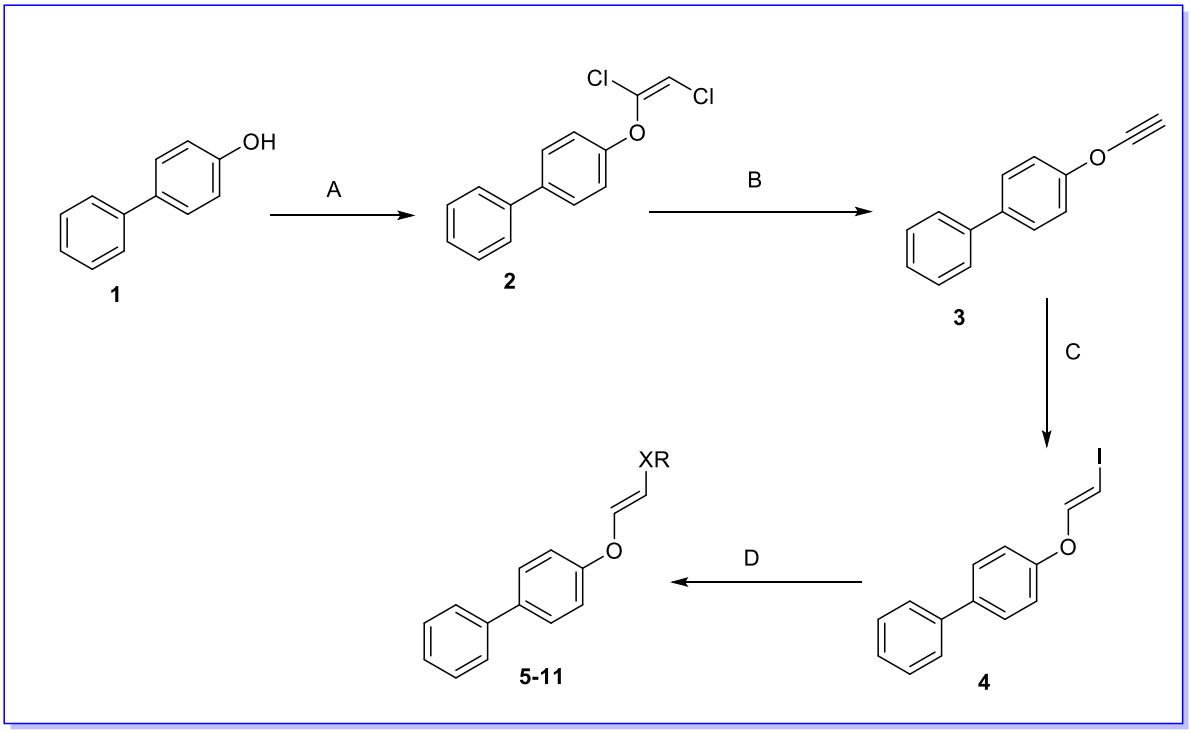

Scheme 1. General synthetic scheme for vinyl diethers and analogs: A) i) KH (55 mmol), **1** (37 mmol) at rt, THF, ~30 min, ii) Trichloroethylene (44mmol) at -78 ^{o}C warm to rt, overnight, B) **2** (7.67 mmol), TMEDA (23 mmol), n-BuLi (23 mmol) at -78 ^{o}C , 1h to -40 ^{o}C, 40 min, Et_2O, C) i) Cp_2ZrCl_2 (20.3 mmol), $LiEt_3BH$ (20 mmol) at rt, THF, 1 h, ii) **3** (10.2 mmol) at rt, 30 min, iii) I_2 (20.5 mmol) , 40 min, D) 10 mol % CuI, 10 mol % ligand, 2 eq Cs_2CO_3, 1 eq HXR , 50-80 ^{o}C, 10-48 h.

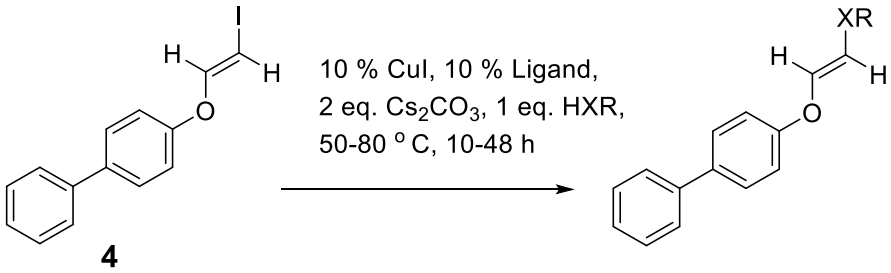

4 **5-11**

Entry	Substrate (HXR)	Ligand [rx. temp (°C), time (hr)]	Yield (%)
5	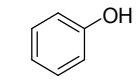	L1 [a] (75, 36)	65
		L2 [b] (75, 16)	70
6	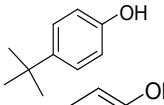	L1 (80, 48)	65
7	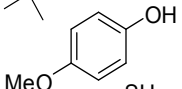	L1 (80, 48)	40
8	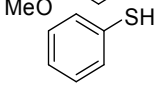	L1 (60, 10)	90
9	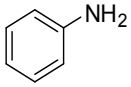	L1 (70-100, 36)	-[c]
		L2 (70-100, 36)	-
10	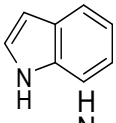	L2 (70, 12)	87
11		L2 (65, 12)	85

[a] L1 = *trans*-*N*-(2pyridylmethylene)aniline
[b] L2 = 2-pyridin-2-yl-benzoimidazole
[c] Not isolable quantity

Table 2. Reaction Products from vinylation reactions at the final step

2.3. Synthesis of Compounds

2.3.1. **Synthesis of** ***4-((1,2-dichlorovinyl)oxy)-1,1'-biphenyl (2)***: To a two-necked, round bottom flask (250 mL) equipped with a magnetic stirrer, pressure equalizing funnel and rubber septum was suspended oil free potassium hydride (2.20 g, 55 mmol, 1.50 eq) in tetrahydrofuran (THF, 25 mL). 4-Phenylphenol (6.30 g, 37 mmol, 1.00 eq) in THF (50 mL) was then added drop-wise with stirring for over 20 min via the funnel. After the evolution of hydrogen was complete, the orange-yellow slurry was cooled to -78 ^{o}C, and then treated with drop-wise solution of trichloroethylene (5.8 g, 44 mmol, 1.2 eq.) in THF (25 mL) for over 10 min. The cooling bath was removed and the reaction mixture was allowed to warm to room temperature (rt) and then maintained for overnight (12 h). To the dark brown mixture was carefully added water (10 mL) using a syringe and then partitioned between water (200 mL) and ethyl acetate (200 mL). The organic phase was then washed with brine (200 mL). Extraction of the combined aqueous layers was done using ethyl acetate (150 mL x 3). The combine organic phases were dried over anhydrous magnesium sulfate, filtered and concentrated using the rotary evaporator to give yellowish brown oil. Silica gel (200 g) column chromatography was done using hexane as eluent to afford **2** (10.5 g, 85 %) as colorless oil that later crystallized to white crystals: mp 52-55 ^{o}C. ^{1}H NMR (300

MHz, $CDCl_3$): 7.62-7.54 (m, 4H, HAr), 7.48-7.41 (m, 2H, HAr), 7.39-7.32 (m, 1H, HAr), 7.18-7.12 (m, 2H, HAr), 6.00 [s, 1H, HC(Cl)=C(O)] ppm; ^{13}C NMR (75 MHz, $CDCl_3$): 153.3, 140.2, 137.8, 128.8, 128.5, 127.3, 127.0, 117.4, 103.9 ppm; IR (cm^{-1}): 3105, 3031, 1898, 1658, 1630, 1603, 1585, 1543, 1310, 1203, 1184, 1107, 1074, 1008, 996, 915, 863, 840, 641, 547, 511; HRMS (ESI) Calculated for $C_{14}H_{10}Cl_2O$ $[M-H]^-$ 263.0031; Found 263.0030.

2.3.2. Synthesis of 4-*(ethynyloxy)-1,1'-biphenyl (3):* To a two-necked, round-bottomed flask (100 mL) equipped with a nitrogen inlet adapter and rubber septum was added the vinyl ether **2** (2.0 g, 7.6 mmol, 1.0 eq), anhydrous diethyl ether (30 mL), and TMEDA (23 mmol, 3.3 mL, 3.0 eq), and then cooled at -78 C. 2.5 M n-butyllithium (9.0 mL, 23 mmol, 3.0 eq) was then added drop-wise to the reaction mixture for over 5 min. The reaction mixture was then maintained at -78 C for 1 h and at - 40 ^oC for 40 min, and then cooled to -78 ^oC while 10% ethanol in pentane (10 mL) was added drop-wise. After 10 min, the reaction mixture was then diluted with *n*-pentane (20 mL) and the washed with saturated solution of ammonium chloride (25 mL). The organic phase was later washed twice with water (20 mL) and then finally with brine (20 mL), dried over anhydrous sodium sulfate, filtered and concentrated to give brown oil. The oil was purified by column chromatography with hexane as the eluent to yield **3** as dark brown oil (0.84 g, 70 %) that later crystallized out as brown amorphous solid: mp 48-49 ^oC. The compound was placed in a round bottom flask and was flushed with nitrogen and kept at -78 ^oC to avoid the decomposition if it was not to be used

immediately. ^{1}H NMR (300 MHz, $CDCl_3$): 7.64-7.52 (m, 4H, HAr), 7.48-7.41 (m, 2H, HAr), 7.40-7.34 (m, 3H, HAr), 2.13(s, 1H, ≡C—H) ppm; ^{13}C NMR (75 MHz, $CDCl_3$): 155.0, 140.1, 138.0, 128.9, 128.4, 127.4, 127.0, 115.4, 84.5, 33.5 ppm; IR (cm^{-1}): 3317(≡C—H), 3029, 2927, 2174(C≡C), 1606, 1512, 1484, 1208, 1166, 1062, 1008, 941, 838, 641, 548, 450; HRMS (ESI) Calculated for $C_{14}H_{10}O$ $[M-H]^-$ 193.0654; Found 193.0651.

2.3.3. Synthesis of *(E)-4-((2-iodovinyl) oxy)-1,1'-biphenyl (4):* To an oven dried, two-necked flask (250 mL) under nitrogen and protected from light was added Cp_2ZrCl_2 (5.2 g, 20.3 mmol, 2.0 eq), dry THF (30 mL), and 1M lithium triethylborohydride (Super Hydride) in THF (20 mL, 20 mmol, 1.9 eq). The mixture was stirred for 1 h where the alkyne **3** (1.97 g, 10.2 mmol, 1.0 eq) was added. After 30 min, iodine (2.57 g, 20.3 mmol, 2.0 eq) was added and the reaction mixture was stirred for 30-40 min while protected from light. The reaction was quenched by diluting with ethyl acetate/hexane (1:1, 50 mL). The diluted mixture was then washed twice with saturated solution of sodium bicarbonate (150 mL) and the combined aqueous layers were extracted with ethyl acetate/hexane mixture (1:1). 10% aqueous sodium thiosulphate (100 mL) was used to wash the combined organic phases followed by brine (100 mL), dried over sodium sulfate, filtered, concentrated to yellowish slurry which was purified by silica gel column chromatography using 100% hexane as eluent (silica gel was pretreated with 2.5 % v/v triethylamine) to afford **4** as white amorphous crystals (1.80 g, 55 %): mp 64-66 ^{o}C. ^{1}H NMR (300 MHz, $CDCl_3$): 7.64-7.52 (m,

4H, HAr), 7.49-7.41 (m, 2H), 7.38-7.32 (m, 1H, HAr), 7.13-7.01 (m, 3H, HAr), 5.74 (s, 1H, CH=CH, *J* = 12.2 Hz) ppm; ^{13}C NMR (75 MHz, $CDCl_3$): 155.5, 150.3, 140.3, 137.0, 128.9, 128.4, 127.2, 126.9, 117.5, 57.9 ppm; IR (cm^{-1}): 3316, 3077, 3034, 2960, 2924, 2874, 2174, 1643, 1623, 1601, 1515, 1485, 1330, 1307, 1226, 1186, 1173, 1093, 1008, 919, 854, 837, 697, 579, 549.

2.3.4. General procedure for Coupling Reactions using *trans-N*-(2-pyridylmethylene)aniline (L1): *(E)-4-((2-(4-(tert-butyl)phenoxy)vinyl)oxy)-1,1'-biphenyl (6)*: An oven dried, three- necked, round- bottomed flask (50 mL) equipped with a nitrogen inlet, reflux condenser, rubber septum was repeatedly evacuated and back-filled with dry and pure nitrogen, and was then charged with CuI (0.09 g, 0.50 mmol), **L1** (0.09 g, 0.50 mmol), *tert*-butyl phenol (0.18 g 1.2 mmol), and Cs_2CO_3 (0.81 g, 2.5 mmol), followed by the addition of anhydrous and degassed acetonitrile (1.2 mL). The flask was evacuated and back-filled with nitrogen and *trans* - **4** (0.32 g, 1.0 mmol) added at rt. The reaction mixture was stirred and heated to the required temperature of 80 ^oC for the 48 h. After cooling to rt, the mixture was diluted with dichloromethane (DCM, 20 mL) and filtered through a plug of celite, with the filter cake being further washed with DCM (10 mL). The filtrate was washed with saturated NH_4Cl (15 mL), and twice with water (10 mL). The collected aqueous phases were extracted twice with DCM (10 mL). The organic layers were collected, dried over $MgSO_4$, filtered, and concentrated in *vacuo* to yield brown solid. The crude product was fixed with 6.0 g silica gel and then purified by silica gel chromatography (100 % hexane) to afford **6** a white

solid (0.20 g 65%): mp 59-62 ^{o}C. ^{1}H NMR (300 MHz, $CDCl_3$) 7.59-7.52 (m, 4H, HAr), 7.46-7.40 (m, 2H, HAr), 7.38-7.33 (m, 3H, HAr), 7.15-7.09 (d, 2H, *J* = 8.5 Hz, HAr), 7.02-6.97 (d, 2H, *J* = 8.6 Hz), 6.91 (s, 2H, CH=CH), 1.32 (s, 9H, 3 x -CH_3) ppm**;** ^{13}C NMR (75 MHz, $CDCl_3$) 157.2, 155.3, 145.6, 140.6, 135.7, 135.3, 134.2, 128.8, 128.4, 127.0, 126.8, 126.5, 116.0, 115.3, 34.3, 31.5 ppm**;** IR (cm^{-1}): 3052, 2961, 2931, 2867, 1607, 1512, 1487, 1367, 1298, 1229, 1187, 1127, 1105, 1079, 1006, 839, 723;HRMS(ESI), Calculated for $C_{24}H_{24}O_2$ $[M+H]^+$ 345.1854; Found 345.1849.

2.3.5. Synthesis of *(E)-4-[2-(4-methoxyphenoxy)vinyloxy]biphenyl (7):* Compound **7** was prepared according to the general method described for compound **6** above, employing trans-- **4** (0.20 g, 0.62 mmol, 1.0 eq) and 4-methoxyphenol (0.077 g, 0.62 mmol, 1.0 eq), Cs_2CO_3 (0.50 g, 1.6 mmol, 2.5 eq), CuI (0.59 g, 0.31 mmol, 0.50 eq) and **L1** (0.057 g, 0.31 mmol, 0.50 eq) heating the reaction mixture at 80 ^{o}C for 48 h to furnish the crude product which was purified by column chromatography using hexane as the eluent to afford **7** as white crystals (40 mg, 40 %): mp 112-115 ^{o}C. ^{1}H NMR (300 MHz, $CDCl_3$): 7.61-7.52 (m, 4H, HAr), 7.47-7.40 (m, 2H, HAr), 7.36-7.30 (m, 1H, HAr), 7.10 (d, 2H, *J* = 8.6 Hz), 7.00 (d, 2H, *J* = 9.0 Hz), 6.91-6.84 (m, 4H, HAr and HC(O)=C(O)H), 3.80 (s, 3H, -CH_3) ppm**.** ^{13}C NMR (75 MHz, $CDCl_3$): 156.3, 154.3, 150.5, 139.5, 135.6, 135.1, 132.7, 131.4, 129.0, 127.8, 127.3, 125.8, 116.1, 115.0, 113.8, 54.7 ppm; IR(cm^{-1}): 3059, 1658, 1605, 1517, 1485,1420, 1319, 1264, 1226, 1173,

1122, 896, 838, 737, 639; HRMS(ESI), Calculated for $C_{21}H_{18}O_3$ [M-H]$^-$ 317.1178; Found 317.1158.

2.3.6. Synthesis of *(E)-(2-([1,1'-Biphenyl]-4-yloxy)vinyl)(phenyl)sulfane (8):* The compound **8** was prepared according to the general procedure described for the compound **6** above employing *trans*- **4** (0.15g, 0.47 mmol, 1.0 eq) and thiophenol (0.051g, 0.050 mL, 0.47 mmol, 1.0 eq), Cs_2CO_3 (0.38 g, 1.2 mmol, 2.6 eq), CuI (0.044 g, 0.23 mmol, 0.49 eq) and **L1** (0.042 g, 0.23 mmol, 0.49 eq) heating the reaction mixture at 60 ^oC for 10 h to give crude product, which was purified by silica gel column chromatography (100 % hexane) to give compound **8**, as white crystals (0.12 g, 90 %). [When a mixture of *Z* and *E*-**4** (1:9) was used as the starting material under same conditions at a temperature above 100 ^oC afforded a mixture of *Z* and *E*-**8** (1:9). They were distinguished from each other by their coupling constants. J_{cis} = 5.7 Hz while J_{trans}= 12 Hz (^{1}H-NMR data of these mixtures are found below). The characterization data below is that of pure **8** obtained from the reaction pure **4** with thiophenol: mp 92-96 ^oC. ^{1}H NMR (300 MHz, CD_2Cl_2): 7.66-7.54 (m, 4H, HAr), 7.48-7.40 (m, 2H, HAr), 7.37-7.28 (br s, 6H, HAr), 7.20-7.09 (m, 3H, HAr), 6.09-6.10 (d, 2H CH=CH, *J* = 12.0 Hz) ppm; ^{13}C NMR (300 MHz, $CDCl_3$): 155.9, 150.6, 140.3, 137.5, 137.1, 128.9, 128.8, 128.5, 127.2, 127.0, 126.9, 125.7, 117.4, 102.1; IR(cm^{-1}): 3054, 2985, 1659, 1624, 1599, 1515, 1485, 1265, 1233, 1185, 1174, 1112, 1086, 1025, 1007, 924, 839, 739, 407; HRMS (ESI) Calculated for $C_{20}H_{16}OS$[M+H]$^+$ 305.1000; Found 305.0998.

2.3.7. Synthesis of *(E)-N-(2-(Biphenyl-4-yloxy)vinyl)aniline (9) :* Compound **9** was tried to be prepared according to the general methods described for compound **6 (**and **5**) above, employing *trans*- **4** (0.15 g, 0.47 mmol, 1 eq), aniline (0.043 g, 0.47 mmol, 1 eq), Cs_2CO_3 (0.38 g, 1.1 mmol, 2.5 eq), CuI (0.044 g, 023 mmol, 0.5 eq) and **L1** (0.042 g, .23 mmol, 0.5 eq) at 80 ^oC to give a new weak spot on TLC which might be the product. However, it could not be purified using a silica gel column chromatography.

2.3.8. General procedure for Coupling Reactions using 2-pyridin-2yl-1*H*-benzoimidazole (L2): *(E)-4-((2-(phenoxy) vinyl) oxy)-1,1'-biphenyl (5)*: An oven dried, three- necked, round- bottomed flask (50 mL) equipped with a nitrogen inlet, reflux condenser, rubber septum was repeatedly evacuated and back-filled with dry and pure nitrogen, and was then charged with CuI (0.074 g, 0.39 mmol, 0.5 eq), **L2** (0.076 g, 0.39 mmol, 0.5 eq) and Cs_2CO_3 (0.63 g, 2.0 mmol, 2.5 eq), followed by addition of DMF (2 mL). The solution was stirred for 10 min at rt until reaction turn light green color. The appropriate substrate phenol (0.073 g, 0.78 mmol, 1 eq) was added to the reaction mixture and then stirred for addition 5 min at rt. *Trans*- **4** (0.25 g, 0.78 mmol, 1eq) was dissolved in minimum amount of solvent and then added into the reaction mixture. The reaction mixture was then heated from rt to between 50-75 ^oC for 12-36 hr depending on the substrate. The reaction mixture was cooled and then through pad of silica gel using ethyl acetate and hexane mixture (20:80, 100 mL) and then washed three times with the same solvent mixture (100 mL). Filtrate was washed with water

(100 mL x 3) followed with brine (200 mL), dried using anhydrous sodium sulfate and concentrated in vacuo to yield brown oil. The crude oil was then purified by silica gel column chromatography using 100% hexane to afford **5** as white crystals. (0.18 g, 70 %): mp 60-63 ^{o}C. ^{1}H NMR (300 MHz, $CDCl_3$): 7.59-7.54 (m, 4H, HAr), 7.47-7.40 (m, 2H, HAr), 7.37-7.31 (m, 1H, HAr), 7.16-7.03 (m, 7H), 6.92 (s, 2H, HC=CH); ^{13}C NMR (75 MHz, $CDCl_3$): 157.6, 157.2, 140.4, 135.8, 134.9, 134.6, 129.7, 128.8, 128.4, 127.0, 126.9, 122.7, 116.0, 115.8; IR (cm^{-1}): 3061, 2962, 2870, 1606, 1510, 1485,1419, 1365, 1230, 1183, 1174, 1124, 1105, 1006, 896, 836, 728; HRMS (ESI), Calculated for $C_{20}H_{16}O_2$ $[M-H]^-$ 287.1072; Found 287.1053.

2.3.9. Synthesis of *(E)-1-(2-([1,1'-Biphenyl]-4-yloxy)vinyl)-1H-indole (10):* The compound **10** was prepared following the procedure described for **5** with *trans*- **4** (0.32 g, 1 mmol, 1 eq), indole (0.14 g, 1.2 mmol, 1.2 eq), Cs_2CO_3 (0.81 g, 2.5 mmol, 2.5 eq), CuI (0.095 g, 0.5 mmol, 0.5 eq) and **L2** (0.097 g, 0.5 mmol, 0.5 eq) at 70 ^{o}C for 12 hr to give crude product which were purified by silica gel column chromatography using ethyl acetate-hexane (9:95) to afford compound **10** as white crystals (0.27 g, 87 %): mp 140-142 ^{o}C. ^{1}H NMR (300 MHz, $CDCl_3$): 7.58-7.46 (m, 6H, HAr), 7.40-7.32 (m, 3H, HAr), 7.25-7.21 (m, 1H, HAr), 7.20-7.14 (m, 2H, HAr), 7.12-7.02 (m, 4H, HAr and H(O)C=(N)CH), 6.55 (d, H, *J* = 3.1 Hz, HAr). ^{13}C NMR (75 MHz, $CDCl_3$): 156.8, 140.4, 136.5, 136.4, 128.9, 128.8, 128.5, 127.1, 126.9, 125.7, 125.6, 121.2, 120.5, 116.5, 115.2, 109.8, 104.0 ppm; IR (cm^{-1}): 3034, 2358, 2338, 1682, 1606, 1515, 1485, 1475, 1462, 1358, 1333,

1322, 1301, 1232, 1202, 1186, 1174, 1134, 1115, 1088, 1031, 1007, 907, 865, 834; HRMS (ESI), Calculated for $C_{22}H_{17}NO$ $[M+H]^+$ 312.1388; Found 312.1381.

2.3.10 Synthesis of *(E)-1-[2-(Biphenyl-4-yloxyl)vinyl]-1H pyrrole (11):* The compound **11** was prepared following the procedure described for **5** with *trans*- **4** (0.2 g, 0.62 mmol, 1 eq), pyrrole (0.062 g, 0.93 mmol, 1.5 eq), Cs_2CO_3 (0.40 g, 1.2 mmol, 2.5 eq), CuI (0.059 g, 0.31 mmol, 0.5 eq) and **L2** (0.060 g, 0.31 mmol, 0.5 eq) at 70 ^oC for 12 hr to give crude product which were purified by silica gel column chromatography using ethyl acetate-hexane (9:95) to afford compound **11** as white crystals (0.14 g, 85 %): mp 102-105 ^oC. Olefinic protons coupling on the named compound gave an AB-system with a typical roof effect with peaks centered at 7.04 and 6.99 ppm. ^1H NMR (300 MHz, $CDCl_3$): 7.62-7.53 (m, 4H, HAr), 7.48-7.40 (m, 2H, HAr), 7.38-7.31 (m, 1H, HAr), 7.17-7.09 (m, 2H, HAr), 7.04 (distorted d, 1H, J = 11.1 Hz, (O)-CH=CH(N)), 6.99 (distorted d, 1H, J = 11.1 Hz, (O)-CH=CH(N)), 6.82 (dd, 2H, J_1 = 4.2 Hz, J_2 = 2.2 Hz, CH=CH of pyrrole), 6.28 (dd, 2H, J_1 = 4.2 Hz, J_2 = 2.2 Hz, CH=CH); ^{13}C NMR (75 MHz, $CDCl_3$): 156.8, 140.4, 136.3, 135.0, 128.8, 128.4, 127.1, 126.9, 119.6, 118.3, 116.5, 110.0 ppm; IR (cm^{-1}): 3086, 3034, 2715, 2682, 1659, 1607, 1587, 1517, 1485, 1360, 1326, 1300, 1239, 1229, 1185, 1173, 1119, 1094, 1072, 1056, 1007, 975, 907, 857, 838, 614; HRMS (ESI) Calculated for $C_{18}H_{15}NO$ $[M+H]^+$ 262.1232; Found 262.1233.

2.4. General photooxidation procedure: To a 0.5 mL $CDCl_3$ in an NMR was dissolved an olefin(0.0048 mmol).. The photosensitizer [5-(4-methoxyphenyl)-10,15,20-triphenyl-21-23-dithiaporphyrin, CMP-OMe, 3 mg, 0.0048 mmol] was added to this solution. Then, the reaction mixture was irradiated for 15 min using a diode laser (690 nm, 200 mW/cm^2). The reaction of olefins with singlet oxygen was monitored by the decrease of olefinic peaks, while the formation of the photooxidation products were also measured by the increased in the formate peaks in ^{1}H-NMR spectra.

2.5. RESULTS AND DISCUSSION

For the synthesis of the diheteroatom-substituted olefins, four-step scheme was developed where 4-phenylphenol **1** was used in one side. First, 4-phenylphenol was vinylated using 1,1,2-trichloroethylene [170] to give the corresponding 4-((1,2-dichlorovinyl)oxy)-1,1'-biphenyl **2** with yield of more than 85%.[171,172] Then, 4-(ethynyloxy)-1,1'-biphenyl **3** was prepared by elimination reaction using *n*-BuLi in 70 % yield.[171,172] Although **1** was used in this paper, other types of alcohols and phenols can also be converted to the alkyne form.[171] Hydrozirconation and iodinolysis of **3** led to 2-iodoenol ether **4** in 55 % yield.[173,174] Using the copper-catalyzed coupling reaction, **4** were linked with various substrates bearing the different functional groups.[175-177]

The reaction with thiophenol gave the best yield (**8**: 90%) and short reaction time followed by reactions with aromatic amines (**10**: 87%, **11**: 85%) and least yield by

the reaction with phenols (compounds **5**, **6**, **7**). The trend could be explained by the relative nucleophilicity of the substracts (-SH > -NH > -OH) (Table 1). Two coupling conditions were used; either trans-*N*-(2-pyridylmethylene)aniline as ligand in acetonitrile as solvent [176,178] or 2-pyridin-2-yl-benzoimidazole as ligand in DMF as solvent.[177] For the compound **5**, slightly better yields were obtained using the latter coupling condition and the reaction time was reduced to 16 h compared to the former condition (36 h). To test the robustness of our method, some selected analogues of the phenolic and azole derivatives were synthesized. Phenolic derivatives required high temperatures of 70-80 ^{o}C for 16-48 h of reaction time and yields were poor-good (40-70 %). Further optimization of reaction conditions for these low yielding coupling reactions will be pursued. Reaction with the azole derivatives required low temperatures between 50-75 ^{o}C and shorter reaction time, 12 h. The yields for **10** and **11** were very good (87 and 85 % respectively). Our methodology encountered, however, a limitation in the case of aniline. Coupling using aniline substrate gave an extremely low yield that the product could not be isolated. In all of these reactions the products gave single isomers (*E*-1,2-diheteroatom-substituted olefins) since only the *trans*- **4** was used for the coupling.[177] This is well-known Ullmann-type coupling reaction which proceeds in stereospecific fashion.[175,177] The stereospecificity of the reaction was also supported by the fact that a mixture of *E*/*Z*-**4** (9:1) at > 100 ^{o}C gave a mixture of *E*/*Z*-**8** at the same ration of 9:1 (NMR data in SI).

Unlike typical coupling constants of 12-18 Hz for protons at *E*-olefins and 6-12 Hz at *Z*-counterparts, the coupling constants of the hydrogen atoms on 1,2-diheteroatom-substitituted olefins were found to be reduced and in some cases even to zero. Only a peak was observed from 1,2-diaryloxyalkenes (**5, 6,** and **7)** where the two olefinic protons are in very similar environment. On the other hand, while **8** showed doublet peaks, **11** showed distorted doublet peaks (AB system): *E*-**8** (*J* = 12 Hz), *Z*-**8** (*J* = 5.3 Hz), *E*-**11** (*J* = 11.1 Hz). Such unusual small coupling constants of olefins were also observed in monohetereoatom-substituted olefins, especially the oxygen-substituted olefins.[175-177]

To examine the oxidation rate of these electron rich alkenes with singlet oxygen (Scheme 2), we irradiated compounds **6**, **8**, and **11** in the presence of 5-(4-methoxyphenyl)-10,15,20-triphenyl-21,23-dithiaporphyrin as a photosensitizer.[179] All experiments were done following the standard procedure previously set by our group with a slight modification by using a 690 nm diode laser source (200 mW/cm^2).[180] The 1:1 ratio of olefin and photosensitizer was used to mimic the situation of prodrug where the olefinic linker could be used for connecting one drug and one photosensitizer (14, 15). The reaction solutions were irradiated for 15 min and monitored every 5 min using olefinic peaks in ^{1}H-NMR each time to monitor the progress of the reactions. Upon the oxidation by singlet oxygen, the olefinic peaks decreased.

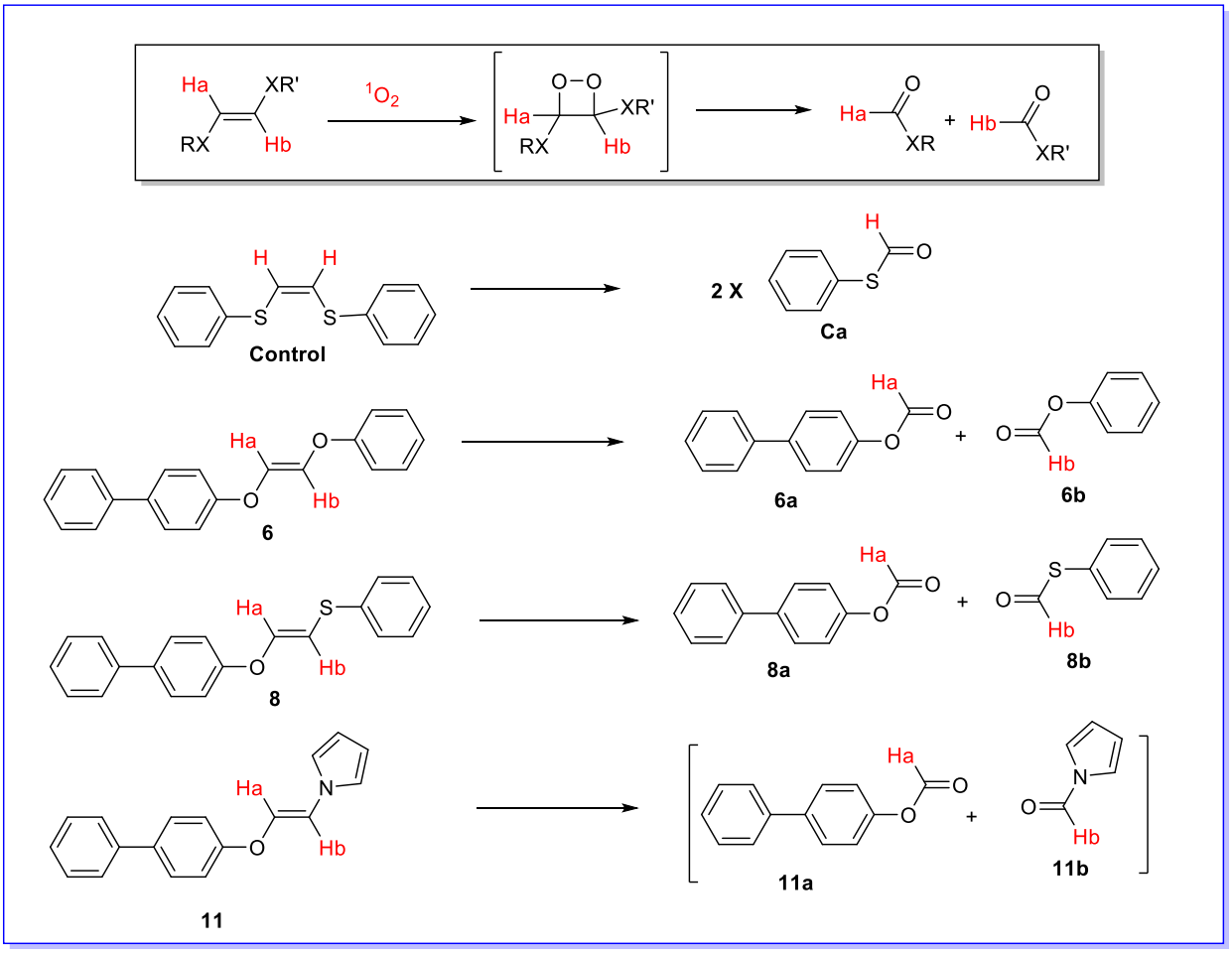

Scheme 2. Cleavage Products from Heteroatom substituted Alkenes

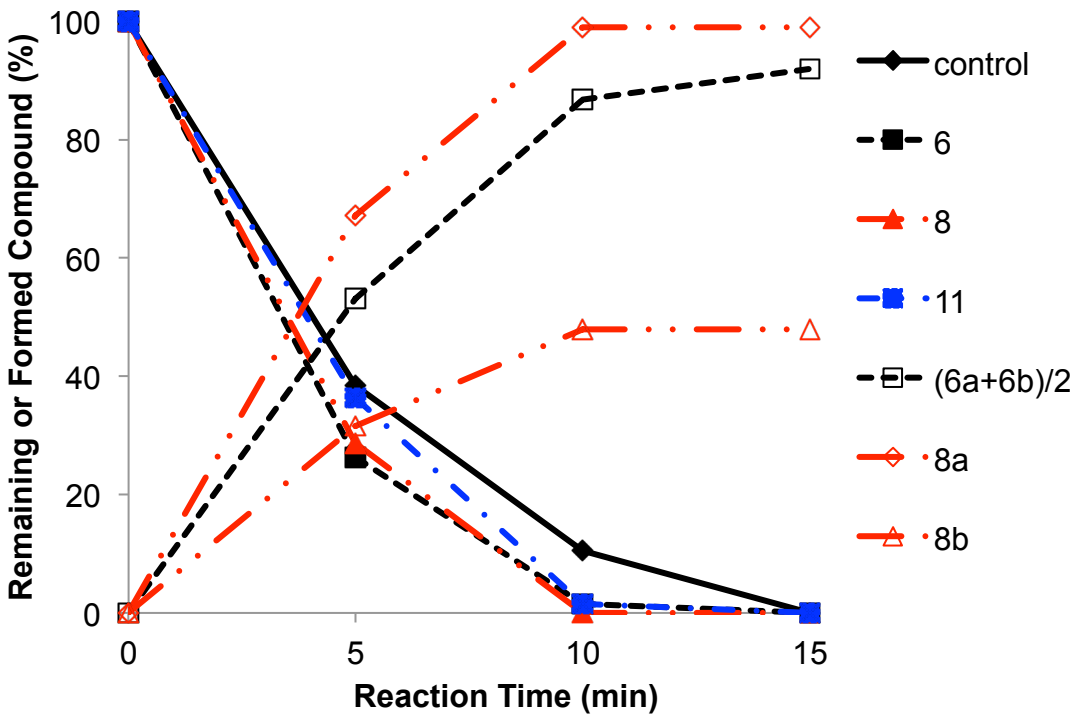

Figure 11. Rate of decomposition and formation of cleavage product singlet oxygen- mediated oxidation of the heteroatom substituted alkenes

(*E*)-1,2-*Bis*(phenylthio)ethylene was used as a control against which the reaction rates were compared. Analysis of the data indicated that not much difference exists amongst these linkers with respect to their rate of reaction with singlet oxygen (Fig. 11 and Table 3). Double bond peaks of all the four substrates disappeared within 15 min of the irradiation. The fast reaction of **6** (*1,2*-diaryloxyalkene) and **8** (*1*-aryloxy-*2*-arythio-alkene) is consistent with our previous report [180]. The cleaved formate products **6a**, **6b**, **8a** were formed consistent with the decrease of the olefins **6** and **8** (Table 3). On the other hand, cleaved thioformate products **8b** was formed much less (about half) than

oxidized olefin 8, presumably, due to the oxidation at sulfur[180]. The fast reaction of **11** (*1*-aryloxy-*2*-amino-alkene) with singlet oxygen was also observed. The olefinic peaks of **11** completely disappeared in 10 min. In addition, we also observed the decrease of the peaks of protons at the pyrrole ring at a little bit slower rate: 73% (olefinic proton) vs. 60% (protons at the pyrrole ring) reduction after 5 min. One notable observation is that the formate product **11a** was not detected in the ^{1}H-NMR from the oxidation of **11**. Further investigation is needed to reveal the detailed mechanism of oxidation of **11**.

2.6. POTENTIAL FOR BIOLOGICAL APPLICATION

For our synthetic scheme to be useful we set out to synthesize a model compound constituted of combretastatin A4, CA-*4*, a compound, structurally related to colchicines [181] (tubulin-binding agents) which has been shown to interact with tubulin [182] and caused vascular shutdown in solid tumors with a *5*-(*4*-hydroxyphenyl)-*10,15,20*-triphenyl-*21,23*-dithiaporphyrin, CMP, (**15**) as a photosensitizer using the vinyl diether linker to give a prodrug, **16**, that can easily be cleaved using a laser diode or NIR.. Our intention was to get the model compound then test it *in vitro* and subsequently *in vivo.* The target compound, **16**, was synthesized but due to its high reactivity, we could not handle the product due to its instability even in NMR solvent.

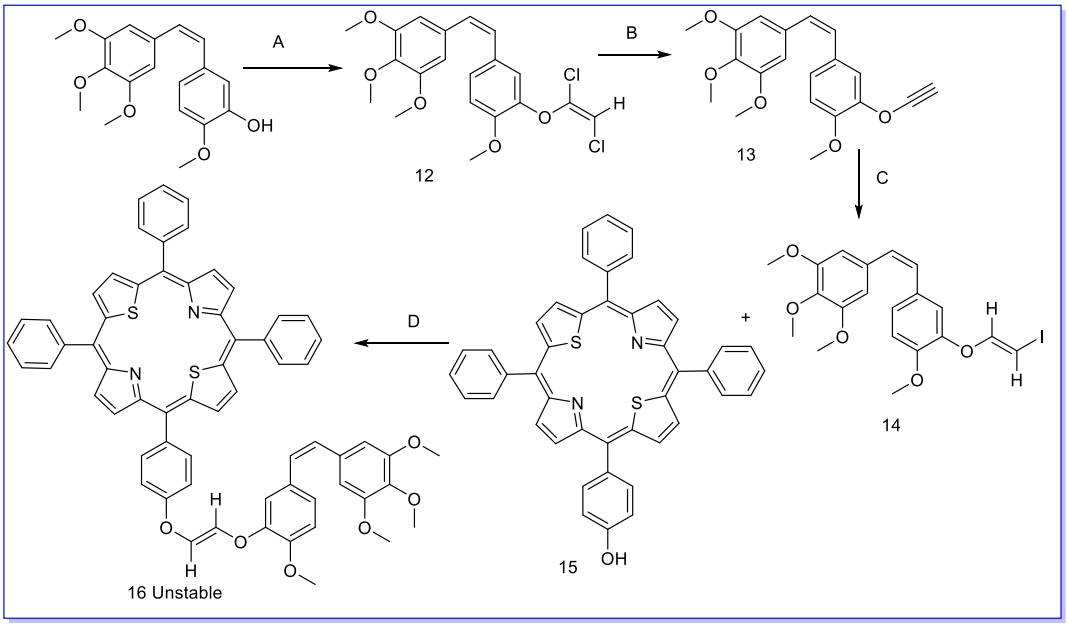

Scheme 3. Proposed scheme for the synthesis of CMP-L-CA4 using vinyl diether linker: A) i) KH (0.55 mmol), **CA-4** (0.37 mmol) at rt, THF, ~30 min, ii) Trichloroethylene (0.44mmol) at -78 ^{o}C warm to rt, overnight, B) **12** (0.37 mmol), TMEDA (3.65 mmol), *n*-BuLi (3.65 mmol) at -78 ^{o}C, 1h to -40 ^{o}C, 40 min, Et_2O, C) i) Cp_2ZrCl_2 (0.42 mmol), $LiEt_3BH$ (0.42 mmol) at rt, THF, 1 h, ii) **13** (0.23 mmol) at rt, 30 min, iii) I_2 (1.05 mmol) , 40 min, D) 10 mol % CuI, 10 mol % ligand, 2 eq. Cs_2CO_3, 1 eq. **14**, 1 eq. **15** , 50-80 ^{o}C, 10-48 h

2.6.2. EXPERIMENTAL SECTION

2.6.2.1. Synthesis of combretastatin A-4 (CA-4). The compound was synthesized as reported in literature.[183]. ^{1}H-NMR (300 MHz, CD_2Cl_2): 3.70 (s, 6H), 3.84 (s, 3H), 3.87 (s, 3H), 5.53 (s, 1H), 6.41 (d, *J* = 12.3 Hz, 1H), 6.47 (d, *J* = 12.3 Hz, 1H), 6.53 (s, 2H), 6.73 (d, *J* = 8.5 Hz, 1H), 6.80 (dd, *J* = 2.0, 2.0 Hz, 1H), 6.92 (d, *J* = 2.0 Hz, 1H). HRMS-ESI (m/z): Calculated for $C_{18}H_{20}O_5$ $[M+ Na]^+$: 339.1300; found: 339.1206

2.6.2.2. Synthesis of compound 12: compound **12** was prepared according to the method described for compound **2** employing combretastatin A-4 (CA-4) (1 eq.), potassium hydride (1.5 eq.), trichloroethylene (1.2 eq.) to give a white solid compound 12 (0.4g, 80 %).^{1}H-NMR (300 MHz, CD_2Cl_2): 3.70 (s, 6H), 3.84 (s, 3H), 3.87 (s, 3H), 5.53 (s, 1H), 6.41 (d, *J* = 12.3 Hz, 1H), 6.47 (d, *J* = 12.3 Hz, 1H), 6.53 (s, 2H), 6.73 (d, *J* = 8.5 Hz, 1H), 6.80 (dd, *J* = 2.0, 2.0 Hz, 1H), 6.92 (d, *J* = 2.0 Hz, 1H).

2.6.2.3. Synthesis of compound 13: Compound **13** was prepared according to the method described for compound **3** employing compound **12** (150 mg, 0.37 mmol), 1.60 M *n*-BuLi (2.28 mL, 3.65 mmol), TMEDA (1.08 mL, 3.65 mmol) in 6 mL of dry Et_2O to afford **13** as orange brown solid (86.70 mg, 60%). ^{1}H-NMR (300 MHz, $CDCl_3$): 3.02 (s. 1H), 3.70 (s, 6H), 3.84 (s, 3H), 3.87 (s, 3H), 5.53 (s, 1H), 6.41 (d, *J* = 12.3 Hz, 1H), 6.47 (d, *J* = 12.3 Hz, 1H), 6.53 (s, 2H), 6.73 (d, *J* = 8.5 Hz, 1H), 6.80 (dd, J = 2.0, 2.0 Hz, 1H), 6.92 (d, *J* = 2.0 Hz, 1H).

2.6.2.4. Synthesis of compound 14: Compound **14** was prepared according to the method described for compound **4** by employing compound **13** (80 mg, 0.23 mmol), Cp_2ZrCl_2 (128.97 mg, 0.42 mmol), $LiEt_3BH$ (0.42 mL, 0.42mmol) and Iodine (I_2) (132.82 mg, 1.05 mmol) to obtain **14** as white crystals.

2.6.2.5. of compound 15: Compound **15** was synthesized and characterized as reported in literature.[184]

2.6.3 Results and discussion

Synthesis of the intermediates for the conjugates was successful until the final step. In the coupling reaction we followed the method described for compounds **6**. Separation of the final conjugate was performed using the preparative TLC but the NMR of the final compound could not be obtained as it decomposed spontaneously within the NMR tube. The result could be interpreted as such; CMP has a very high singlet oxygen quantum yield, hence, minimum amount of light could excite it. Direct conjugation of the electron-rich (vinyl diether) bond led to the generation of $^1O_2$ at the vicinity of the bond with minimum light that cleaved the bond and was responsible with the observed instability of **16**. Therefore, the strategy to ensure the stability of the prodrug should be developed.

2.7. CONCLUSION

In summary, a facile and versatile synthetic scheme for *E*-*1,2*-diheteroatom-substituted electron-rich alkenes was established for the first time. Not only symmetric vinyl diethers but also unsymmetrically heteroatom-substituted olefins could be prepared using phenols, thiols, and *N*-heterocycles with high stereospecificity. In addition to *1,2*-diaryloxyalkene and *1*-aryloxy-*2*-arylthio-alkene, *1*-aryloxy-*2*-amino-alkene also seems to react fast with singlet oxygen.

Because we were faced with the challenge of the synthesis of the prodrug, using the vinyl diether linker, we resort to use the alternative linker (aminoacrylate linker) was developed which offer a number of advantages compared to the vinyl diether such as synthesis via easy and high yield reactions, stability, and regeneration of parent drug after cleavage. Moreover, the use of *n*-Buli in one of the steps limited the used of the scheme especially when the drugs were sensitive or unstable to the *n*-BuLi.

Chapter 3: DESIGN, SYNTHESIS AND CHARACTERIZATION OF FOLATE AND BIOTIN TARGETED PRODRUG DELIVERY SYSTEM OF PC-CA4

3.1. Introduction

Chemotherapy is often used to treat cancer, and it is expected to destroy the tumor cells for maximum treatment efficacy, while minimizing the side effects to other organs.[185] However, conventional anticancer agents often have such a poor distribution, normal tissue damage and lack of target specificity. The development of tumor targeting drug delivery systems, able to selectively transport cytotoxic agents into the tumor site by exploiting subtle morphological and physiological differences between healthy and malignant cells, currently stands as one of the attractive strategies to overcome the selectivity problems of conventional chemotherapy. Active investigation in cancer treatment is being carried out on new targeted chemotherapeutic drugs that can report on the localization and activation of the drug upon selective internalization.[186-188] As mentioned in the introduction, to actively target the drug delivery system or carrier, chemical modification by tumor targeting ligands is popular, e.g., biotin, antibody[91], transferrin, folic acid epidermal growth factor and RGD peptide, among others. [189]

Folic acid (FA) is a prominent ligand capable of specific interaction with cells expressing the folate receptor (FR). The folate receptor is a well-known tumor–associated receptor that is overexpressed in many tumors, including those of the breast, lung, kidney, and brain and has little expression in normal tissues.[187,190-192] The overexpression of FR provides tumor cells with increased amounts of FA essential for DNA synthesis and seems to aid in aggressive tumor growth. Seminar observation of cancer patients overexpressing folate isoform α (FR-α) is that it tends to correlates with higher histological grade and more advanced stage of this disease.[105] Therefore, FR can serve as both as a marker and target molecule for diagnosis and therapy of cancer.[187] Various folate – drug conjugates such as folate conjugated to cytotoxic drugs e.g., camptothecin,[193] taxol,[194] mitomycin C,[195-197] and folate tethered protein toxins such as momordin[198] and Pseudomonas exotoxins,[199] etc. have been developed and tested in culture cells, animal models, and in human clinical trials with successful results as stated in the introduction. The drugs are conjugated through cleavable linker that constitute prodrugs that are released upon cell internalization but none of these conjugates possesses both activatable cytotoxicity and fluorescent imaging capabilities and intracellular localization upon cell entry.[193-197] Although folate conjugates with florescent dyes and nanoparticles have been developed to determine the intracellular localization and presence of folate receptor, they lack therapeutic modality.[200,201]. Moreover, some of the folate conjugates such as; *bis*-(haloethyl) phosphoramidites,[202] PEG carboplatin,[203] 10–mer a conjugate of thymidylate synthase inhibitor, *5*-fluoro-*2*'-deoxyuridine-*5'-O*-monophosphate

(FdUMP),[204] and paclitaxel,[205] although synthesized, were of limited success (lower potencies)[206] probably due to lack of active release mechanisms within the conjugates. Hence, there is need for multimodal folate targeting drug delivery system which can actively target the cancer cells, release the payload, image and carryout therapeutic functions.

Biotin (vitamin B_7, vitamin H, Figure 12) is an essential micronutrient for normal cellular function growth and development.[207] Biotin is involved in two ways in targeted cancer therapy. 1) In rapidly dividing cancer cell lines, biotin uptake is greater than that seen in normal tissues.[208] Biotin receptors are over expressed more than FA receptors on several cancer cell lines, including leukemia (L1210FR), lung (M109), renal (RENCA, RD0995) and breast cancer cells (4T1, JC, MMT06056).[209]Although the structure(s) of the biotin receptor is /are not known,[209,210] it has been suggested that the sodium-dependent multivitamin transporter is involved in biotin uptake.[211,212] Cells that overexpressed biotin receptors are known to be targeted by the biotin conjugates via endocytosis.[213] (ii) Biotin has the highest affinity to two proteins avidin and streptavidin with a dissociation constant of 10^{-15}.[214] We will not focus on this biotin streptavidin drug targeting methodology but rather we will focus on the targeting of active species by conjugation to biotin via their receptors. Since its research has indicated that cancer cell lines that overexpress folate receptors, most of time equally show the overexpression of the biotin receptors,[209] it stands to reason that developing a drug delivery system using the biotin as the homing device[211,215-217] should be

possible since not much clinical work has been done that far on this newly discovered receptor and can possibly be a substitute for the folate or serve as a dual targeting ligand together with the folate in the same construct.

‘

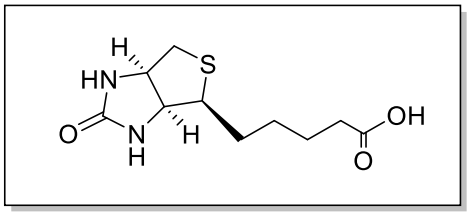

Figure 12. Structure of Biotin

As I said in the introduction, PDT is a promising new therapeutic tool for the management of a variety of solid tumors. It involves the administration of a nontoxic photosensitizer a drug, followed by activation of the drug with light of specific wavelength (600-800 nm). PDT generates singlet oxygen and other reactive oxygen species (ROS) that cause an oxidative stress and membrane damage in the treated cells and eventually cell death. The selectivity of PDT is a result of a low-to-moderate degree of selective photosensitizer uptake caused by proliferating malignant lesion followed by the focused illumination of tumor with red or NIR that is able to penetrate the tissue. The conventional PDT has been less commonly used for cancer therapy because the current non-targeted photosensitizers are also taken up by normal tissues, which causes side effects,

including skin photosensitization.[10,62,218] Various methods used in targeting chemotherapeutic agents have also been used to target the photosensitizers. Various combinations of conventional photosensitizers and monoclonal antibodies (mAbs) have been tested to improve their selectivity with limited success, especially when measured by *in vivo* therapeutic effects.[219-223] Polymeric carriers including polymer–photosensitizer conjugates,[224,225] PS-loaded nanocarriers, long circulating liposomes[226] and polymeric micelles,[227-230] have also been developed to passively target the tumor via enhanced permeability and retention (EPR) effect.[231] PSs have also been conjugated to peptides, [232]as well as other small ligands such as folic acid [233,234] for site-specific targeting photosensitizers to tumor tissues. Each of this targeting methodology has always been encountered with other challenges at the animal models. *Hence, there is need to design specifically targeted photosensitizers in order to enhance phototoxicity as a result of higher and more selective accumulation in tumor cells and reduction in skin phototoxicity of this therapy.*

3.2. Hypothesis

We hypothesized that by conjugating prodrug to folic acid via a PEG spacer we could actively target the prodrug to the tumor tissue by exploiting the high affinity of the FA to the FR ultimately improving the photodynamic response and at the same time actively triggering the release of the CA-4 into the tumor mass while sparing the healthy tissues.

3.3. Experimental Design

In this study we evaluated the ability of both folate and biotin targeted prodrugs to deliver the conjugates to the tumor by exploiting the overexpression of their receptors on the cancer cells as compared to the normal cells. Seven conjugates: **FA-PC-CA4, PC-CA4, FA-PEG2-PC-CA4, Boc-PEG897-PC-CA4, FA-PEG897-PC-CA4, Biotin-PEG897-PC-CA4 and FA-PEG2K-PC-CA4** were designed and synthesized. They were synthesized by conjugating PC-CA4 (generated click reaction of **17** to **16**) to FA directly or PEGylated folic acid or biotin of variable lengths as seen in the synthetic schemes below. To evaluate the efficiency of the conjugates as photosensitizers, some of the photophysical properties of all the six conjugates and the *in vitro* photodynamic activities of three lead conjugates selected from *in vivo* imaging screening were studied.

Photophysical studies: the UV/Visible absorption spectra, molar extinction coefficients and the aggregation tendency were studied.

In vitro studies of dark toxicity, phototoxicity, cellular uptake, competition assays, and sub-cellular localization of selected conjugates were evaluated using colon 26 cell lines.

In vivo optical screening: The rate of uptake and receptor targeting capabilities of the conjugates were evaluated in vivo in balb/c mice bearing colon 26 cancer cell lines and leads were then selected for further studies.

These conjugates were designed and synthesized combining the two basic principles that may be necessary to fulfill “Paul Ehrlich’s” vision of “magic bullet” for the treatment of diseases. 1) Site-specific delivery by targeting either the FR or biotin receptors in the tumor to direct the drug (CA-4) away from normal tissues that is particularly sensitive to the toxic action of the carried payload. 2) Site-specific triggering mechanism which by incorporating the photocleavable aminoacrylate linker could increase the release and therapeutic efficiency of the carried drug dramatically (this concept has been proven by Dr. Bio Moses in our lab).[158] The combination of these two principles could lead to high local drug bioavailability specifically in tumor tissue while maintaining the stability of the drug delivery system in circulation. Furthermore, in designing the folate conjugates other useful criteria for producing active lead compounds were also taken.

3.3.1. Design of FA- and biotin-prodrug conjugates and their intracellular release mechanism

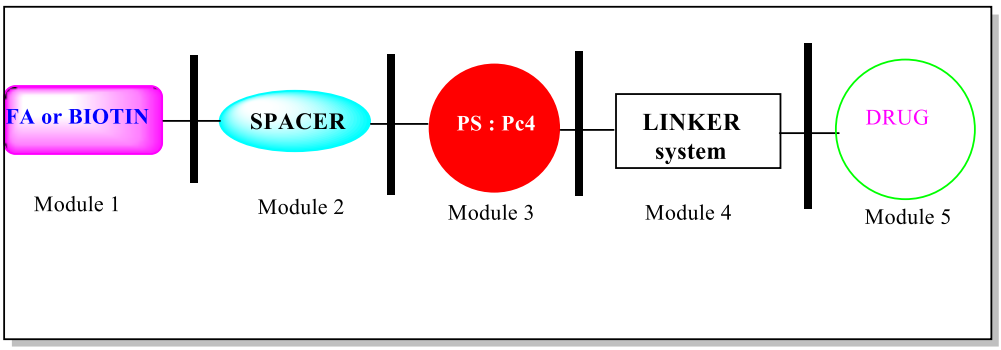

Figure 13. Schematic design of multifunctional prodrug.

- Use of highly potent drug (module 5): Since there is finite number of FR per cell and the folate recycling rate is 8-12 h, there will be a saturable period of exposure to the CA-4 and under these conditions CA-4 with its intrinsic IC50 value in the low μM range will produce the required cytotoxic effects.

- Enhanced hydrophilicity: The PC-CA4 prodrug is highly lipophilic and can passively diffuse through the cell membrane bilayer. By PEGylation or introducing a hydrophilic spacer (module 2) between the FA (module 1) and PC (module 3) we hope not only to increase the biocompatibility of the prodrug but to also enhance the hydrophilicity, thereby forcing the greasy prodrug to exclusively enter the FR positive cells via FR-mediated endocytosis rather than indiscriminate diffusion into the cells. The spacers used by other groups for this purpose are peptides [195,235-239] or carbohydrates.[235,240-242] By using PEGs of variable lengths we wanted to achieve a minimum chain length that can not only

ensure the hydrophility of our prodrug but also easy targetability of FR on tumor tissue *in vivo*.

- Choice of photosensitizer. We choose silicon dichloride phthalocyanine because it could easily be functionalized at the axial position, let alone the fact that most metallated phthalocyanines are used clinically as PDT and imaging agents. Therefore using the two axial positions available in pc-4 we could asymmetrically functionalized them with homing device and the drug- linker. In this study, we developed a folate base photosensitizer that is activated by NIR light for theranostic purpose when uptaken by the cancer cells. Further, because this agent also emits fluorescence, it can also be used to direct the application of light to minimize exposure to non-relevant tissues and to noninvasively monitor any therapeutic effects of excitation light.

- Low molecular weight: By limiting the average size of our conjugates well below 4000Da we anticipate that they will allow for better penetration into the solid tumors with simultaneous rapid systemic clearance.

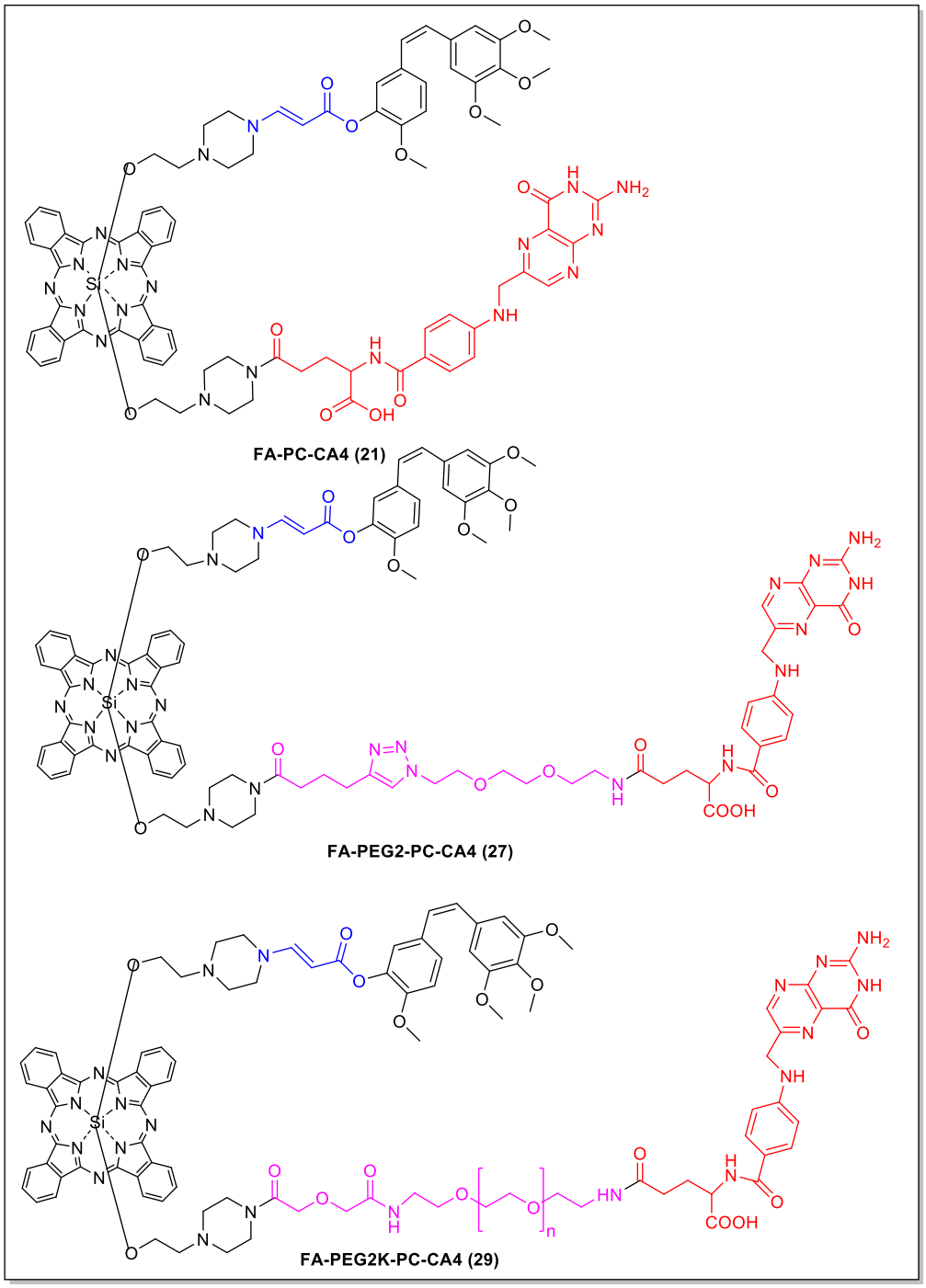

Figure 14. Structures of compounds **21, 27**, and **29** synthesized

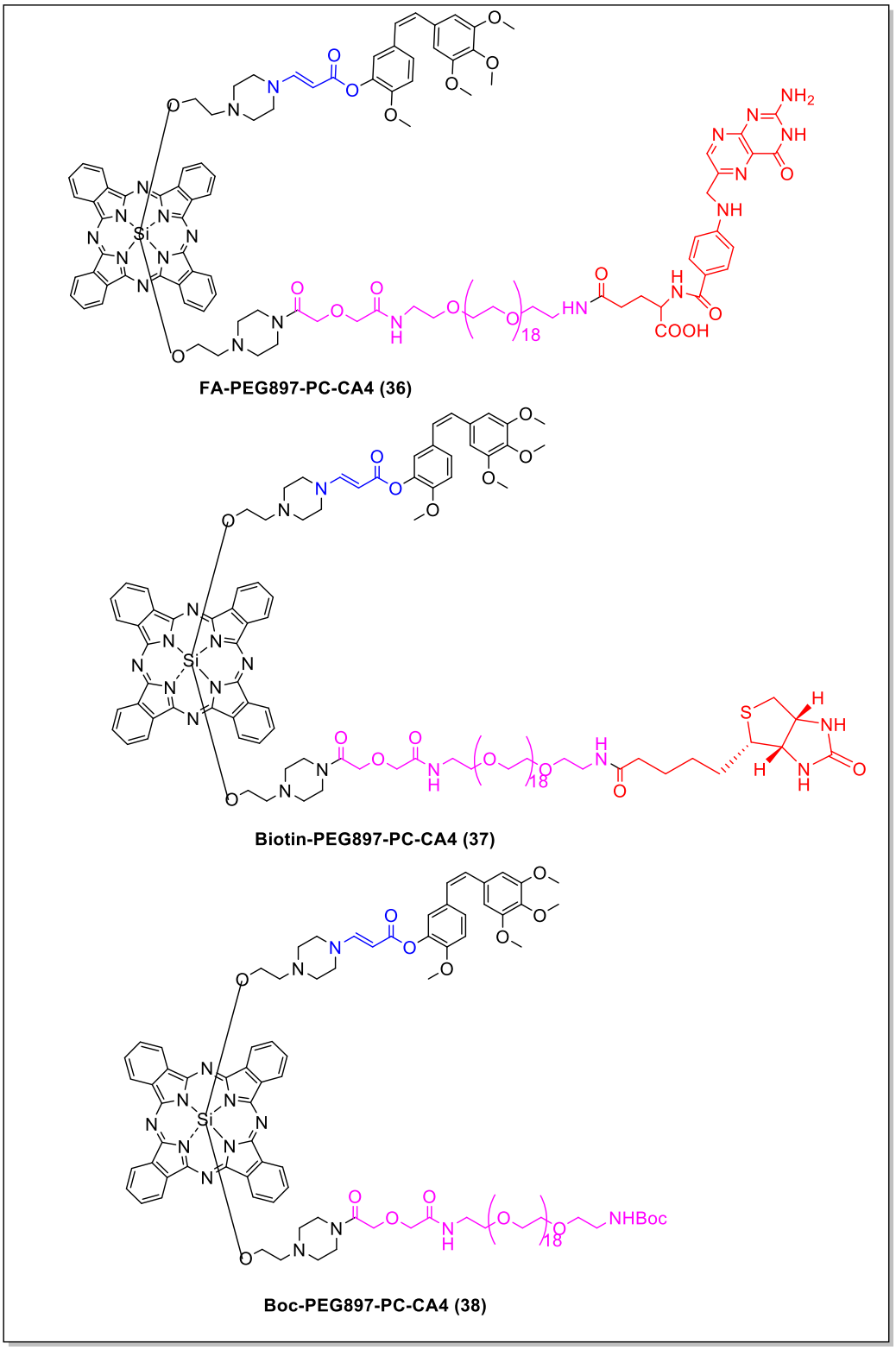

Figure 15. Structures of compounds **36, 37 and 38** synthesized

3.4 Experimental Procedure

3.4.1. General Method

All solvents and reagents used were obtained from Sigma-Aldrich, Alfa Aesar, Thermo Fisher Scientific, Polypure Inc., and Nanocs Technology Inc. unless otherwise stated. All reactions were monitored by TLC using 5-17 μm silica gel plates with fluorescent indicators from Sigma Aldrich (catalog # Z193291-1PAK). All chromatography was performed using 32-63 μm silica gel Sorbent Technologies (Catalog # 02826-26). All preparative TLC separations were performed using silica gel GF preparative layer uniplate chromatography plates with UV254 prep-scored 20 X 20 microns from Analtech Inc. (Catalog # 02003) All dialysis were performed using 7 Spectra/Por dialysis membrane (MWCO: 1000 DA) from Spectrum Laboratories, Inc. NMR solvents with residual solvent signals were used as internal standards and NMR spectra were recorded using a Mercury 300 MHz spectrometer.

3.4.2. Organic Synthesis

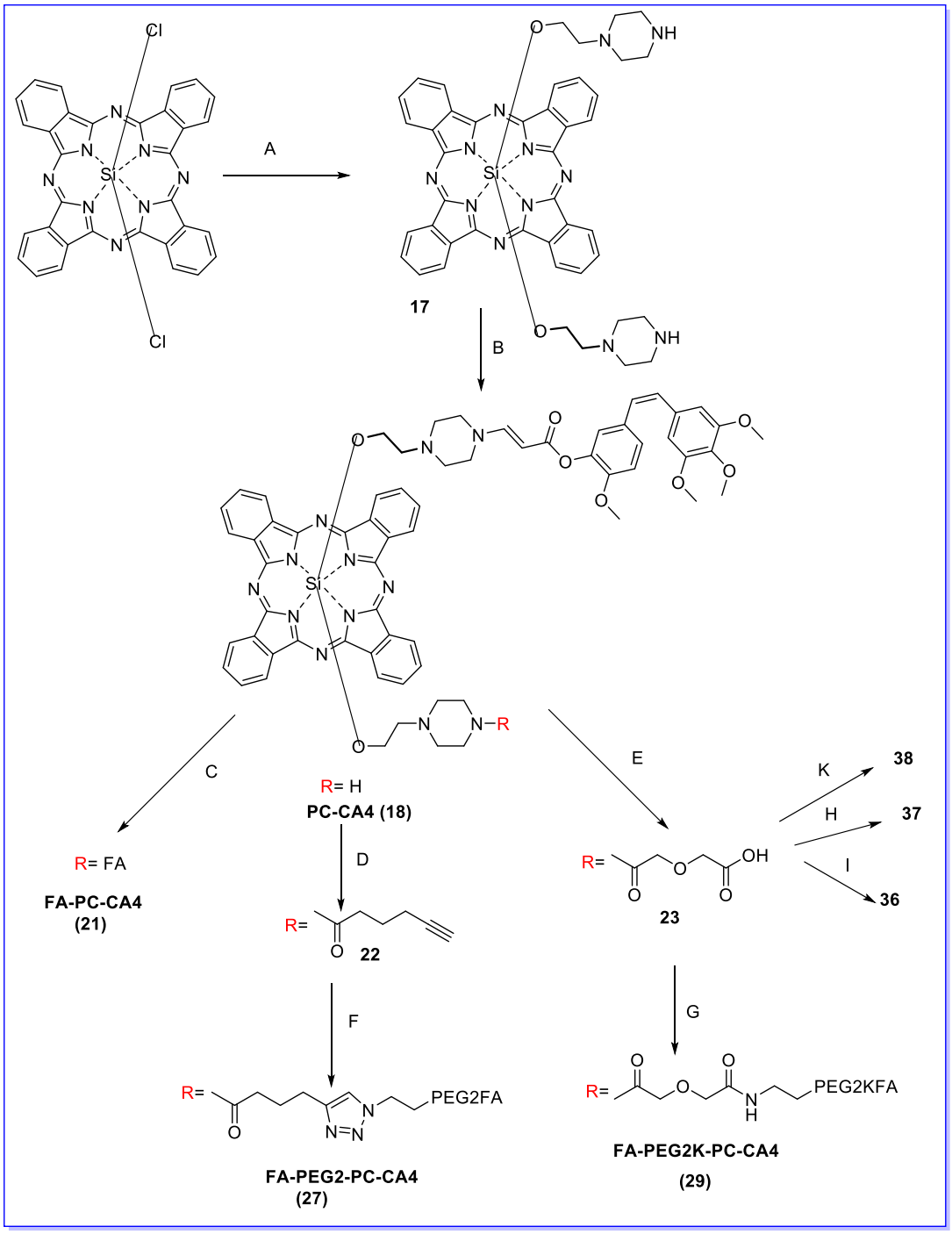
Cl
Si
A
17
B
C
R= H
PC-CA4 (18)
D
E
R= FA
FA-PC-CA4
(21)
R=
22
F
PEG2FA
FA-PEG2-PC-CA4
(27)
23
K
38
H
37
I
36
G
PEG2KFA
FA-PEG2K-PC-CA4
(29)

Scheme 4. General synthetic scheme for the conjugates. A) Silicon phthalocyanine dichloride (1), (1.15 mmol), *1*-(*2*- Hydroxyethyl)piperazine (10.30 mmol), Reflux, Toluene/Pyridine (70 mL/1.75 mL) overnight, 80% yield. B) **17** (0.47 mmol), **16** (0.47 mmol), in THF (150 mL) at rt for 1 h, 60% yield. C) i) **19** (0.034 mmol) DCC (0.21 mmol) DMF/Pyridine (5:1 v/v), Sonicate, 30 min, ii) add **18** (0.034 mmol) at rt, 24 h, iii) precipitate, Et_2O/Acetone (3:1 v/v), iv) Dialysis, 48 h, 60% yield. D) **18** (0.086 mmol), *5*-Hexynoic acid (0.17 mmol), HBTU (0.17 mmol), DIPEA (0.34 mmol), DCM (4 mL) at rt, 1 h, 80% yield. E) **18** (0.072 mmol), Digycolic anhydride (0.072 mmol) at rt, DMF (6 mL), 36 h, 70% yield. F) i) **22** (0.033 mmol), $N_3CH_2CH_2$PEG2FA (**26**) (0.033 mmol), CuBr (0.033 mmol), PMDETA (0.033 mmol) at 37 ^oC, DMF (2 mL), 48 h, ii) Dialysis, 72 h, 60% yield. G) **23** (0.033 mmol), $NH_2CH_2CH_2$PEG2KFA (**28**) (0.033 mmol), HBTU (0.050 mmol), DIPEA (0.099 mmol) at rt DMF (4 mL) overnight, 70%.

3.4.2.1. Synthesis of compound 17

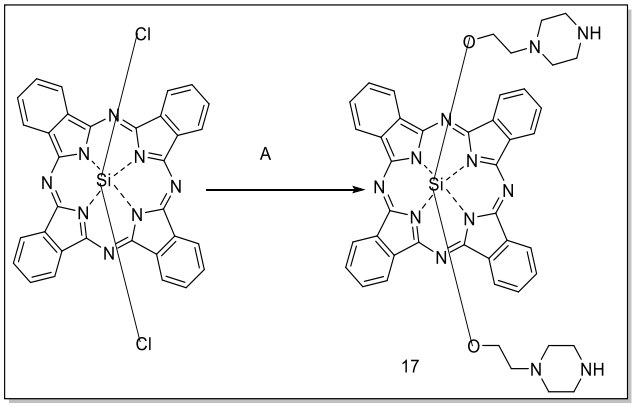

Scheme 5. Synthesis of compound **17:** A) 9 eq *1*-(*2*-Hydroxyethyl)piperazine , toluene/pyridine (5:1 v/v), reflux 8 h

A mixture of silicon (IV) Phthalocyanine dichloride (0.7 g, 1.15 mmol), *1-(2*-Hydroxyethyl) piperazine (1.34 g, 10.30 mmol), and pyridine (1.75 mL) in toluene (70 mL) was refluxed overnight. After evaporation of the solvent at reduced pressure using the rotavap, the residue was then dissolved in DCM (300 mL) and then washed with water (400 mL x 4). The organic layer was collected and evaporated to dryness and the crude product recrystallized from DCM/ Hexane (1:9 v/v) to give a deep solid product (0.74 g, 80% yield).[243]

^{1}H-NMR (300 MHz, CD_2Cl_2): -1.19 (t, *J* = 5.8 Hz, 4H), -0.82 (t, *J* = 5.8 Hz, 4H), 0.29 (m, 8H), 1.75 (m, 8H), 8.30 - 8.40 (m, 8H, Pc-H), 9.55-9.69 (m, 8H, Pc-H), MS-ESI (m/z): Calculated for $C_{46}H_{49}N_{12}O_2Si$ $[M+H]^+$ 828.38 Found: 828.37

3.4.2.2. Synthesis of PC-CA4 (18)

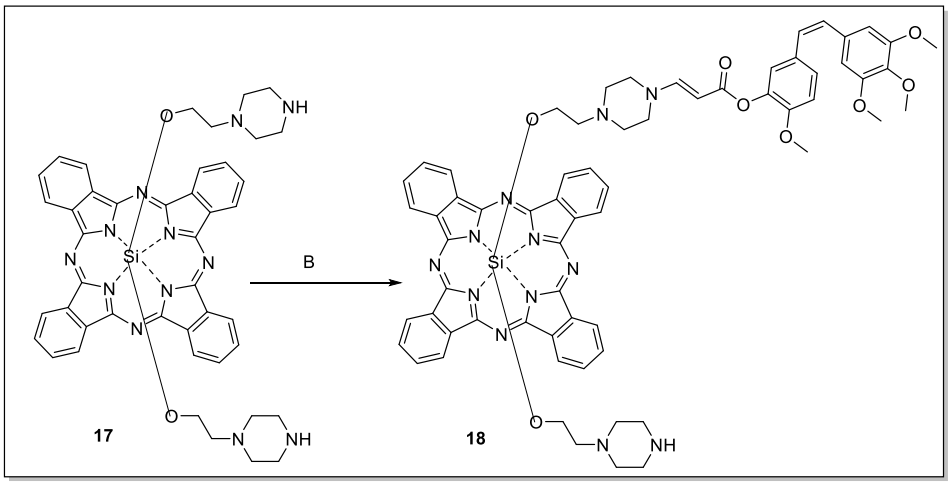

Scheme 6. Synthesis of compound **18:** B) **17** (0.47 mmol), **16** (0.47 mmol), in THF (150 mL) at rt, 1 h, 60% yield.

To a 150 mL dry THF solution in a round-bottom flask equipped with a magnetic stirring bar was added **17** (0.38 g, 0.47 mmol). The solution was purged and maintained for 10 min in N_2 atmosphere. CA-alkyne (**16**) (0.17 g, 0.47 mmol) dissolved in 30 mL dry THF was then added drop-wise into a vigorously stirring solution of **17** for over 1.5 h and then allowed to stir for further 15 min. The reaction mixture was then evaporated under reduced pressure and the crude product was purified using either the preparative TLC or a short column chromatography first using the solvent system ethylacetate/methanol (4:1 v/v) to remove the di-substituted product, followed by DCM/MeOH/NH_4OH (79:17: 4 % v/v/v) to afford the target compound **18** as a blue solid (0.32 g, 60%). This compound then served as an intermediate for all the conjugates.[244]

^{1}H-NMR (300 MHz, CD_2Cl_2-d_2): 9.67 (br s, m, 8H), 8.38 (br s, 8H), 7.19 (d, *J* = 11.9 Hz, 1H), 7.00 (m, 2H), 6.85 (d, *J* = 11.9 Hz, 1H), 6.52 (s, 2H), 6.46 (m, 2H), 4.35 (d, *J* = 12.99 Hz, 1H) 3.76 (s, 3H, OMe), 3.70 (s, 3H, OMe), 3.65 (s, 6H, OMe), 2,19 (br s, 8H), 1.65 (br s, 1H, NH), 0.29 (br s, 8H), -0.37 (m, 4H), -1.94 (m, 4H). HRMS-ESI: Calcd for $C_{84}H_{79}N_{19}O_{13}Si$: m/z 1166.4583; $[M+H]^+$, 1167.4661, $[M+Na]^+$, 1189.4481. Found: $[M+H]^+$, 1167.4665, $[M+Na]^+$,1189.4479.

3.4.2.3. Synthesis of FA-PC-CA4 (21)

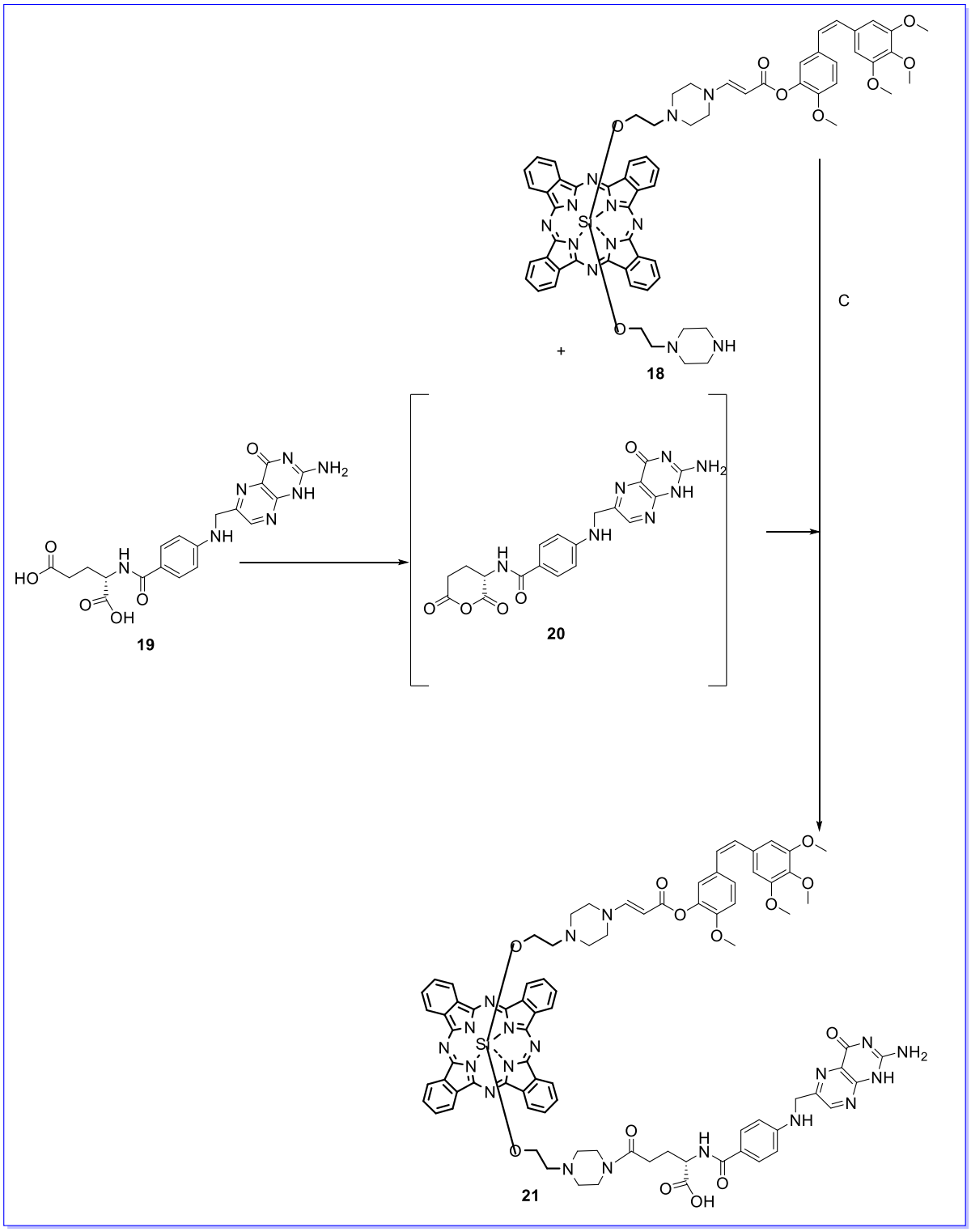

Scheme 7. Synthesis of compound **21:** C) i) **19** (0.034 mmol) DCC (0.21 mmol) DMF/Pyridine (5:1 v/v), Sonicate, 30 min, ii) add **18** (0.034 mmol) at rt, 24 h, iii) precipitate, Et_2O/Acetone (4:1 v/v), iv) Dialysis, 48 h, 60%.

To a stirring solution of folic acid (0.015 g, 0.034 mmol) in anhydrous DMF/pyridine (5:1 v/v) solution, DCC (0.043 g, 0.21 mmol) was added in one portion. The reaction mixture was kept in an ultrasound bath in the dark for 30 min. Then the resulting suspension was quickly filtered over a sintered funnel and the precipitate was washed with minimum amount of DMF/pyridine solution.[245] Solution of **18** (0.040 g, 0.034 mmol) was added into the filtrate. The resulting mixture was further stirred at room temperature in the dark for 24 h. The crude reaction mixture was then purified either by passed through gel permeation G-15 Sephadex column, using DMF as the eluent to separate the product from the unreacted folic acid starting material. The top stop was then collected and poured drop-wise into a stirred solution of cold Et_2O/ acetone (4:1 v/v) to afford a green precipitate that was collected over a sintered glass funnel. An alternative method wash by simply precipitating in cold Et_2O/ acetone (4:1 v/v) then followed by dialysis in DMF with cellulose membrane of MWCO of 1000 Da for 48 h. After washing several times with cold acetone and Et_2O the material was dried to give a deep blue solid product (33.5 mg, 60%) with more than 90% purity. See SI for the HPLC chromatogram.

^{1}H-NMR (300 MHz, DMSO-d_6): 9.67 (br s, 9H), 8.65 (s, 1H), 8.49 (m, 8H), 7.64 (d, J = 7.75 Hz, 2H), 7.11-6.90 (m, 5H), 6.67 (d, J = 8.0 Hz, 2H), 6.55 (br s, 2H),

6.48 (m, 2H), 4.49 (br s, 2H), 4.30 (d, *J* = 11.43 Hz), 4.17 (m, 1H), 3.71 (s, OCH_3, 3H), 3.61 (s, $3OCH_3$, 9H), 2.35 (m, 2H), 2.20 (br s, 8H), 1.21 (br s 2H), 0.22-0.12(0.18) (m, 8H), -0.7 (m, 4H). ^{13}C-NMR (75 MHz, DMSO-d_6): 166.64, 152.98, 152.98, 151.33, 149.25, 140.37, 135.42, 132.57, 132.41, 129.02, 124.03, 112.86, 106.39, 60.48, 56.11, 56.06, 31.16. MS-ESI: Calcd for $C_{84}H_{79}N_{19}O_{13}Si$: m/z 1589.59; $[M+H]^+$, 1590.60; $[M+H]^{+2}$, 795.30. Found: $[M+H]^+$, 1590.59; $[M+H]^{+2}$, 795.30

3.4.2.4. Synthesis of 22

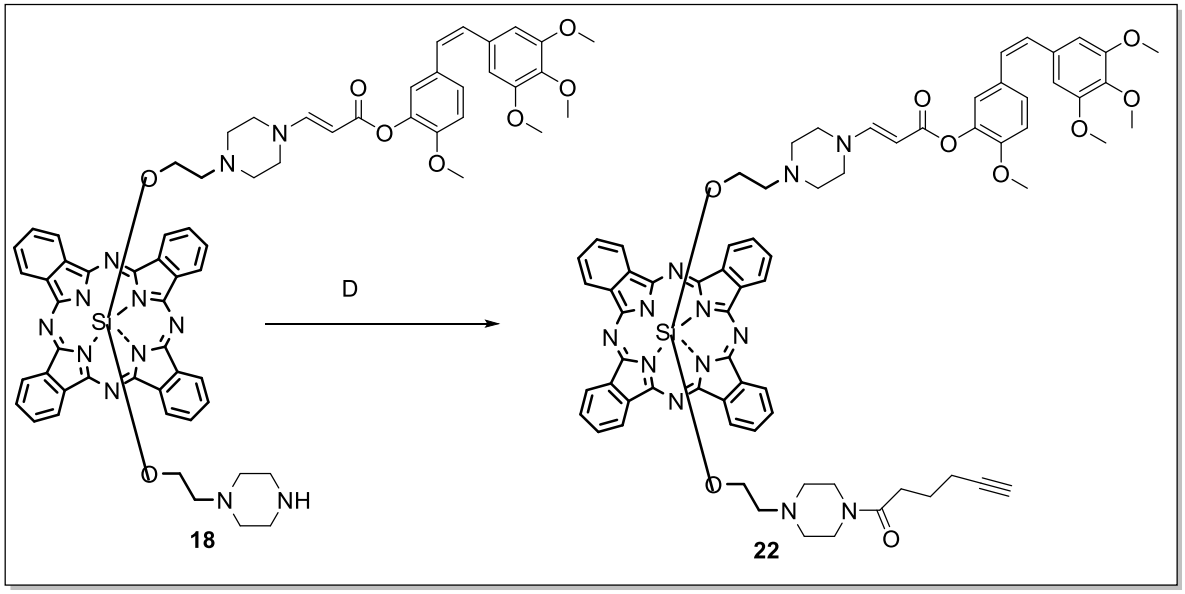

Scheme 8. Synthesis of compound **22: 18** (0.085 mmol), 5-Hexynoic acid (0.17 mmol), DIEA (0.34 mmol), HBTU (0.17 mmol), DCM (5 mL) at rt, 2h, 80 %.

To a 5 mL dry DCM stirring solution of **18** (0.10 g, 0.085 mmol), was added *5*-hexynoic acid (0.019 g, 0.17 mmol) and *N,N*-diisopropylethylamine (DIEA) (56.6 µL, 0.044 g, 0.34 mmol) and *O*-(benzotriazol-yl)-*N,N,N',N'*-tetramethyluronium hexafluorophosphate (HBTU) (0.065 g, 0.17 mmol). The reaction mixture was left for 2 h at room temperature and monitored using the TLC. At the end of the reaction, the reaction mixture was diluted with 60 mL of DCM and washed with water (200 ml x 3 times). The organic filtrate was then dried using anhydrous sodium sulfate (Na_2SO_4) and evaporated to dryness *in vacuo*. The crude was re-dissolved in minimum DCM, and the recrystallized using a mixture of cold hexane/ Et_2O. The solid residue was washed several times with diethyl ether to afford a deep blue solid product (87 mg, 80%).

^{1}H-NMR (300 MHz, CD_2Cl_2-d_2): 9.67 (br s, m, 8H), 8.38 (br s, 8H), 7.19 (d, *J* = 11.9 Hz, 1H), 7.00 (m, 2H), 6.85 (d, *J* = 11.9 Hz, 1H), 6.52 (s, 2H), 6.46 (m, 2H), 4.35 (d, *J* = 12.99 Hz, 1H) 3.76 (s, 3H, OMe), 3.70 (s, 3H, OMe), 3.65 (s, 6H, OMe), 2.51 (s, 1H) 2,19 (br s, 8H), 1.95(m, 2H), 1.56 (m, 4H), 0.29 (br s, 8H), -0.37 (m, 4H), -1.94 (m, 4H). HRMS-ESI: Calcd for: $C_{71}H_{68}N_{12}O_9Si$ m/z 1260.5001; $[M+Na]^+$,1283.4899; Found $[M+Na]^+$,1283.4879.

3.4.2.5. Synthesis of 23

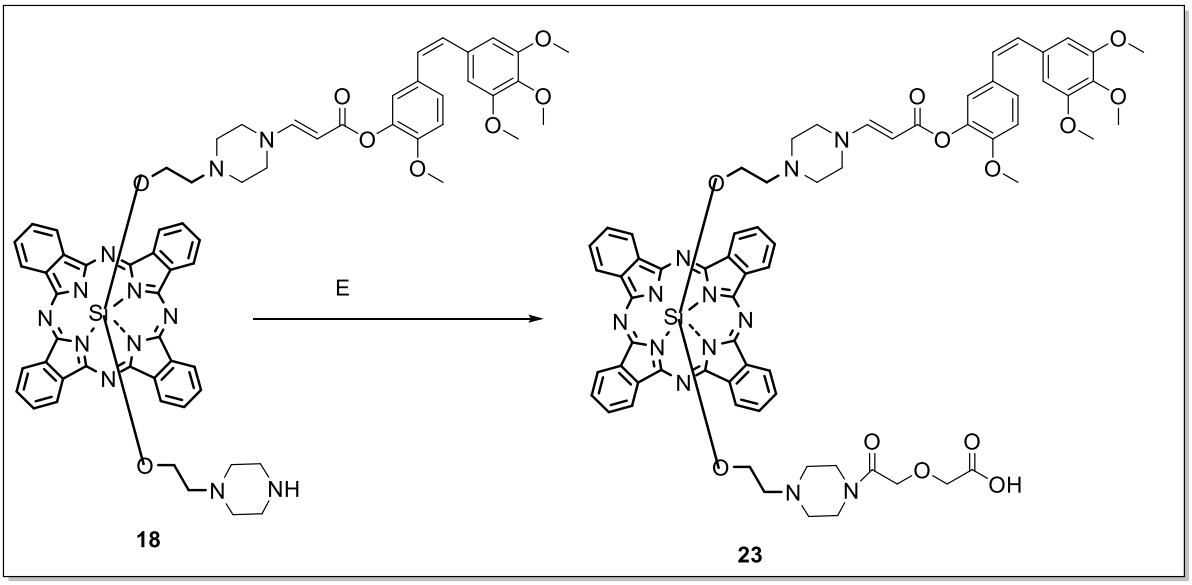

Scheme 9. Synthesis of compound **23:** E) **18** (0.072 mmol), Digycolic anhydride (0.072 mmol) at rt, DMF (6 mL), 36 h, 70%.

To a 6 mL anhydrous DMF in 10 mL round bottomed flask equipped with magnetic stir bar was added **18** (0.084 g, 0.072 mmol), and diglycolic anhydride (0.0084 g, 0.072 mmol) at room temperature and allowed to run for 36 h. The reaction mixture was poured drop-wise into cold Et_2O and the blue precipitate was filtered using a sintered glass funnel. This was further washed with more diethyl ether solvent to obtain a blue solid (64 mg, 70 %).

^{1}H-NMR (300 MHz, CD_2Cl_2): 9.67 (br s, m, 8H), 8.38 (br s, 8H), 7.19 (d, *J* = 11.9 Hz, 1H), 7.00 (m, 2H), 6.85 (d, *J* = 11.9 Hz, 1H), 6.52 (s, 2H), 6.46 (m, 2H), 4.35 (d, *J* = 12.99 Hz, 1H), 3.98 (s, 2H), 3.91 (s, 2H) 3.76 (s, 3H, OMe), 3.70 (s, 3H, OMe), 3.65 (s, 6H, OMe), 2,19 (br s, 8H), 1.65, 0.29 (br s, 8H), -0.37 (m, 4H), -

1.94 (m, 4H). HRMS-ESI: Calcd for $C_{69}H_{67}N_{12}O_{12}Si$, m/z 1282.4692; $[M+H]^+$, 1283.48. Found $[M+H]^+$ 1283.4761.

3.4.2.6. Synthesis of FA-PEG2-PC-CA4 (27)

Folate-PEG2-N_3 **[$N_3CH_2CH_2$PEG2FA, (26)]** (0.020 g, 0.033 mmol) and **22** (0.042 g, 0.033 mmol) were dissolved in 1.5 mL anhydrous DMF. After purging with nitrogen gas at room temperature, *N,N,N′,N″,N‴*-pentamethyldiethylenetriamine (PMDETA) (0.0058 g, 0.033 mmol, 7 µL) and CuBr (0.0048g, 0.033 mmol) were added and the solution stirred at 37 ^oC for 48 h. The reaction was stopped by opening to air and mixture diluted with DMF. It was then washed with water to eliminate copper and the crude extensively dialyzed against DMSO for 72 h (cutoff MW 1000) and then precipitated using cold Et_2O / acetone mixture (4:1 v/v) to afford **27** as green precipitate, 60%.

HRMS-ESI: Calcd for $[C_{96}H_{120}N_{123}O_{16}SiNa]^{+2}$; $[M+H_2O+Na+H]^{+2}$, 951.45 (100 %); 951.95 (40 %). Found $[M+H_2O+Na+H]^{+2}$, 951.4401(100 %), 951.9423 (40 %)

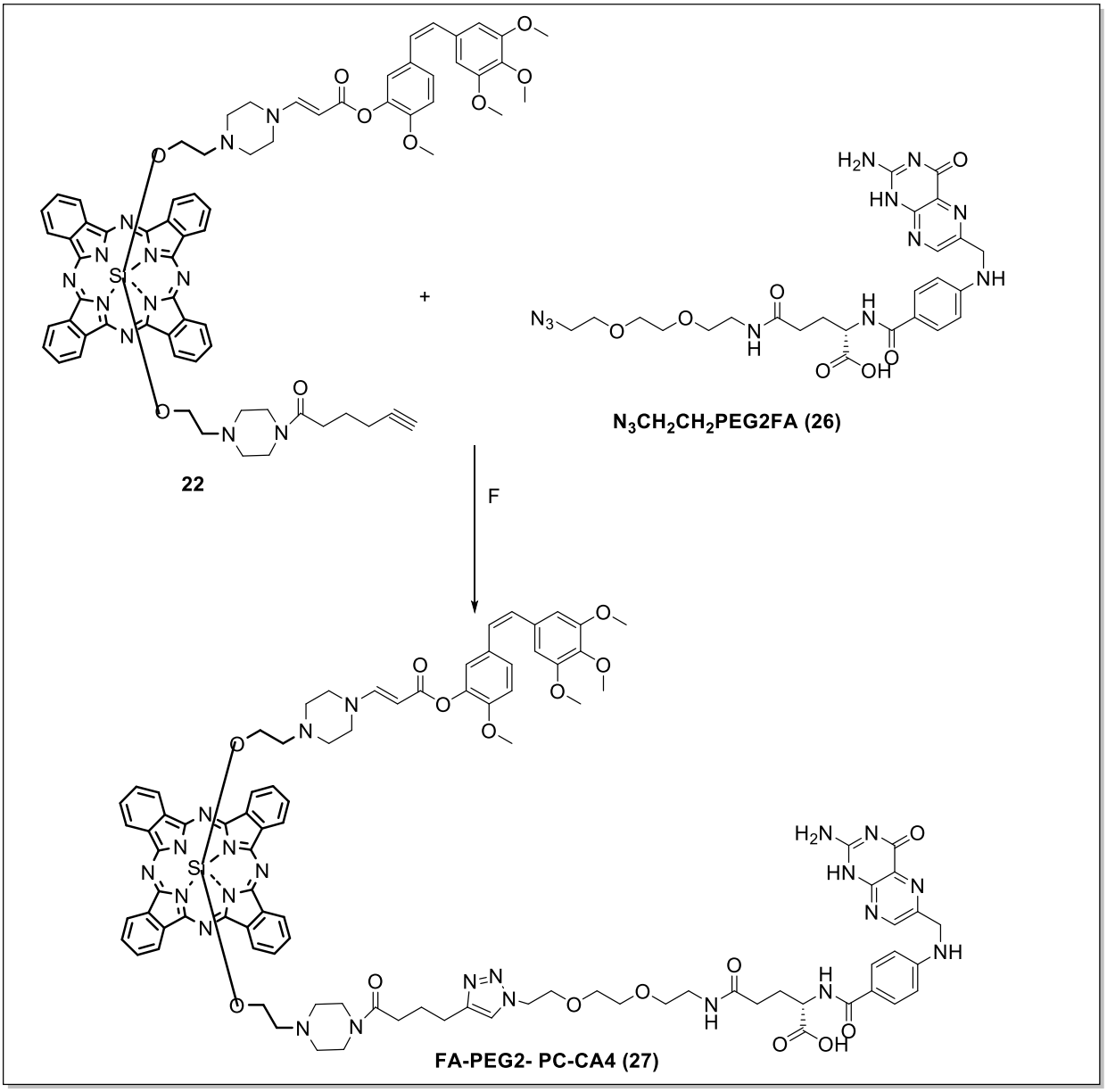

Scheme 10. Synthesis of compound **27. 22** (0.033 mmol), $N_3CH_2CH_2PEG2FA$ (**26**) (0.033 mmol), CuBr (0.033 mmol), PMDETA (0.033 mmol) at 37 ^oC, DMF (2 mL), 48 h, ii) Dialysis, 72 h, 60%.

3.4.2.7. Synthesis of $N_3CH_2CH_2PEG2$-FA (26)

Following the same method described for the synthesis of compound **21 (PC-CA4),** compound **25** (217 mg, 1.25 mmol), FA (**19**) (500 mg, 1.13 mmol), DCC (1440 mg, 6.99 mmol) and 48 mL toluene/pyridine (5:1 v/v) were employed to obtain compound **26** as yellow solid (450 mg, 65 %).[245]

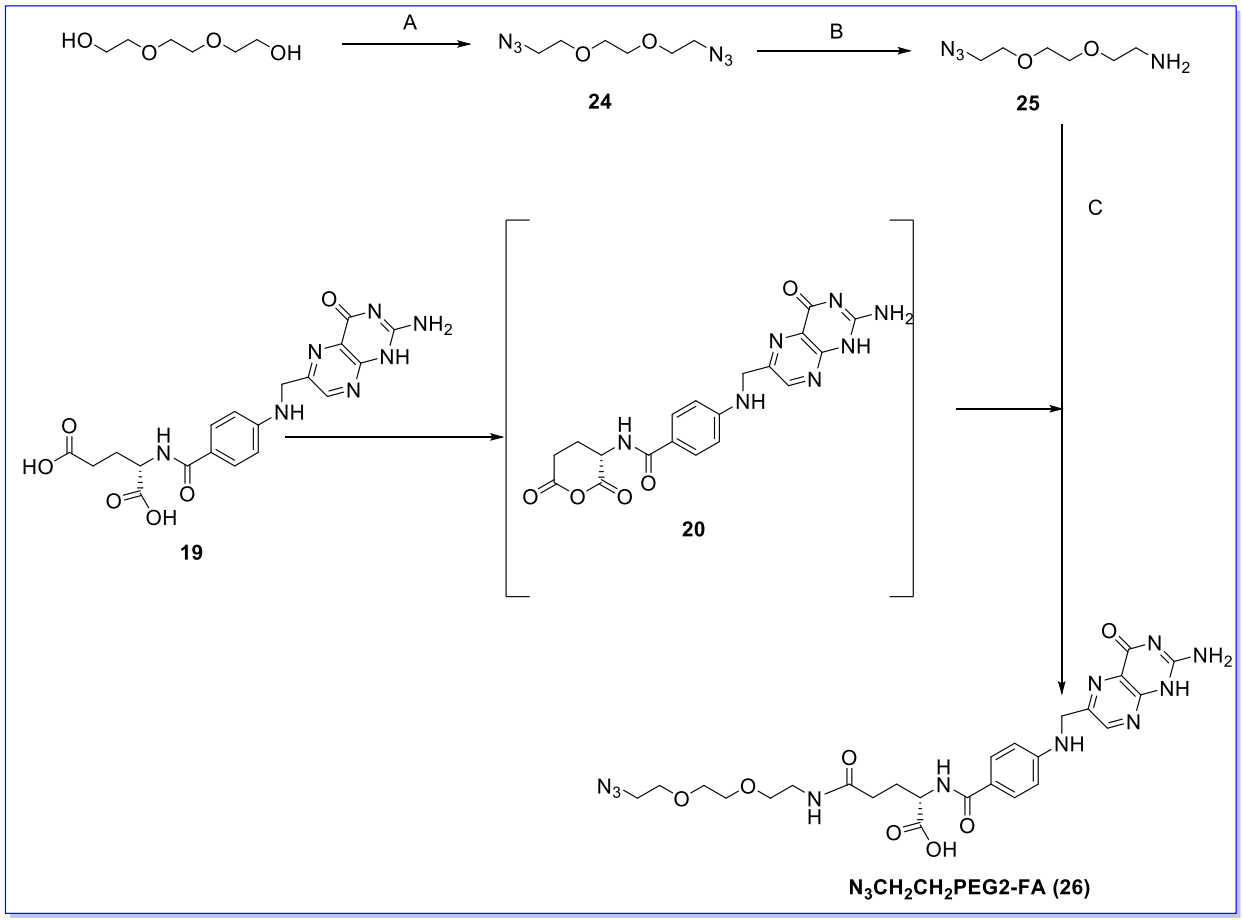

Scheme 11. Synthesis of compound **28.** A) Triethylene glycol (25.7 mmol), methanesulfonyl chloride (51.50 mmol) TEA (51.50 mmol) in 10 mL THF reflux at 120 ^{o}C. B) **24** (15.40 mmol), 0.65M H_3PO_4 (40 mL), PPh_3 (15.20 mmol, 30 mL), C) i) **19** (0.034 mmol) DCC (0.21 mmol) DMF/pyridine (5:1 v/v), sonicate, 30 min, ii) add

25 (0.034 mmol) at rt, 24 h, iii) precipitate, Et_2O/Acetone (4:1 v/v), iv) Dialysis, 48 h, 60%.

3.4.2.8. Synthesis of compound 24

To 40 mL of dry THF under N_2 was added triethylene glycol (3859.37 mg, 24.7 mmol). methanesulfonyl chloride (4.01 mL, 51.50 mmol) was added by syringe, and the solution was stirred in an ice bath as TEA (7.24 mL, 51.50 mmol) in 10 mL of THF was added for 30 min. The ice bath was removed after 1 h of stirring, and the mixture stirred for an additional 5 h with occasional swirling. The yellow-white precipitate was dissolved by addition of H_2O (24.40 mL), and the resulting two phases were chilled on a cold water bath. $NaHCO_3$ (2.50 g, to pH 8) was added followed by NaN_3 (3.35 g, 51.50 mmol), and stirring was commenced. Then, THF was removed by distillation, and the solution was refluxed for 48 h at a temperature of 120 ^oC. The aqueous layer was extracted five times with 20 mL aliquots of Et_2O, with each layer of Et_2O back-extracted with the same 20 mL aliquot of brine (saturated NaCl). The organic layers were then combined, dried over anhydrous Na_2SO_4 and filtered. Concentration of the organic layers by rotary evaporation yielded **24** as a yellow oil (4.40 g, 80 %) .[246]

^{1}H-NMR (300 MHz, $CDCl_3$): 3.61 (m, 8H), 3.32 (m, 4H). MS-ESI: Calcd for $C_6H_{12}N_6O_2$: m/z 200.10; $[M+H]^+$, 201.11. Found; $[M+H]^+$, 201.12

3.4.2.9. Synthesis of compound 25

Aqueous H_3PO_4 (40 mL of 0.65 M) was added to the diazide **24** (2894.53 mg, 15.4 mmol) and the solution was brought to stirring with PPh_3 (3390 mg, 15.20 mmol) in 30 mL of Et_2O was added drop-wise over 1 h. The addition funnel was then rinsed with 10 mL of ether, and the solution was placed under N_2 and stirred for 24 h. The aqueous layer was separated and washed with 4 x 30 mL of Et_2O and 3.20 g of KOH was added. The mixture was cooled to 4 ^oC after removal of traces of ether by evaporation. After 16 h, the PPh_3 was removed by filtration followed by addition of 9.20 g of KOH (to 4.0 M). The aqueous solution was then extracted several times with 20 mL aliquots of DCM, which were then dried over anhydrous Na_2SO_4, filtered and concentrated under reduced pressure to afford **25** as a brownish oil (1.07 g, 70 %) .[246]

^{1}H-NMR (300 MHz, $CDCl_3$): 3.63 (m, 6H), 3.51 (m, 2H), 3.32 (m, 2H), 2.83 (m, 2H), 2.0 (br s 2H, NH_2). MS-ESI: Calcd for $C_6H_{14}N_4O_2$: m/z 174.11; $[M+H]^+$, 175.12. Found; $[M+H]^+$, 175.12.

3.4.2.10. Synthesis of FA-PEG2K-PC-CA4 (29)

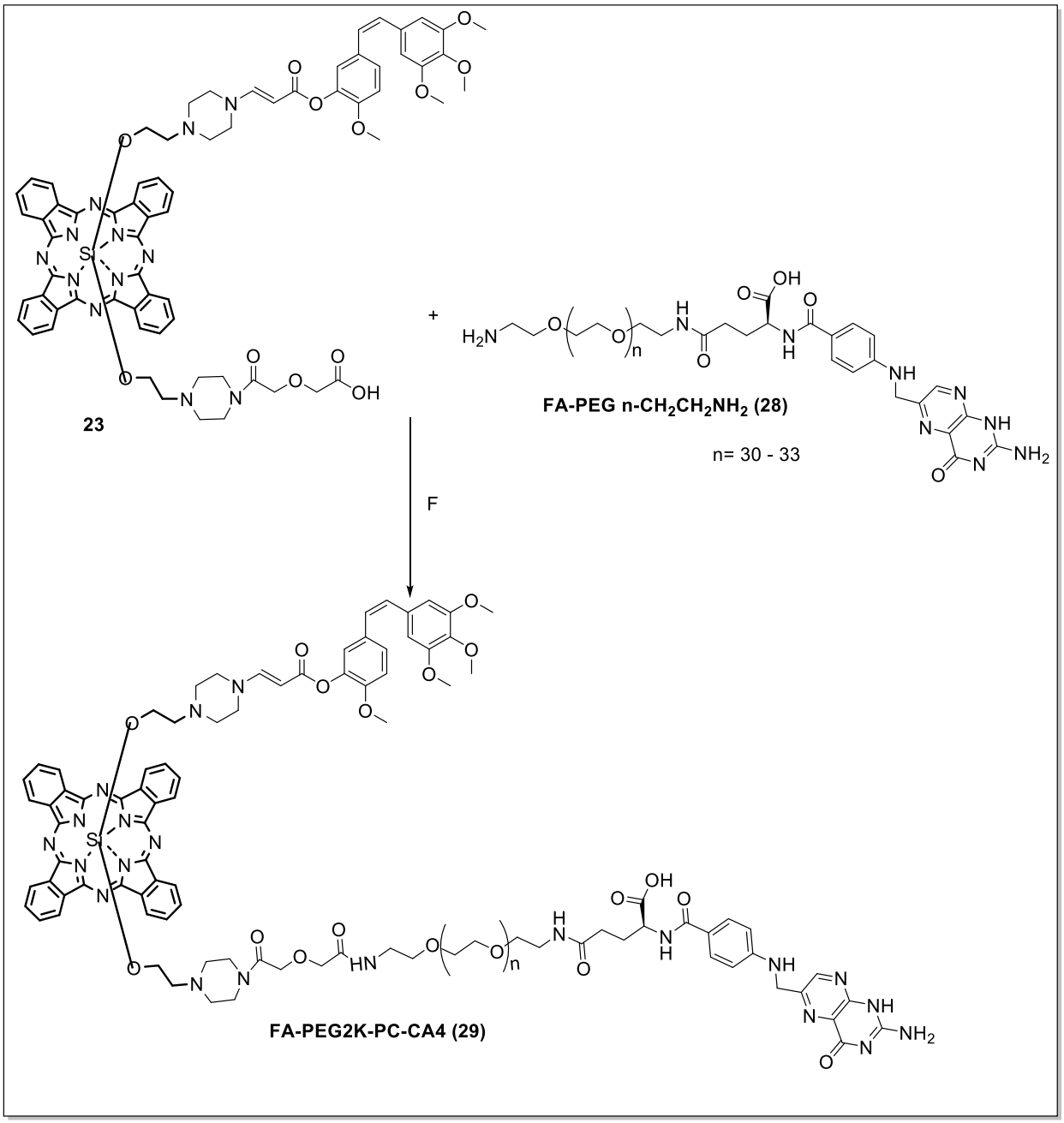

Scheme 12. Synthetic scheme for compound **29:** G) **23** (0.033 mmol), $NH_2CH_2CH_2$PEGnFA (**28**) (0.033 mmol), HBTU (0.050 mmol), DIEA (0.099 mmol) at rt, DMF (4mL), overnight, 70%.

To a 4 mL anhydrous DMF in a 10 mL round-bottom flask equipped with a magnetic stir bar was added FA-PEGn-$CH_2CH_2NH_2$ (**28**) (0.078 g, 0.033 mmol), **23** (0.044 g, 0.034 mmol), DIEA (0.099 mmol), and HBTU (0.019 g, 0.050 mmol) at room temperature and allowed to stir for 3 h. The crude reaction mixture was passed through a G-15 Sephadex column using DMF as the eluent. With the molecular weight of the final product greater than 1500 g/mol, the products passed through the void volume and were collected as the fast moving spot from the solvent front. The product was dialyzed for 48 h against DMF and subsequently DCM for 12 h to get rid of the DMF. (MWCO 1000 Da). The Product in DCM was concentrated *in vacuo* and precipitated into 71 mg sticky dark green solid product using cold Et_2O. ^{1}H-NMR (300 MHz, DMSO-d_6) (Figure 63): 9.67 (m, 9H, 1', 4', 20), 8.40 (m, 8H, 2',3'), 7.96 (br s, DMF peak), 7.69 (m, 1H), 7.41 (m, 2H, 14, 17), 7.10 d, *J* = 11.9 Hz, 1H, 5), 7.00 (m, 2H, 9, 7), 6.85 (m, 2H, 6, 13), 6.52 (br s, 4H, 15,16,1,2), 6.46 (m, 1H, 12), 4.35 (d, *J* = 12.99 Hz, 1H, 8), 4.24 (m, 1H, 12), 3.85 (br s, 2H, g, m), 3.78 (s, 4H, e, f), 3.73 (s, OMe, 3H), 3.68 (s, 3xOMe, 9H), 3.58 (br s, complex, j, t, h), 2.91 (s, DMF), 2.82 (s, DMF), 2.21 (m, 8H, c), 1,67 (br s, H_2O), 0.31 (m, 8H, d, d'), -0.58 (m, 4H, b), -1.90 (br s, 4H, a)

3.4.2.11. Synthesis of FA-PEG897-NH_2 (35) and Biotin-PEG897-NH_2 (36)

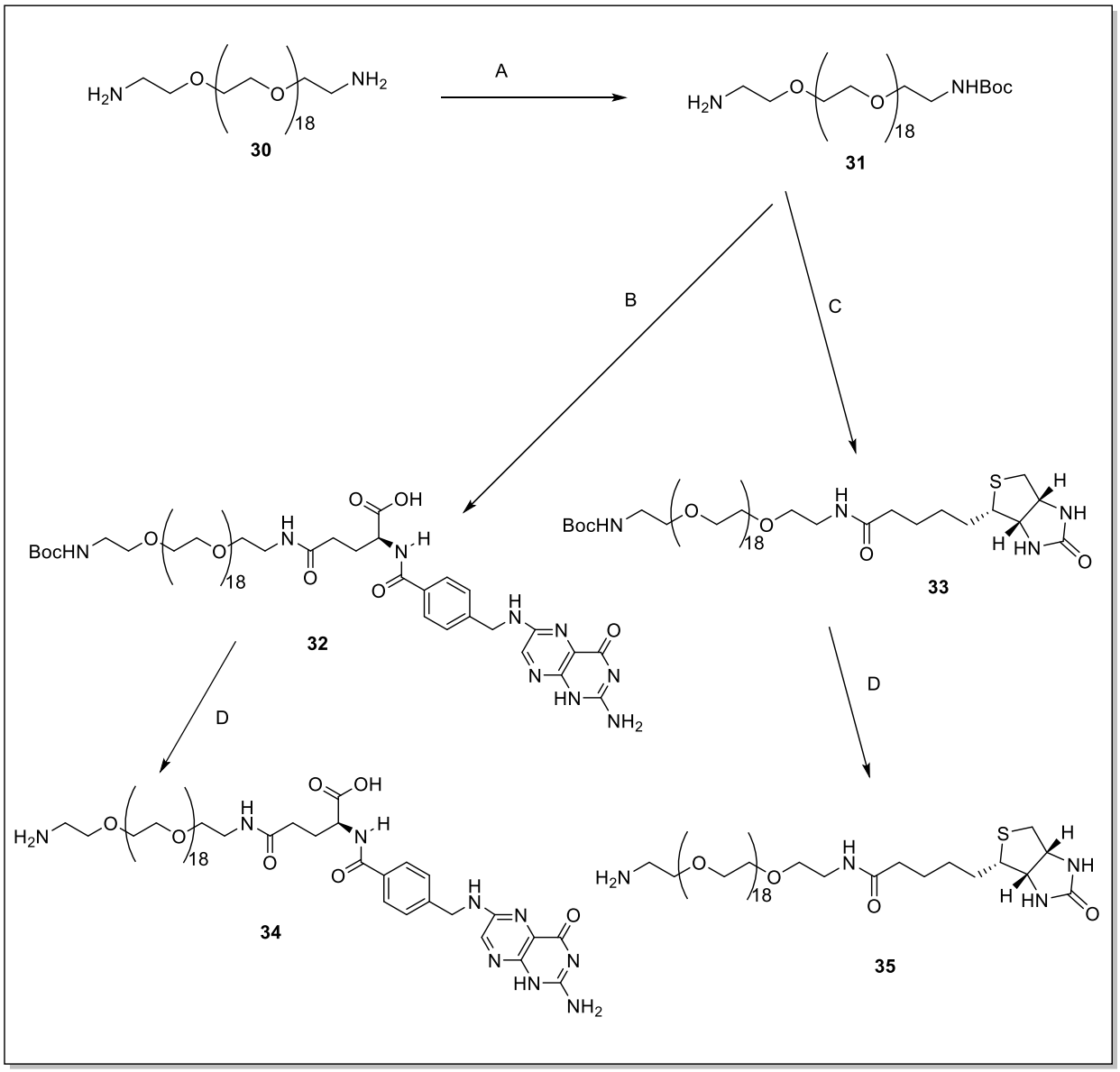

Scheme 13. Synthesis for compound **34** and **35.** A) **30** (0.56 mmol), Boc_2O (0.56 mmol) TEA (1.67 mmol), anhydrous MeOH (9.31 mL), reflux, 24 h. B) sonicated FA, (0.19 mmol) in DCC (1.13 mmol), 30 min, DMF/Pyridine (5:1 v/v), **31** (0.19 mmol) at rt, 36 h precipitate in Et_2O/Acetone (3:1 v/v). C) **31**(0.23 mmol), *D*-Biotin

(0.23 mmol), HBTU (0.23 mmol), DIEA (0.23 mmol), anhydrous DMF (4 mL) at rt , 3 h. D) TFA at rt, 4 h.

3.4.2.12. Synthesis of mono-protected diamine (31)

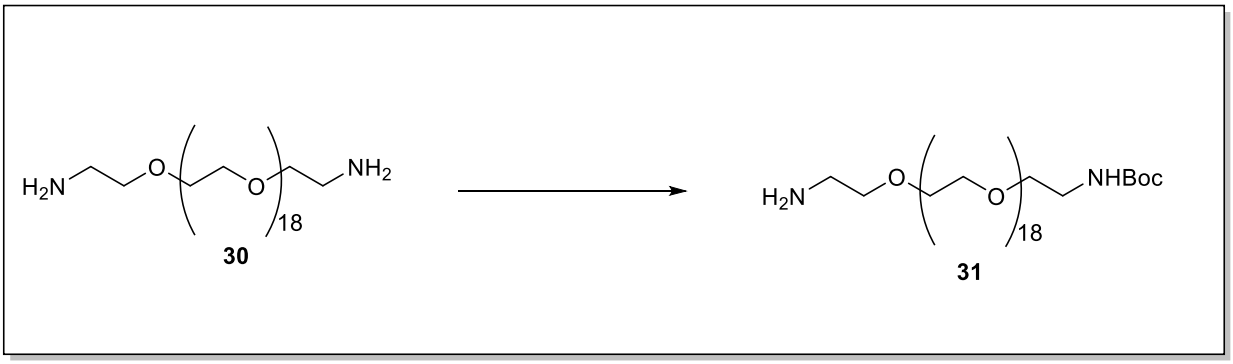

Scheme 14. Synthesis of compound **31:** **30** (0.56 mmol), Boc_2O (0.56 mmol), TEA (1.67 mmol), reflux, anhydrous MeOH (9.31 mL), 24 h, 75%.

A stirring solution of PEG-diamine (**30**) (500 mg, 0.56 mmol) in anhydrous MeOH (9.31 mL) was treated with Boc_2O (122.50 mg, 0.56 mmol) and TEA (177.60 µL, 1.67 mmol). The reaction mixture was left at reflux for 24 h. The solvent was removed under reduced pressure and the resulting yellow oil was purified by silica gel chromatography using DCM/MeOH/NH_4OH (79:17:4 % v/v/v) as the eluent to give **31** as a colorless/white solid after freezing (400 mg, 75 %). [245]

^{1}H-NMR (300 MHz, D_2O-d_2): 3.64 (br s, -CH_2- of PEG), 3.20 (m, 4H), 3.00 (m, 4H), 1.43 (s, 9H, *t*-butyl group). MS-ESI: Calcd for $C_{45}H_{92}N_2O_{21}$: m/z 996.62; $[M+H]^+$, 997.63. Found; $[M+H]^+$, 997.70.

3.4.2.13. Synthesis of Boc-PEG 897-FA (32).

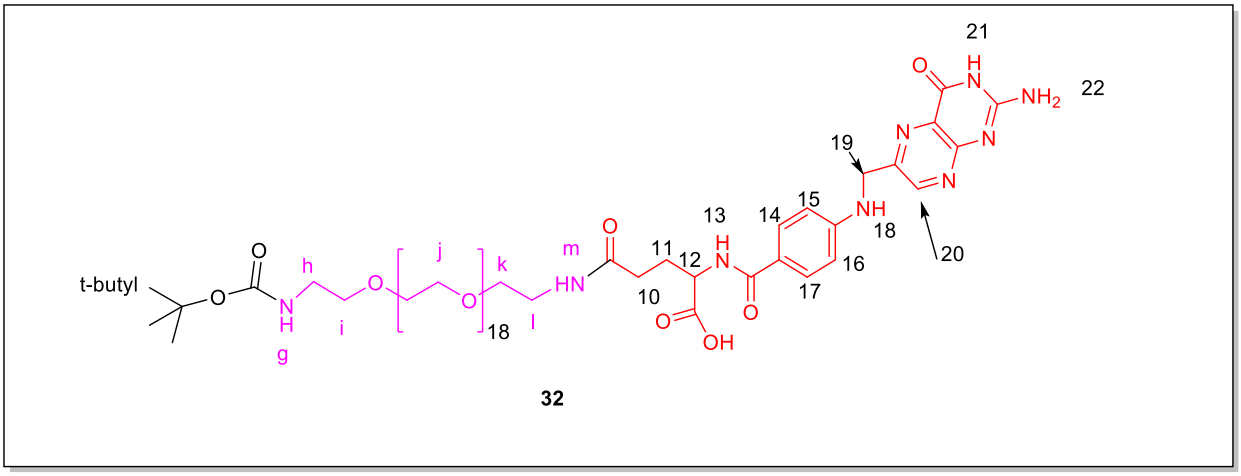

Figure 16. Structure of compound **32**

To a stirring solution of FA (0.083 g, 0.19 mmol) in anhydrous DMF/pyridine (5:1 v/v) solution, DCC (0.23 g, 1.13 mmol) was added in one portion. The reaction mixture was kept in an ultrasound bath in the dark for 30 min. Then the resulting suspension was quickly filtered over a sintered funnel and the precipitate was washed with minimum amount of DMF/pyridine solution. Mono-protected diamine **(31)** (180 mg, 0.19 mmol) was then added to the filtrate and allowed to stir in dark for 36 h. The reaction mixture was then poured drop-wise into a stirred

solution of cold Et_2O/ acetone (4:1 v/v) to afford a yellow precipitate that was collected on a sintered glass funnel. After washing several times with cold acetone and Et_2O the material was dried to give a deep yellow solid product which was further purified by passing over Sephadex G-15 using deionized water as a solvent to remove any unreacted folic acid (196 mg, 80 %).

^{1}H-NMR (300 MHz, D_2O-d_2) [Figure 82]: 8.60 (s, 1H, 20), 7.52 (br s, 2H, 15, 16), 6.62 (br s, 2H, 14, 17), 3.52 (br s, -CH_2- of PEG block), 1.27 (s, 9H, *t*-butyl group). MS-ESI: Calcd for $C_{64}H_{109}N_9O_{26}$: m/z 1419.75; $[M+H]^+$, 1420.76. Found; $[M+H]^+$, 1420.70, $[M+Na]^+$, 1442.70.

3.4.2.14. Synthesis of Boc-PEG 897-Biotin (33)

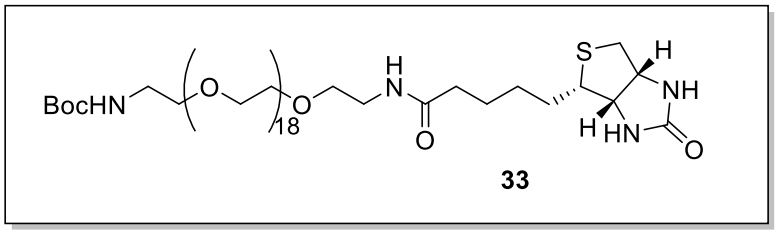

33

Figure 17. Structure of compound **33**

A mixture of *D*-(+)-Biotin, (54.88 mg, 0.23 mmol), compound **31,** (214.10 mg, 0.23 mmol), HBTU (85.22 mg, 0.23 mmol) and DIEA (37 µL, 0.45 mmol) in 3 mL DMF was stirred at rt for 2 h. The reaction mixture was concentrated *in vacuo*,

and the residue was purified by silica gel column chromatography using DCM /MeOH as eluent (9:1 v/v) to give a gray colored solid (84 %).

^{1}H-NMR (300 MHz, $CDCl_3$) [Figure 83]: 7.79 (d, *J* = 8 Hz, 1H), 7.60 (d, *J* = 8.2 Hz, 1H), 7.38- 7.25 (m, 1H), 7.00 (m, 1H), 4.46 (m, 1H) 4.30-4.20 (m, 1H), 3.59-3.49 (complex, PEG, H), 2.24 (m, 2H), 1.71-1.51 (m, 5H), 1.42 (br s, 9H). MS-ESI: Calcd for $C_{64}H_{109}N_9O_{26}$: m/z 1419.75; $[M+H]^+$, 1420.76. Found; $[M+H]^+$, 1420.70, $[M+Na]^+$, 1442.70

3.4.2.15. Synthesis of H_2N-PEG 897-FA (34) and H_2N-PEG 897-Biotin (35)

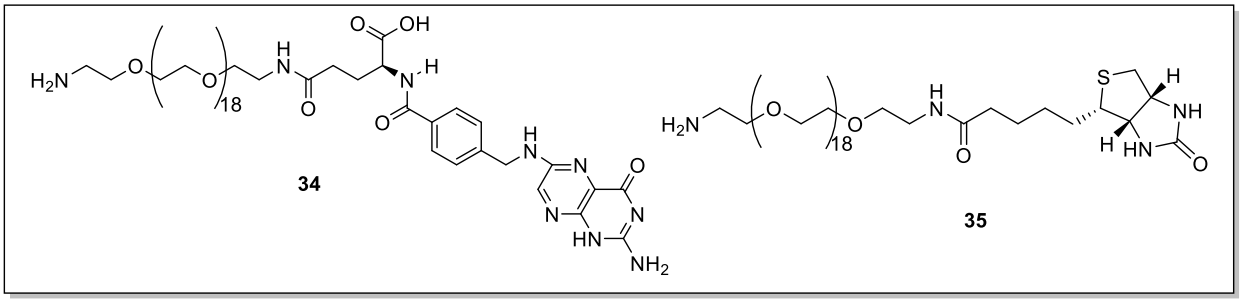

Figure 18. Structures of compound s **34** and **35**

Boc deprotection on both compound **32** and **33** were accomplished using TFA at room temperature and the deprotected products used for the next respective steps without further purification.

3.4.2.16. Synthesis of FA-PEG897-PC-CA4 (36)

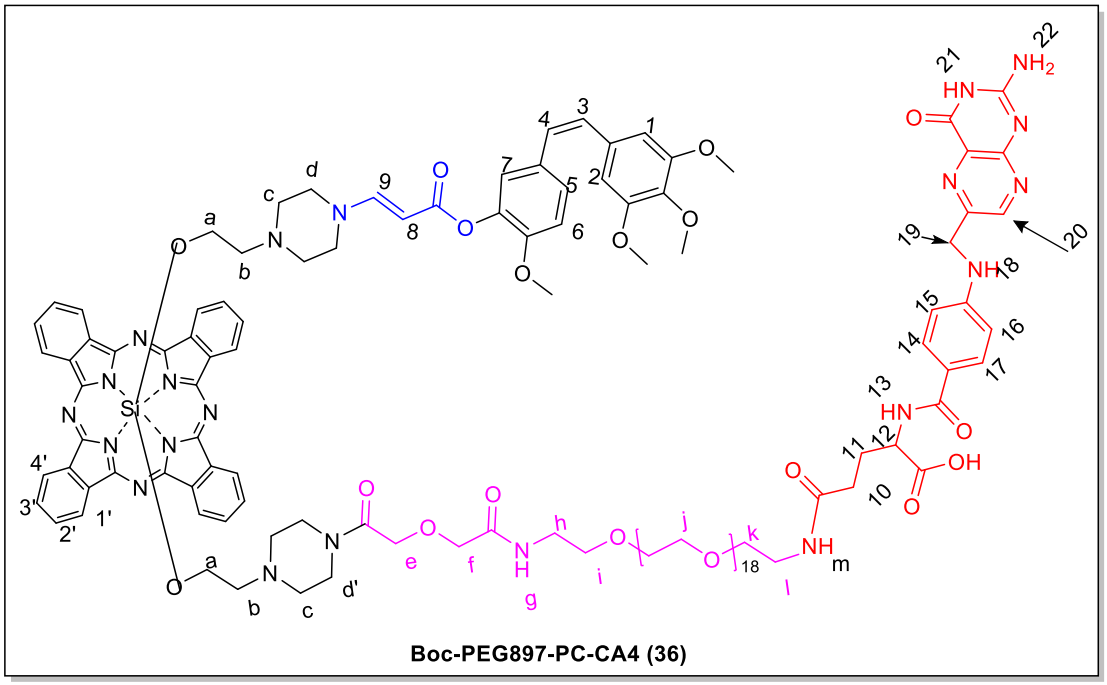

Figure 19. Structure of compound **36**

The procedure for this synthesis was similar to that of compound **29.** Compound **34** (0.082 g, 0.062 mmol), compound **23** (0.080 g, 0.062 mmol), HBTU (0.026 g, 0.069 mmol) and DIEA (22.80 µL, 0.14 mmol) in 4 mL anhydrous DMF afforded a dark green solid product after similar purification process (100.90 mg, 70 %).

^{1}H-NMR (300 MHz, CD_2Cl_2-d_2) [Figure 73]: 9.67 (m, 8H, 1', 4', 2), 8.40 (m, 8H, 2',3'), 7.69 (m, 1H), 7.41 (m, 2H, 14, 17), 7.10 d, *J* = 11.9 Hz, 1H, 5), 7.00 (m, 2H, 9, 7), 6.85 (m, 2H, 6,), 6.52 (br s, 2H, 15, 1,2), 12), 4.35 (d, *J* = 12.99 Hz, 1H, 8), 3.85 (br s, 2H, g, m), 3.78 (s, 4H, e, f), 3.73 (s, OMe, 3H), 3.68 (s, 3xOMe, 9H), 3.58 (br s, complex, j, t, h), 2.21 (m, 8H, c), 1,67 (br s, 9H, 10), 0.31 (m, 8H, d, d'), -0.58 (m, 4H, b), -1.90 (br s, 4H, a).

3.4.2.17. Synthesis of Biotin-PEG897-PC-CA4 (37)

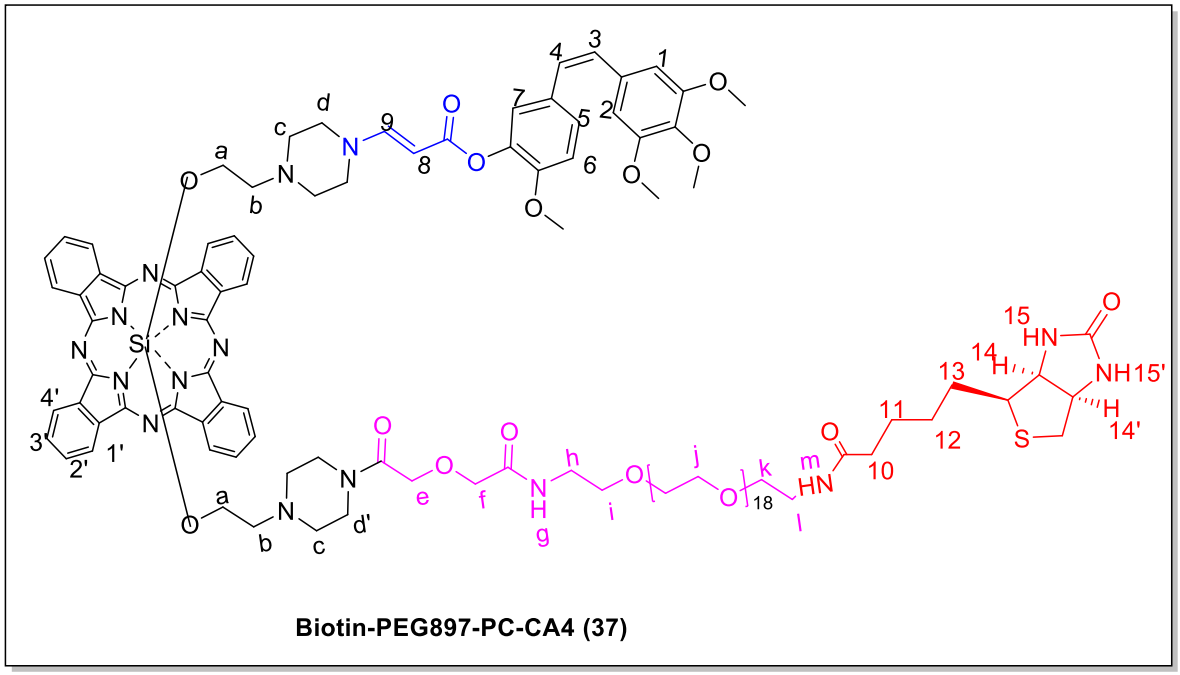

Figure 20. Structure of compound **37**

The procedure was similar to that of compound **29. H_2N-PEG 897-Biotin (35)** (48 mg, 0.043 mmol), compound **23** (55.42 mg, 0.043 mmol), HBTU (18.02 mg, 0.047 mmol) and DIEA (16 µL, 0.095 mmol) in 4 mL of anhydrous DMF stirring at room temperature for 4 h gave dark green solid (51.25 mg, 60 %).

^{1}H-NMR (300 MHz, CD_2Cl_2-d_2) [Figure 148]: 9.64 (m, 9H, 1', 4',), 8.38 (m, 8H, 2',3'), 7.69 (m, 1H), 7.41 (m, 2H, 14, 17), 7.09 (d, *J* = 11.9 Hz, 1H, 5), 6.94 (m, 2H, 9, 7), 6.83 (m, 1H, 6,), 6.50 (br s, 2H, 1,2), 6.43 (m, 2H, 3, 4), 4.44 (m, 1H, 14'), 4.34 (d, *J* = 12.99 Hz, 1H, 8), 4.25 (m, 1H, 14), 3.94 (br s, 2H, e), 3.85 (br s,

2H, f), 3.76 (s, 3H, OMe, 3H), 3.70 (s, OMe, 3H), 3.65 (s, 2 x OMe, 6H) 3.58 (br s, complex, j, t, h), 2.19 (m, 10H, c, 10), 1.59 (m, alkyl chain), 1.22 (from PEG chain), , 0..29 (m, 8H, d, d'), -0..37(m, 4H, b), -1.93(br s, 4H, a). MS-ESI: Calcd for $C_{119}H_{162}N_{16}O_{32}SSi$: m/z 2388.83; $[M+H]^+$, 2389.11. Found; $[M+H]^+$, 2389.20.

3.4.2.18. Synthesis of Boc-PEG897-PC-CA4 (38)

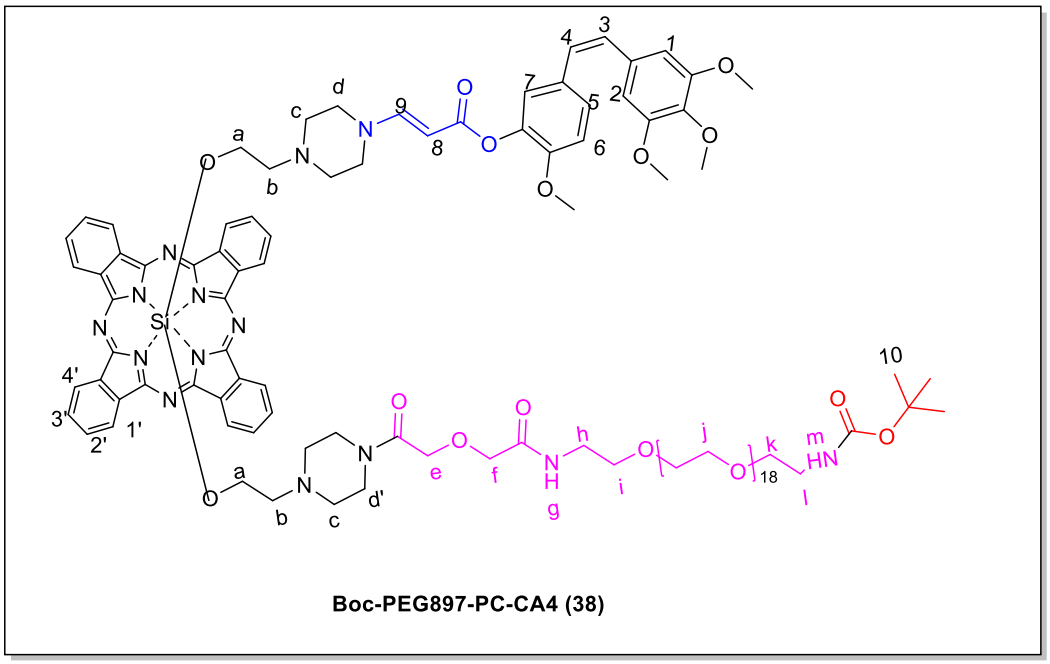

Figure 21. Structure of compound **38**

This compound was synthesized as a control following the same procedure described for compound **29.** Compound **23** (102 mg, 0.080 mmol), compound **31** (75.73 mg, 0.078 mmol), HBTU (33.18 mg, 0.088 mmol) and DIEA (28 µL, 0.18 mmol) in 4 mL anhydrous DMF gave a green solid (130 mg, 80 %).

^{1}H-NMR (300 MHz, CD_2Cl_2-d_2) [Figure 150]: 9.67 (m, 8H, 1', 4'), 8.40 (m, 8H, 2',3'), 7.69 (m, 1H), 7.10 (d, *J* = 11.9 Hz, 1H, 5), 7.00 (m, 2H, 9, 7), 6.85 (m, 1H, 6,), 6.52 (br s, 2H,1,2), , 4.35 (d, *J* = 12.99 Hz, 1H, 8), 4.24 (m, 1H, 12), 3.85 (br s, 2H, g, m), 3.78 (s, 4H, e, f), 3.73 (s, OMe, 3H), 3.68 (s, 3xOMe, 9H), 3.58 (br s, complex, j, t, h), 2.21 (m, 8H, c), 1.46 (br s, 9H, *t*-butyl), 0.31 (m, 8H, d, d'), -0.58 (m, 4H, b), -1.90 (br s, 4H, a). MS-ESI: Calcd for $C_{114}H_{156}N_{14}O_{32}$: m/z 2261.08; $[M+Na]^+$, 2284.07. Found; $[M+Na]^+$, 2284.02.

3.5. Photophysical studies

3.5.1. Aggregation tendencies

Aggregation tendency involves an association of solute molecules that does not involve covalent bonding to give assemblies of individual units in solutions.[247] Being a critical problem in PDT, photosensitizers readily aggregate in aqueous media producing species with lower quantum yields of singlet oxygen generation and thus lower photodynamic activities.[248] The energy absorbed by a photosensitizer upon irradiation is lost to other photosensitizer molecules in the aggregates by collisional quenching leading to reduced fluorescence and singlet oxygen generation. When the fluorescence of PS is monitored in an aqueous media compared to that in organic solvents, then the aggregation tendency in the biological media such as blood and cytosol can be estimated.[249]

To determine the aggregation tendency of the conjugates in aqueous media, the fluorescence emission was compared with that observed in organic solvents (where the samples exist in monomeric forms). All experiments were carried out in aqueous media; thus, a comparison of the decrease in fluorescence observed in media compared to that observed in DMSO was used to estimate the aggregation. Although the aggregation tendency of dyes generally increases with their concentrations, only one concentration was chosen to test the solubility in different solvents.

2 mM stock solutions of the respective conjugates were prepared in DMSO and diluted to 1 mL of 10 uM concentrations with the distilled water and DMSO respectively. The solutions were left 1 h after which the fluorescence readings were taken at 605 nm excitation and 640-800 nm emission wavelengths. The change in the fluorescence of the conjugates in water compared to that in DMSO was used as a measure of the aggregation tendencies which indirectly translates to their solubility.

3.6. *In vitro* studies

3.6.1. Dark Toxicity

In order to determine the cytotoxicity of the conjugates in the absence of light (dark toxicity), folated, biotinylated and non-targeted prodrugs were evaluated for cytotoxicity without illumination against the colon 26 cell line. A total 5-10 x 10^3 cells in 190 µL of the complete medium per well were plated in a 96-well plate, followed by incubation for 24 h at 37 ^oC in 5 % CO_2. 10 µL of respective dilute solutions of the conjugates (previously diluted from the 4 mM stock solution to the appropriate concentrations using complete media) was then added to 190 µL of complete media in each well to achieve final concentrations ranges (0.0001- 2 µM) and the well plates incubated for 24 h. Then the medium was removed and cell monolayers washed with ice-cold PBS (190 µL) three times. Clear medium, with neither phenol red nor bovine growth serum, was then added to the wells and the well plates were kept in the dark for 1 h. The clear medium was removed after this time and 190 µL of the complete medium was added. The plates were then incubated for 3 days at 37 ^oC in 5 % CO_2 after which the cell viability was determined by MTT assay. In brief, a volume of 10 µL of MTT at a concentration of 10 mg/mL was added to 190 µL of complete media in each well. After 4 h of incubation, MTT solutions were removed and formazan crystals formed were dissolved in 200 µL of DMSO and the absorbance was measured at 570 nm with background subtraction at 650 nm. The cell viability was then quantified by measuring the absorbance of the treated wells, compared to that of the untreated wells (controls). The controls in the assays involve tests done with cells not incubated with the conjugates.

The IC_{50} value for each was calculated using nonlinear regression curve in GraphPad Prism 5.03 software based on the Hill (sigmoid Emax) equation.[184,250]The logarithmic concentrations of the conjugates were plotted against the percentage viability of cells grown in the absence of conjugate prodrugs.

$$\% \text{ Cell Survival} = \frac{(A570nm - A650nm)Treated\ cells}{(A570nm - A650nm)control} X\ 100\%$$

3.6.2. Phototoxicity

In order to determine the cytotoxicities of the folated, biotinylated and non-targeted prodrugs upon light exposure (phototoxicity), colon 26 cells were seeded on a 96 well plates at densities of 5-10 x 10^3 cells/well. The same procedure and concentrations ranges were used as in the determination of the dark toxicity and after 24 h incubation; the medium was removed and rinsed twice with 0.9 % NaCl solution. Clear medium, without phenol red and bovine growth serum, was then added to the wells and well plates irradiated for 30 min. To ensure a uniform distribution or illumination of light, the well plate was placed on an orbital shaker (Lab-line, Barnstead International) and the well plate lid removed before exposing the wells for 30 min to a 5.6 mW/cm^2 from a 690 nm diode source and then gently orbiting the well plate over the entire 30 min. After the 30 min irradiation, the clear medium was then removed, and 190 µL of complete medium was added to the wells. The well plates were then incubated at

37 ^{o}C in 5 % CO_2 for 3 days after which the cytotoxicity was determine by MTT assay and expressed as a percentage of the controls to that of cells exposed to light and not treated with the conjugates.[184]

3.6.3. Cell Uptake Experiments

To determine the intracellular accumulations of the folated, biotinylated, PC-CA4 and non-targeted PEGylated conjugates, colon 26 cells were seeded in 6 well plates at 5 x 10^4 cells/well in 1.5 mL complete medium and incubated at 37 ^{o}C in 5 % CO_2 for 24 h. The 4 mM stock solutions of the conjugates in DMSO were diluted to 100 μM with cremophor formulation mixture composed PBS/EtOH/Cremophor (18:1:1 v/v) before addition to the wells. 300 μL of the respective dilute solutions were then added to 1200 μl of complete media in each well to achieve a 20 μM final concentration of conjugate per well and the well plates incubated at various time points. After every time point of incubation, the medium was removed and the cell monolayer was rinsed twice with PBS. 120 uL of DMSO was then added to each well to solubilize the cells for 5 min after which an additional 280 μL of absolute EtOH was added to the DMSO solution already in the wells and the fluorescence from PC was read using the multi-well plate reader (Molecular Devices, SpectraMax M2 model) set at 605 nm excitation and 640 – 800 nm emission wavelengths. The intracellular concentrations of the conjugates were determined from the standard fluorescence curve obtained by

dissolving the stock solutions of the conjugates in DMSO/EtOH in the same ratio as used in the used in fluorescence uptake experiment to obtain dilute solutions. The results were expressed in concentrations (M).

3.6.4. Competitive binding assay of conjugates with excess folic acid or excess biotin

In order to demonstrate that FA and FA-conjugates and biotin and biotin conjugates compete for of receptors, we preincubated 5 x 10^4 colon 26 cells in 6 well plates which are FR-alpha receptor positive as well as biotin receptor positive with 1 mM FA and 1 mM biotin respectively. After 1 h in this condition we added **FA-PEG2K-PC-CA4** or **Biotin-PEG 897-PC-CA4** (all at 20 μM). At the end of each incubation period, fluorescence emission was taken as indicated in the uptake experiment.

Briefly, colon 26 cells were incubated at cell densities of 5 x 10^4 cells in complete medium in 6 well-plates at 37 ^oC in 5 % CO_2 for 24 h. The 5 mM folic or biotin stock solutions were prepared by dissolving appropriate amounts of the respective compounds in 1 mL DMSO at 60 ^oC and later diluting them in deionized water to make a total volume of 10 mL. 200 μL of the solution was then added to 1000 μL of complete medium in the well plate and incubated for 1 h prior to the addition of 300 μl of the prodrug conjugates to compete with

receptors available on cancer cell membranes. At various time points, fluorescence of wells with free FA or biotin is taken following the same protocol as in the uptake experiment and compared with wells without free FA or biotin at that same time point. The results are expressed as fluorescence units within a given volume of solvent.

3.6.5. Estimation of cellular uptake of conjugates by confocal fluorescence microscopy

To assess the specificity of the conjugates to the cancer cells, colon 26 cells were seeded at densities of $1x10^4$ cells/well in 24 well-plates containing 12 mm diameter cover slides and was then incubated for 24 h. **FA-PEG2K-PC-CA4** and **Boc-PEG897-PC-CA4** conjugates were diluted to appropriate concentration and 25 µl of each diluted solution then added to the well-plates to achieve 10 uM final concentrations per well. The cells were incubated for 1.5 h and then the media was removed and cell monolayer rinsed three times with the complete media. The cover slides were removed and then mounted on the glass slide. The fluorescence caused by the two conjugates (all excited at 633 nm, monitored at 650-750 nm) was recorded using confocal scanning microscope and images were taken using a leica DMI4000B fluorescence microscope fitted with QI imaging Fast camera and the spot advance version 4.6 processing software. [251]

3.7. *In vivo* optical imaging

All animal experiments were carried out in compliance with the Animal Management Rules of IACCUC and the guidelines for the Care and Use of Laboratory Animals of the University of Oklahoma Health Sciences Center.

Three to 4-week old female balb/c mice (n=3) (approximately 20 g, Charles Rivers Laboratories Inc.) were used to monitor, the bio-distribution and the tumor targeting ability of the seven conjugates synthesized (viz; **PC-CA4, FA-PC-CA4, FA-PEG2-PC-CA4, FA-PEG2K-PC-CA4, Boc-PEG897-PC-CA4, FA-PEG897-PC-CA4** and **Biotin-PEG897-PC-CA4)**. The mice were implanted sub-cutaneously with 2 X 10^6 colon 26 cells in PBS (100 µL) on the lower back neck region and tumor growth was monitored with digital caliper for 10 days until when the tumor diameter reached 5-6 mm length. The mice were then anesthetized in acrylic chamber with 2.5 % isoflurane/air mixture followed by injection with cremophor solutions (consisting of PBS/EtOH/Cremophor, 18:1:1 v/v) of the conjugates (2 umol/kg, i.v.). Then the images were taken using the IVIS imaging system (Caliper Life Sciences), which consisted, of cryogenically cooled imaging system coupled to the data acquisition computer running Living Image software. Fluorescence images were taken at 0, 15 min, 1h, 3 h, 7 h, 9 h 24 h, 48 h, and 72 h post injection. During the imaging process, five different exposure times were selected viz; 0.5 s, 1 s, 2 s, 3 s and 5 s. The excitation and emission wavelengths were 633 nm and 675-720 nm respectively. Prior to the imaging the

mice were anesthetized and during the post processing, image counts were adjusted to 5 x10^3 as minimum and 3 x 10^4 a.u. as maximum color scale.[252]

3.8. RESULTS AND DISCUSSION

3.8.1. Synthesis

We design the conjugates base on the following principles 1) Phthalocyanine is an effective imaging and therapeutic agent. 2) PEG is a biocompatible and stable linker that increases the hydrophilicity of the conjugate and is recommended by FDA for biomedical applications. 3) Folate and biotin are effective homing molecules targeting FR and biotin receptor expressing tumors respectively. 4) CA-4 is chemotherapeutic agent (antitubulin agent). On the basis of this design, we synthesized four folated and one biotinylated PC-CA4 prodrugs as seen in the scheme following very versatile methods and high yields as seen in the scheme above.

3.8.2. Electronic absorption and photophysical properties

The absorption spectra of six out of the seven conjugates are summarized in Table 4. The compounds gave absorption spectra that were typical phthalocyanine derivatives showing the B- band at 354-356 nm, Q- band at 672-

676 and two other vibronic bands at 604-607 and 642-647 nm.[243] The similarity in their Q- bands absorption indicates that the π-system of these compounds is not perturbed by the axial ligands. It is worth noting that λ_{max} for both **FA-PC-CA4** and **FA-PEG897-PC-CA4** are quite similar in almost all the wavelengths and a bit lower than those of the other conjugates. The explanation for **FA-PC-CA4** may be due to the direct conjugation of FA (which is highly insoluble in most organic solvent except DMF and DMSO) to a highly lipophilic prodrug (**PC-CA4**) introduce some ampiphilicity to the molecule that may lead to π- π stack stacking and subsequent aggregation even in the organic solvent. But the introduction of PEG 897 which is shorter between FA and PC seems not to alleviate the situation hence a need for a longer PEG. There may be some other reason attached to that reduced extinction coefficient for this compound. We did expect similar results from **FA-PEG2-PC-CA4** due to the short nature of the spacer but contrary to this, the compound had similar extinctions coefficients like the other compounds. May be the nature of the spacer also has an attribute since there is the presence of the tetrazole ring within this chain coupled with the saturated alkyl chain. We may conclude that solubility of the conjugates contributed a lot to the observed results.

Compd	λ_{max} (nm) (log ε)			

PC-CA4	674(5.25)	645(4.40)	607(4.47)	355(4.79)
FA-PC-CA4	674(5.08)	646(4.24)	607(4.30)	355(4.66)
FA-PEG2K-PC-CA4	676(5.36)	646(4.52)	607(4.59)	355(4.93)
FA-PEG2-PC-CA4	675(5.26)	646(4.46)	607(4.50)	355(4.80)
FA-PEG897-PC-CA4	674(5.08)	645(4.24)	607(4.29)	355(4.73)
Biotin-PEG897-PC-CA4	675(5.30)	646(4.46)	607(4.53)	355(4.85)

Table 4: Extinction coefficient at various λ_{max}

3.8.3. Aggregation Tendency

The fluorescence of the conjugates in DMSO was compared with those in aqueous medium. The following observations were made. The fluorescence of all

the conjugates in DMSO was quite similar except that of **FA-PC-CA4** which might be attributed to aggregation of the molecule (we have observed the reduction in its extinction coefficient above). The decrease in the fluorescence intensities of the conjugates in culture media compared to that of the DMSO was quite apparent (Figure 22), since they contain the highly lipophilic photosensitizer (phthalocyanine). The reduction was quite conspicuous with **FA-PC-CA4** (aggregated most). The least aggregated of all the conjugates was **FA-PEG2K-PC-CA4** with a long PEG that increases the hydrophilicity of the molecule. Although **FA-PEG897-PC-CA4** and **Biotin-PEG897-PC-CA4** had the same PEG lengths, **FA-PEG897-PC-CA4** aggregated more in the media than **Biotin-PEG897-PC-CA4.** This discrepancy could be attributed the less solubility of FA compared to that of biotin. The order of aggregation in culture medium were; **FA-PC-CA4 > FA-PEG2-PC-CA4 > PC-CA4 > FA-PEG897-PC-CA4 > FA-PEG897-PC-CA4 > FA-PEG2K-PC-CA4.** This data suggests that the longer the PEG spacer, the more hydrophilic the conjugate becomes and the less prone to form aggregates in aqueous medium.[243]

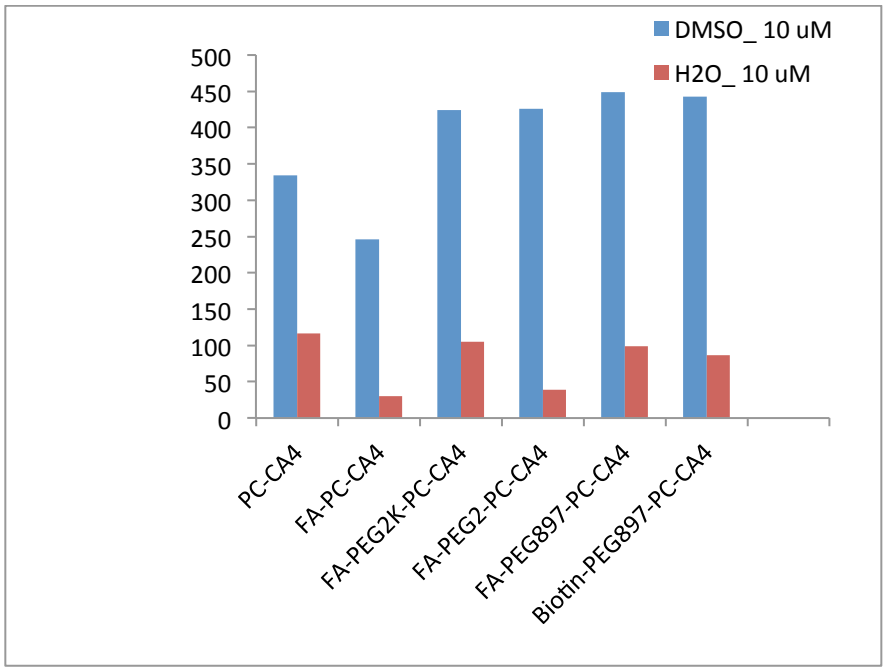

Figure 22. Aggregation tendency of various conjugates

3.8.4. Phototoxicity

Boc-PEG897-PC-CA4, Biotin-PEG897-PC-CA4 and **FA-PEG2K-PC-CA4** all selected from *in vivo* imaging were evaluated against colon 26 cells for *in vitro* studies. Figure 24 shows the phototoxicity of the three conjugates. All three conjugates showed similar survival curves.

3.8.5. Preliminary antitumor efficacy study of FA-PC-CA4 and PC-CA4

The preliminary antitumor efficacy study *in vivo* was performed for FA-PC-CA4 and PC-CA4 (Figure 25 and 26). Tumor growth in balb/c mice implanted with

colon 26 cells were completely suppressed for 9 days by the treatment with PC-CA4 [dose of 2 μmole/kg in 200 μL cremorphor EL 5 % in PBS, and light of 200 W/cm^2 intensity from a 690 nm diode laser for 30 min] while **FA-PC-CA4** showed a substantial reduction in the size of the tumor compared to the control group (Figure 27). No significant body weight loss was observed from any group (Figure 26). *(Drs. Pallavi Rajaputra and Bio Moses performed this study.)*

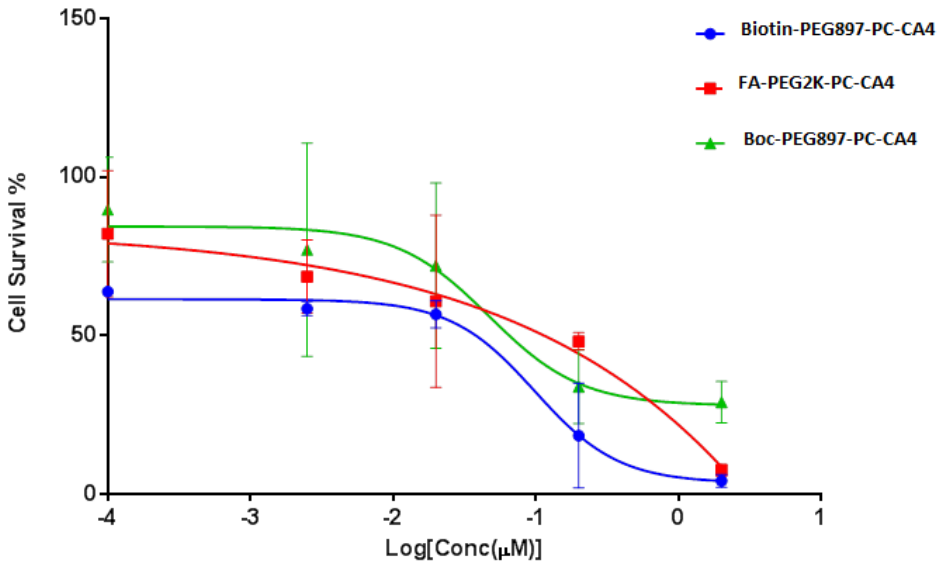

Figure 24. Phototoxicity of the three conjugates

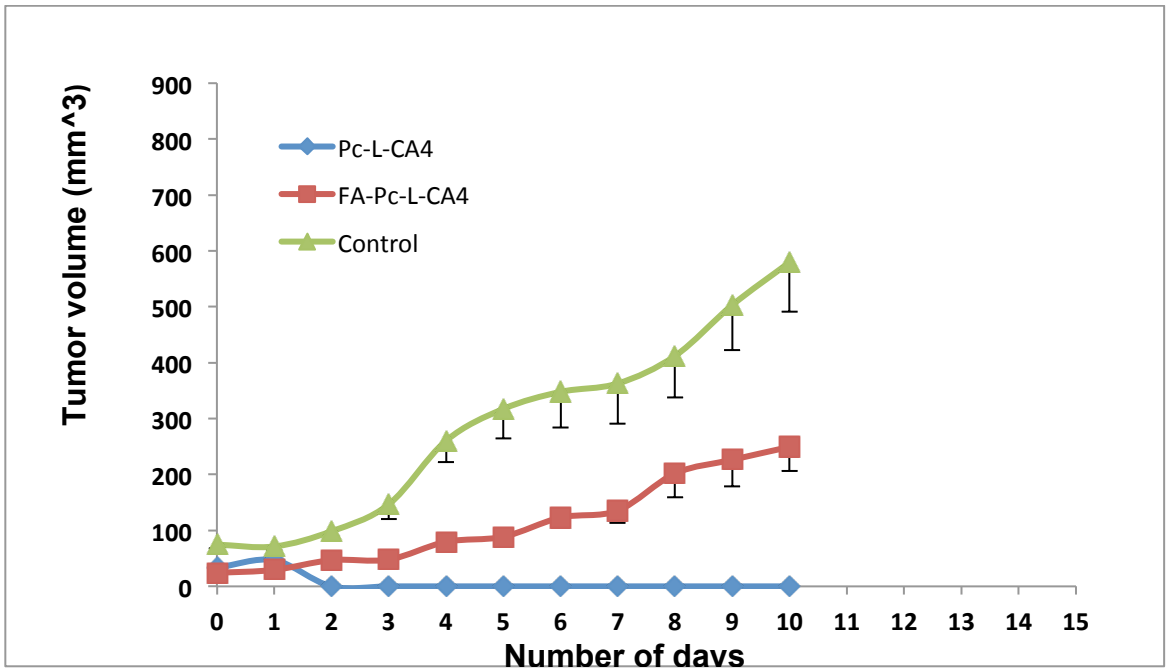

Figure 25. *In vivo* PDT efficacy of **PC-CA4** treated, **FA-PC-CA4** treated and **conrol** group of mice

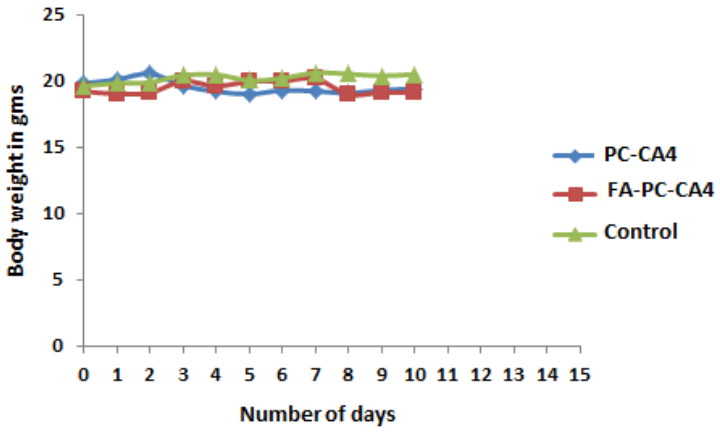

Figure 26. *In vivo* PDT acute toxicity test on **PC-CA4** treated, **FA-PC-CA4** treated and **control** group or mice

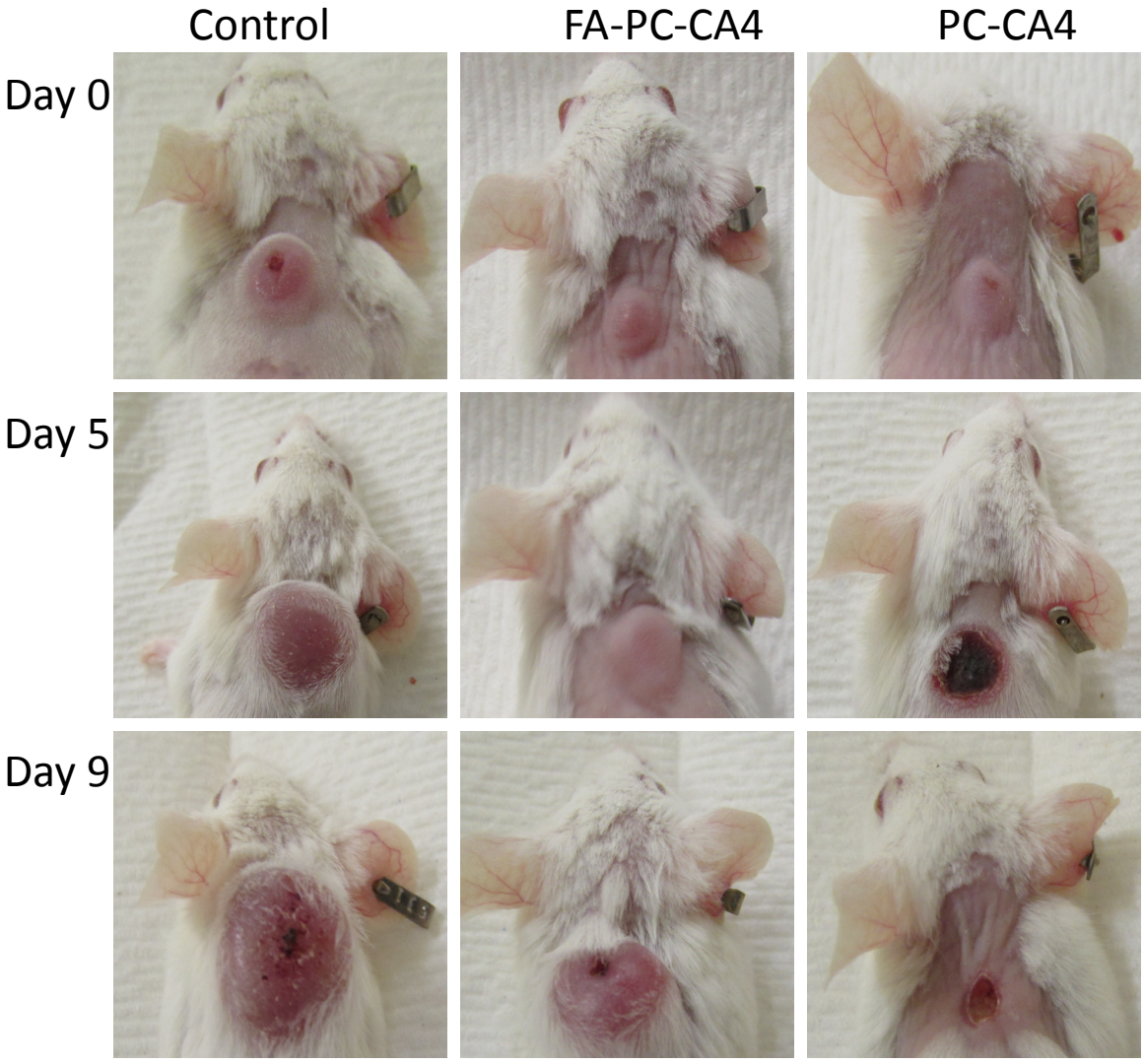

Figure 27: Pictures of balb/c mice treated with **FA-PC-CA4** and **PC-CA4** and **control** group

3.8.6. Estimation of cellular uptake of conjugates by confocal fluorescence microscopy

Cellular uptake of the **FA-PEG2K-PC-CA4** and **Boc-PEG897-PC-CA4** were estimated using an Olympus FV 1000 confocal laser scanning microscopy and the multi-plate reader. Strong fluorescence of the **FA-PEG2K-PC-CA4** was observed after treatment for 1.5 h in colon 26 cells, a folate receptor positive cell line. (Figure 28) In contrast, the fluorescence of the **Boc-PEG 897-PC-CA4** was negligible (not bright) suggesting the folate moieties in the folated conjugate accelerated its uptake in the colon 26 cells. This may have been expected as targeted and non-targeted conjugate were water soluble and the major means of transport across the cell membrane would be through folate mediated-endocytosis for the targeted conjugate while hydrophilic non-targeted conjugate could not easily diffuse across cell membrane. This has been attested with the *in vitro*-uptake data that although some random diffusion may occur but that uptake was quite negligible. The results showed that these two conjugates had no organelle specificity and were distributed throughout the cytoplasm.

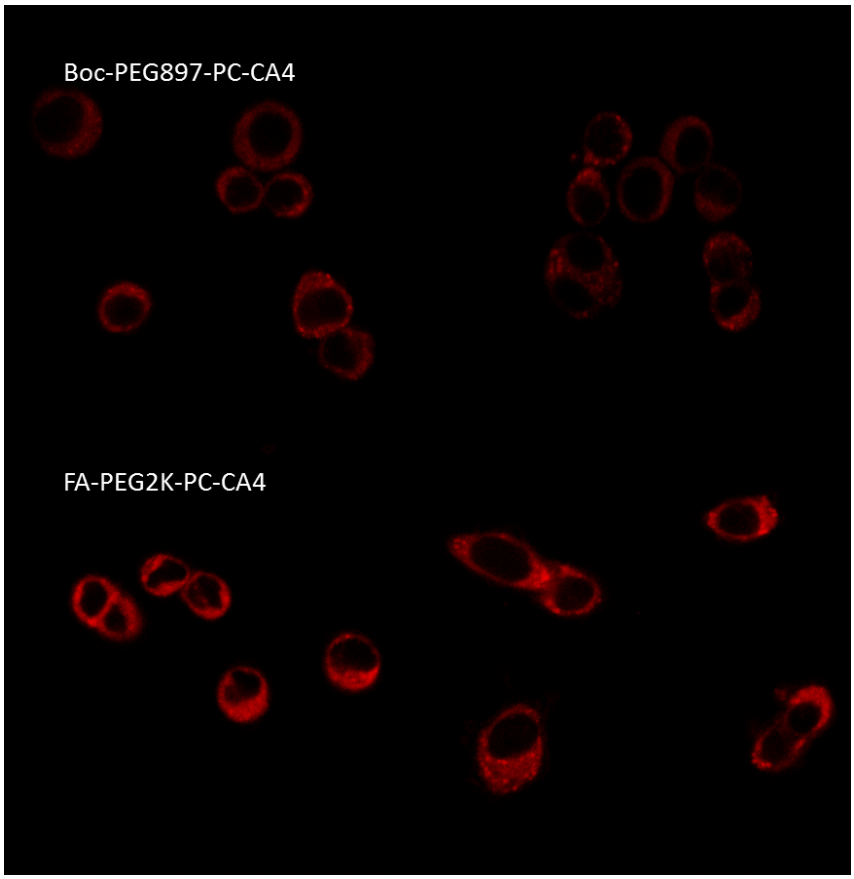

Figure 28. Estimation of cellular uptake by confocal microscopy of **Boc-PEG897-PC-CA4** and **FA-PEG2K-PC-CA4**

3.8.7. Cellular uptake

The cellular uptake of **Boc-PEG897-PC-CA4,** used as reference in this study **FA-PEG2K-PC-CA4** and **Biotin-PEG897-PC-CA4** conjugates as function of incubation time was examined at 20 μM concentration. (Figure 29 and 30) Summarily within the first 6 h of incubation of the conjugates, the uptake increased rapidly and almost saturated or increased gradually from 6-9 h for both

conjugates. Compared to the reference conjugate, the uptake of **FA-PEG2K-PC-CA4** was 7-fold higher while that **Biotin-PEG897-PC-CA4** was 4-fold within this time period. The rapid increase and then followed by a plateau within 6-9 h is not strange because the folate recycling rate has been estimated to be 8-12 h depending on the cell line.[253] Within the saturation period not many receptors are available to cause any meaningful change in the uptake rate. At the end of 24 h exposure, the uptake of **FA-PEG2K-PC-CA4** was 18.8-fold higher than the concentration **Boc-PEG897-PC-CA4** while the uptake **Biotin-PEG897-PC-CA4** was 4-fold higher than the concentration of **Boc-PEG897-PC-CA4.** The steady increase of the cellular uptake of the conjugates over a 24 h period suggested active transport via receptor- mediated endocytosis rather than nonspecific absorption. Better results will have been achieved if a folate free medium was used in the incubation of the cells.

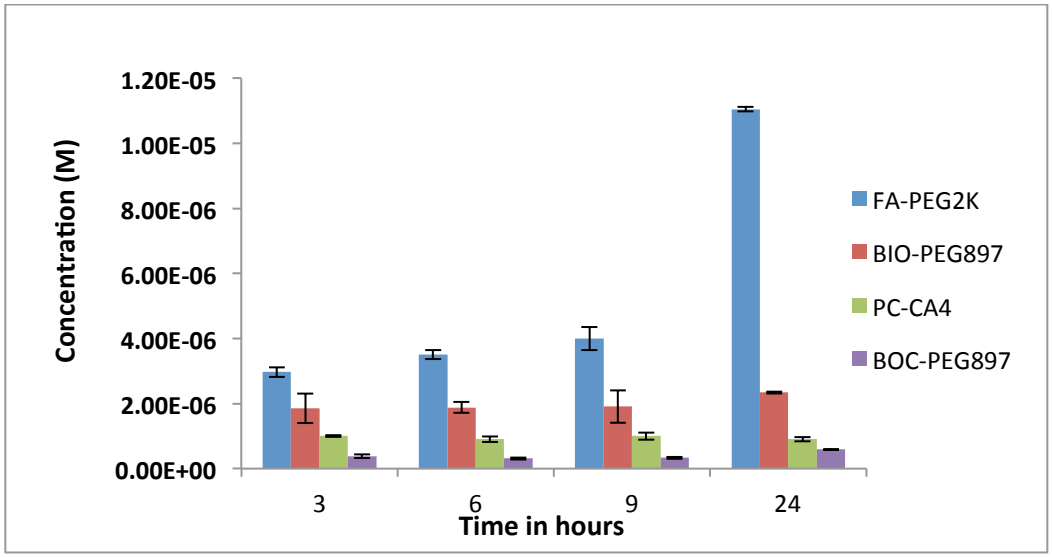

Figure 29. Cellular uptake of four selected conjugates in concentration/ M

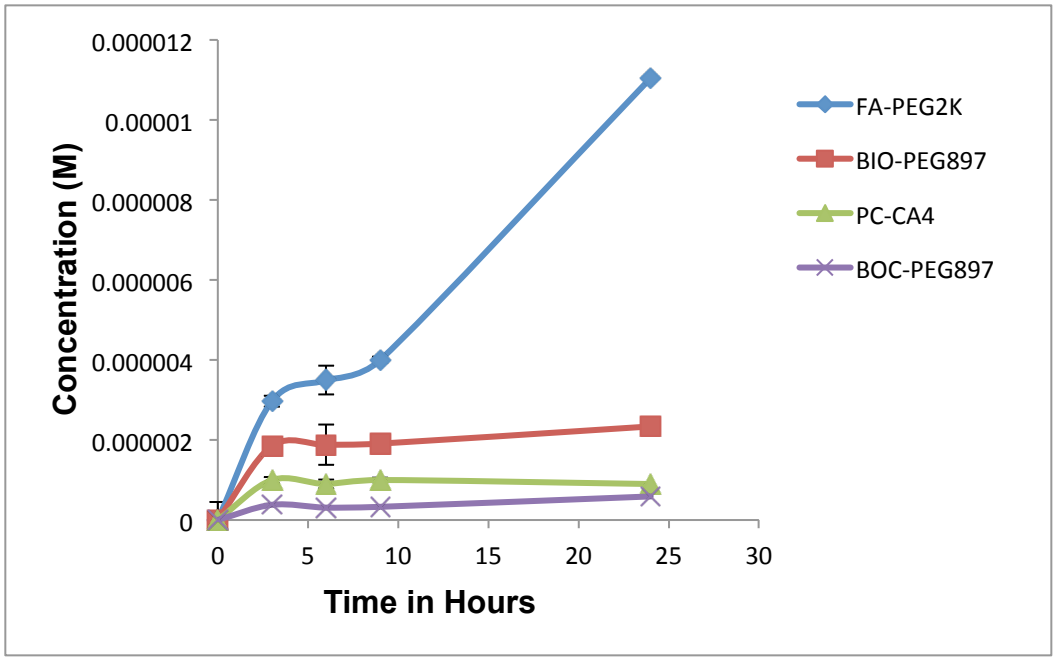

Figure 30. Graphic Representations of the cellular uptake in concentration/M

3.8.8. Competition Assays.

The dependence of uptake on the folate or biotin receptor in colon 26 cells was evaluated by performing a competitive uptake assay in the presence of excess folic acid or biotin (1 mM, 500-fold higher than the conjugates). After 6 h of exposure, the accumulation of **FA-PEG2K-PC-CA4** and **Biotin-PEG897-PC-CA4** were higher than that of non-targeted conjugate. Figure 31 shows that 1 mM FA and I mM biotin significantly reduced the uptake of **FA-PEG2K-PC-CA4** and **Biotin-PEG897-PC-CA4** produgs respectively, but no significant effect was observed for **Boc-PEG897-PC-CA4**. The cellular uptake of **Boc-PEG897-PC-**

CA4 conjugate was not significantly influenced by the presence of either a competitive folic acid or biotin in the medium. While the introduction of excess folic acid (500-fold) reduced the uptake of **FA-PEG2K-PC-CA4** by 60 %, that of excess biotin (500-fold) was reduced by approximately 40 %. The cellular uptake study clearly indicates that both the folate and biotin targeted conjugates were internalized by folate or biotin receptor-mediated endocytosis, consistent with previous reports on folate or biotin receptor-mediated cellular uptake of the folate or biotin-conjugated nanocarriers.[254] [255] Although these compounds were synthesized to improve targeting to cancer cells compared to normal tissues or cells, some uptake was also observed which suggest that the presence of folic acid and biotin could also enhance nonspecific uptake or that better results will have been seen had it been a folate free medium was used in the case of folated conjugate.

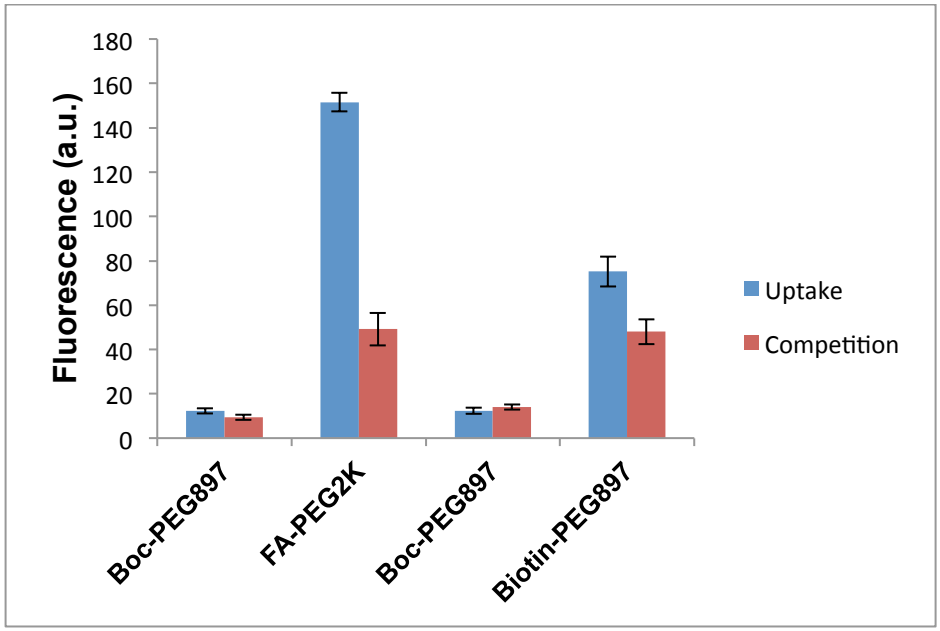

Figure 31. Competition Assays of **Boc–PEG897-PC-CA4**, **FA-PEG2K–PC-CA4** and **Biotin-PEG897-PEG-PC-CA4**

3.8.9. *In vivo* optical imaging

In order to access the specificity of the conjugates to tumor *in vivo* optical imaging was performed with the following compounds **FA-PC-CA4, PC-CA4, FA-PEG2-PC-CA4, Boc-PEG897-PC-CA4, FA-PEG897-PC-CA4, Biotin-PEG897-PC-CA4 and FA-PEG2K-PC-CA4** using IVIS imaging system (Caliper Life Sciences). Generally, all the targeted conjugates accumulated in the tumor but worth noting is the fact some accumulated gradually while others were fast up taken by the tumor tissue. We set our exposure time to 0.5 s. Using these criteria, three hits were selected for further studies, viz; **FA-PEG897-PC-CA4, Biotin-PEG897-PC-CA4 and FA-PEG2K-PC-CA4.** From Figure 32, **FA-PEG2K-PC-CA4** was fastest to be accumulate with bright fluorescence appearing on tumor within the first 3 h and being maximum (peak or brightest fluorescence) at 7 h time point. Fluorescence reduced gradually after 7 h time point but still a hot spot still concentrated at the tumor until after 48 h post injection. It was also observed that the conjugate was cleared via the kidney as intensity fluorescence from the kidney regions increased with time. **Biotin-PEG897-PC-CA4** was the second conjugate to be accumulated in the tumor (Figure 33). The accumulation of this this was gradual compared to **FA-PEG2K-PC-CA4** reaching a maximum tumor-to-skin fluorescence between 9-24 h post injections. The difference between the two conjugates may stem from differences in binding affinities of the

receptors to their respective targeting ligands (folate receptors are known to bind folic acid with nanomolar affinity,[106] thus, indicating a fast up take when compared with biotin receptor(s)). **FA-PEG897-PC-CA4 (**Figure 34**)** was the least of the conjugates to have brighter fluorescence on tumor. Although **FA-PEG897-PC-CA4** has the same PEG chain lengths like **Biotin-PEG897-PC-CA4** and similar FA like in **FA-PEG2K-PC-CA4** its kinetics were slow but similar to that **FA-PEG2K-PC-CA4**. We observed that **FA-PEG897-PC-CA4** compound had some solubility issues from the aggregation tendency as a result of PEG chain not being long enough to completely solubilize FA conjugated to the **PC-CA4** prodrug in aqueous medium. This could probably explain the difference in *in vivo* optical imaging of **FA-PEG897-PC-CA4** which is poorly soluble (aggregates more) and **Biotin-PEG897-PC-CA4** which is highly soluble in aqueous medium although they have the same PEG chain lengths. The exceptional high tumor to skin fluorescence when treated with these targeted conjugates can be attributed to folate and biotin-mediated targeting of the conjugates to the colon 26 cell lines that overexpress both FR-α and biotin receptors. The **PC-CA4** conjugate was used as one of the standard non-targeted prodrug. From the *in vivo* images this prodrug was not localized compared to the targeted counter-parts. It was distributed everywhere within the system (Figure 35). **Boc-PEG897-PC-CA4** was another non-targeted prodrug used to assess the effect of PEG to the localization into the tumor (Figure 36). Boc-PEG897-PC-CA4 showed the high photon counts in both tumor and skin with low maximum tumor/skin ratio (~ 1.70) after 72 h post IV injection. It seemed PEG897 did not specifically delivery the prodrug to tumor.

From the tumor/ skin photon count ratios the following conclusions could be made about the conjugates. 1) Maximum tumor/skin ratio (3.12, 7 h post-IV injection) for FA-PEG2K-PC-CA4 was greater than that for FA-PEG897-PC-CA4 (2.31, 7 h post-IV injection). This may imply that the longer PEG was better. 2) The maximum tumor/ skin ratio for FA-PEG897-PC-CA4 was higher than that of Boc-PEG897-PC-CA4 (1.36, 7 h post-IV injection). Since both conjugates are similar but for the ligand (FA), FA seemed necessary for localization. 3) Biotin-PEG897-PC-CA4 had higher tumor/skin ratio (3.2, 9 h post-IV injection) than FA-PEG897-PC-CA4. Both conjugates only differ in their ligands. We may come to conclude that biotin (it also showed a slow and decreased clearance rate from the tumor) is may be better than FA in targeting for this tumor model, although some factors such as solubility of the conjugate may also contribute to the observed difference. The longer the PEG length the more soluble the conjugate becomes and the higher the accumulation in the tumor compared to the skin or normal tissue. This is why conjugates with either no PEG (Figure 37) or shorter PEG chain length (Figure 38) showed no significant or little fluorescent brightness in the respective tumor accumulation of the conjugates due partly to solubility and to aggregation in the blood stream of the mice.

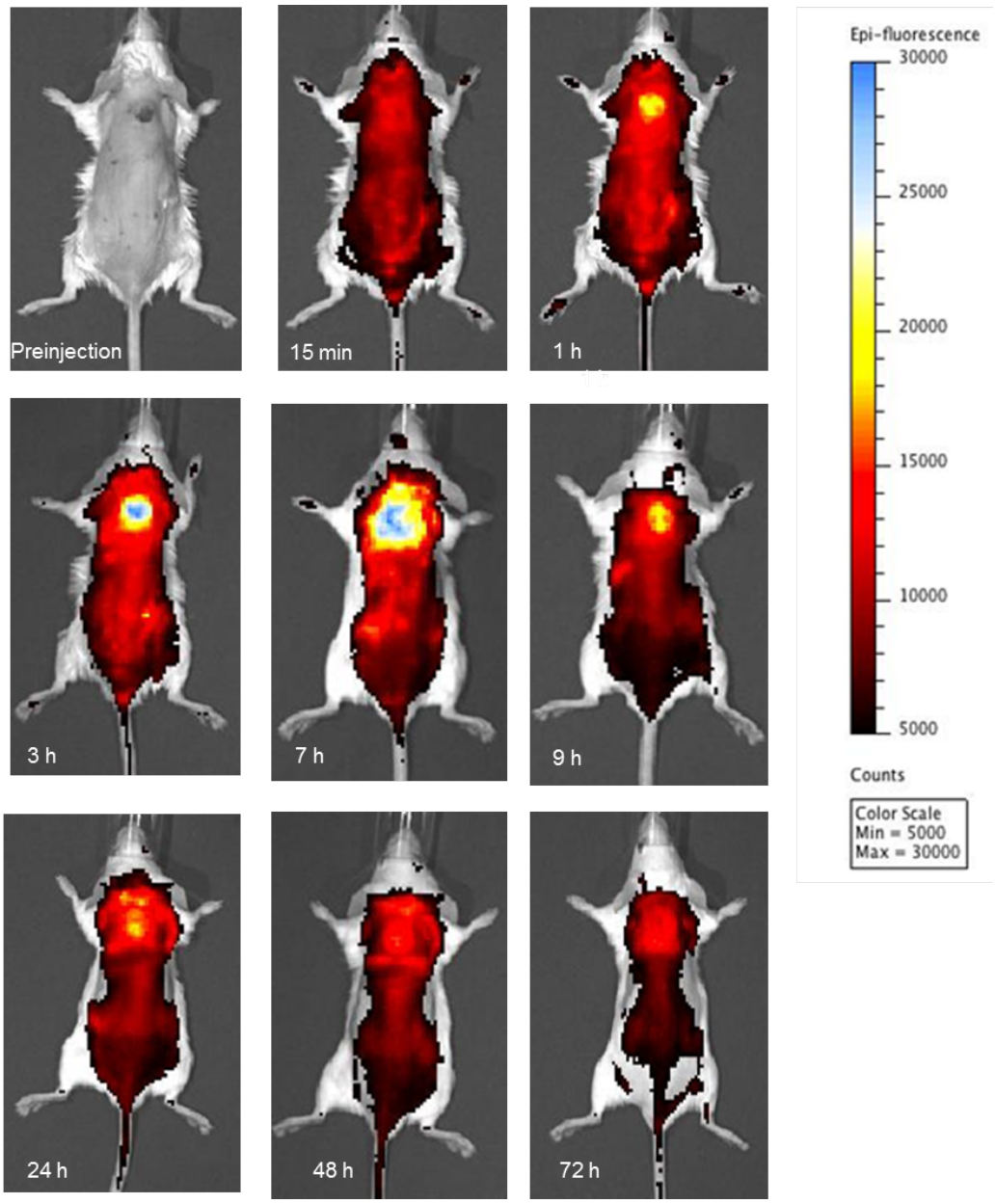

Figure 32. *In vivo* images of **FA-PEG2K-PC-CA4** uptake

.

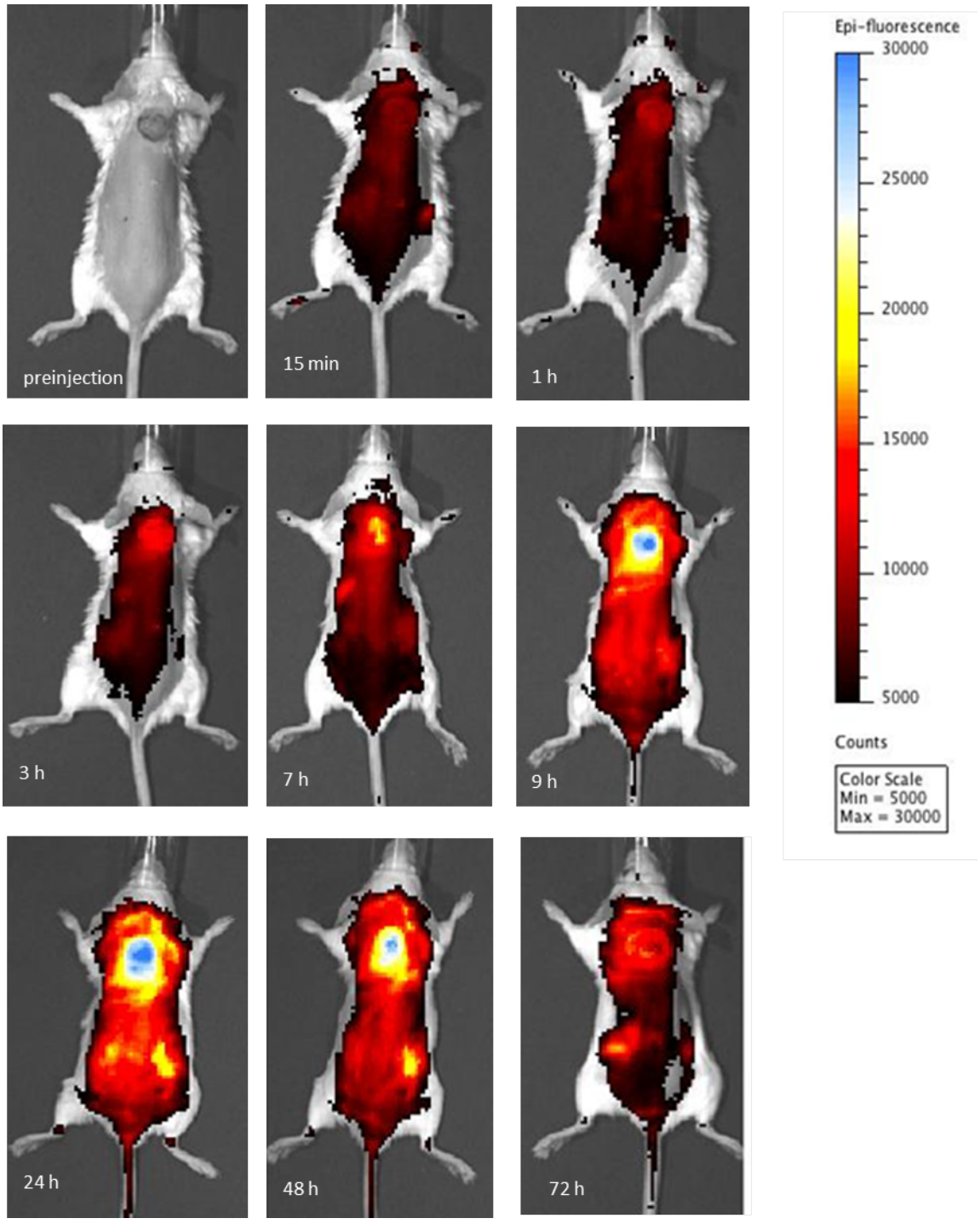

Figure 33. *In vivo* images **Biotin-PEG897-PC-CA4** uptake

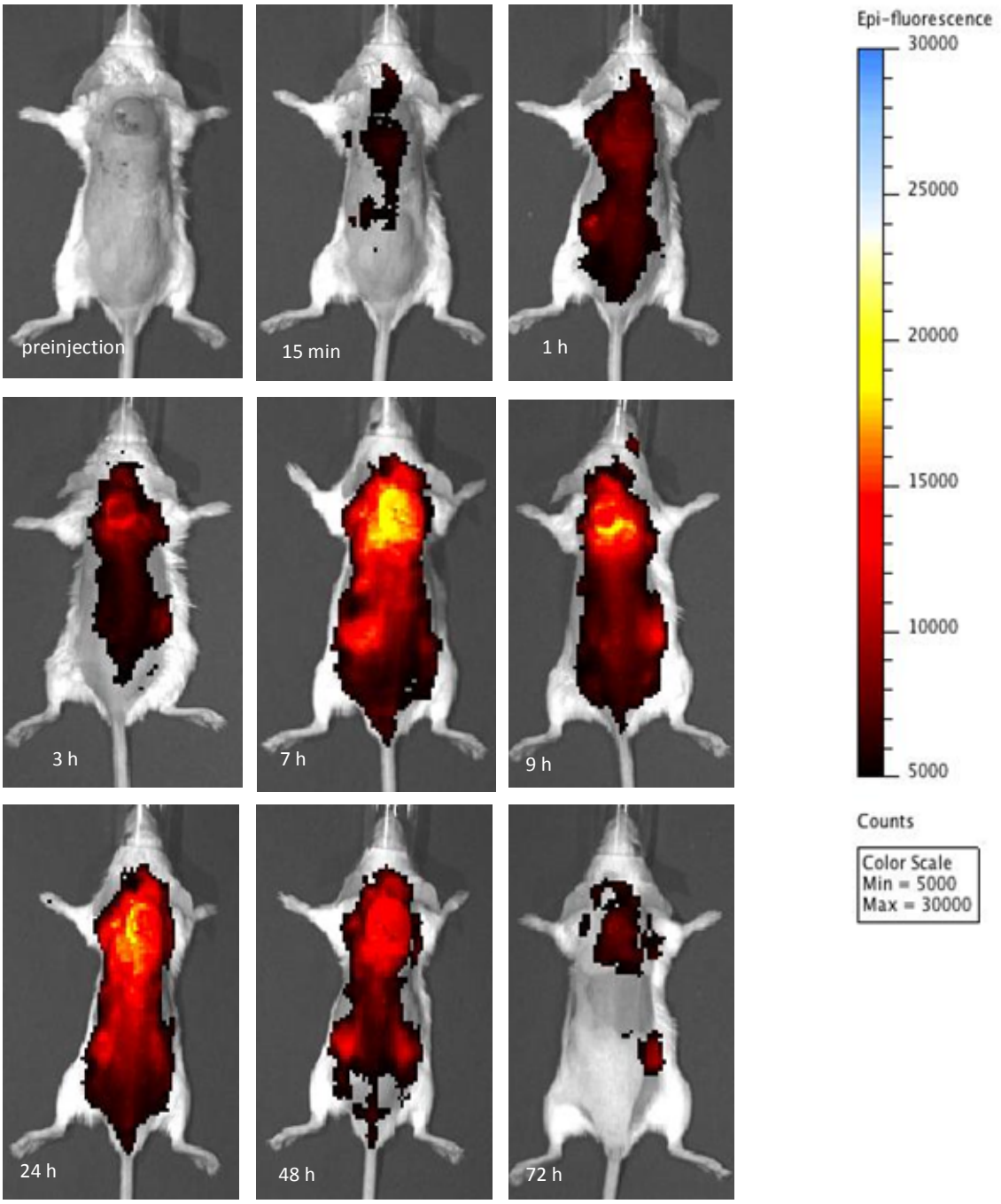

Figure 34. *In vivo* images of **FA-PEG897-PC-CA4** uptake

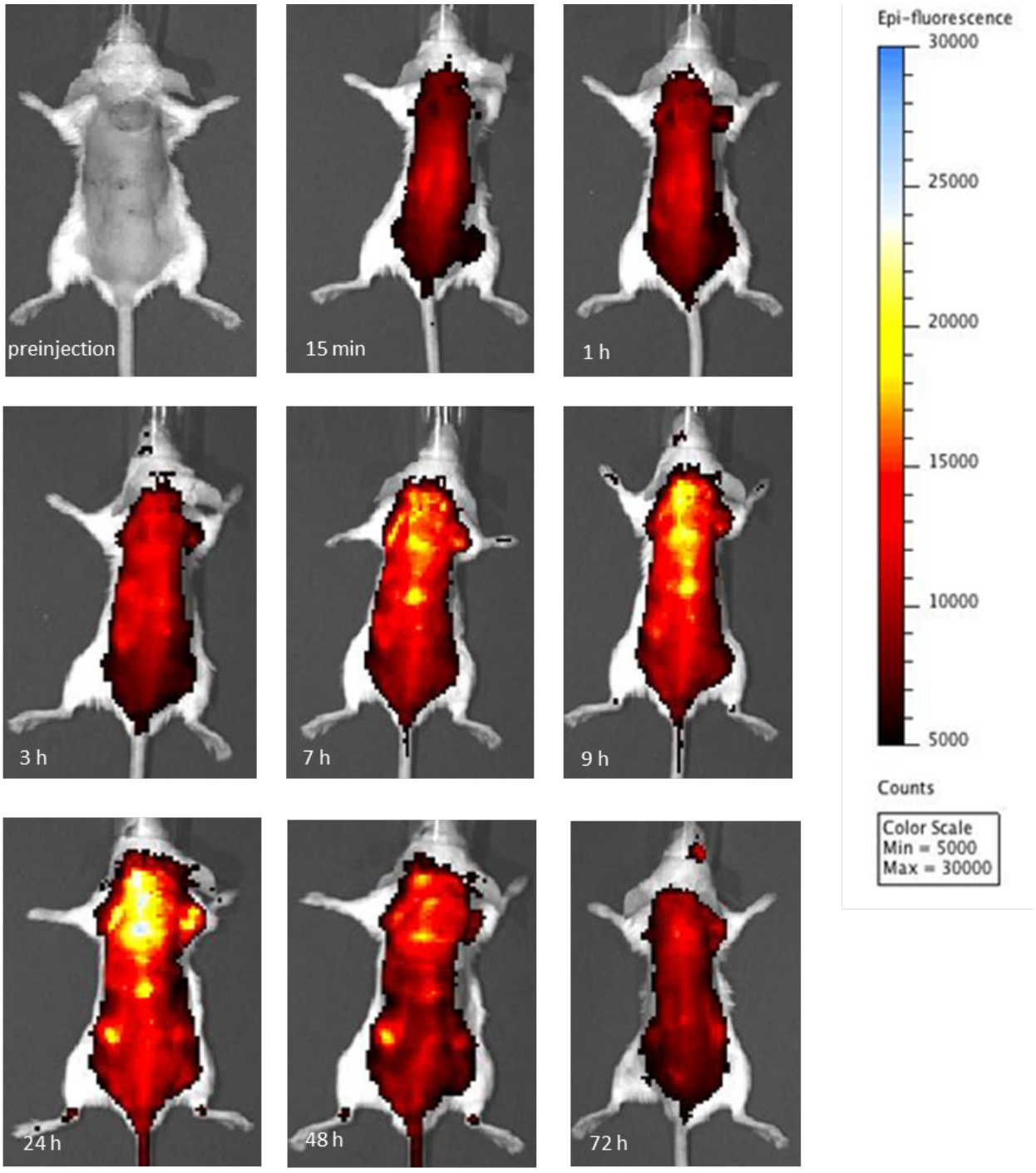

Figure 35. *In vivo* images of **PC-CA4**

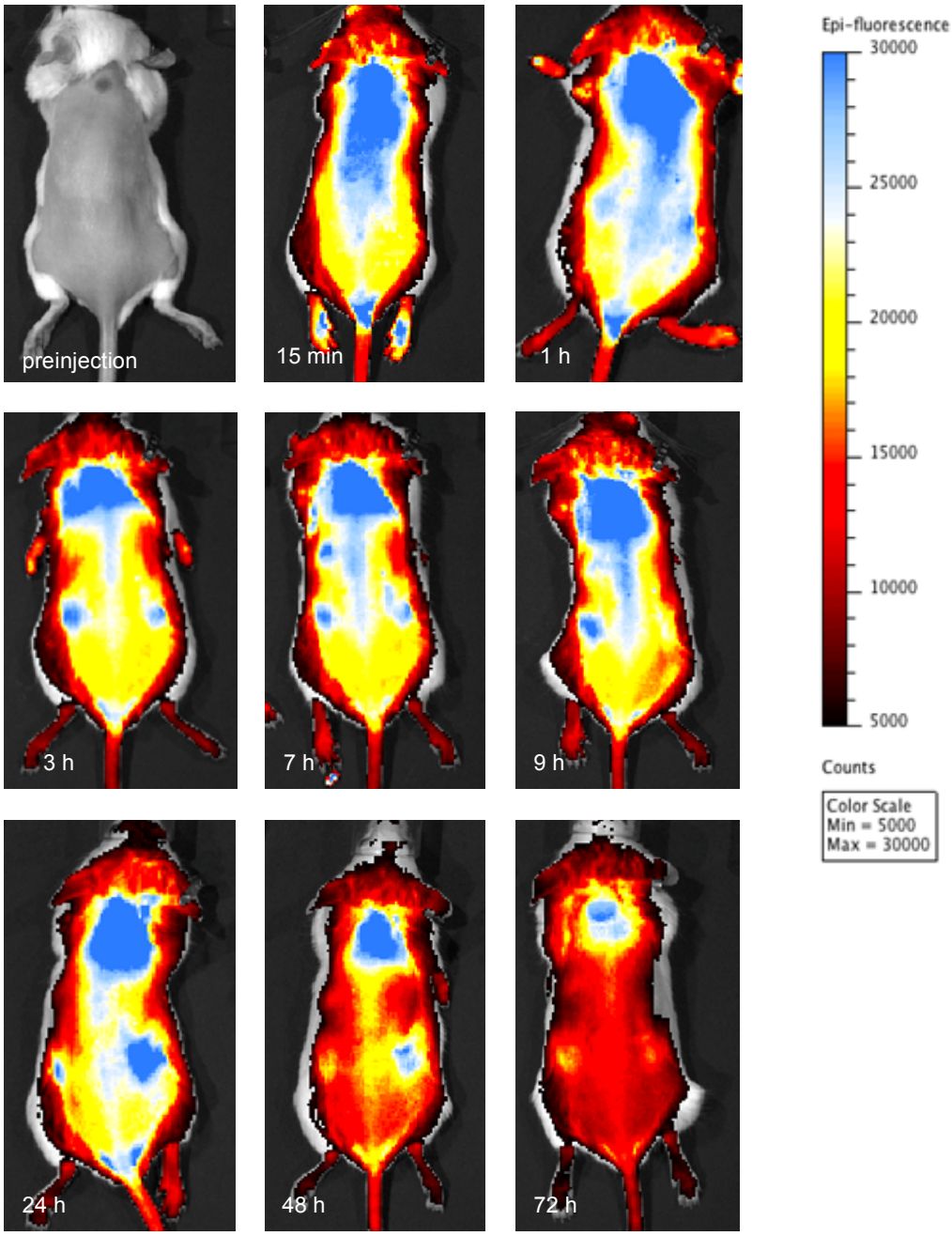

Figure 36. *In vivo* images of **Boc-PEG897-PC-CA4** uptake

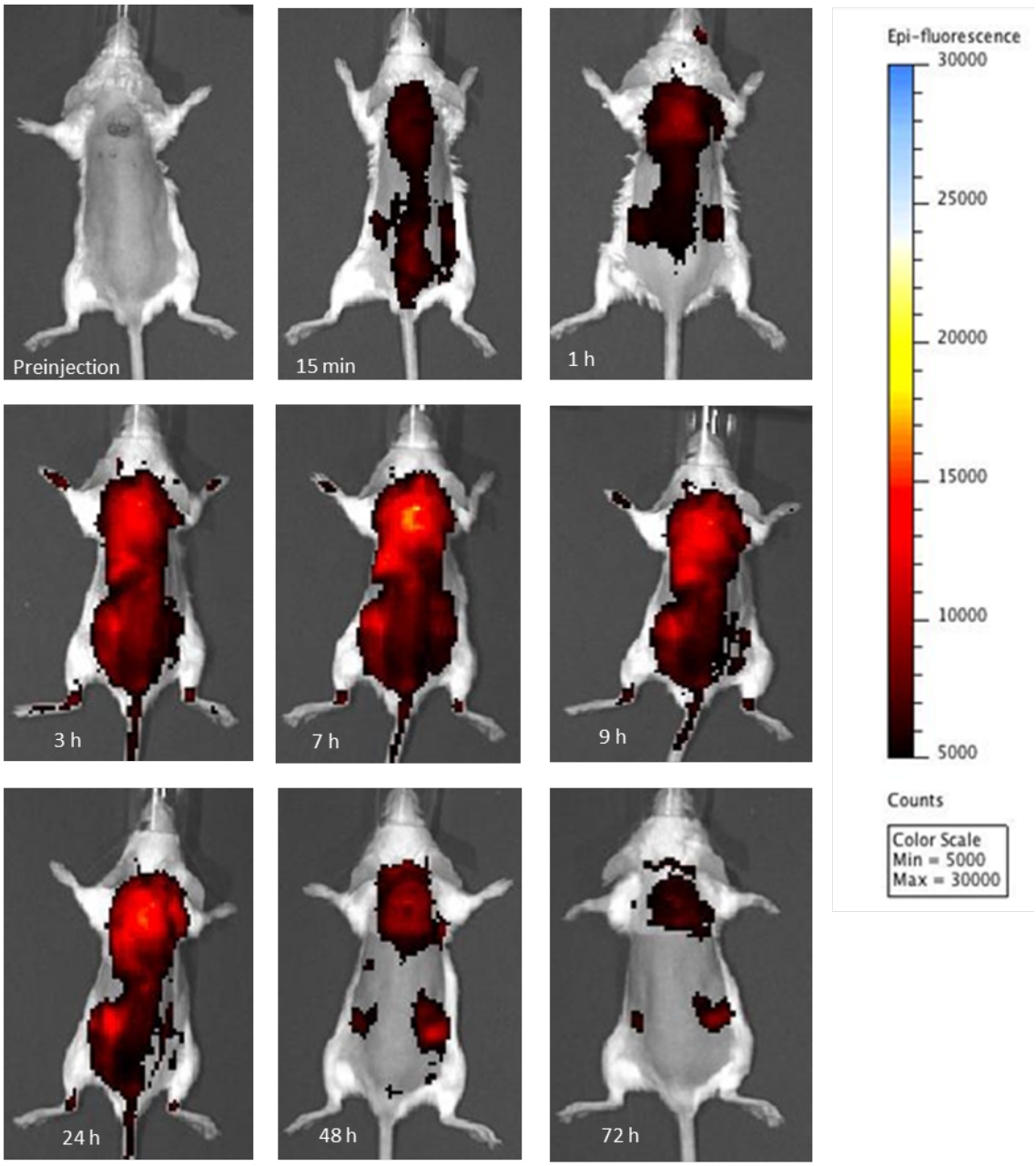

Figure 37. *In vivo* images of **FA-PEG2-PC-CA4** uptake

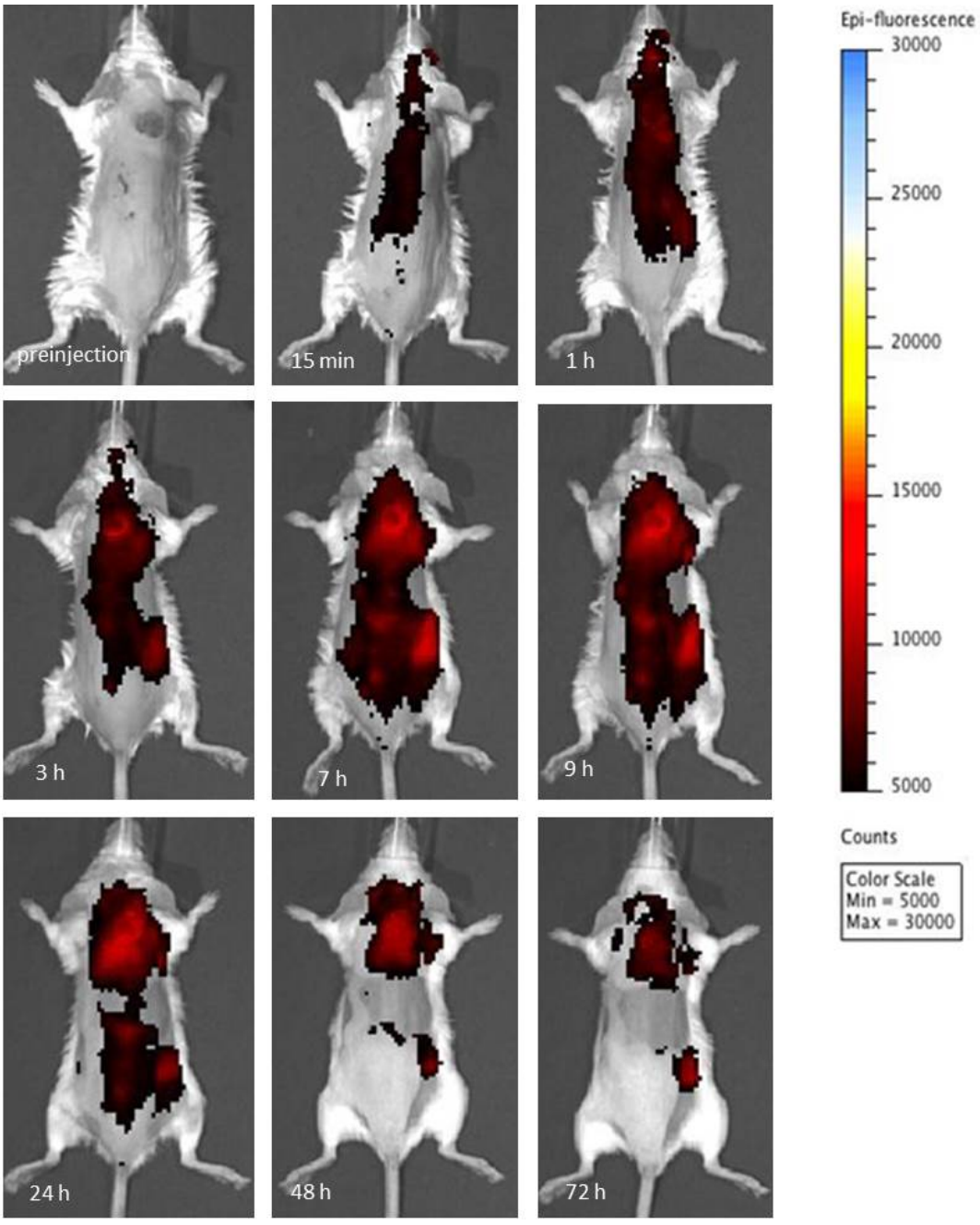

Figure 38. *In vivo* images of **FA-PC-CA4** uptake

3.9. Conclusions

We have been able to design multifunctional conjugates of silicon phthalocyanine, evaluate the cellular uptake using the confocal microscopy and fluorescence from multiplate reader. *In vivo* uptake using the fluorescence from *in vivo* imaging in balb/c mice inoculated with colon 26 cells was also evaluated therefore proving the concept of folate- and biotin-mediated uptake of these prodrugs at cellular and animal model.

CHAPTER 4. CONCLUSIONS

The main goal of this study was to develop a tumor-targeting drug delivery system with the capabilities of selectively transport of cytotoxic agents into tumor by exploiting overexpressed receptors on malignant cells, and an active or remote controlled release of the drug by near infra-red (NIR) light as an externally activating agent. A combination of active site-specific targeting and site–specific triggering release of an anticancer drug from a drug delivery system is expected to increase the local bioavailability of a cytotoxic at the tumor site and stands as attractive local treatment to overcome the selectivity problems of conventional chemotherapy. Several tumor-targeted delivery vehicles (prodrugs, liposomes, dendrimers, micelles, etc.) have been designed, synthesized and some are in clinical studies, but most of them lack the active release mechanisms within the construct. Although some may be equipped with the release mechanism, most of them relied on intrinsic activating agents such as enzymes, pH, etc. of the tumor micro-environment. The use of light as an extrinsic activating agent looks attractive for the site specific release mechanism, but the major hurdle to achieving our aim was to develop a synthetic scheme for the vinyl diether linker that was screened in our lab as potential linker to use in the release of a drug from the caged molecule or prodrug using NIR light.

The electron rich-alkenes activated by heteroatoms have been shown to react with singlet oxygen through 1,2-cycloaddition reaction and have been proposed for photo – triggerable drug release systems in the form of liposomes, cyclodextrin complex and prodrugs. While these linkers and other hetero-olefinic bonds appear to be potentially excellent linkers to drug delivery, no facile approach to the synthesis have been reported, even though the linkers look very simple. Previous methods were limited to symmetric molecules, lengthy steps, harsh reaction conditions and low yields. Hence, in collaboration with lab colleagues (Drs. Praveen and Bio Moses), we were able to develop new synthetic route for O-, N-, and S- vinylation for singlet oxygen labile linkers and the kinetic study of the cleavage of these linkers was done.

To apply our synthetic scheme to biologically active molecule, we set to conjugate combretastatin A-4 (CA-4) to core modified porphyrin (CMP) to make CA4-L-CMP prodrug linked by the vinyl diether bond, but to our greatest dismay the final product was unstable even in an NMR solvent. The intermediates were synthesized with great purity and successfully, but the final product, although seen as being formed from the TLC pattern, could not be isolated and characterized. Owing to the high instability of the prodrug synthesized presumably due to the close proximity of the CMP photosensitizer to the electron rich double bond, we attempted using a spacer but still failed due to the incompatibility of the spacer with the reaction conditions. Moreover, one of the main disadvantages of using this scheme was that *n*-BuLi was used in one of the

steps; hence, drug molecules that carry sensitive functional groups could not be used in this scheme.

With a few problems concerning the vinyl diether linker, we turned our attention to an alternative linker (aminoacrylate linker) that was developed in our lab. The amino acrylate linker has advantages that could not be met with the vinyl diether linker such as easy synthesis, high yields, and mild reaction conditions leading to functional group tolerance, and regeneration of parent drugs after cleavage. Dr. Bio Moses used this linker to synthesize a prodrug of CA-4 and CMP and the first ever prove of the concept of site–specific release mechanism of cytotoxic agent both *in vitro* and *in vivo* using NIR light.

With site-specific triggering prodrug concept proven, I set out to synthesize the multifunctional prodrug system combining the triggering capabilities to active targeting in order to increase local bioavailability of the drug at the tumor site. The targeting vector I set was the folic acid and/or biotin whose receptors are overexpressed on cancer cells and that are common vitamins required by rapidly proliferating tumor cells. The prodrug was envisaged to rapidly accumulate in tumor tissue compared to the normal tissue. The prodrug delivery system to be synthesized was supposed to be three-in-one tumor targeting system. This system consisted of a tumor recognition moiety (FA) that binds to folate receptors frequently overexpressed on the surface of malignant cells) linked by a spacer to photosensitizer and a cytotoxic warhead (drug) also connected by the aminoacrylate linker to the photosensitizer. The three are supposed to form a

conjugate that is inactive and sufficiently stable while in circulation; then once selectively internalized into cancer cells, cleavage of the conjugate upon irradiation with visible light or NIR light restores the active cytotoxic warhead (drug). Two of these conjugates were initially synthesized, which consisted of FA-TPP-CA4 (results not presented in the dissertation) and FA-PC-CA4 by direct conjugation of the FA to the photosensitizers.

From the synthetic point of view, even though the two conjugates can be synthesized in principle by straightforward coupling reactions between the linkers, FA, CA-4 and photosensitizer, some problems regarding FA-containing reaction intermediates must be pointed out.

- The main hurdle in the synthesis is extreme sensitivity of these reactions especially when the drug-linker is attached to the PS. This made it difficult to get the high mass of these conjugates from other methods other than the ESI since the aminoacrylate linker was being cleaved by laser light used, the inability of some of the conjugates to be ionized easily when they are conjugated to FA and with molecules above a certain molecular weight range.

- Secondly, the synthesis of FA-derivatives is represented by very poor solubility of all the FA-containing products in organic solvents (except DMSO and DMF). On the one hand, this made most of the reaction intermediates unsuitable for purification on common solid chromatographic supports. For this reason, precipitation was always preferred to purify reaction productions to eliminate

traces of unreacted reagents and other byproducts. On the other hand, solubility problems often resulted in slow reaction rates, both in the coupling of FA with various nucleophiles and in the following synthetic steps; this led to low yields and, after prolonged reaction times, to the formation of a complex mixture of products. Therefore accurate tuning of reaction conditions was considered to avoid contamination of reaction products by undesired compounds and thus to ensure efficient purification of the desired folate conjugates.

- Thirdly, the problem was also in the characterization of the final products. Due to high instability, the high mass could not be determined using other mass spect methods except ESI. The final molecules seemed to be completely ablated by laser light used in MALDI, FAB, etc. The low volatility of FA conjugates above a certain mass range made the analysis difficult (above 1800 the signal for the internal standards are always too low to get the molecular ion peak). Concerning the problem of mass, SUNY at Buffalo is developing a method for the determination of the masses of these unstable molecules. NMR of FA conjugates are poorly resolved, which has thus led to alternative methods of characterization such as UV, IR, etc.

Despite all the challenges faced in the synthesis, preliminary *in vitro* test (figure U) conducted on the first conjugate (**FA-PC-CA4)** synthesized by direct reaction of the FA to the photosensitizer indicate that it was not accumulating in the colon 26 cell line. When we investigated the behavior of this conjugate in cell culture media or aqueous medium, we realized that this conjugates was highly

aggregating, and that is why their fluorescence was completely quenched, and it was stacked in the medium (due to its ampiphilicity) and not taken up by cells. The NMR this conjugate (**FA-PC-CA4)** was not good, which indicated the aggregation even in DMSO as the most polar NMR solvent in use. We decided to pursue the modification of the PC4 core by sequentially increasing its solubility by varying the PEG chain length. Interestingly, the first modification with short PEG could not improve the solubility, but after adding a longer spacer of approximately 2000 Da, the conjugate showed marked uptake by the cells. It is noteworthy that the effect of PEG lengths on target ability of the FA has been investigated by several research groups on the receptor-mediated uptake of nano-particulate conjugates such as liposomes, micelles but not with the prodrug delivery systems and photosensitizers. With **FA-PEG2K** conjugates being non-monodisperse polymers, we decided to synthesize prodrugs of FA and biotin with pure (>95 %) PEG (897 Da). The prodrugs showed good uptake in the cell culture medium. The best of the conjugates was **FA-PEG2K-PC-CA4** followed by **Biotin-PEG897-PC-CA4** and lastly **FA-PEG897-PC-CA4**. With all the seven conjugates synthesized, we decided to assess the accumulation in mice tumor models using *in vivo* imaging. Interestingly, **FA-PEG2K-PC-CA4** showed the best accumulation with fluorescence peaking between 3 to 7 h post injections followed by the biotin conjugate (**Biotin-PEG897-PC-CA4**) with fluorescence peaking between 9 to 24 h post-injection. **FA-PEG897-PC-CA4** had the similar kinetic like that of **FA-PEG2K-PC-CA4,** but the uptake was not all that great compared to the latter. With these three leads selected, we went ahead to carry out the *in vitro*

test using both the confocal microscopy and cellular accumulation with a multi-plate reader at every time point. Finally using the competition assays we were able to demonstrate folate- and biotin-mediated uptake of these conjugates. We were able to achieve 19 fold cellular accumulations in the cells after 24 h of incubation of our folate prodrugs while that of the biotin was 4 folds compared to the standard compound **Boc-PEG897-PC-CA4**. Uptake accumulations of folate prodrug were done in normal medium having some folic acid. This indicates that we would have achieved better results had a folate free medium been used.[256] I was able to design, synthesize and demonstrate the concept of folate or biotin mediated uptake of our prodrug using PEG of various chain lengths to solubilize the highly hydrophobic PC molecules. Although folate active targeting has been used in other delivery vehicles such as liposomes, micelles, nanoparticulate delivery systems, the use of active targeting on the drug or prodrug is more appealing than targeting the macromolecules since there is always an issue of the stability of these polymers in circulation. To best of my knowledge very little has done in the development of drug delivery system the can actively target and actively release the carried payload using NIR light. Moreover our prodrugs function as multimodal drug delivery system performing the following functions:

1) Imaging (diagnostic application)
2) PDT agent
3) Targeting agent due folate or biotin attached
4) A therapeutic agent; Delivery system for chemotherapeutic drugs.

To the best of our knowledge, the systems developed so far may constitute only three of the above four functions as theranostic agents, which thereby indicates the importance of our prodrug delivery system. Because of the high expression of folate receptors and biotin receptors in most cancer cell lines such as ovarian, breast, lung, etc., our prodrugs will definitely find good use not only in the treatment of aggressive solid tumors such as those mentioned above (ovarian and breast cancer especially) but in the delivery of bioactive molecule. *In vivo* PDT is underway to determine the efficacy of these prodrugs to treat bigger tumors although the non-targeted analog (Figure Z) has proven to be quite effective in our lab.

^{1}H- NMR (upper) and ^{13}C-NMR (lower) spectra of the compounds

2

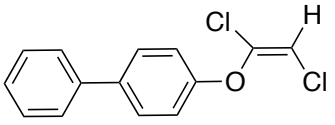

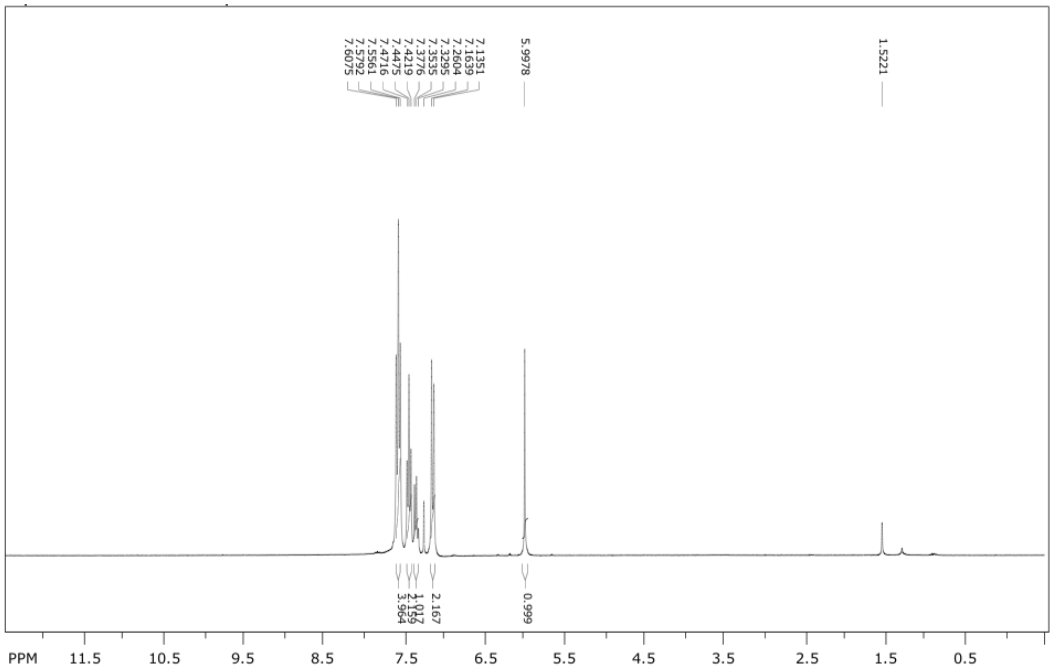
7.6075
7.5792
7.5561
7.4475
7.4219
7.3776
7.3535
7.3295
7.2604
7.1359
7.1351
5.9978
1.5221
3.924
1.017
2.167
0.999
PPM
11.5
10.5
9.5
8.5
7.5
6.5
5.5
4.5
3.5
2.5
1.5
0.5

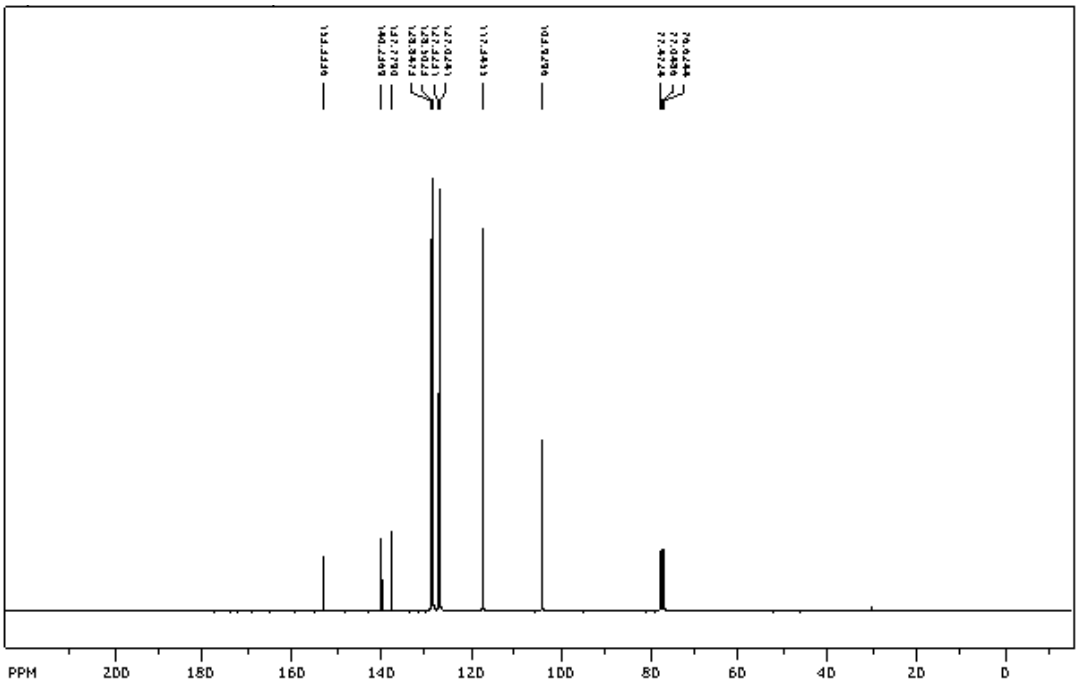
PPM
200
180
160
140
120
100
80
60
40
20
0

Figure 33

3

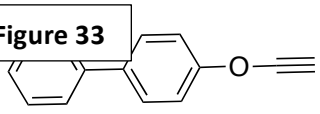
O

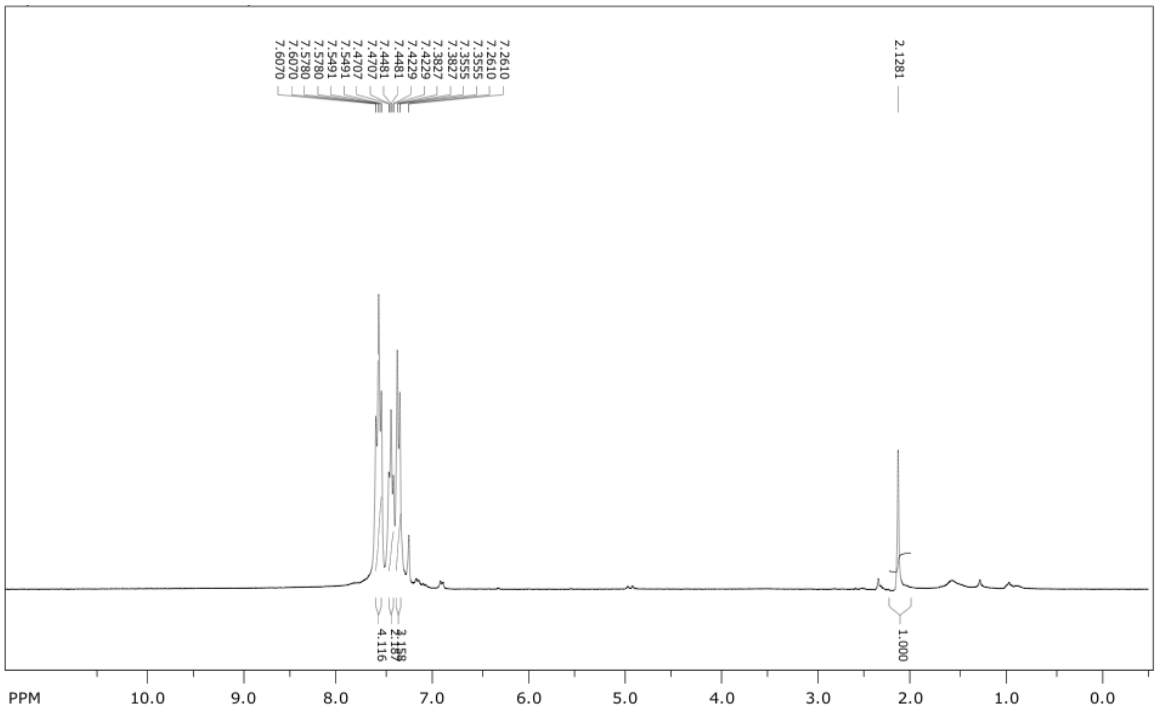
7.6070
7.5780
7.5491
7.4707
7.4481
7.4229
7.3827
7.3555
7.2610
2.1281
4.116
2.158
1.000
PPM
10.0
9.0
8.0
7.0
6.0
5.0
4.0
3.0
2.0
1.0
0.0

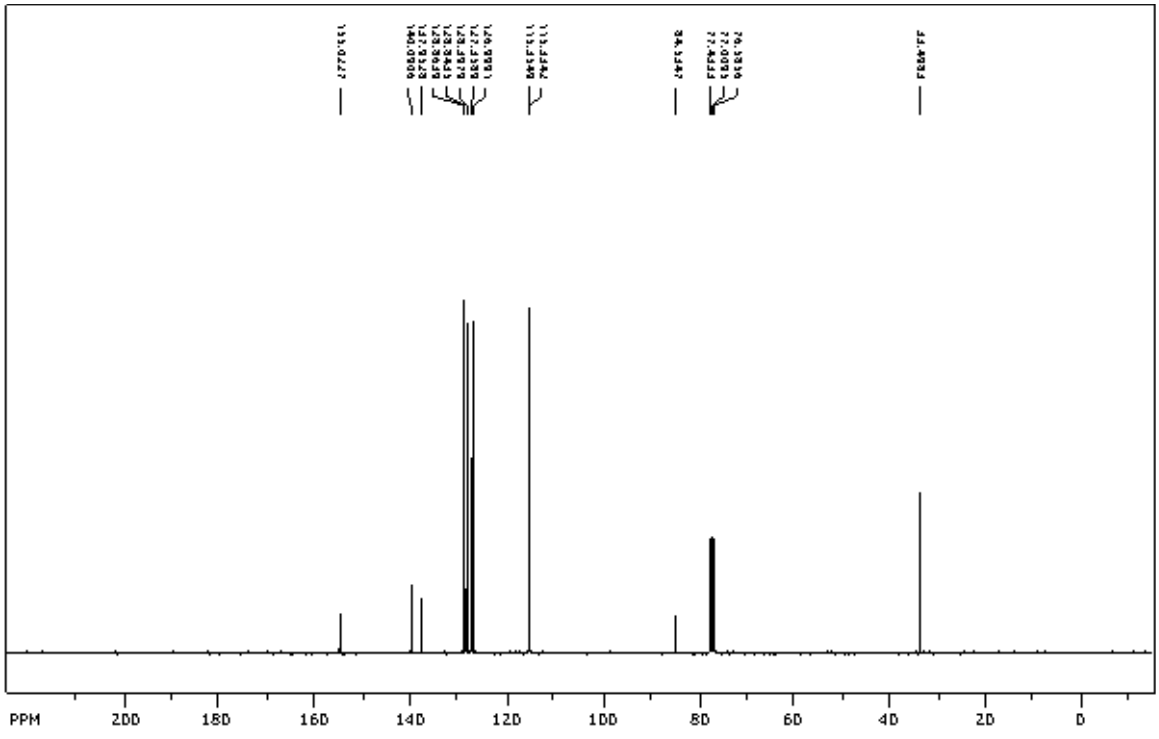
PPM
200
180
160
140
120
100
80
60
40
20
0

Figure 39

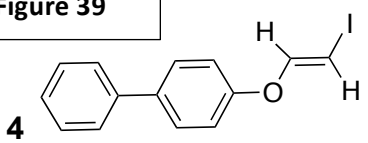
H
I
O
H

4

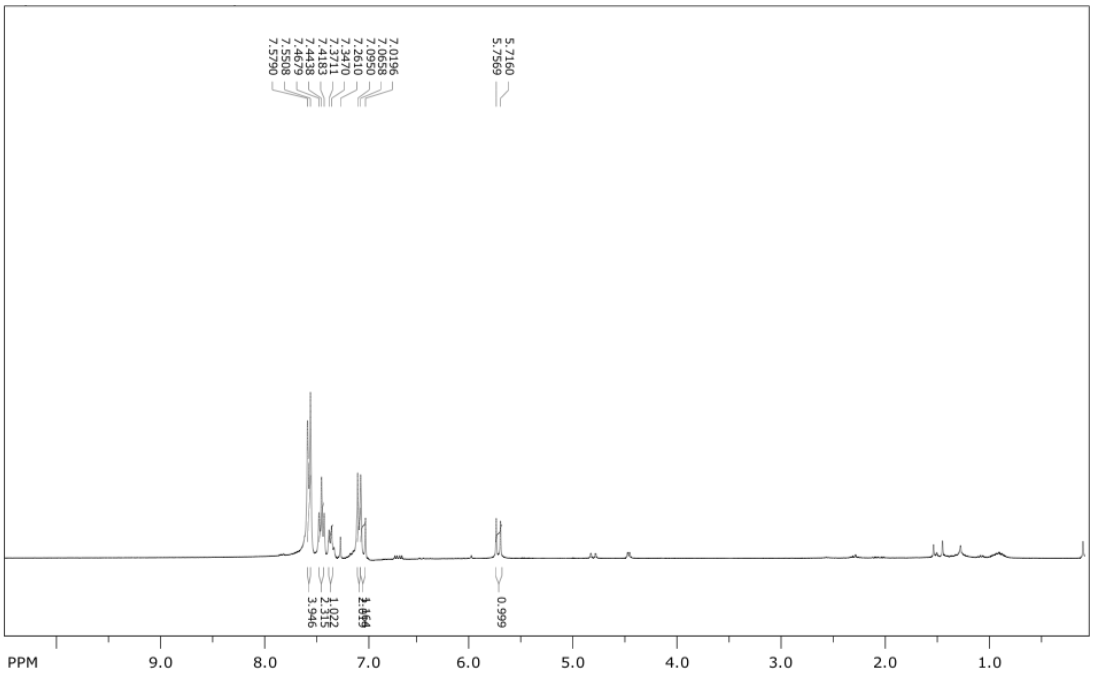
7.0196
7.0058
7.0050
7.2610
7.3470
7.3711
7.4183
7.4438
7.4679
7.5508
7.5790
5.7160
5.7569
3.946
2.315
1.022
0.999
PPM
9.0
8.0
7.0
6.0
5.0
4.0
3.0
2.0
1.0

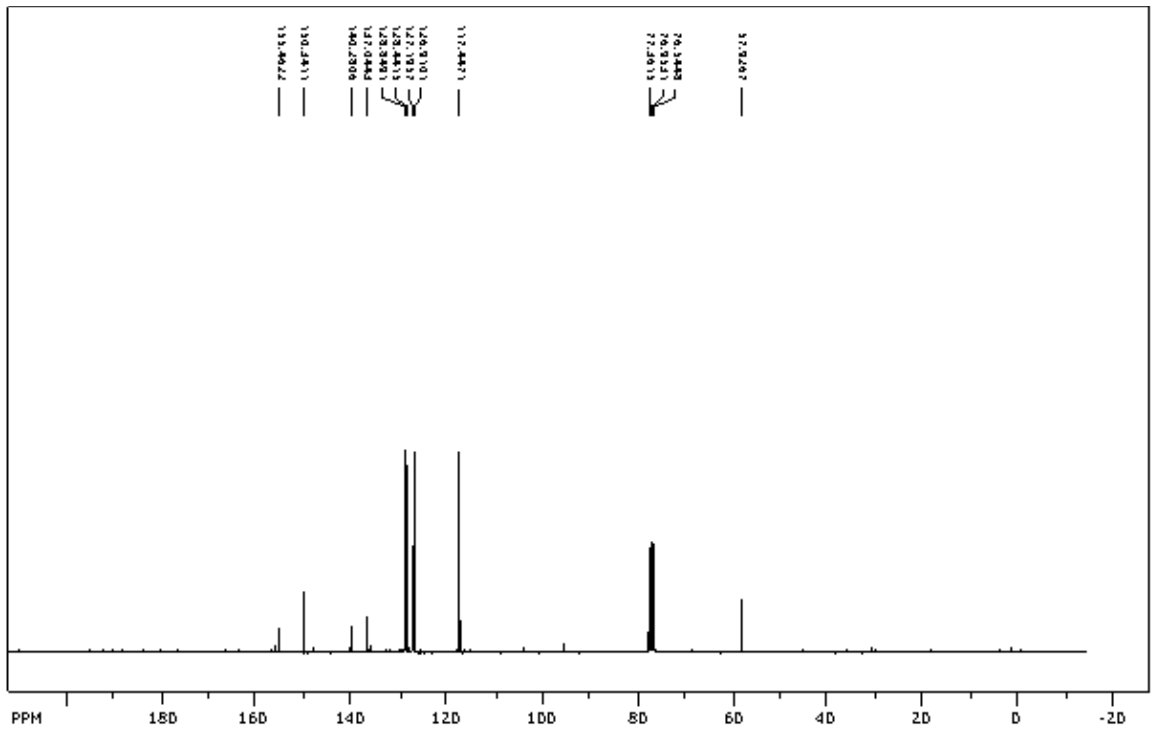
PPM
180
160
140
120
100
80
60
40
20
0
-20

Figure 40

5

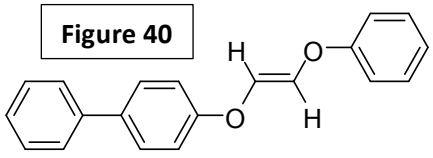
H
O
O
H

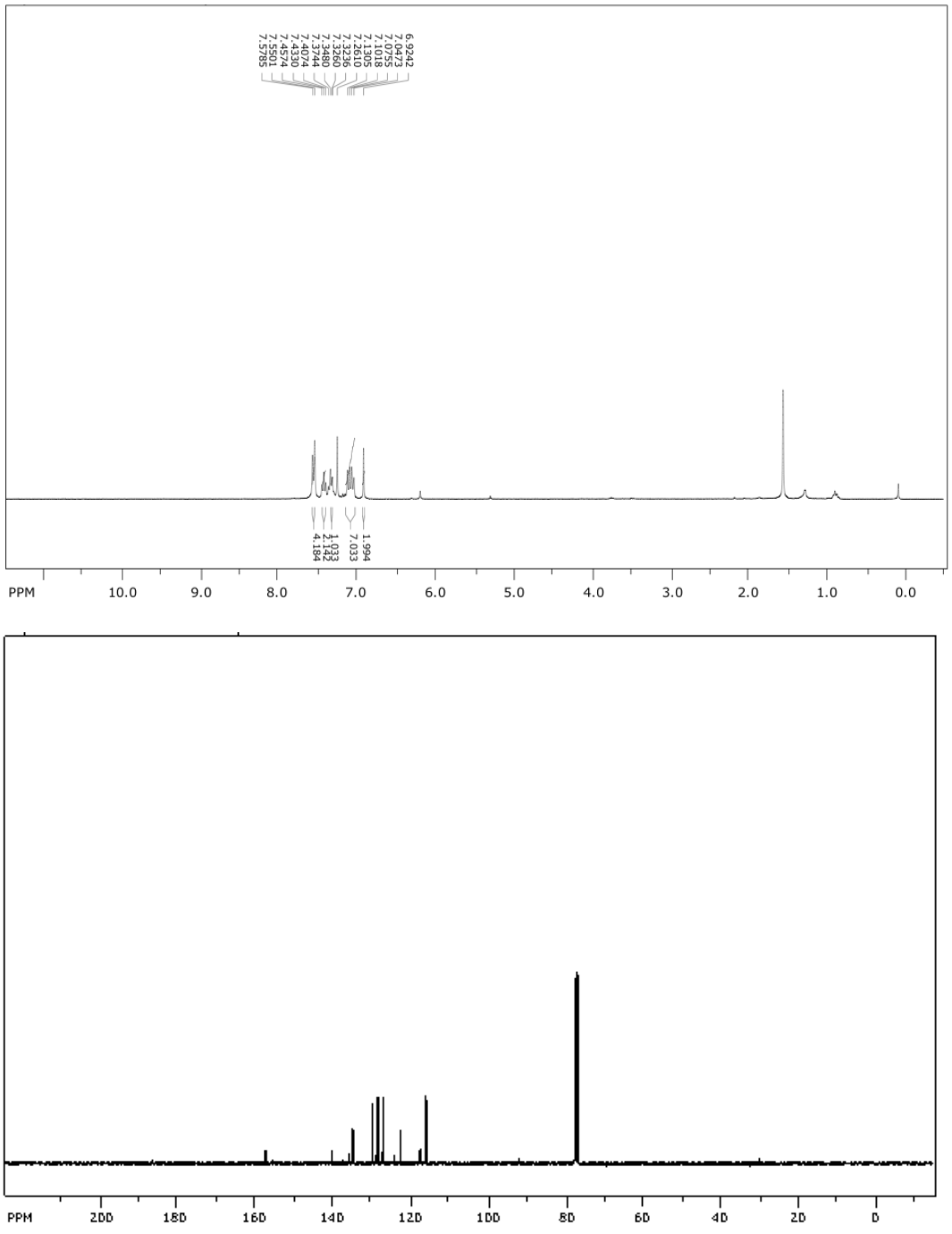
7.5785
7.5501
7.4574
7.4074
7.3744
7.3480
7.3260
7.2236
7.2060
7.1305
7.1018
7.0755
7.0473
6.9242
4.184
2.142
1.033
7.033
1.994
PPM
10.0
9.0
8.0
7.0
6.0
5.0
4.0
3.0
2.0
1.0
0.0
PPM
200
180
160
140
120
100
80
60
40
20
0

Figure 41

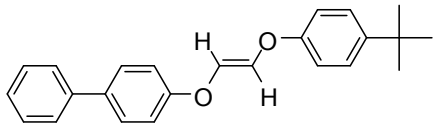
H
O
O
H

6

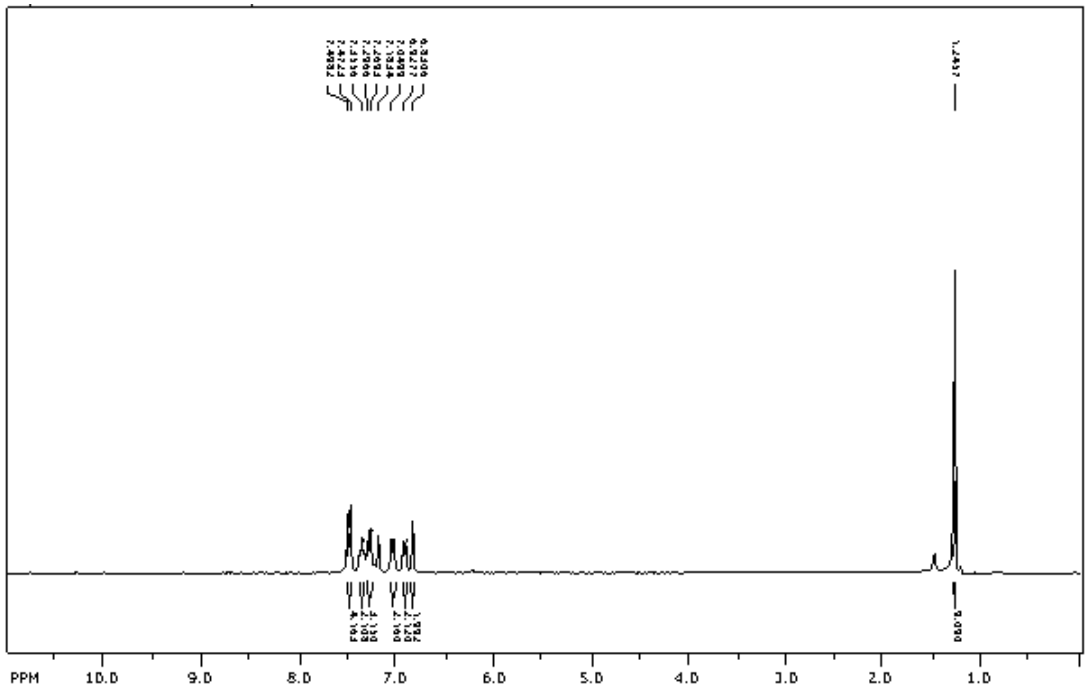
PPM
10.0
9.0
8.0
7.0
6.0
5.0
4.0
3.0
2.0
1.0

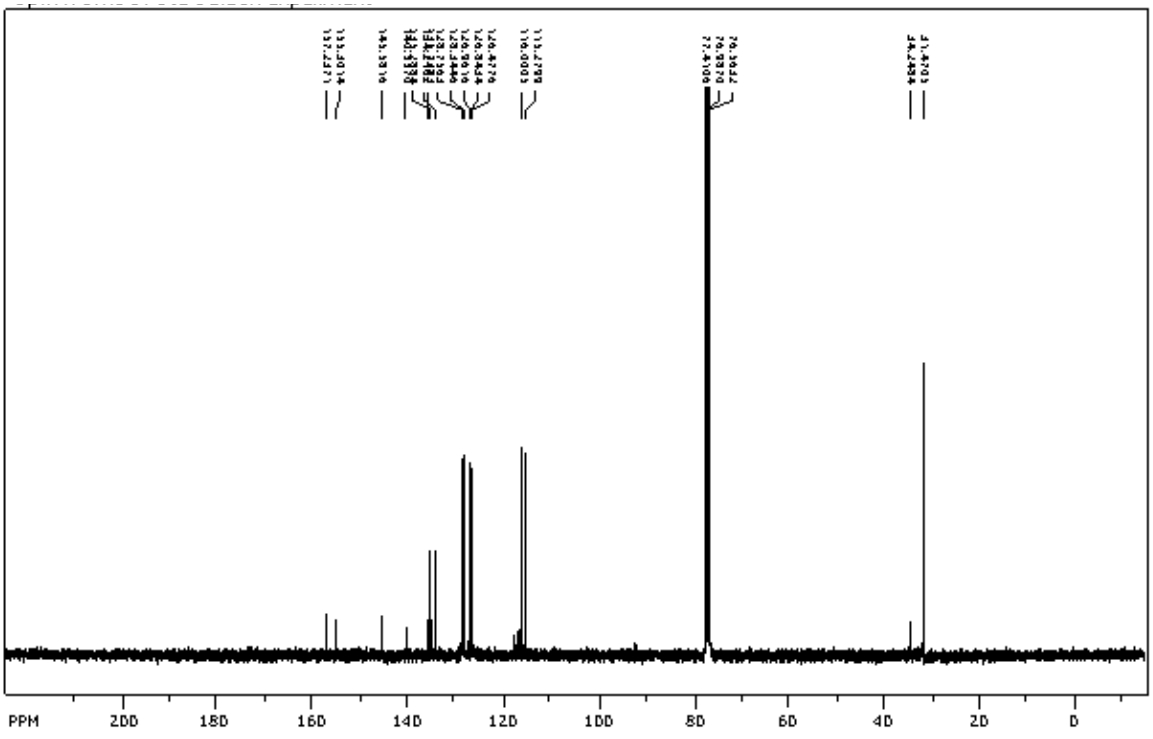
PPM
200
180
160
140
120
100
80
60
40
20
0

Figure 42

7

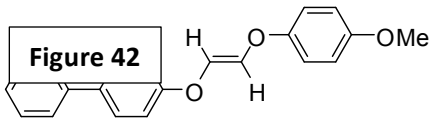
H
O
OMe
O
H

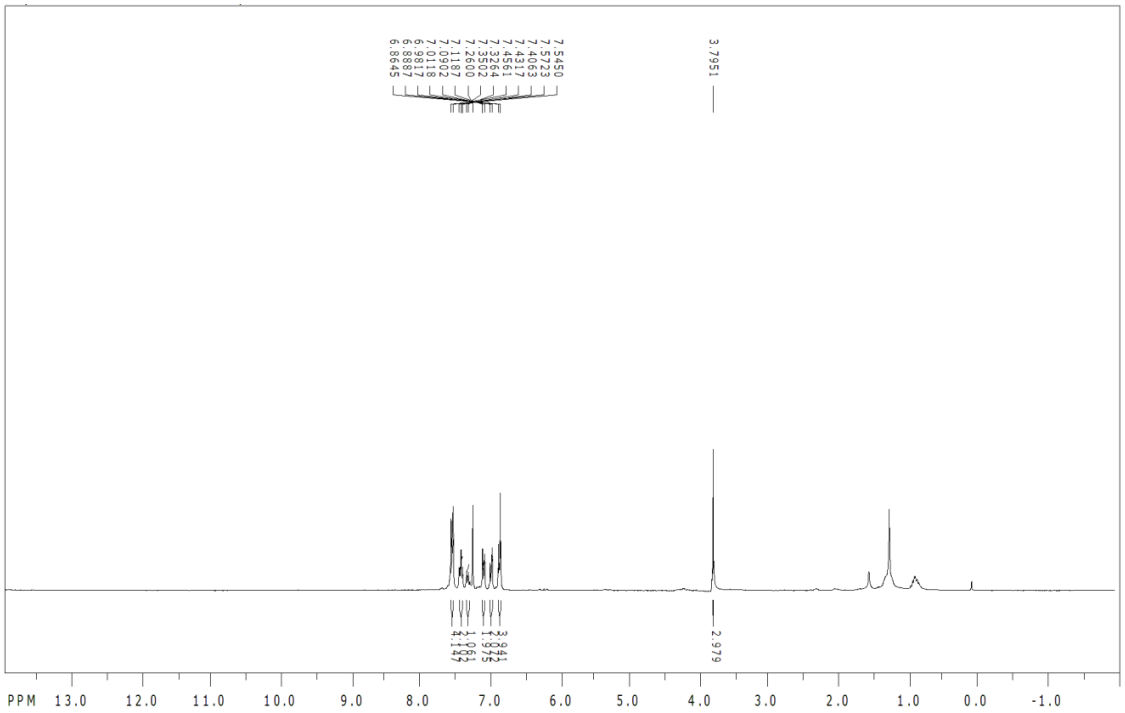
7.5450
7.5723
7.4063
7.4317
7.4561
7.3254
7.3266
7.1187
7.0982
7.0118
6.9817
6.8887
6.8645
3.7951
4.1187
1.0961
4.1967
3.9410
4.0975
2.9790
PPM 13.0 12.0 11.0 10.0 9.0 8.0 7.0 6.0 5.0 4.0 3.0 2.0 1.0 0.0 -1.0

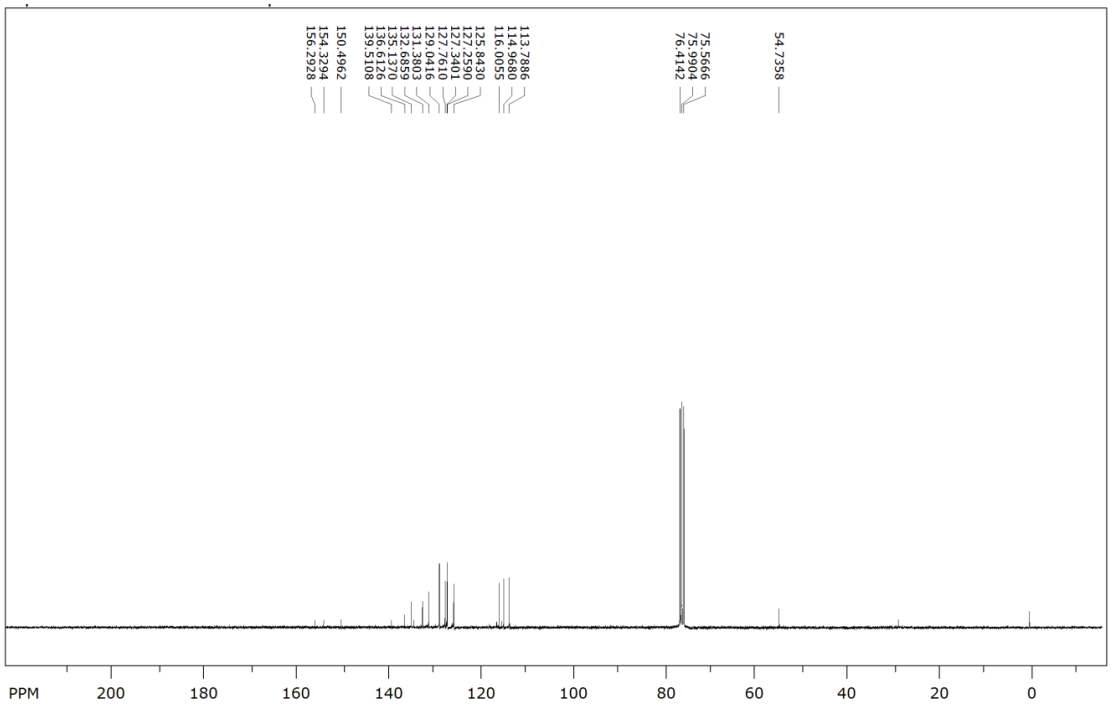
156.2928
154.3294
150.4962
139.5108
136.6126
135.1370
132.6859
131.3803
129.0416
127.7401
127.2590
125.8430
116.0055
114.9685
113.7886
76.4142
75.9904
75.5666
54.7358
PPM 200 180 160 140 120 100 80 60 40 20 0

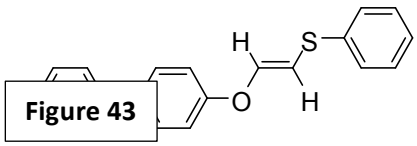
H
S
O
H

Figure 43

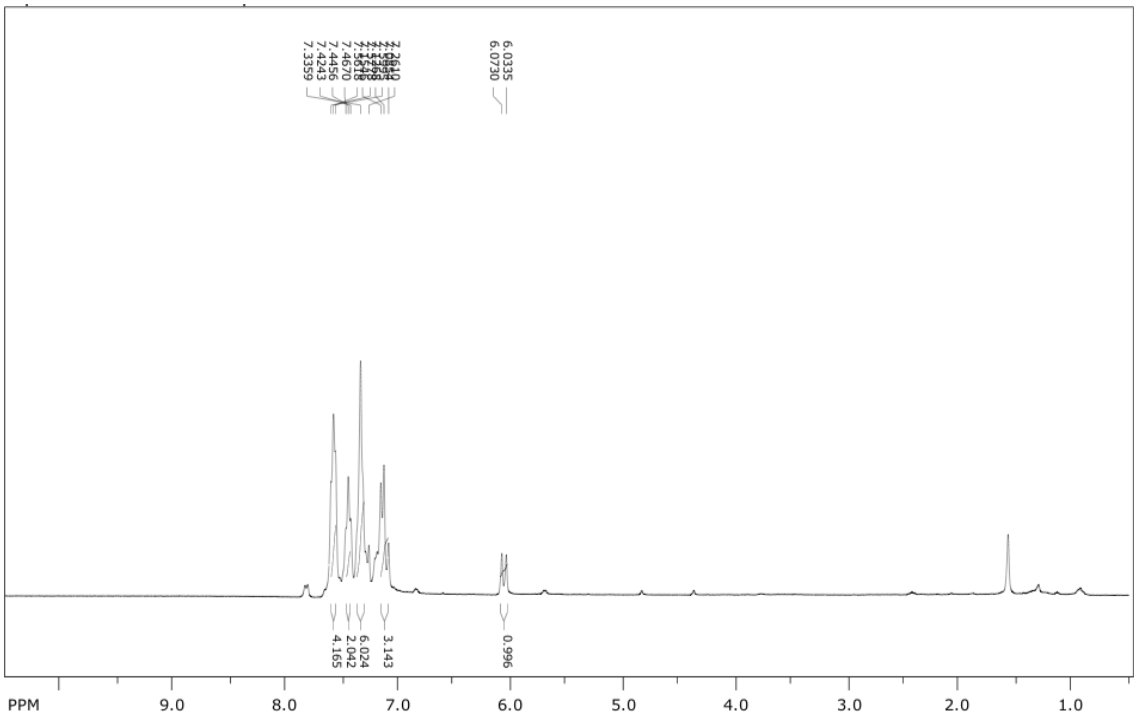
7.3359
7.4243
7.4456
7.4670
6.0335
6.0730
4.165
2.042
6.024
3.143
0.996
PPM
9.0
8.0
7.0
6.0
5.0
4.0
3.0
2.0
1.0

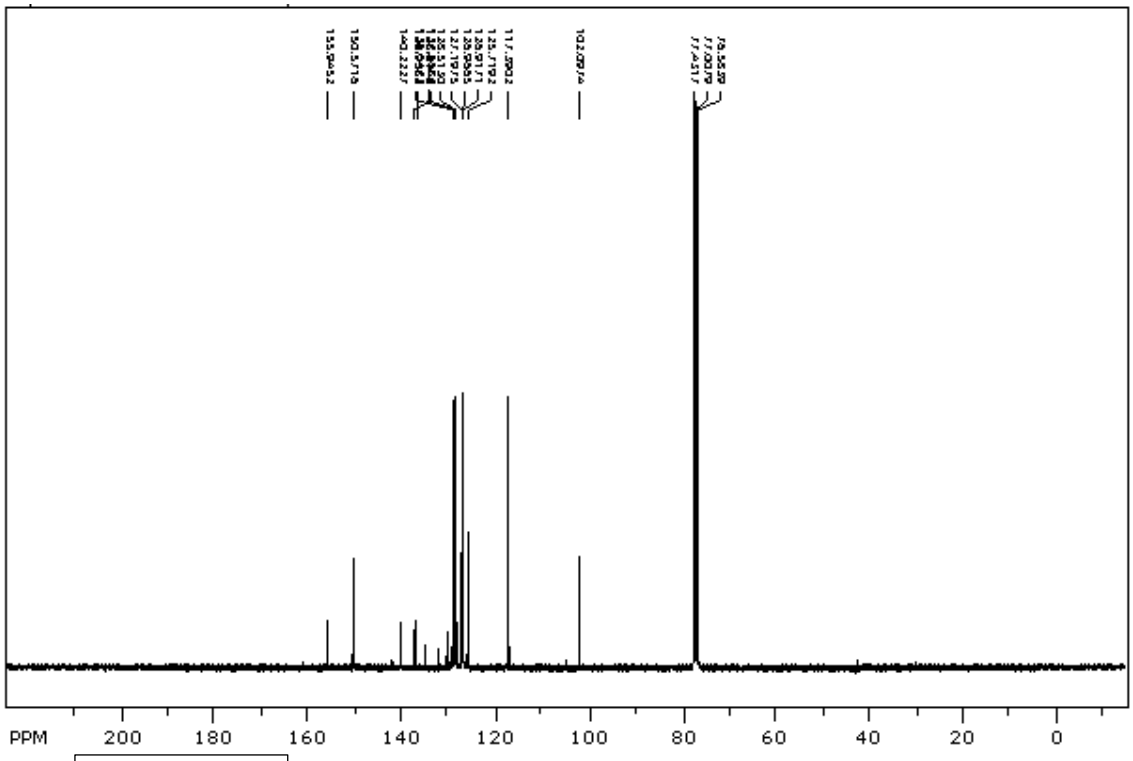
PPM
200
180
160
140
120
100
80
60
40
20
0

Figure 44

10

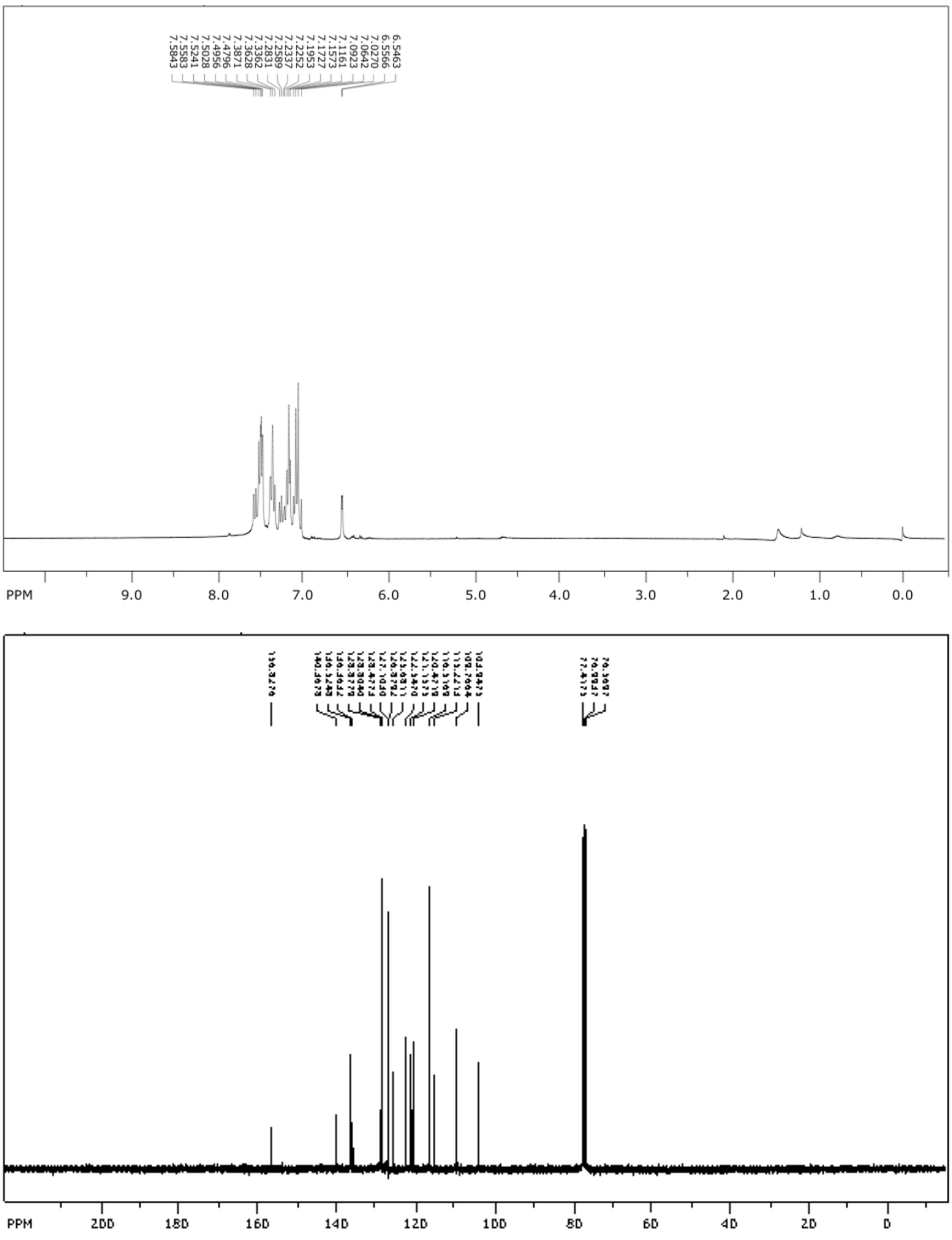
PPM
9.0
8.0
7.0
6.0
5.0
4.0
3.0
2.0
1.0
0.0
PPM
200
180
160
140
120
100
80
60
40
20
0

Figure 45

11

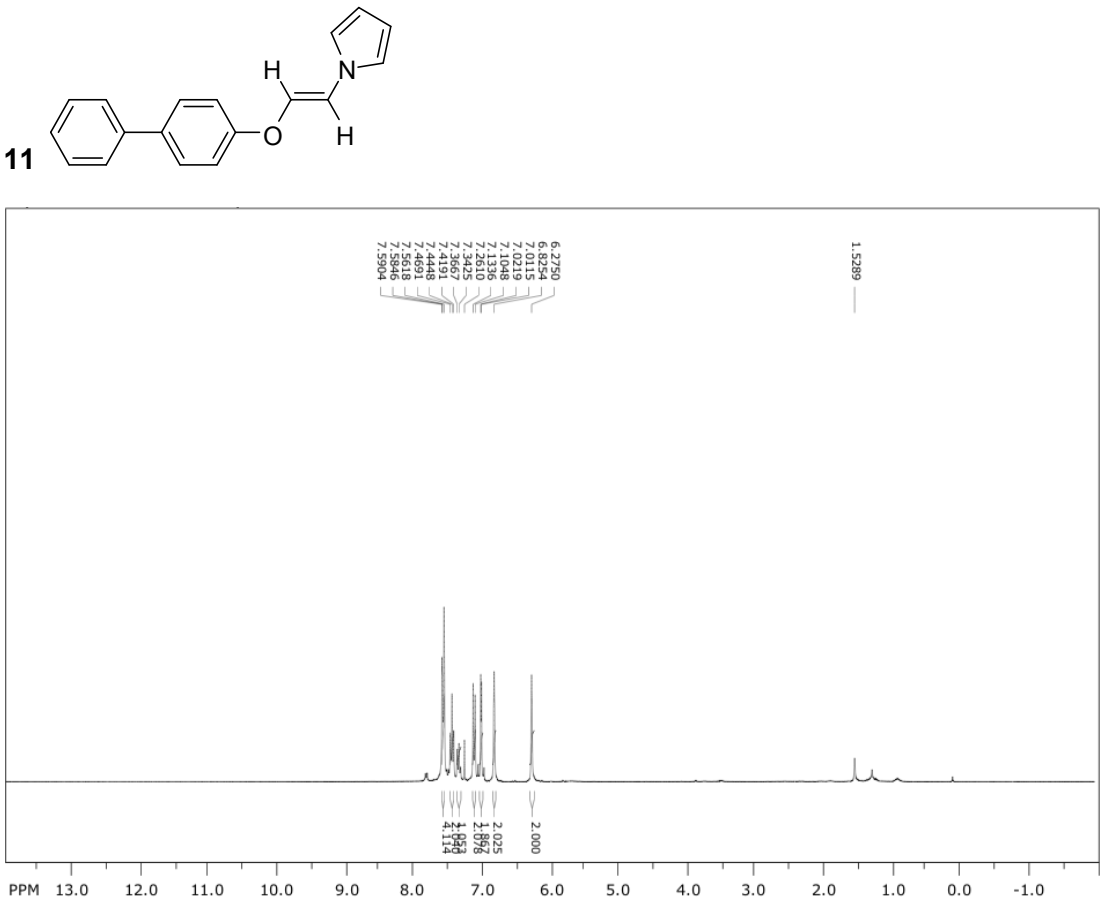
7.5904
7.5846
7.5618
7.4691
7.4448
7.3567
7.3425
7.2610
7.1336
7.1048
7.0219
7.0115
6.8254
6.2750
1.5289
4.114
1.953
2.878
2.025
2.000
PPM 13.0 12.0 11.0 10.0 9.0 8.0 7.0 6.0 5.0 4.0 3.0 2.0 1.0 0.0 -1.0

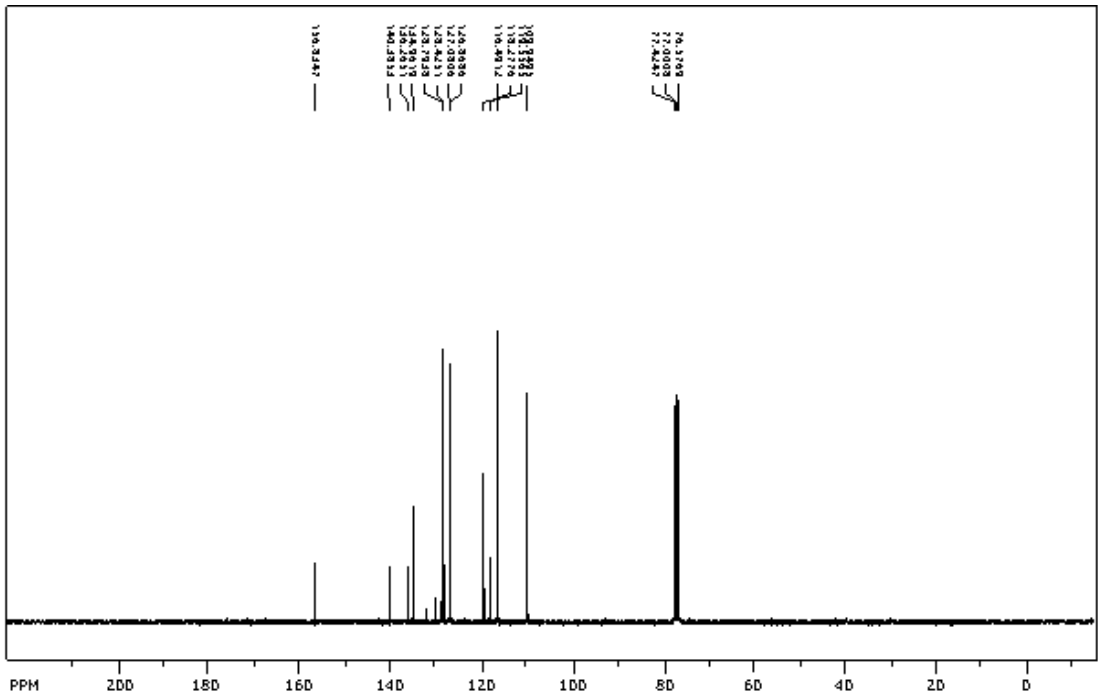
PPM 200 180 160 140 120 100 80 60 40 20 0

Figure 46

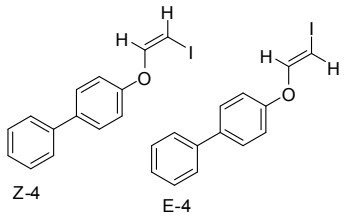
Z-4
E-4

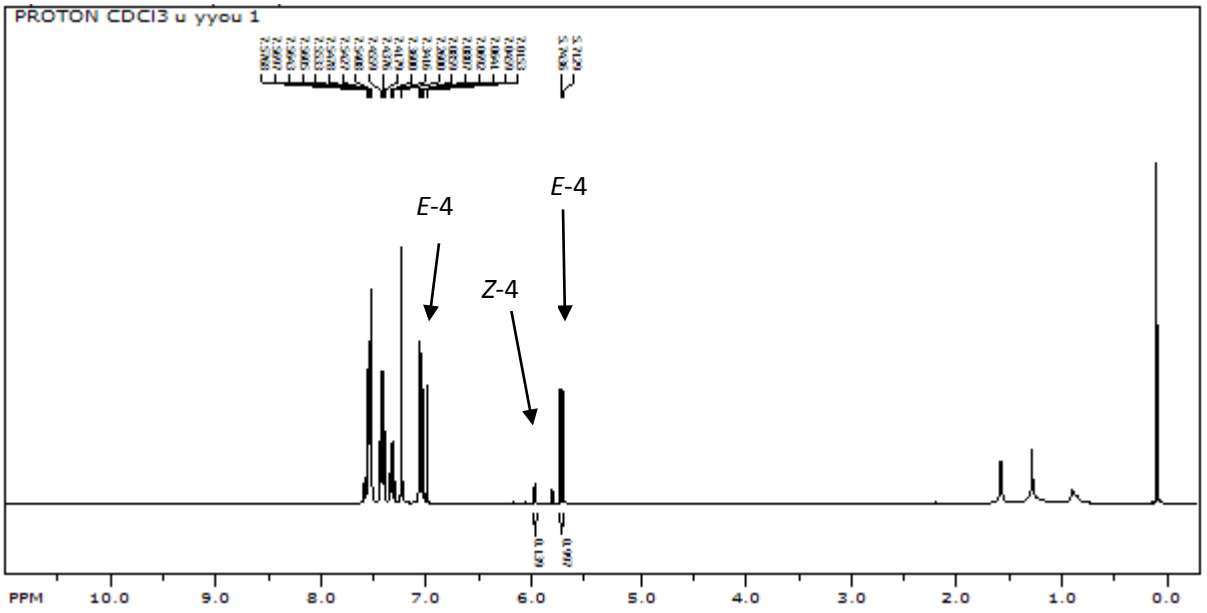
PROTON CDCl3 u yyou 1
E-4
E-4
Z-4
PPM
10.0
9.0
8.0
7.0
6.0
5.0
4.0
3.0
2.0
1.0
0.0

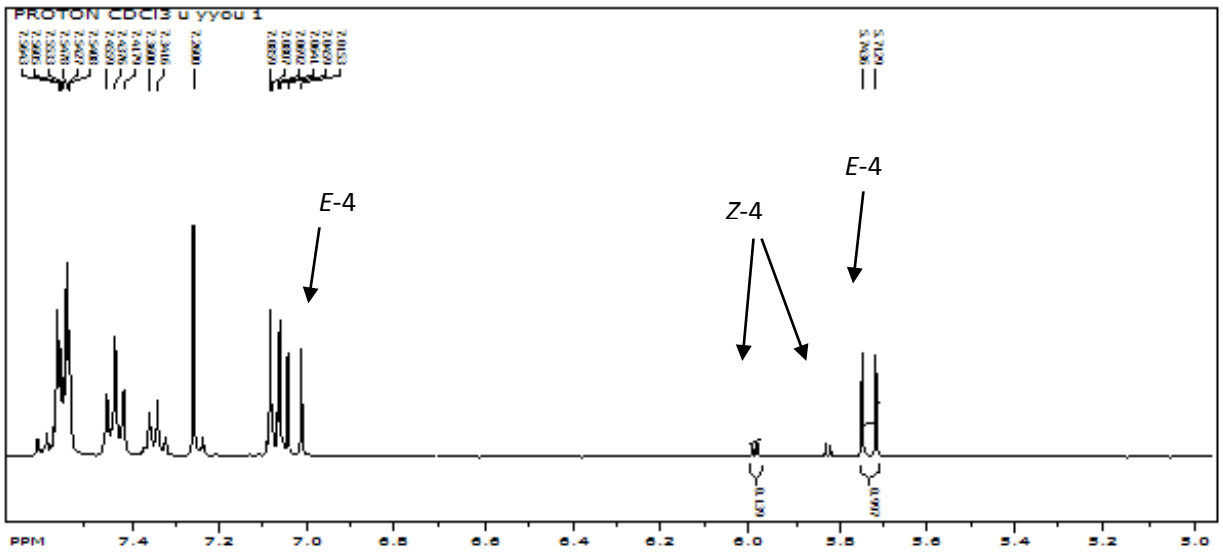
PROTON CDCl3 u yyou 1
E-4
Z-4
E-4
PPM
7.4
7.2
7.0
6.8
6.6
6.4
6.2
6.0
5.8
5.6
5.4
5.2
5.0

Figure 47

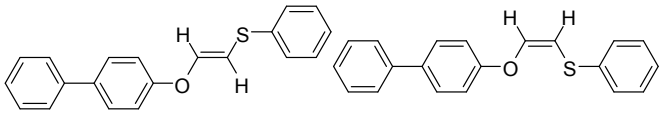

E-**8** *Z*-**8**

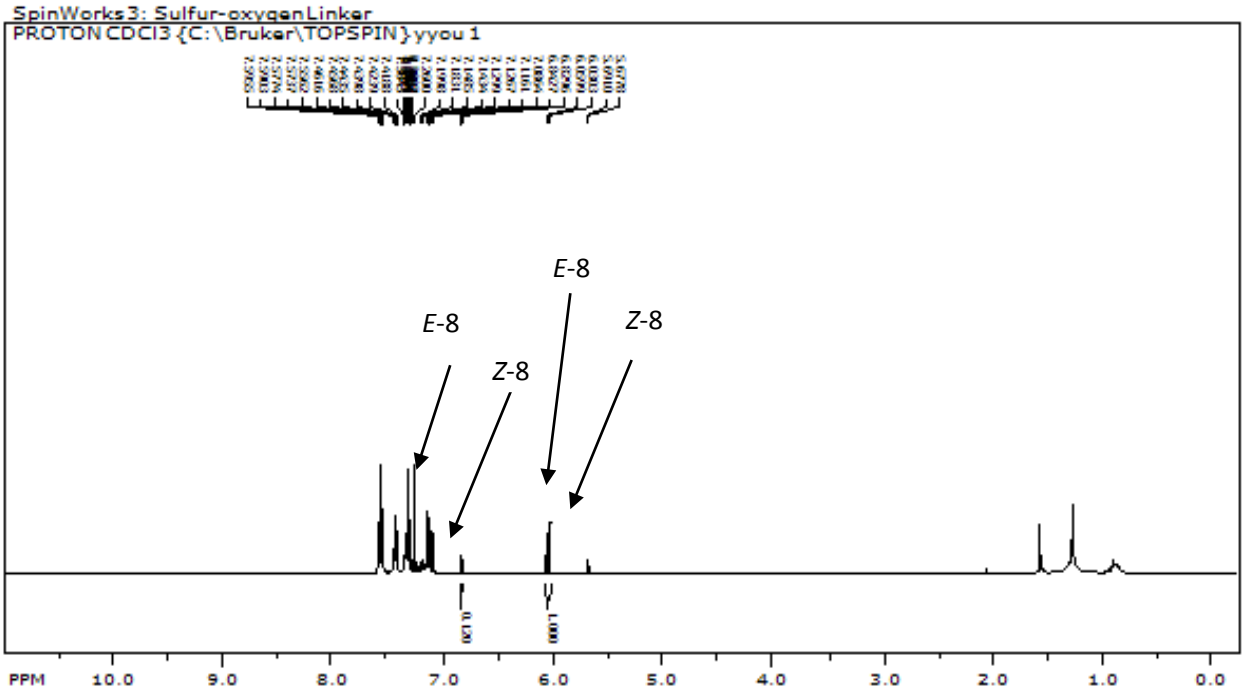

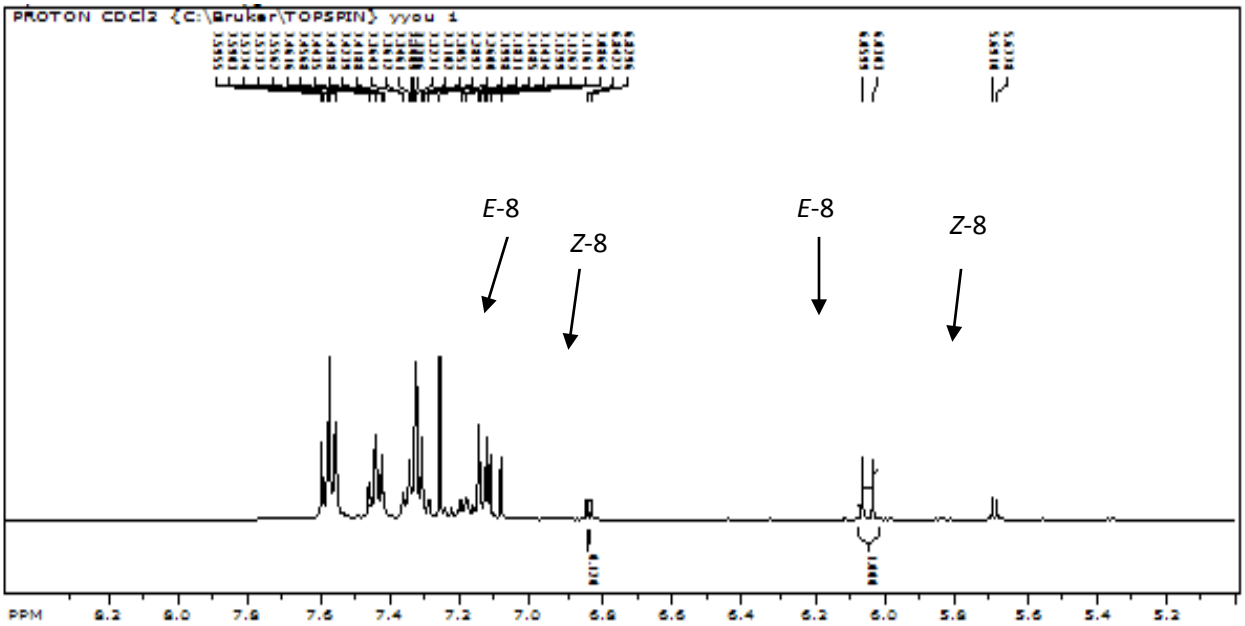

Figure 48

Table 3. Kinetic data of oxidation of olefins.

	Remaining Starting Compound (%)				Observed Product (%)			
Time (min)	**control**	**6**	**8**	**11**	**Ca**	**(6a+6b)/2***	**8a**	**8b**
0	100	100	100	100	0	0	0	0
5	38	26	29	27	0	53	67	32
10	11	2	0	0	1	87	99	48
15	0	0	0	0	2	92	99	48

* In 1H-NMR, the formate peaks of expected products of **6** (**6a** and **6b**) were too close. Thus, two peaks were integrated together and divided by 2.

Figure 49: Kinetic NMR Spectra of Control

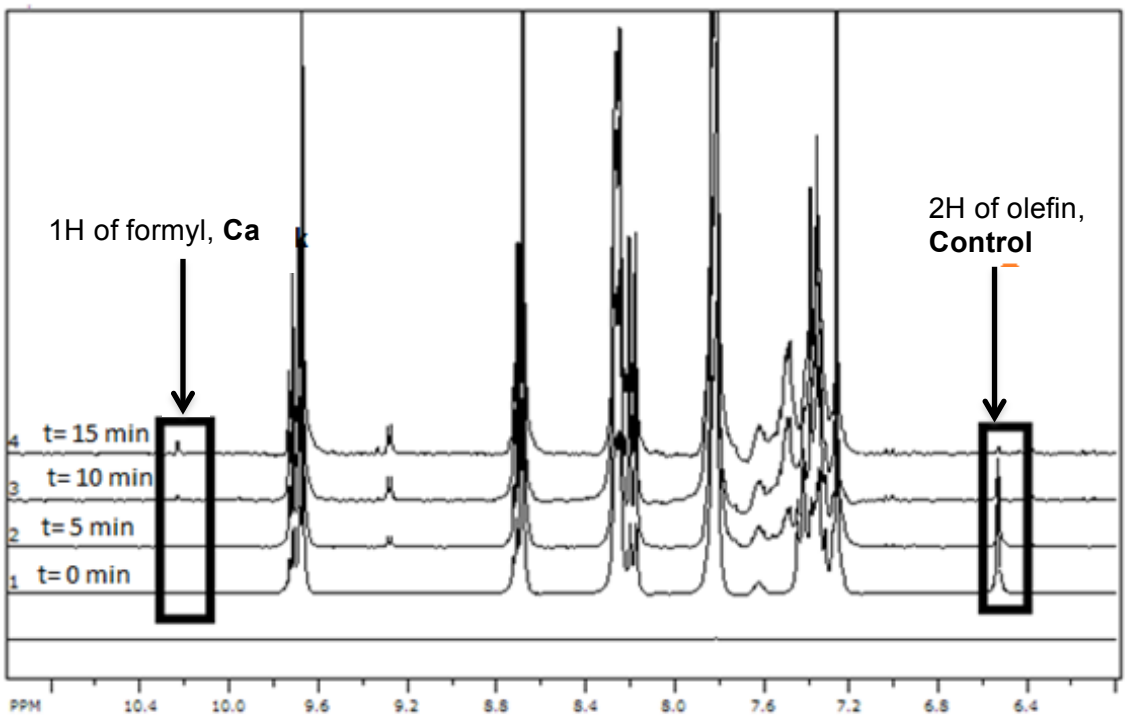

Figure 49: Kinetic NMR spectra of **6**

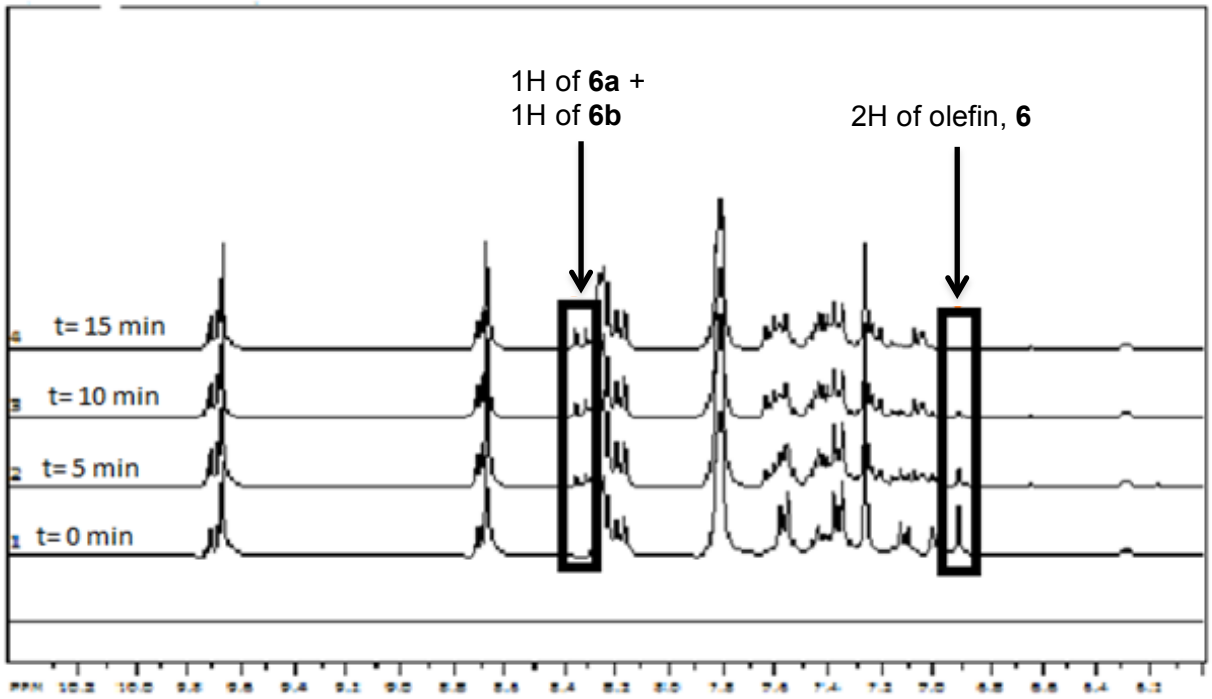

Figure 50: Kinetic NMR spectra of **8**

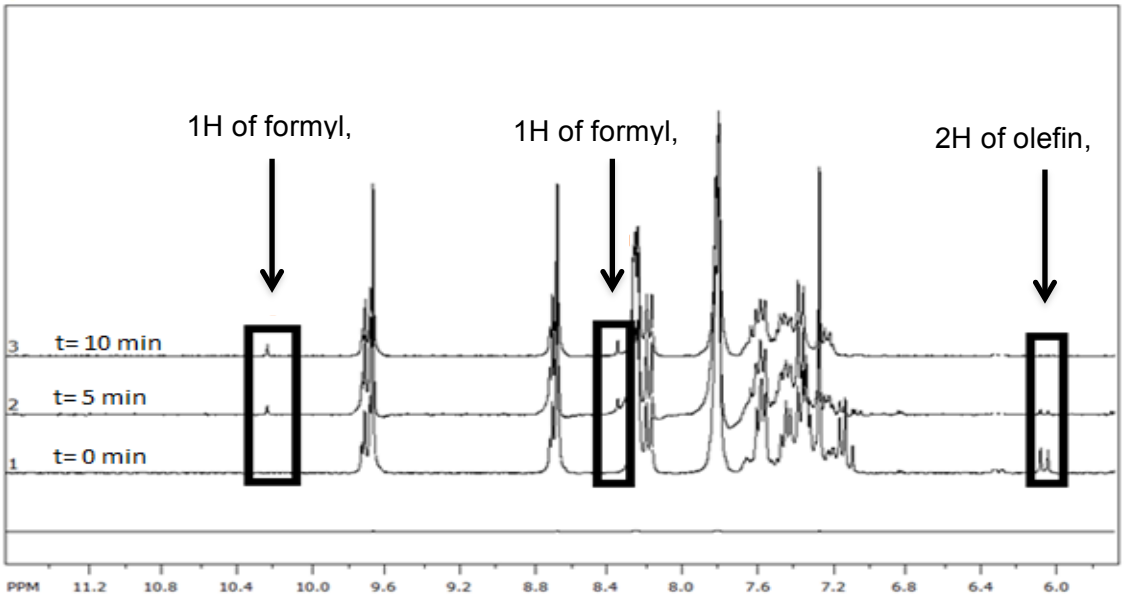

Figure 51: Kinetic NMR spectra of **11**

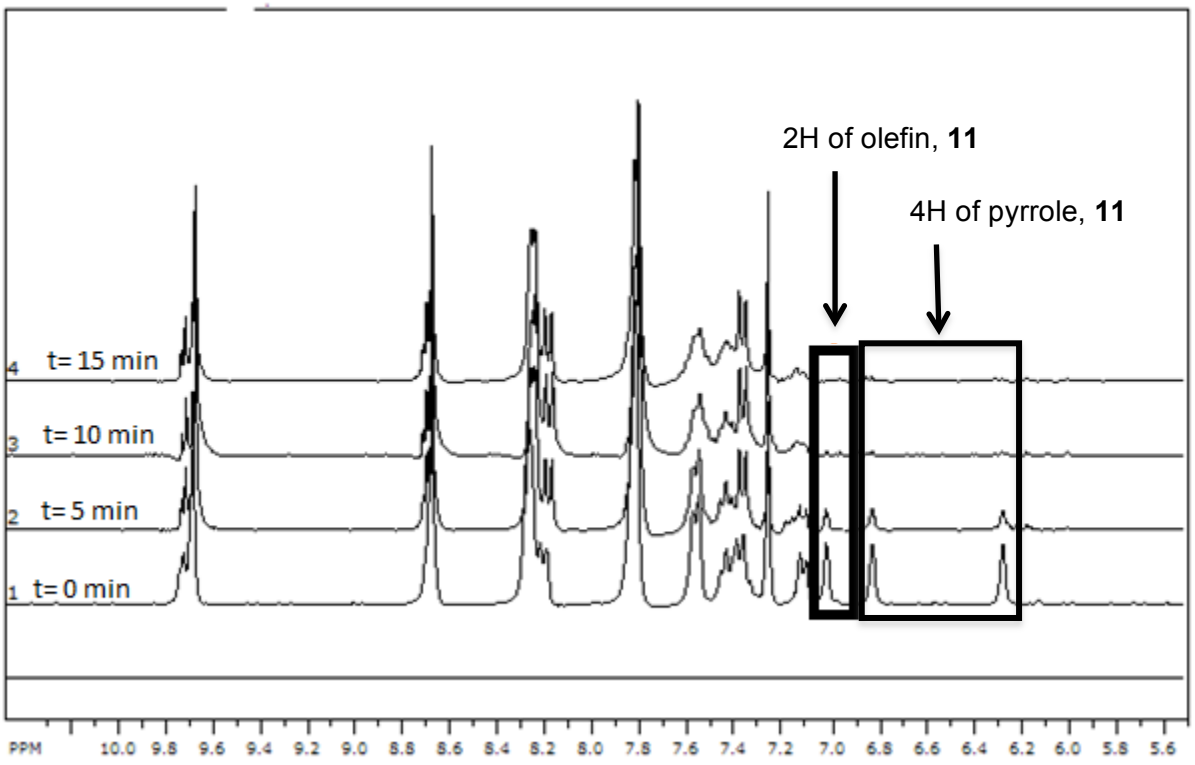

Figure 52

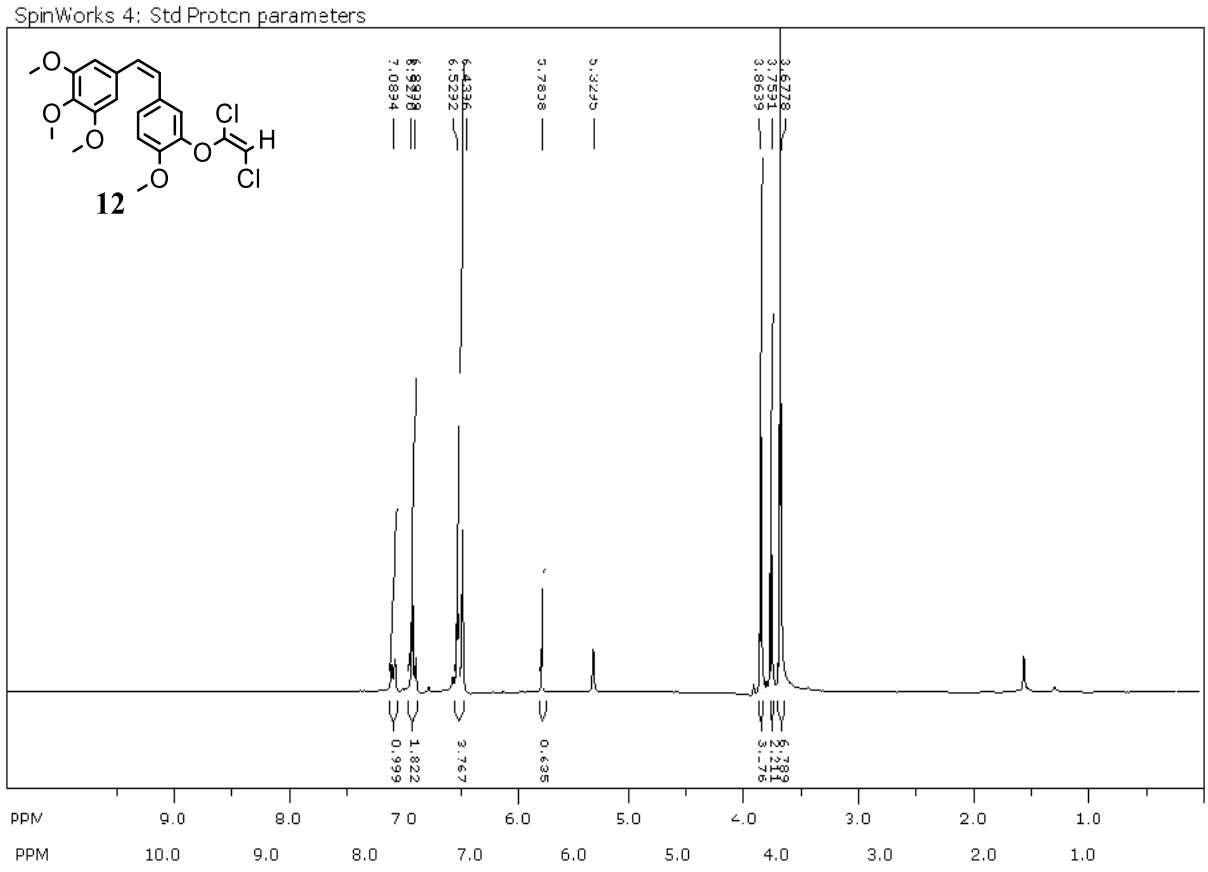
SpinWorks 4: Std Protcn parameters
12
Cl
H
Cl
O
O
O
O
7.0894
6.8838
6.8670
6.5292
5.7838
5.3295
3.8639
3.7531
3.6778
0.999
1.822
3.767
0.635
3.178
2.211
6.789
PPM
9.0
8.0
7.0
6.0
5.0
4.0
3.0
2.0
1.0
PPM
10.0
9.0
8.0
7.0
6.0
5.0
4.0
3.0
2.0
1.0

Figure 54

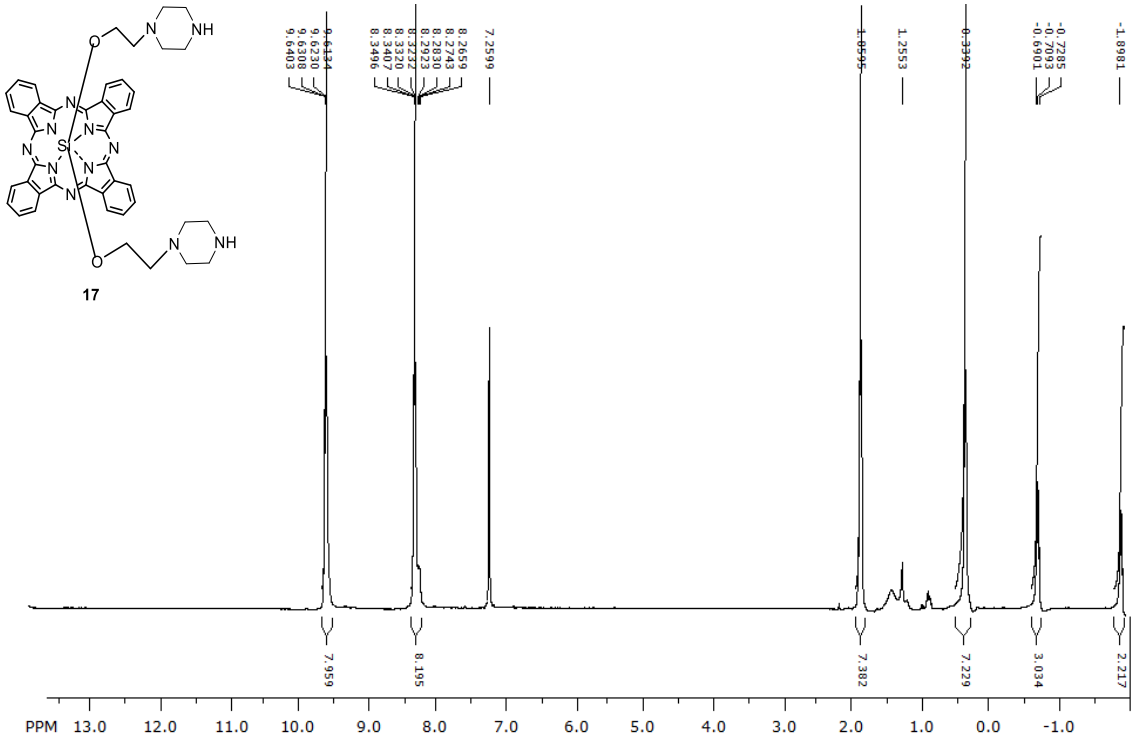

Figure 56

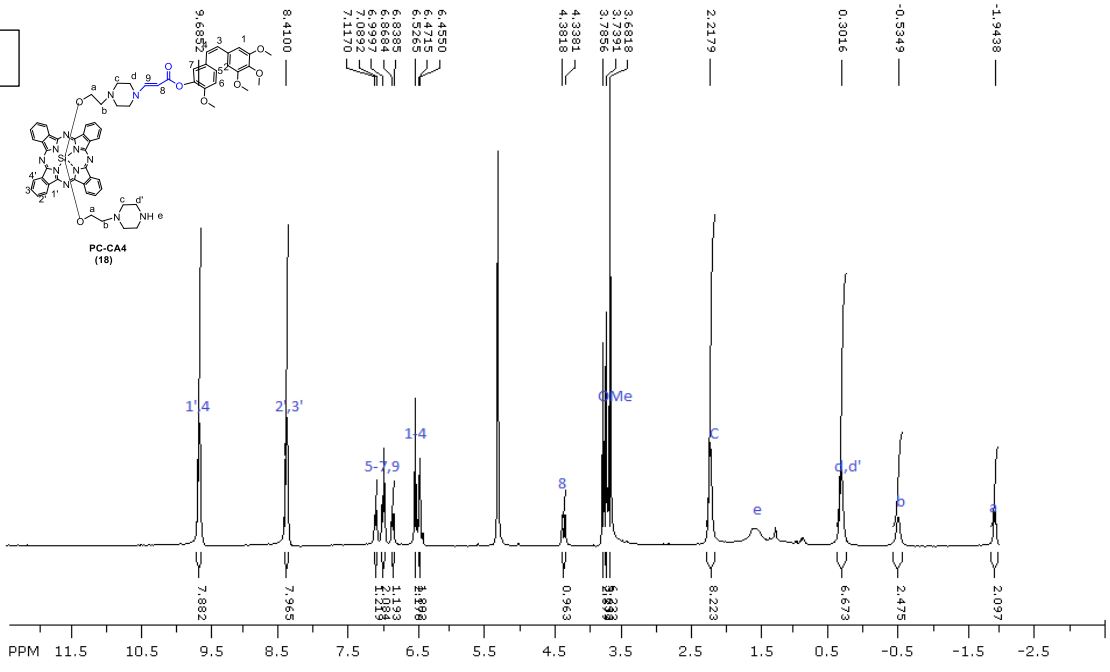

Figure 57: ^{1}H NMR of FA-PC-CA4

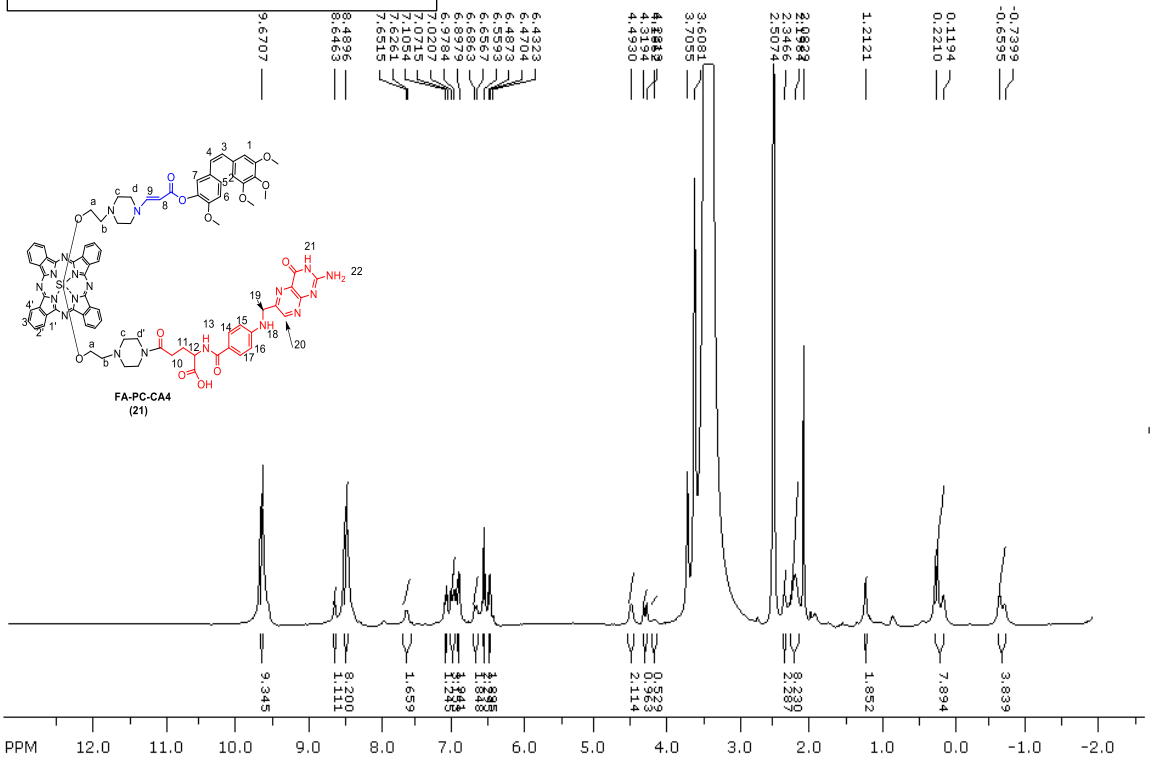

Figure 58 HRMS of FA-PC-CA4

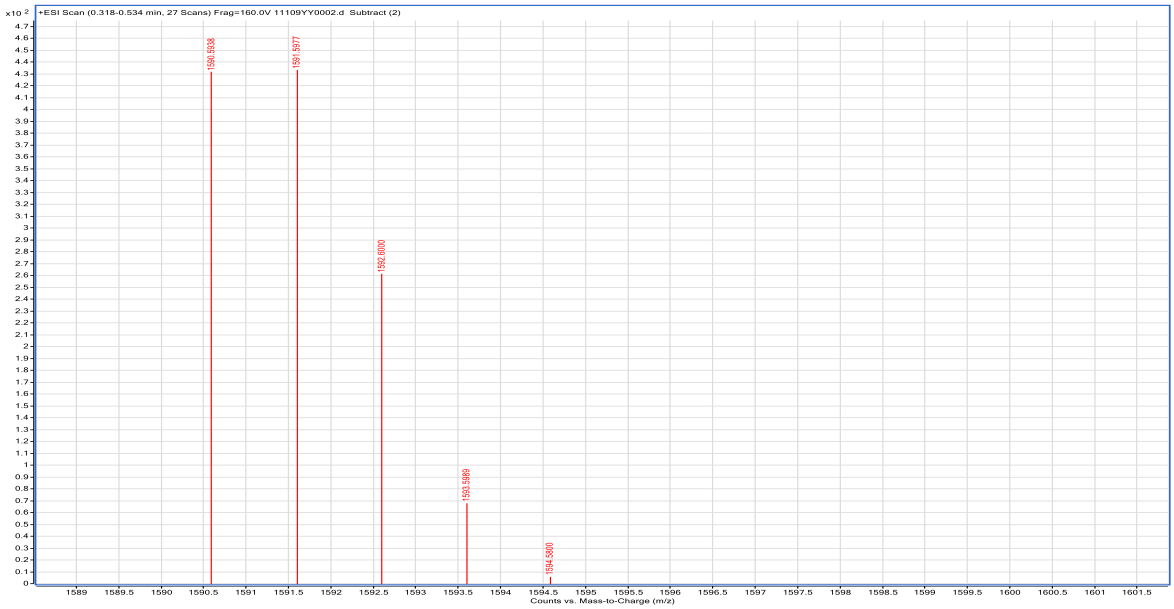

Figure 58: HPLC of FA-PC-CA4

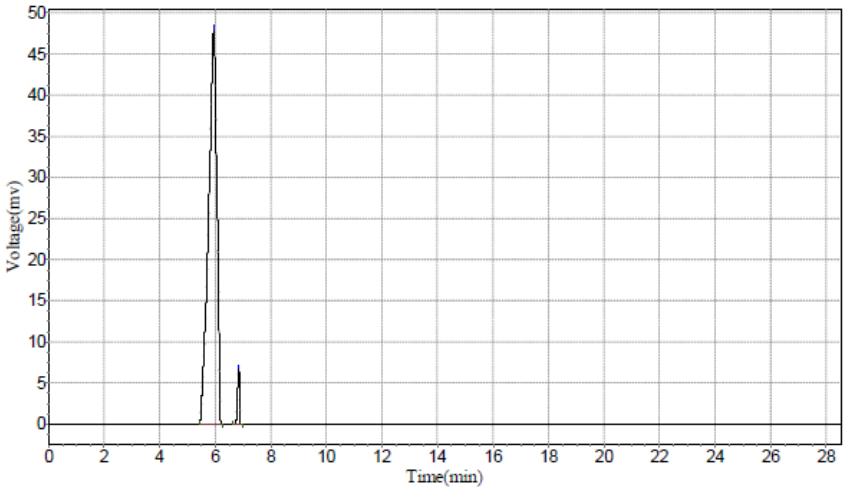

Results

Peak No.	Peak ID	Ret Time	Height	Area	Conc.
1		5.940	47965.398	1001771.625	96.2589
2		6.848	6831.381	38933.301	3.7411
Total			54796.779	1040704.926	100.0000

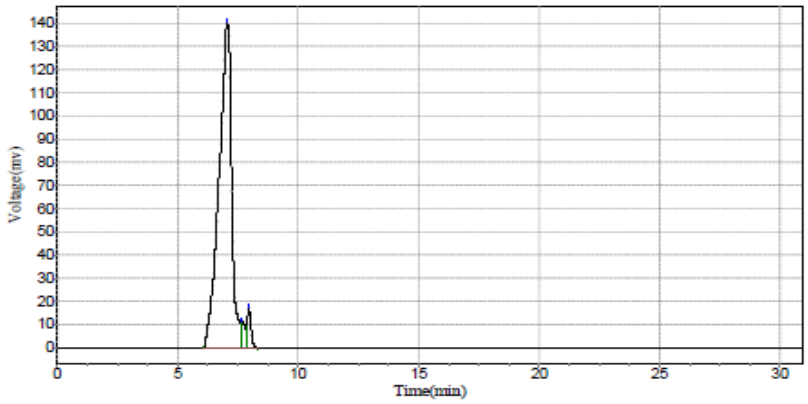

Results

Peak No.	Peak ID	Ret Time	Height	Area	Conc.
1		7.040	140291.438	5093423.500	94.0081
2		7.665	11172.711	145596.516	2.6872
3		7.948	17850.838	179045.891	3.3046
Total			169314.986	5418065.906	100.0000

Figure 60: NMR or FA-PEG2-PC-CA4

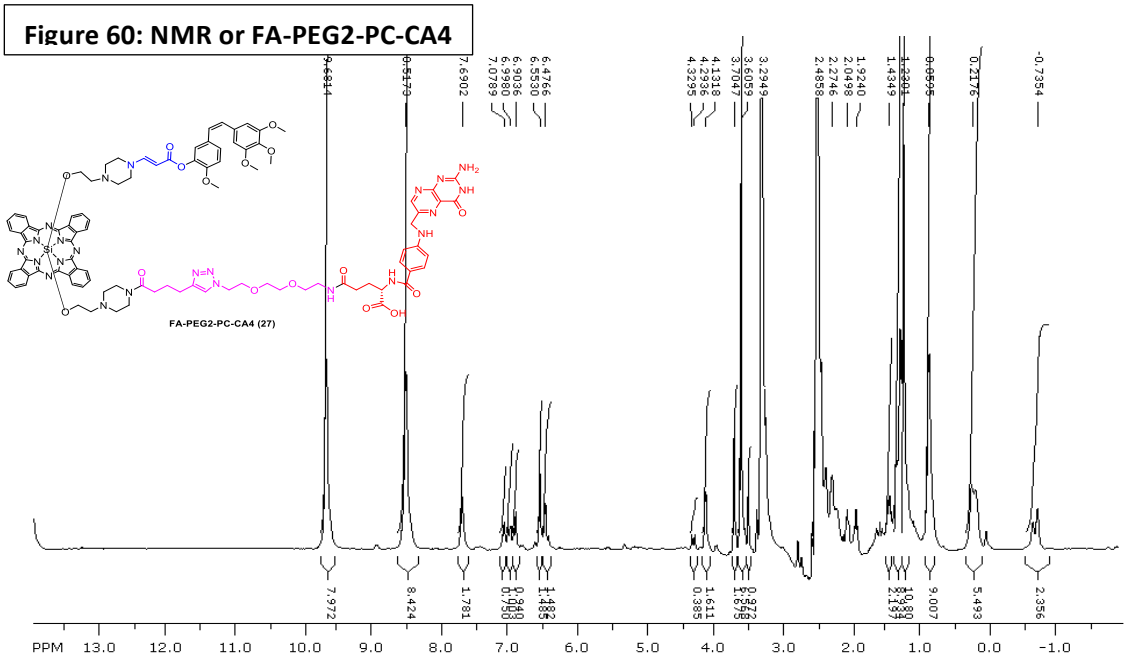

Figure 60: Mass Spec of FA-PEG2-PC-CA4

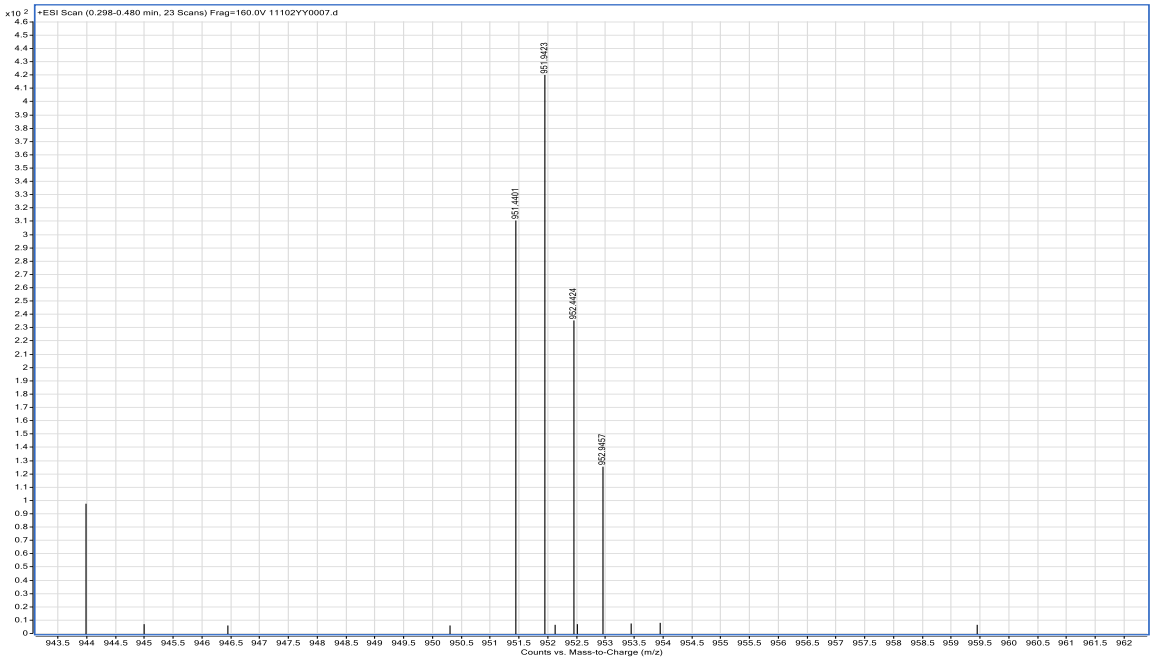

Figure 62: HPLC chromatogram of FA-PEG2-PC-CA4

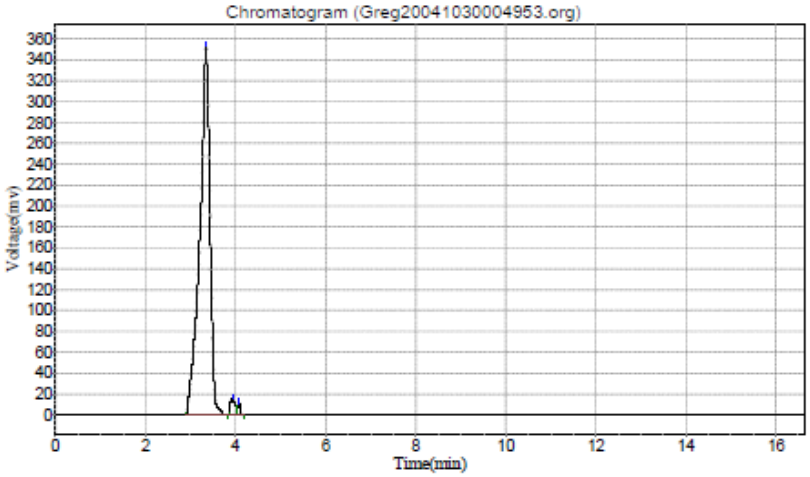

Results

Peak No.	Peak ID	Ret Time	Height	Area	Conc.
1		3.348	355075.969	5549544.500	97.0861
2		3.932	16456.631	129944.125	2.2733
3		4.073	11506.306	36620.211	0.6406
Total			383038.905	5716108.836	100.0000

Figure 62: NMR of FA-PEG2K-PC-CA4

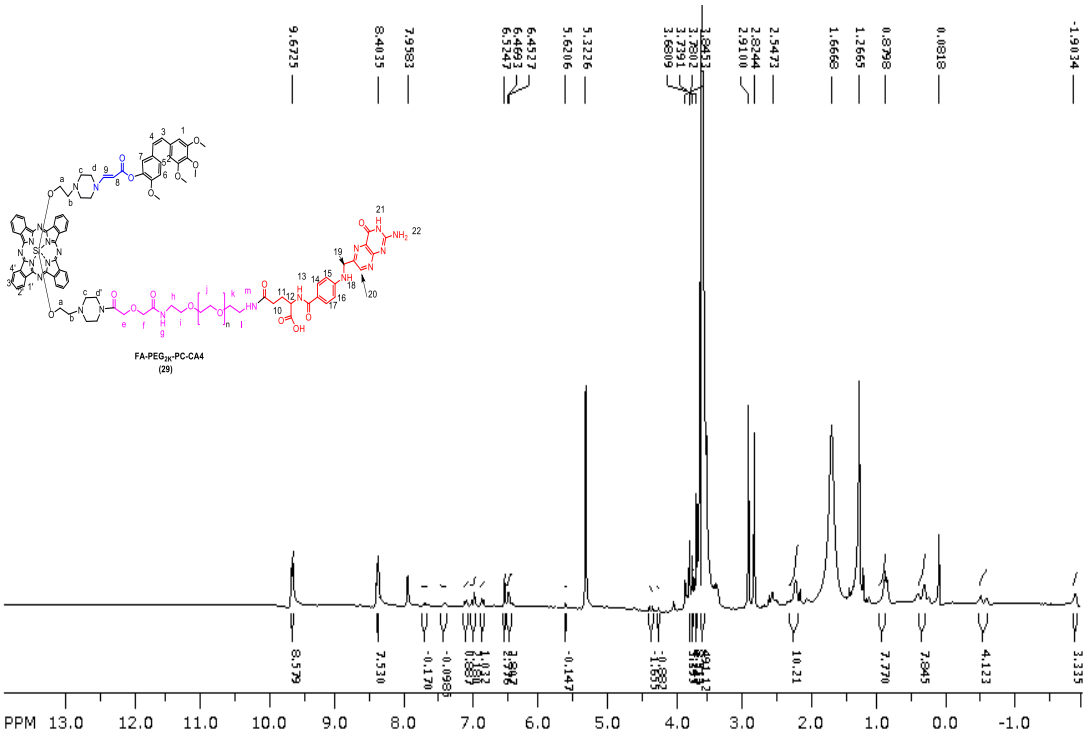

Figure 63: NMR of Compound 28

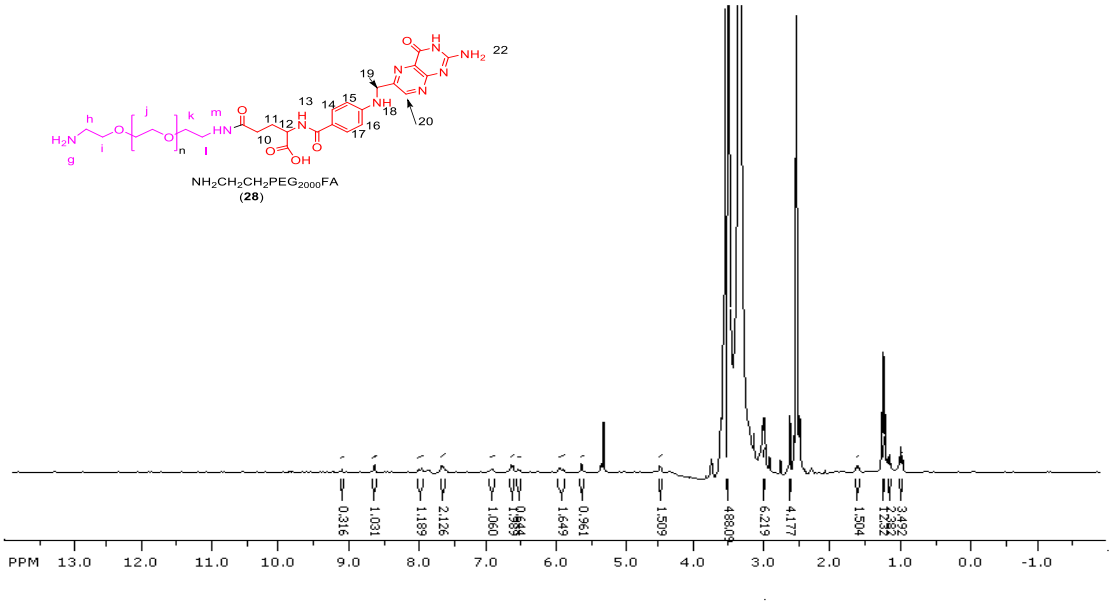

Figure 64: Stacked NMR of FA-PEG2000-NH2 (28) and FA-PEG2K-PC-CA4

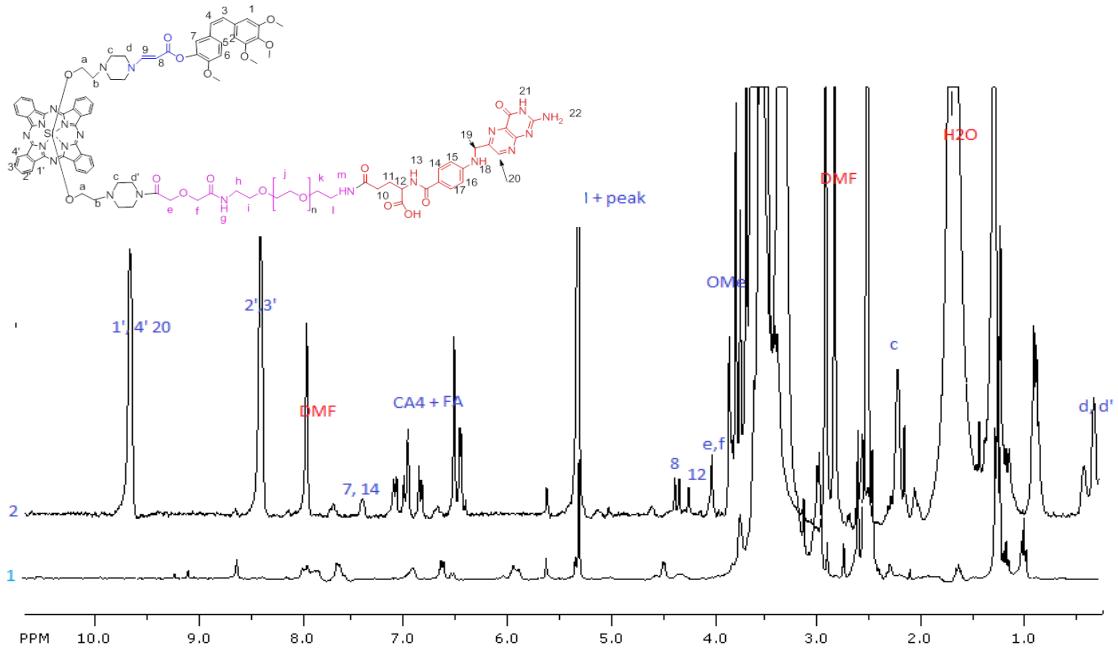

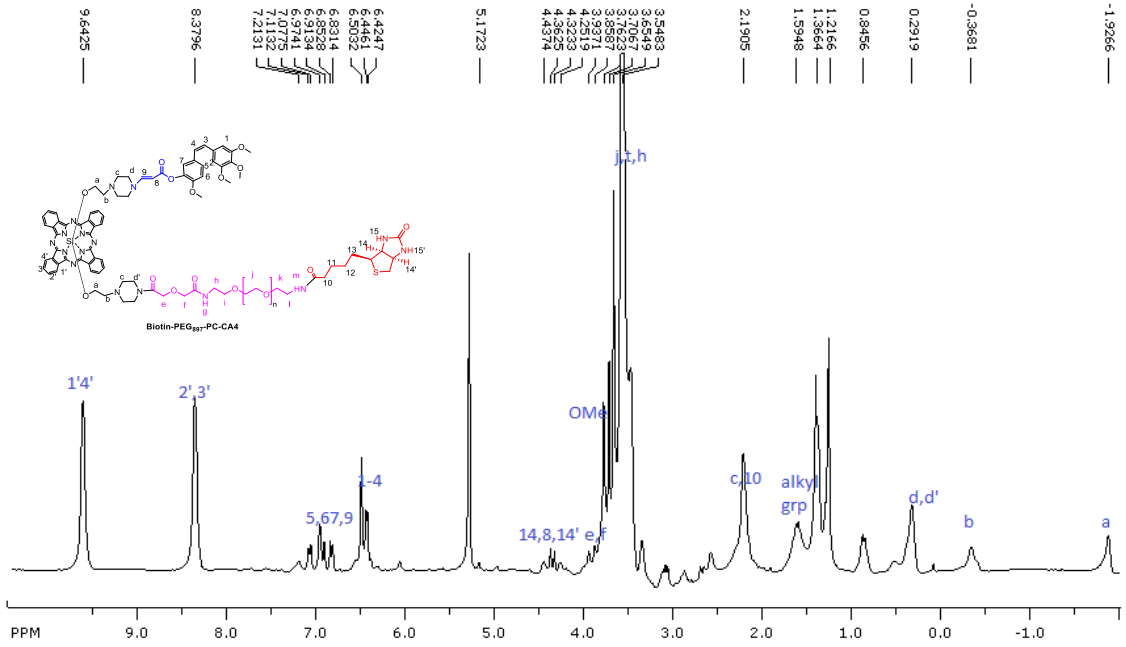

Figure 65: NMR of Biotin-PEG-PC-CA4

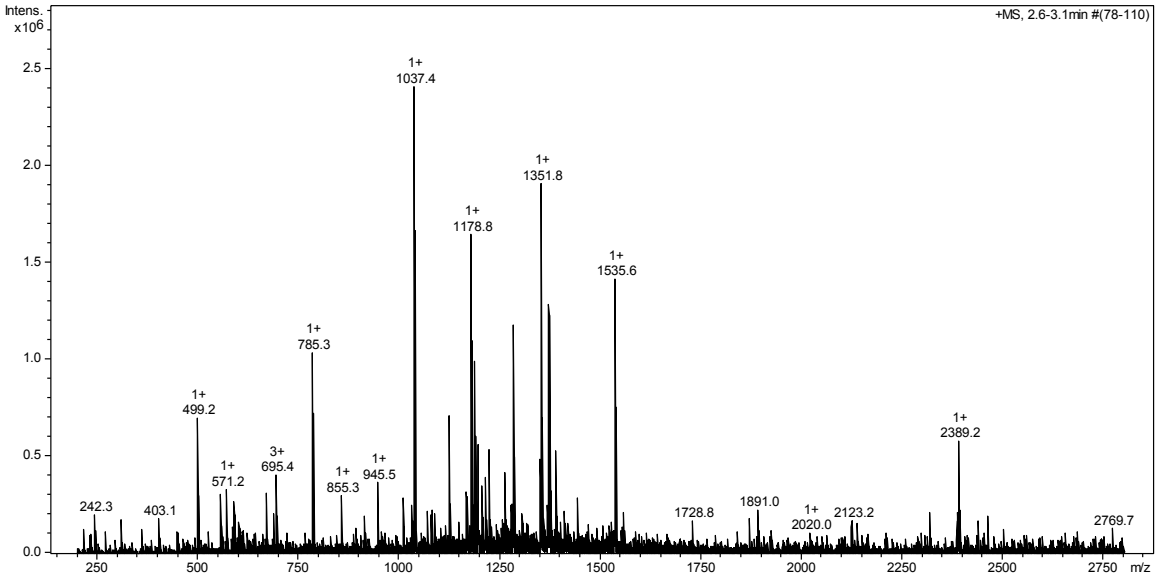

Figure 66: ESI (Ion trap) of Biotin-PEG897-PC-CA4

Figure 67: Stacked NMRs of Boc-PEG897-Biotin and Biotin-PEG897-PC-CA4

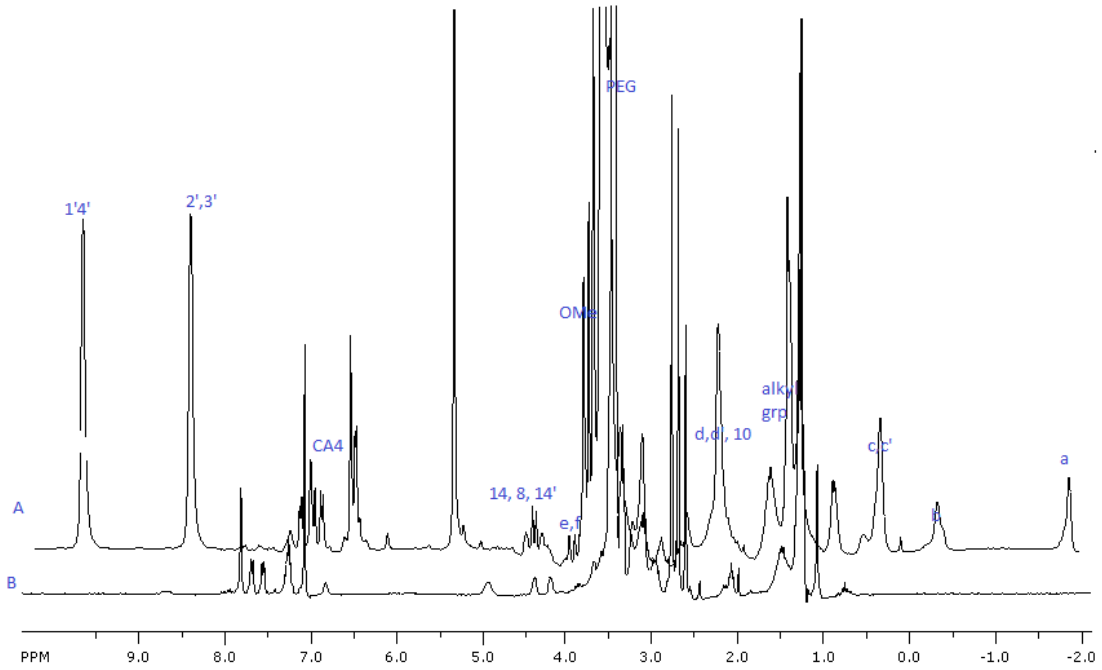

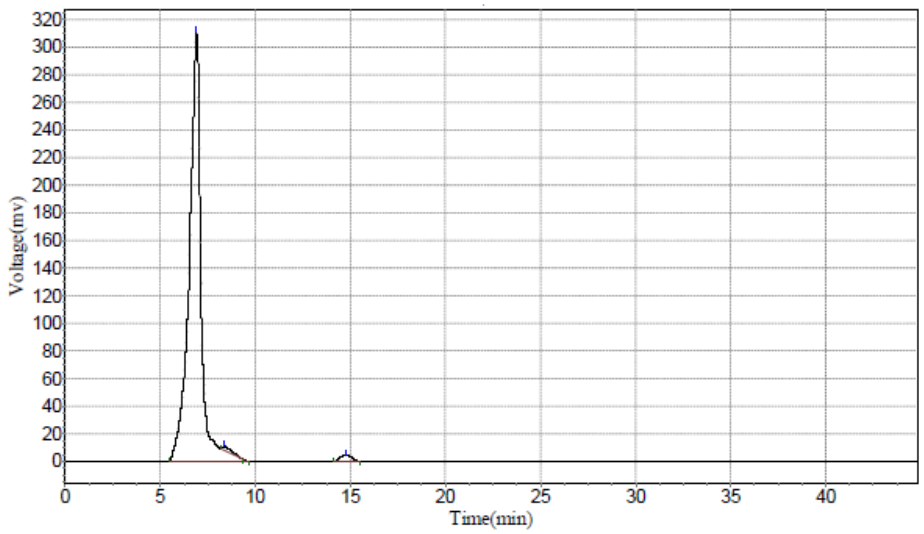

Results

Peak No.	Peak ID	Ret Time	Height	Area	Conc.
1		6.907	311290.656	13409531.000	97.9027
2		8.390	3366.042	101677.000	0.7423
3		14.790	4155.000	185592.000	1.3550
Total			318811.698	13696800.000	100.0000

Figure 68: HPLC of Biotin-PEG897-PC-CA4

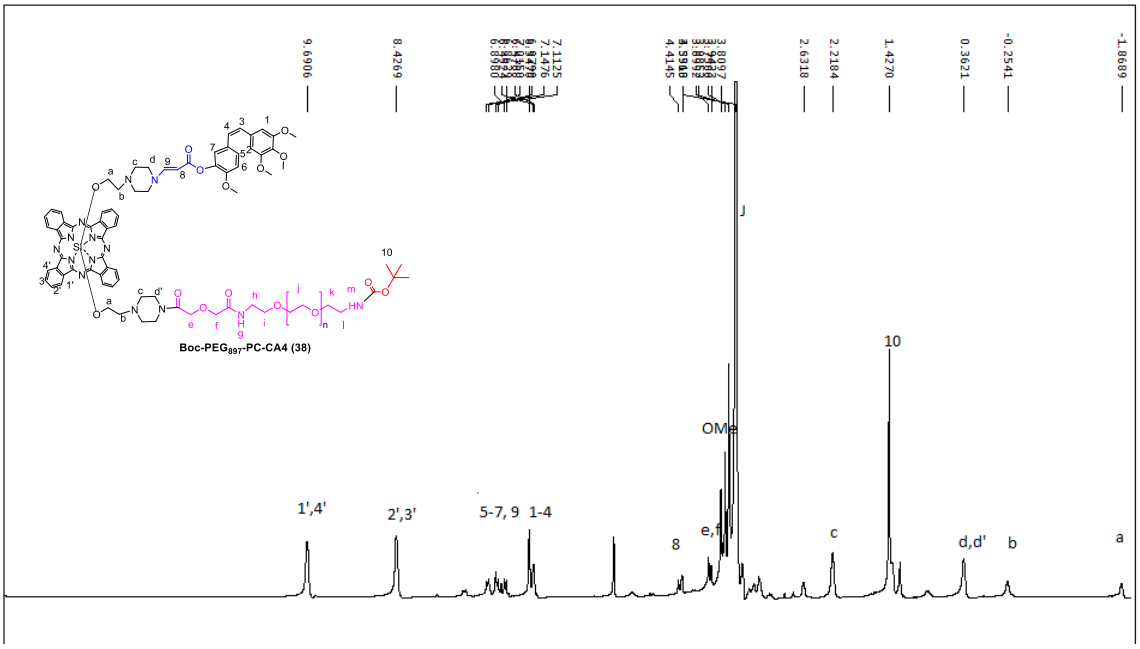

Figure 69: NMR of Boc-PEG897-PC-CA4

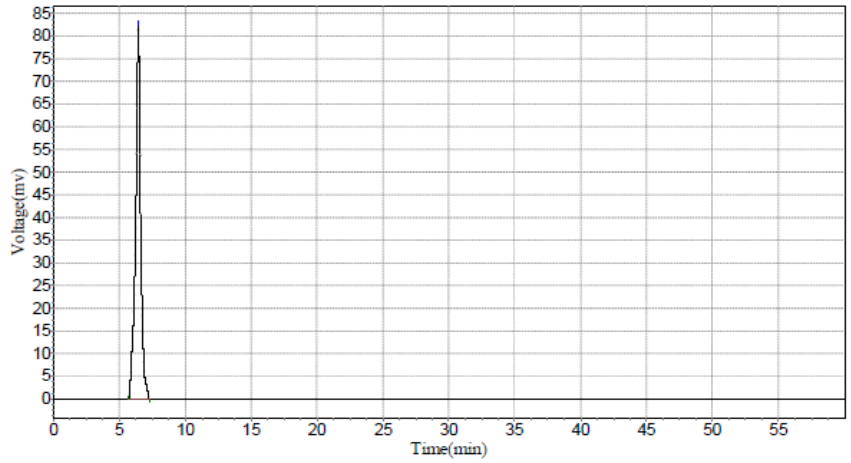

Results

Peak No.	Peak ID	Ret Time	Height	Area	Conc.
1		6.440	82370.523	2283782.500	100.0000
Total			82370.523	2283782.500	100.0000

Figure 70: HPLC of Boc-PEG897-PC-CA4

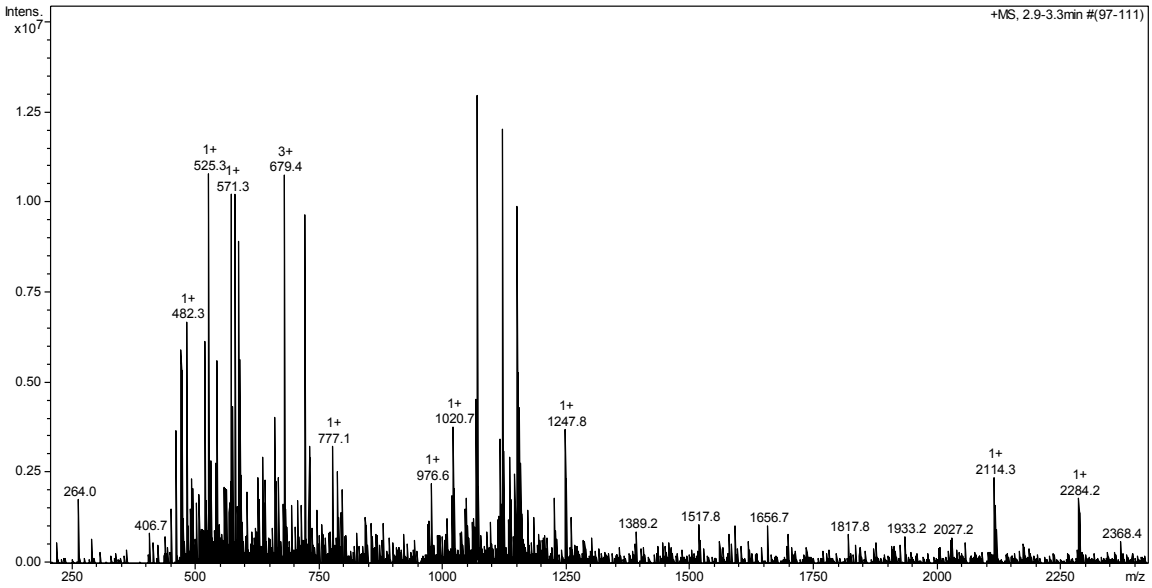

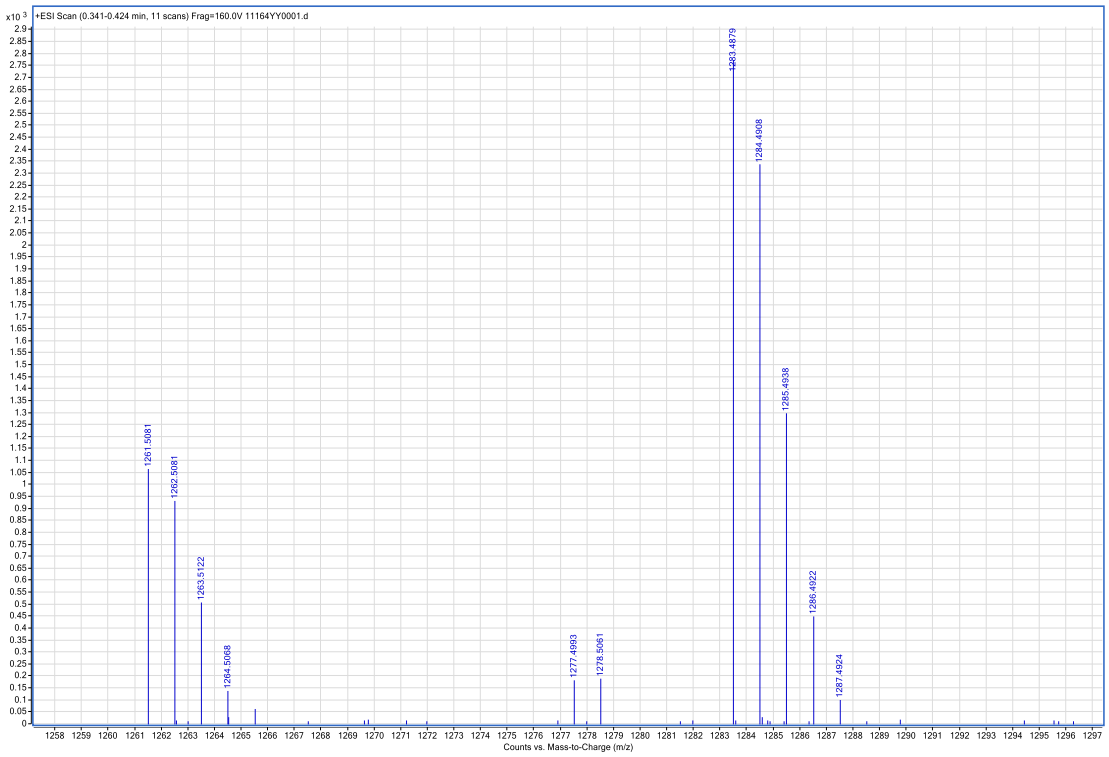

Figure 71: HRMS-ESI or Boc-PEG897-PC-CA4

Figure 73: ^{1}H-NMR FA-PEG897-PC-CA4

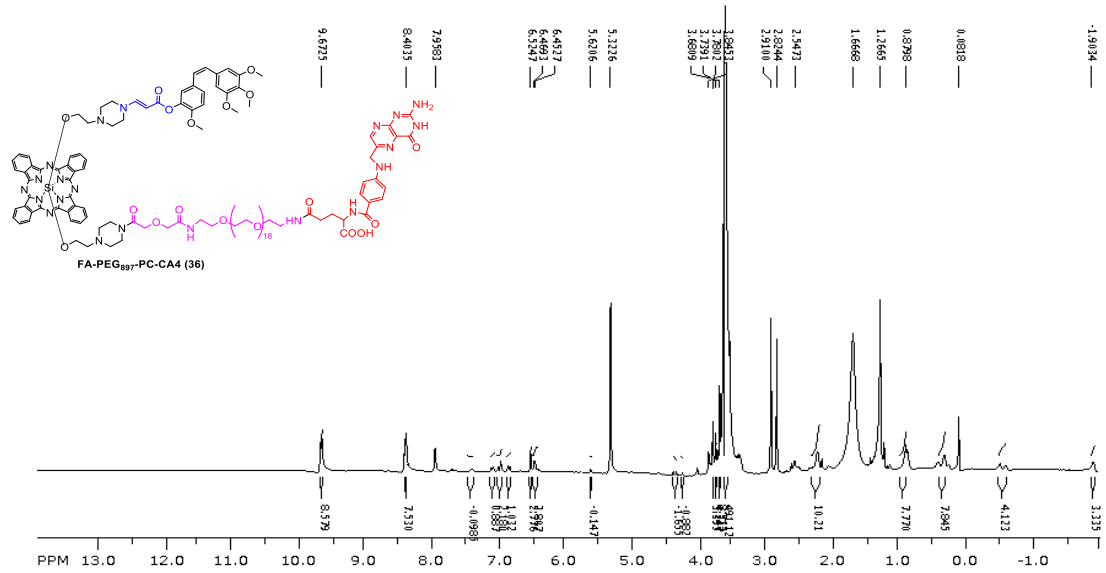

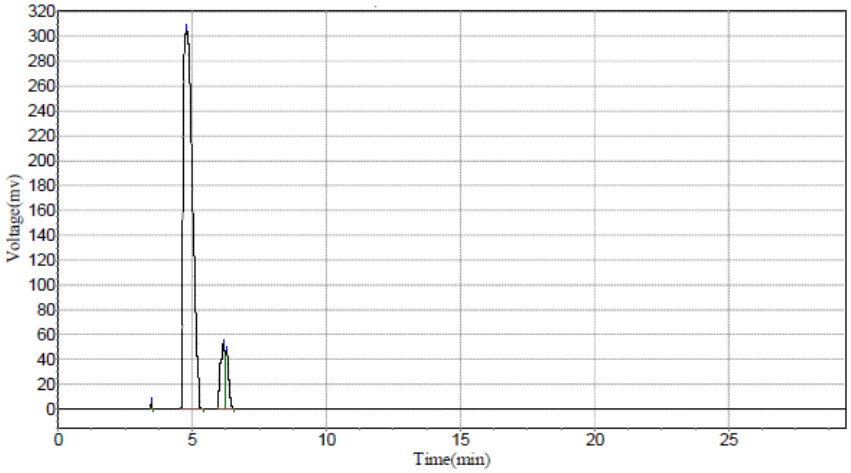

Results

Peak No.	Peak ID	Ret Time	Height	Area	Conc.
1		3.465	5709.000	14762.400	0.1774
2		4.782	306122.813	7286394.000	87.5451
3		6.157	52182.656	622986.875	7.4851
4		6.273	47067.473	398874.313	4.7924
Total			411081.941	8323017.588	100.0000

Figure 73: HPLC of FA-PEG897-PC-CA4

Figure 74: ^{1}H-NMR of compound 22

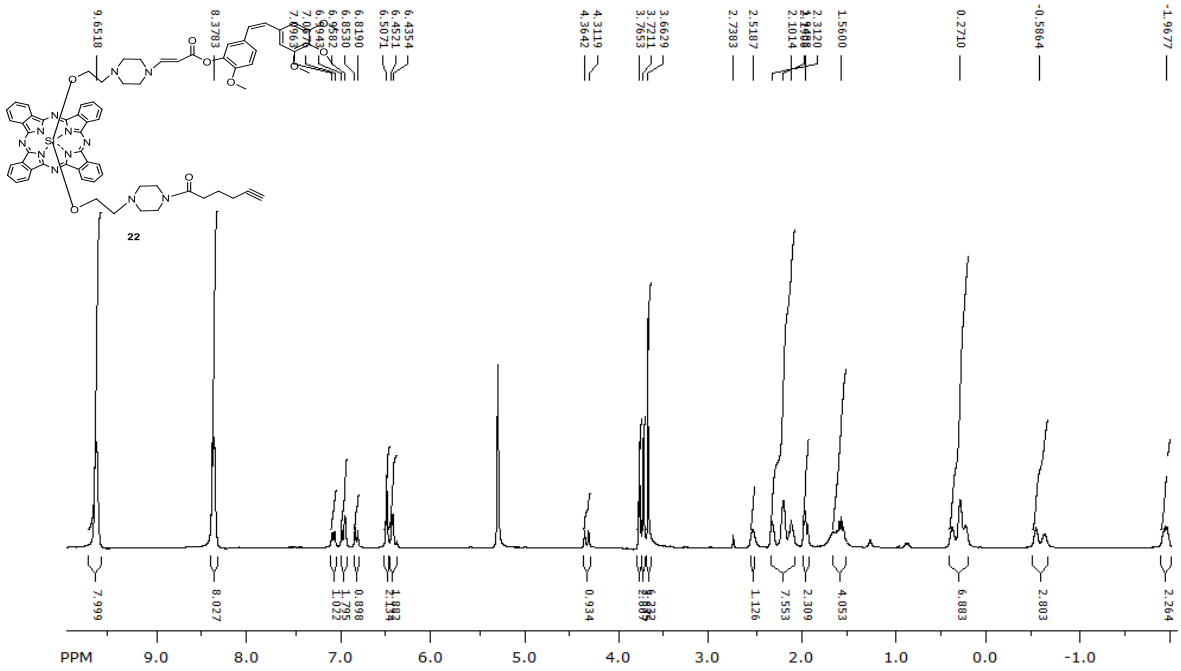

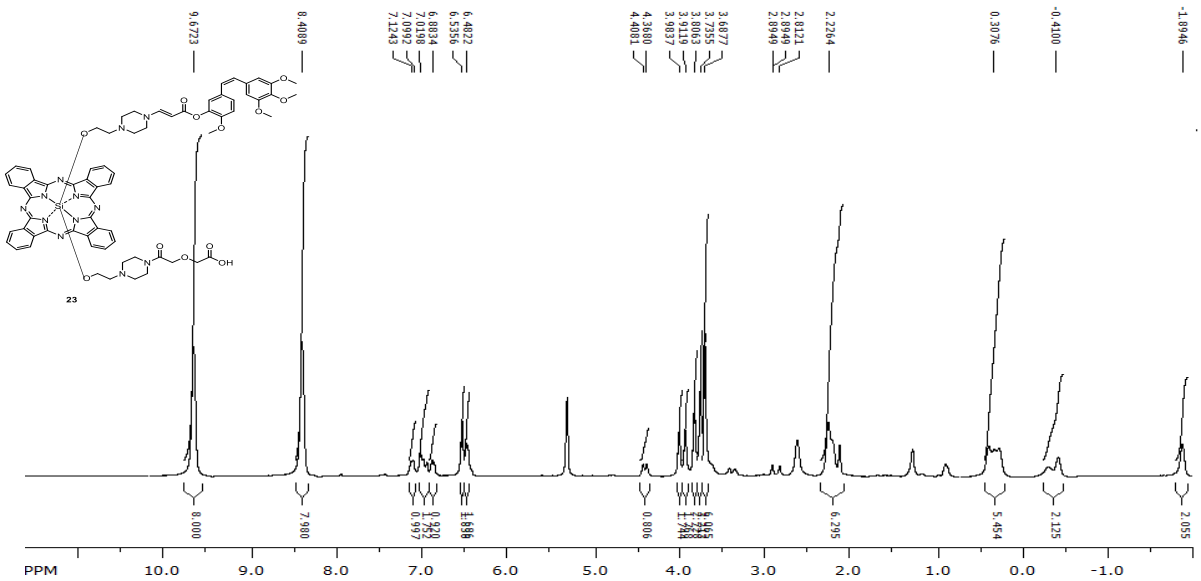

Figure75: ^{1}H-NMR of compound 23

Figure 76: 1H-NMR of compound 24

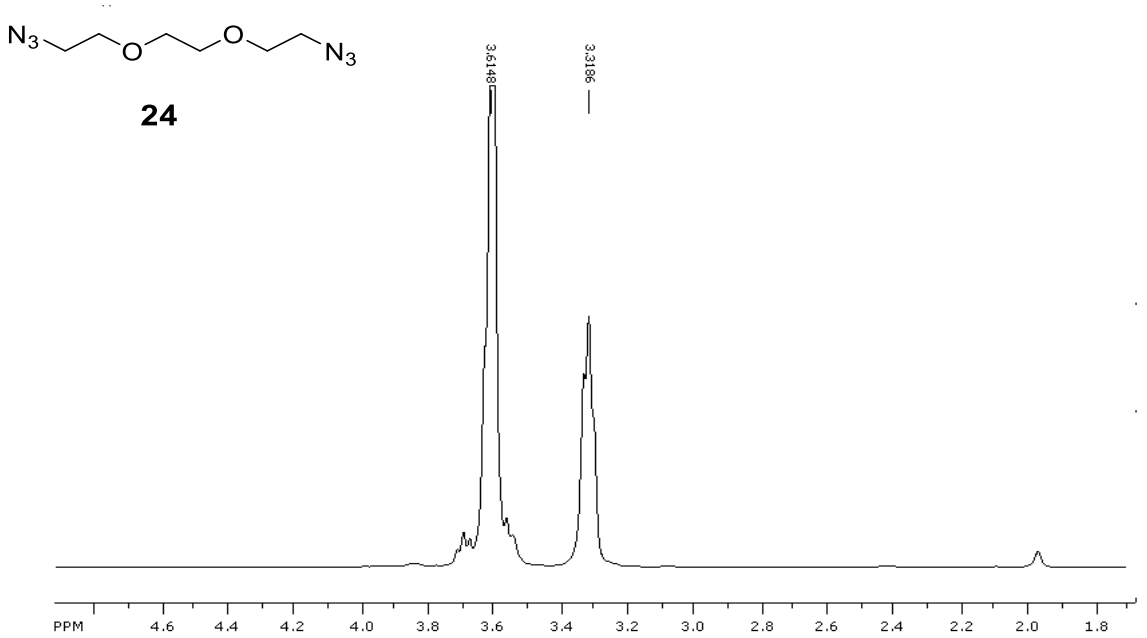

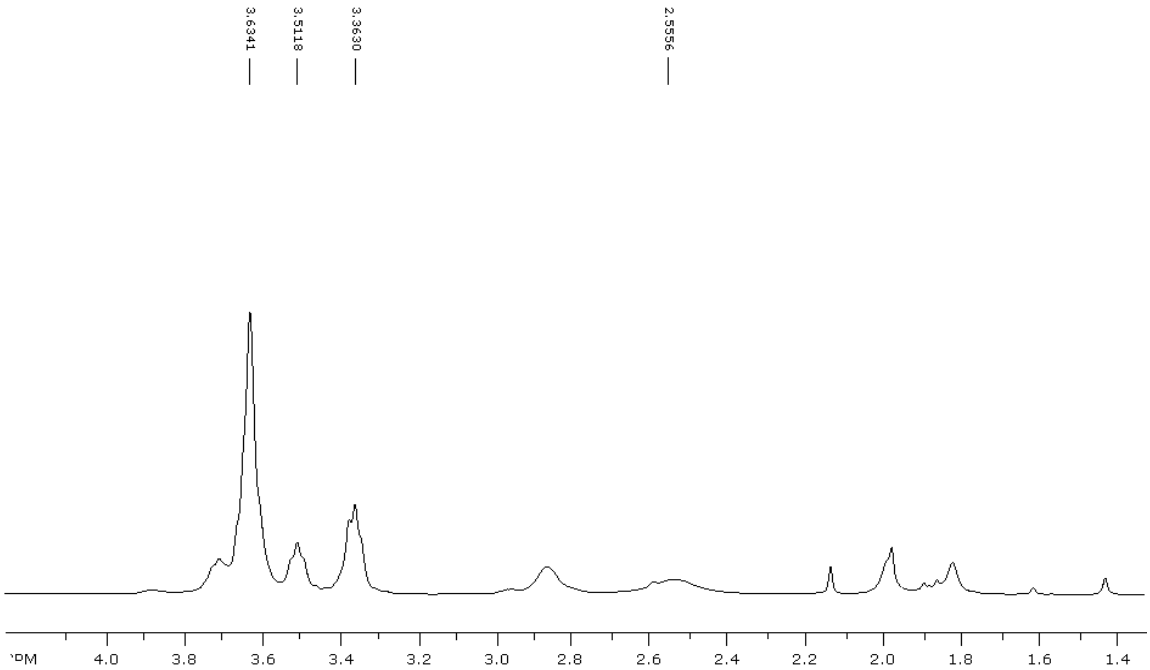

Figure 77: 1H-NMR of compound 25

Figure 78: ^{1}H-NMR of compound 31

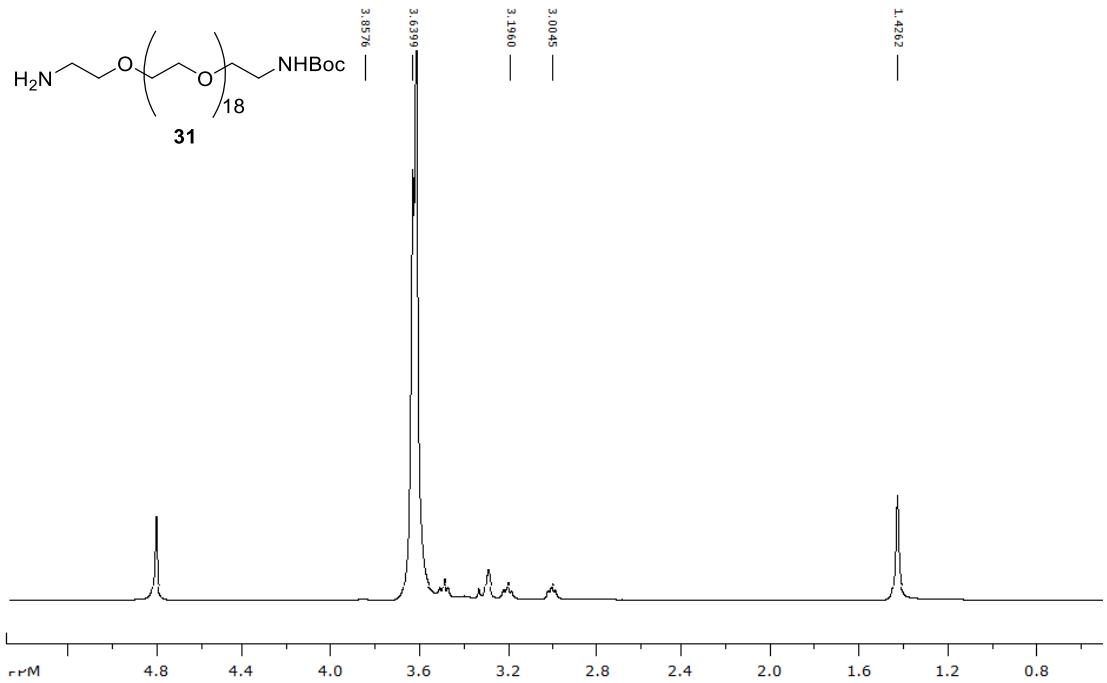

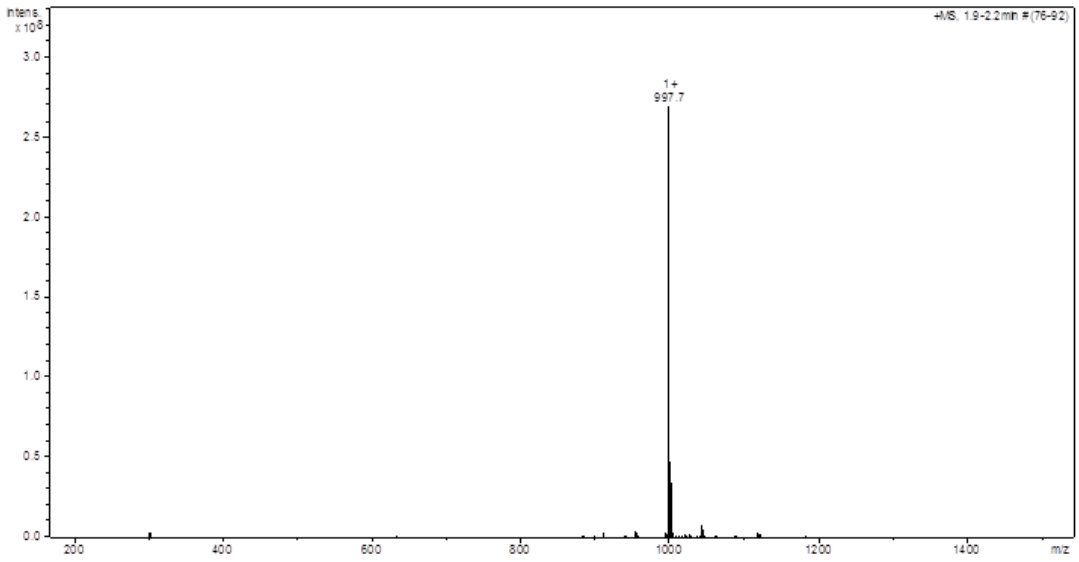

Figure 79: HRMS-ESI of compound 31

Figure 80

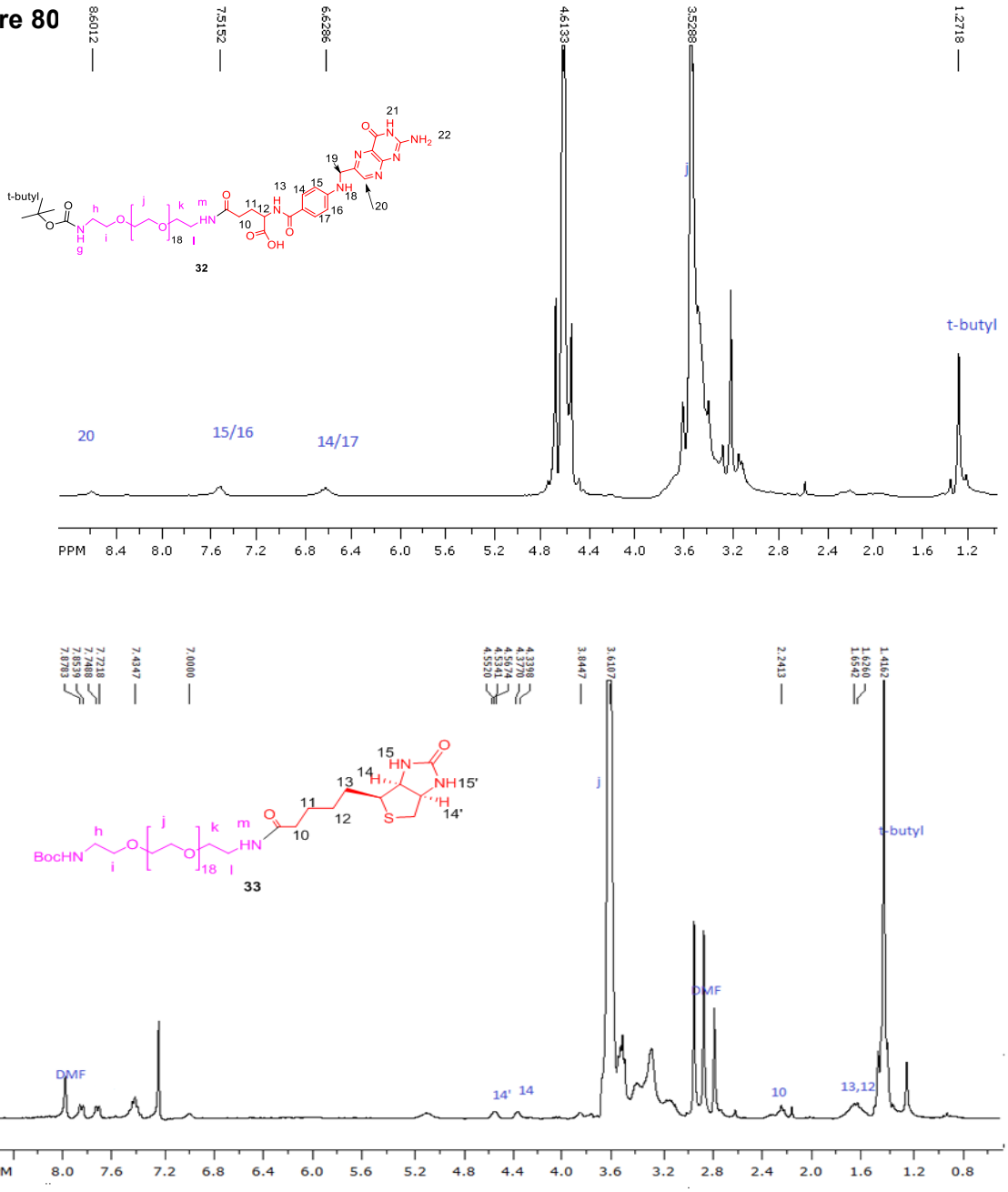

Figure 81: ^{1}H-NMR of Boc-PEG897-Biotin

REFERENCES

(1) Master, A. M.; Rodriguez, M. E.; Kenney, M. E.; Oleinick, N. L.; Gupta, A. S. *J Pharm Sci* **2010**, *99*, 2386.

(2) Wang, K. K.; Wilson, J. D.; Kenney, M. E.; Mitra, S.; Foster, T. H. *Photochem Photobiol* **2007**, *83*, 1056.

(3) Kamb, A.; Wee, S.; Lengauer, C. *Nat Rev Drug Discov* **2007**, *6*, 115.

(4) Menon, U.; Jacobs, I. J. *Curr Opin Obstet Gynecol* **2000**, *12*, 39.

(5) Li, C. *Adv Drug Deliv Rev* **2002**, *54*, 695.

(6) Pizzolato, J. F.; Saltz, L. B. *Lancet* **2003**, *361*, 2235.

(7) Mross, K.; Richly, H.; Schleucher, N.; Korfee, S.; Tewes, M.; Scheulen, M. E.; Seeber, S.; Beinert, T.; Schweigert, M.; Sauer, U.; Unger, C.; Behringer, D.; Brendel, E.; Haase, C. G.; Voliotis, D.; Strumberg, D. *Ann Oncol* **2004**, *15*, 1284.

(8) Agostinis, P.; Berg, K.; Cengel, K. A.; Foster, T. H.; Girotti, A. W.; Gollnick, S. O.; Hahn, S. M.; Hamblin, M. R.; Juzeniene, A.; Kessel, D.; Korbelik, M.; Moan, J.; Mroz, P.; Nowis, D.; Piette, J.; Wilson, B. C.; Golab, J. *CA Cancer J Clin* **2011**, *61*, 250.

(9) Detty, M. R. *Expert Opin Ther Pat* **2001**, *11*, 1849.

(10) Dolmans, D. E.; Fukumura, D.; Jain, R. K. *Nat Rev Cancer* **2003**, *3*, 380.

(11) Pervaiz, S.; Olivo, M. *Clin Exp Pharmacol P* **2006**, *33*, 551.

(12) Brown, S. B.; Brown, E. A.; Walker, I. *Lancet Oncol* **2004**, *5*, 497.

(13) Hamblin, M. R.; Hasan, T. *Photochem Photobiol Sci* **2004**, *3*, 436.

(14) Sibata, C. H.; Colussi, V. C.; Oleinick, N. L.; Kinsella, T. J. *Expert Opin Pharmacother* **2001**, *2*, 917.

(15) Gomer, C. J. *Semin Hematol* **1989**, *26*, 27.

(16) Dougherty, T. J. *Oncol (Williston Park)* **1989**, *3*, 67.

(17) Berg, K.; Folini, M.; Prasmickaite, L.; Selbo, P. K.; Bonsted, A.; Engesaeter, B. O.; Zaffaroni, N.; Weyergang, A.; Dietze, A.; Maelandsmo, G. M.; Wagner, E.; Norum, O. J.; Hogset, A. *Curr Pharm Biotechno* **2007**, *8*, 362.

(18) Rosenthal, I.; Ben-Hur, E. *Int J Radiat Biol* **1995**, *67*, 85.

(19) Moan, J.; Christensen, T. *Cancer Lett***1979**, *6*, 331.

(20) Niedre, M. J.; Secord, A. J.; Patterson, M. S.; Wilson, B. C. *Cancer Res* **2003**, *63*, 7986.

(21) Niedre, M.; Patterson, M. S.; Wilson, B. C. *Photochem Photobiol* **2002**, *75*, 382.

(22) Sonoda, M.; Krishna, C. M.; Riesz, P. *Photochem Photobiol* **1987**, *46*, 625.

(23) Weishaupt, K. R.; Gomer, C. J.; Dougherty, T. J. *Cancer Res* **1976**, *36*, 2326.

(24) Foote, C. S. *Photochem Photobiol* **1991**, *54*, 659.

(25) Davies, M. J. *Biochem Bioph Res Co* **2003**, *305*, 761.

(26) Girotti, A. W. *J Photochem Photobiol B* **2001**, *63*, 103.

(27) Herzberg, G. *Nat* **1934**, *133*, 759.

(28) Childs, W. H. J.; Mecke, R. *Z Phys* **1931**, *68*, 344.

(29) Ogryzlo, E. A. *Photophys* **1970**, *5*, 35.

(30) Foote, C. S. *Acc Chem Res* **1968**, *1*, 104.

(31) Pathak, M. A.; Joshi, P. C. *Biochimet Biophy Acta* **1984**, *798*, 115.

(32) Corey, E. J.; Taylor, W. C. *J Am Chem Soc* **1964**, *86*, 3881.

(33) Foote, C. S.; Wexler, S. *J Am Chem Soc* **1964**, *86*, 3879.

(34) Foote, C. S.; Wexler, S. *J Am Chem Soc* **1964**, *86*, 3880.

(35) Duncan, C. K.; Kearns, D. R. *Chem Phys Lett* **1971**, *12*, 306.

(36) Kearns, D. R. *Chem Rev* **1971**, *71*, 395.

(37) Duncan, C. K.; Kearns, D. R. *J Chem Phys* **1971**, *55*, 5822.

(38) Ackroyd, R.; Kelty, C.; Brown, N.; Reed, M. *Photochem Photobiol* **2001**, *74*, 656.

(39) Alberti, M. N.; Orfanopoulos, M. *Tetrahedron* **2006**, *62*, 10660.

(40) Stratakis, M.; Orfanopoulos, M. *Tetrahedron* **2000**, *56*, 1595.

(41) Nickon, A.; Bagli, J. F. *J Am Chem Soc* **1959**, *81*, 6330.

(42) Higgins, R.; Foote, C. S.; Cheng, H. *Adv Chem Ser* **1968**, 102.

(43) Young, R. H.; Wehrly, K.; Martin, R. L. *J Am Chem Soc* **1971**, *93*, 5774.

(44) Murray, R. W.; Lin, J. W. P.; Kaplan, M. L. *Ann Ny Acad Sci* **1970**, *171*, 121.

(45) Oshea, K. E.; Foote, C. S. *J Org Chem* **1989**, *54*, 3475.

(46) Sheu, C.; Foote, C. S. *J Am Chem Soc* **1993**, *115*, 10446.

(47) Matsumoto, M.; Dobashi, S.; Kondo, K. *Tetrahedron Lett* **1977**, 2329.

(48) Matsumoto, M.; Kondo, K. *J Am Chem Soc* **1977**, *99*, 2393.

(49) Gollnick, K. *Adv Chem Ser* **1968**, 78.

(50) Bartlett, P. D.; Schaap, A. P. *J Am Chem Soc* **1970**, *92*, 3223.

(51) Mazur, S.; Foote, C. S. *J Am Chem Soc* **1970**, *92*, 3225.

(52) Mazur, S.; Foote, C. S. *J Am Chem Soc* **1970**, *92*, 3225.

(53) Bartlett, P. D.; Schaap, A. P. *J Am Chem Soc* **1970**, *92*, 3223.

(54) Belyakov, V. A. *Photochem Photobiol* **1970**, *11*, 179.

(55) Wilson, T.; Schaap, A. P. *J Am Chem Soc* **1971**, *93*, 4126.

(56) Merkel, P. B.; Kearns, D. R. *J Am Chem Soc* **1972**, *94*, 7244.

(57) Long, C. A.; Kearns, D. R. *J Am Chem Soc* **1975**, *97*, 2018.

(58) Moan, J. *J Photochem Photobiol B* **1990**, *6*, 343.

(59) Skovsen, E.; Snyder, J. W.; Lambert, J. D.; Ogilby, P. R. *J Phys Chem B* **2005**, *109*, 8570.

(60) Sitkovsky, M.; Lukashev, D. *Nat Rev Immunol* **2005**, *5*, 712.

(61) Brown, J. M.; William, W. R. *Nat Rev Cancer* **2004**, *4*, 437.

(62) MacDonald, I. J.; Dougherty, T. J. *J Porphyr Phthalocya* **2001**, *5*, 105.

(63) Sharman, W. M.; Allen, C. M.; van Lier, J. E. *Drug Discov Today* **1999**, *4*, 507.

(64) Brown, S. B.; Brown, J. E.; Vernon, D. I. *Expert Opin Investig Drugs* **1999**, *8*, 1967.

(65) Allison, R. R.; Downie, G. H.; Cuenca, R.; Hu, X. H.; Childs, C. J. H.; Sibata, C. H. *Photodiagn Photodyn* **2004**, *1*, 27.

(66) Sternberg, E. D.; Dolphin, D.; Bruckner, C. *Tetrahedron* **1998**, *54*, 4151.

(67) Josefsen, L. B.; Boyle, R. W. *Met Based Drugs* **2008**, *2008*, 276109.

(68) Jori, G. *J Photochem Photobiol A* **1992**, *62*, 371.

(69) Boyle, R. W.; Dolphin, D. *Photochemand Photobiol***1996**, *64*, 469.

(70) Brasseur, N.; Menard, I.; Forget, A.; el Jastimi, R.; Hamel, R.; Molfino, N. A.; van Lier, J. E. *Photochem Photobiol* **2000**, *72*, 780.

(71) Ferreira, J.; Menezes, P. F. C.; Kurachi, C.; Sibata, C. H.; Allison, R. R.; Bagnato, V. S. *Laser Phys Lett* **2007**, *4*, 743.

(72) Fickweiler, S.; Abels, C.; Karrer, S.; Baumler, W.; Landthaler, M.; Hofstadter, F.; Szeimies, R. M. *J Photochem Photobiol B* **1999**, *48*, 27.

(73) Jori, G. *J Photochem Photobiol B* **1996**, *36*, 87.

(74) Karrer, S.; Abels, C.; Szeimies, R. M.; Baumler, W.; Dellian, M.; Hohenleutner, U.; Goetz, A. E.; Landthaler, M. *Arch Dermatol Res* **1997**, *289*, 132.

(75) Mathai, S.; Bird, D. K.; Stylli, S. S.; Smith, T. A.; Ghiggino, K. P. *Photochem Photobiol Sci* **2007**, *6*, 1019.

(76) Mody, T. D. *J Porphyr Phthalocya* **2000**, *4*, 362.

(77) Nyman, E. S.; Hynninen, P. H. *J Photoch Photobio B* **2004**, *73*, 1.

(78) Palumbo, G. *Expert Opin Drug Del* **2007**, *4*, 131.

(79) Usuda, J.; Kato, H.; Okunaka, T.; Furukawa, K.; Tsutsui, H.; Yamada, K.; Suga, Y.; Honda, H.; Nagatsuka, Y.; Ohira, T.; Tsuboi, M.; Hirano, T. *J Thorac Oncol* **2006**, *1*, 489.

(80) Rosenthal, M. A.; Kavar, B.; Hill, J. S.; Morgan, D. J.; Nation, R. L.; Stylli, S. S.; Basser, R. L.; Uren, S.; Geldard, H.; Green, M. D.; Kahl, S. B.; Kaye, A. H. *J Clin Oncol* **2001**, *19*, 519.

(81) Ochsner, M. *J Photoch Photobio B* **1996**, *32*, 3.

(82) Hanahan, D.; Folkman, J. *Cell* **1996**, *86*, 353.

(83) Danhier, F.; Feron, O.; Preat, V. *J Control Release* **2010**, *148*, 135.

(84) Matsumura, Y.; Maeda, H. *Cancer Res* **1986**, *46*, 6387.

(85) Talekar, M.; Kendall, J.; Denny, W.; Garg, S. *Anticancer Drugs* **2011**, *22*, 949.

(86) Schiffelers, R. M.; Koning, G. A.; ten Hagen, T. L.; Fens, M. H.; Schraa, A. J.; Janssen, A. P.; Kok, R. J.; Molema, G.; Storm, G. *J Control Release* **2003**, *91*, 115.

(87) Maruyama, K. *Adv Drug Deliv Rev* **2011**, *63*, 161.

(88) Hong, R. L.; Huang, C. J.; Tseng, Y. L.; Pang, V. F.; Chen, S. T.; Liu, J. J.; Chang, F. H. *Clin Cancer Res* **1999**, *5*, 3645.

(89) Roche, A. C.; Fajac, I.; Grosse, S.; Frison, N.; Rondanino, C.; Mayer, R.; Monsigny, M. *Cell Mol Life Sci* **2003**, *60*, 288.

(90) Nakamura, H.; Miyajima, Y.; Takei, T.; Kasaoka, S.; Maruyama, K. *Chem Commun (Camb)* **2004**, 1910.

(91) Harata, M.; Soda, Y.; Tani, K.; Ooi, J.; Takizawa, T.; Chen, M. H.; Bai, Y. S.; Izawa, K.; Kobayashi, S.; Tomonari, A.; Nagamura, F.; Takahashi, S.; Uchimaru, K.; Iseki, T.; Tsuji, T.; Takahashi, T. A.; Sugita, K.; Nakazawa, S.; Tojo, A.; Maruyama, K.; Asano, S. *Blood* **2004**, *104*, 1442.

(92) Sugahara, K. N.; Teesalu, T.; Karmali, P. P.; Kotamraju, V. R.; Agemy, L.; Girard, O. M.; Hanahan, D.; Mattrey, R. F.; Ruoslahti, E. *Cancer Cell* **2009**, *16*, 510.

(93) Sugahara, K. N.; Teesalu, T.; Karmali, P. P.; Kotamraju, V. R.; Agemy, L.; Greenwald, D. R.; Ruoslahti, E. *Science* **2010**, *328*, 1031.

(94) Lu, Y. J.; Low, P. S. *Adv Drug Deliver Rev* **2002**, *54*, 675.

(95) Gupta, Y.; Kohli, D. V.; Jain, S. K. *Crit Rev Ther Drug Carrier Syst* **2008**, *25*, 347.

(96) Ojima, I. *Acc Chem Res* **2008**, *41*, 108.

(97) Chen, S.; Zhao, X.; Chen, J.; Kuznetsova, L.; Wong, S. S.; Ojima, I. *Bioconjug Chem* **2010**, *21*, 979.

(98) Bareford, L. M.; Swaan, P. W. *Adv Drug Deliv Rev* **2007**, *59*, 748.

(99) Bildstein, L.; Dubernet, C.; Couvreur, P. *Adv Drug Deliv Rev* **2011**, *63*, 3.

(100) Lu, J. Y.; Lowe, D. A.; Kennedy, M. D.; Low, P. S. *J Drug Target* **1999**, *7*, 43.

(101) Sabharanjak, S.; Mayor, S. *Adv Drug Deliv Rev* **2004**, *56*, 1099.

(102) Elnakat, H.; Ratnam, M. *Adv Drug Deliv Rev* **2004**, *56*, 1067.

(103) Garin-Chesa, P.; Campbell, I.; Saigo, P. E.; Lewis, J. L., Jr.; Old, L. J.; Rettig, W. J. *Am J Pathol* **1993**, *142*, 557.

(104) Toffoli, G.; Cernigoi, C.; Russo, A.; Gallo, A.; Bagnoli, M.; Boiocchi, M. *Int Jof Cancer* **1997**, *74*, 193.

(105) Toffoli, G.; Russo, A.; Gallo, A.; Cernigoi, C.; Miotti, S.; Sorio, R.; Tumolo, S.; Boiocchi, M. *IntJof Cancer* **1998**, *79*, 121.

(106) Kamen, B. A.; Caston, J. D. *Biochem Pharmacol* **1986**, *35*, 2323.

(107) Antony, A. C. *Annu Rev Nutr* **1996**, *16*, 501.

(108) Reddy, J. A.; Low, P. S. *Crit Rev Ther Drug Carrier Syst* **1998**, *15*, 587.

(109) Wang, S.; Low, P. S. *J Control Release* **1998**, *53*, 39.

(110) Xia, W.; Low, P. S. *J Med Chem* **2010**, *53*, 6811.

(111) Chen, H.; Ahn, R.; Van den Bossche, J.; Thompson, D. H.; O'Halloran, T. V. *Mol Cancer Ther* **2009**, *8*, 1955.

(112) Gabizon, A.; Tzemach, D.; Gorin, J.; Mak, L.; Amitay, Y.; Shmeeda, H.; Zalipsky, S. *Cancer Chemoth Pharm* **2010**, *66*, 43.

(113) Riviere, K.; Huang, Z. H.; Jerger, K.; Macaraeg, N.; Szoka, F. C. *J Drug Target* **2011**, *19*, 14.

(114) Watanabe, K.; Kaneko, M.; Maitani, Y. *Int J Nanomed* **2012**, *7*, 3679.

(115) Wang, Y.; Cao, X. Y.; Guo, R.; Shen, M. W.; Zhang, M. G.; Zhu, M. F.; Shi, X. Y. *Polym Chem-Uk* **2011**, *2*, 1754.

(116) Sahu, S. K.; Mallick, S. K.; Santra, S.; Maiti, T. K.; Ghosh, S. K.; Pramanik, P. *J Mater Sci-Mater M* **2010**, *21*, 1587.

(117) Scomparin, A.; Salmaso, S.; Bersani, S.; Satchi-Fainaro, R.; Caliceti, P. *Eur J Pharm Sci* **2011**, *42*, 547.

(118) Kim, D.; Lee, E. S.; Oh, K. T.; Gao, Z. G.; Bae, Y. H. *Small* **2008**, *4*, 2043.

(119) Leamon, C. P.; Low, P. S. *J Biol Chem* **1992**, *267*, 24966.

(120) Atkinson, S. F.; Bettinger, T.; Seymour, L. W.; Behr, J. P.; Ward, C. M. *J Biol Chem* **2001**, *276*, 27930.

(121) Ward, C. M. *Curr Opin Mol Ther* **2000**, *2*, 182.

(122) Wang, S.; Lee, R. J.; Cauchon, G.; Gorenstein, D. G.; Low, P. S. *P Natl Acad Sci USA* **1995**, *92*, 3318.

(123) Ginobbi, P.; Geiser, T. A.; Ombres, D.; Citro, G. *Anticancer Res* **1997**, *17*, 29.

(124) Li, S.; Deshmukh, H. M.; Huang, L. *Pharmaceut Res* **1998**, *15*, 1540.

(125) Lee, R. J.; Huang, L. *J Biol Chem* **1996**, *271*, 8481.

(126) Douglas, J. T.; Rogers, B. E.; Rosenfeld, M. E.; Michael, S. I.; Feng, M. Z.; Curiel, D. T. *Nat Biotechnol* **1996**, *14*, 1574.

(127) Xu, L.; Pirollo, K. F.; Chang, E. H. *J Control Release* **2001**, *74*, 115.

(128) van Dam, G. M.; Themelis, G.; Crane, L. M.; Harlaar, N. J.; Pleijhuis, R. G.; Kelder, W.; Sarantopoulos, A.; de Jong, J. S.; Arts, H. J.; van der Zee, A. G.; Bart, J.; Low, P. S.; Ntziachristos, V. *Nat Med* **2011**, *17*, 1315.

(129) Mathias, C. J.; Wang, S.; Waters, D. J.; Turek, J. J.; Low, P. S.; Green, M. A. *J Nucl Med***1998**, *39*, 1579.

(130) Kennedy, M. D.; Jallad, K. N.; Thompson, D. H.; Ben-Amotz, D.; Low, P. S. *J Biomed Opt* **2003**, *8*, 636.

(131) Themelis, G.; Yoo, J. S.; Soh, K. S.; Schulz, R.; Ntziachristos, V. *J Biomed Opt* **2009**, *14*, 064012.

(132) Gillies, E. R.; Frechet, J. M. J. *Drug Discovery Today* **2005**, *10*, 35.

(133) Najlah, M.; Freeman, S.; Attwood, D.; D'Emanuele, A. *Int J Pharmac***2006**, *308*, 175.

(134) Wiener, E. C.; Brechbiel, M. W.; Brothers, H.; Magin, R. L.; Gansow, O. A.; Tomalia, D. A.; Lauterbur, P. C. *Magnetic resonance in medicine : official J Soc of Magnetic Resonance in Med / Soc Magnetic Resonance Med***1994**, *31*, 1.

(135) Mullen, D. G.; McNerny, D. Q.; Desai, A.; Cheng, X. M.; Dimaggio, S. C.; Kotlyar, A.; Zhong, Y.; Qin, S.; Kelly, C. V.; Thomas, T. P.; Majoros, I.; Orr, B. G.; Baker, J. R.; Banaszak Holl, M. M. *Bioconjug Chem* **2011**, *22*, 679.

(136) Ward, B. B.; Dunham, T.; Majoros, I. J.; Baker, J. R., Jr. *J oral and maxillofacial surgery : official J Am Assoc of Oral and Maxillofacial Surgeons* **2011**, *69*, 2452.

(137) Li, M. H.; Choi, S. K.; Thomas, T. P.; Desai, A.; Lee, K. H.; Kotlyar, A.; Banaszak Holl, M. M.; Baker, J. R., Jr. *Eur JMed Chem***2012**, *47*, 560.

(138) D'Emanuele, A.; Attwood, D. *Adv Drug Deliv Rev* **2005**, *57*, 2147.

(139) Alexis, F.; Pridgen, E. M.; Langer, R.; Farokhzad, O. C. *Handbook of Experimental Pharmacology* **2010**, 55.

(140) Yu, W.; Pirollo, K. F.; Rait, A.; Yu, B.; Xiang, L. M.; Huang, W. Q.; Zhou, Q.; Ertem, G.; Chang, E. H. *Gene therapy* **2004**, *11*, 1434.

(141) Jhaveri, M. S.; Rait, A. S.; Chung, K. N.; Trepel, J. B.; Chang, E. H. *Mol Cancer Ther* **2004**, *3*, 1505.

(142) Haran, G.; Cohen, R.; Bar, L. K.; Barenholz, Y. *Biochim et Biophy Acta* **1993**, *1151*, 201.

(143) Goren, D.; Horowitz, A. T.; Tzemach, D.; Tarshish, M.; Zalipsky, S.; Gabizon, A. *ClinCancer Res : an official J Am Assoc for Cancer Res* **2000**, *6*, 1949.

(144) Yokoyama, M.; Fukushima, S.; Uehara, R.; Okamoto, K.; Kataoka, K.; Sakurai, Y.; Okano, T. *J Control Release* **1998**, *50*, 79.

(145) Lu, Y.; Low, P. S. *Adv Drug Deliv Rev* **2002**, *54*, 675.

(146) Kim, S. C.; Kim, D. W.; Shim, Y. H.; Bang, J. S.; Oh, H. S.; Kim, S. W.; Seo, M. H. *J Control Release* **2001**, *72*, 191.

(147) Werner, M. E.; Cummings, N. D.; Sethi, M.; Wang, E. C.; Sukumar, R.; Moore, D. T.; Wang, A. Z. *Int J Radiat Oncol* **2013**, *86*, 463.

(148) Arnida; Nishiyama, N.; Kanayama, N.; Jang, W. D.; Yamasaki, Y.; Kataoka, K. *J Control Release* **2006**, *115*, 208.

(149) Nishiyama, N.; Kataoka, K. *Nihon rinsho. Jap J Clin Med* **2006**, *64*, 199.

(150) Ulbrich, K.; Subr, V. *Adv Drug Deliv Rev* **2004**, *56*, 1023.

(151) Alexis, F.; Rhee, J. W.; Richie, J. P.; Radovic-Moreno, A. F.; Langer, R.; Farokhzad, O. C. *Urol Oncol* **2008**, *26*, 74.

(152) Alvarez-Lorenzo, C.; Bromberg, L.; Concheiro, A. *Photochemistry and Photobiology* **2009**, *85*, 848.

(153) Choi, S. K.; Thomas, T.; Li, M. H.; Kotlyar, A.; Desai, A.; Baker, J. R. *Chem Commun* **2010**, *46*, 2632.

(154) Mccoy, C. P.; Rooney, C.; Edwards, C. R.; Jones, D. S.; Gorman, S. P. *J Am Chem Soc* **2007**, *129*, 9572.

(155) Normand, N.; Valamanesh, F.; Savoldelli, M.; Mascarelli, F.; BenEzra, D.; Courtois, Y.; Behar-Cohen, F. *Mol Vis* **2005**, *11*, 184.

(156) Donnelly, R. F.; McCarron, P. A.; Cassidy, C. M.; Elborn, J. S.; Tunney, M. M. *J Control Release* **2007**, *117*, 217.

(157) Klohs, J.; Wunder, A.; Licha, K. *Basic Res Cardiology* **2008**, *103*, 144.

(158) Bio, M.; Rajaputra, P.; Nkepang, G.; Awuah, S. G.; Hossion, A. M.; You, Y. *J Med Chem* **2013**, *56*, 3936.

(159) Hossion, A. M. L.; Bio, M.; Nkepang, G.; Awuah, S. G.; You, Y. *ACS Med Chem Lett* **2013**, *4*, 124.

(160) Mahendran, A.; Kopkalli, Y.; Ghosh, G.; Ghogare, A.; Minnis, M.; Kruft, B. I.; Zamadar, M.; Aebisher, D.; Davenport, L.; Greer, A. *Photochem Photobiol***2011**, *87*, 1330.

(161) Zamadar, M.; Ghosh, G.; Mahendran, A.; Minnis, M.; Kruft, B. I.; Ghogare, A.; Aebisher, D.; Greer, A. *Abstr Pap Am Chem S* **2011**, *241*.

(162) Zamadar, M.; Ghosh, G.; Aebisher, D.; Alqaim, M.; Greer, A. *Abstr Pap Am Chem S* **2010**, *240*.

(163) Nkepang, G. a. Y., Y. In The Chemistry of Peroxides; John Wiley $ Sons, Ltd: The Atrium Gate, Chichester, West Sussex England, 2013; Vol. 3, p in Press.

(164) Nkepang, G.; Pogula, P. K.; Bio, M.; You, Y. *Photochem Photobiol* **2012**, *88*, 753.

(165) Baganz, H. *Angew Chem Int Edit* **1959**, *71*, 366.

(166) Sales, F.; Serratosa, F. *Tetrahedron Lett* **1979**, 3329.

(167) Yang, J. K.; Bauld, N. L. *J Org Chem* **1999**, *64*, 9251.

(168) Jiang, M. Y.; Dolphin, D. *J Am Chem Soc* **2008**, *130*, 4236.

(169) Bychkova, T. I.; Vasileva, M. A.; Kalabina, A. V.; Rozova, T. I.; Ratovskii, G. V. *Zh Org Khim+* **1984**, *20*, 524.

(170) Kaberdin, R. V.; Potkin, V. I. *Uspekhi Khimii* **1994**, *63*, 673.

(171) Moyano, A.; Charbonnier, F.; Greene, A. E. *J Org Chem* **1987**, *52*, 2919.

(172) Dudley, G. B.; Takaki, K. S.; Cha, D. D.; Danheiser, R. L. *Org Letts* **2000**, *2*, 3407.

(173) Lipshutz, B. H.; Ellsworth, E. L. *J Am ChemSoc* **1990**, *112*, 7440.

(174) Dussault, P. H.; Han, Q.; Sloss, D. G.; Symonsbergen, D. J. *Tetrahedron* **1999**, *55*, 11437.

(175) Taillefer, M.; Ouali, A.; Renard, B.; Spindler, J. F. *Chemistry* **2006**, *12*, 5301.

(176) Kabir, M. S.; Van Linn, M. L.; Monte, A.; Cook, J. M. *Org Lett* **2008**, *10*, 3363.

(177) Cook, J. M.; Kabir, M. S.; Lorenz, M.; Namjoshi, O. A. *Org Lett* **2010**, *12*, 464.

(178) Kaddouri, H.; Vicente, V.; Ouali, A.; Ouazzani, F.; Taillefer, M. *Angew Chem Int Ed Engl* **2009**, *48*, 333.

(179) You, Y.; Gibson, S. L.; Hilf, R.; Davies, S. R.; Oseroff, A. R.; Roy, I.; Ohulchanskyy, T. Y.; Bergey, E. J.; Detty, M. R. *J Med Chem* **2003**, *46*, 3734.

(180) Murthy, R. S.; Bio, M.; You, Y. J. *Tetrahedron Letters* **2009**, *50*, 1041.

(181) Dark, G. G.; Hill, S. A.; Prise, V. E.; Tozer, G. M.; Pettit, G. R.; Chaplin, D. J. *Cancer Res* **1997**, *57*, 1829.

(182) Lin, C. M.; Singh, S. B.; Chu, P. S.; Dempcy, R. O.; Schmidt, J. M.; Pettit, G. R.; Hamel, E. *Mol Pharmacol* **1988**, *34*, 200.

(183) Gaukroger, K.; Hadfield, J. A.; Hepworth, L. A.; Lawrence, N. J.; McGown, A. T. *J Org Chem* **2001**, *66*, 8135.

(184) You, Y.; Gibson, S. L.; Detty, M. R. *J Photochem Photobiol B* **2006**, *85*, 155.

(185) Wong, H. L.; Bendayan, R.; Rauth, A. M.; Li, Y.; Wu, X. Y. *Adv Drug Deliv Rev* **2007**, *59*, 491.

(186) Kim, K.; Lee, M.; Park, H.; Kim, J. H.; Kim, S.; Chung, H.; Choi, K.; Kim, I. S.; Seong, B. L.; Kwon, I. C. *J Am Chem Soc* **2006**, *128*, 3490.

(187) Low, P. S.; Henne, W. A.; Doorneweerd, D. D. *Acc Chem Res* **2008**, *41*, 120.

(188) Weinstain, R.; Segal, E.; Satchi-Fainaro, R.; Shabat, D. *Chem Commun (Camb)* **2010**, *46*, 553.

(189) Onodera, R.; Motoyama, K.; Okamatsu, A.; Higashi, T.; Arima, H. *Scientific Reports* **2013**, *3*, 1104.

(190) Mattes, M. J.; Major, P. P.; Goldenberg, D. M.; Dion, A. S.; Hutter, R. V.; Klein, K. M. *Cancer Res* **1990**, *50*, 880s.

(191) Ross, J. F.; Chaudhuri, P. K.; Ratnam, M. *Cancer* **1994**, *73*, 2432.

(192) Weitman, S. D.; Lark, R. H.; Coney, L. R.; Fort, D. W.; Frasca, V.; Zurawski, V. R., Jr.; Kamen, B. A. *Cancer Res* **1992**, *52*, 3396.

(193) Henne, W. A.; Doorneweerd, D. D.; Hilgenbrink, A. R.; Kularatne, S. A.; Low, P. S. *Bioorg & Med Chem Lett* **2006**, *16*, 5350.

(194) Lee, J. W.; Lu, J. Y.; Low, P. S.; Fuchs, P. L. *Bioorg & Med Chemistry* **2002**, *10*, 2397.

(195) Vlahov, I. R.; Santhapuram, H. K.; Kleindl, P. J.; Howard, S. J.; Stanford, K. M.; Leamon, C. P. *Bioorg & Med Chem Lett* **2006**, *16*, 5093.

(196) Leamon, C. P.; Reddy, J. A.; Vlahov, I. R.; Kleindl, P. J.; Vetzel, M.; Westrick, E. *Bioconjug Chem* **2006**, *17*, 1226.

(197) Leamon, C. P.; Reddy, J. A.; Vlahov, I. R.; Vetzel, M.; Parker, N.; Nicoson, J. S.; Xu, L. C.; Westrick, E. *Bioconjug Chem* **2005**, *16*, 803.

(198) Leamon, C. P.; Low, P. S. *J Biol Chem* **1992**, *267*, 24966.

(199) Leamon, C. P.; Pastan, I.; Low, P. S. *J Biol Chem* **1993**, *268*, 24847.

(200) Yang, J.; Chen, H.; Vlahov, I. R.; Cheng, J. X.; Low, P. S. *Proc Natl Acad Sci U S A* **2006**, *103*, 13872.

(201) Urano, Y.; Asanuma, D.; Hama, Y.; Koyama, Y.; Barrett, T.; Kamiya, M.; Nagano, T.; Watanabe, T.; Hasegawa, A.; Choyke, P. L.; Kobayashi, H. *Nat Med* **2009**, *15*, 104.

(202) Steinberg, G.; Borch, R. F. *J Med Chem* **2001**, *44*, 69.

(203) Aronov, O.; Horowitz, A. T.; Gabizon, A.; Gibson, D. *Bioconjug Chem* **2003**, *14*, 563.

(204) Liu, J. Q.; Kolar, C.; Lawson, T. A.; Gmeiner, W. H. *J Org Chem* **2001**, *66*, 5655.

(205) Lee, J. W.; Lu, J. Y.; Low, P. S.; Fuchs, P. L. *Bioorg & Med Chem* **2002**, *10*, 2397.

(206) Leamon, C. P.; Reddy, J. A. *Adv Drug Deliv Rev* **2004**, *56*, 1127.

(207) Zempleni, J.; Wijeratne, S. S. K.; Hassan, Y. I. *Biofactors* **2009**, *35*, 36.

(208) Yang, W.; Cheng, Y.; Xu, T.; Wang, X.; Wen, L. P. *Eur Journal MedChem***2009**, *44*, 862.

(209) Russell-Jones, G.; McTavish, K.; McEwan, J.; Rice, J.; Nowotnik, D. *J Inorg Biochem* **2004**, *98*, 1625.

(210) Na, K.; Lee, T. B.; Park, K. H.; Shin, E. K.; Lee, Y. B.; Cho, H. K. *Eur J Pharm Sci* **2003**, *18*, 165.

(211) Yellepeddi, V. K.; Kumar, A.; Palakurthi, S. *Anticancer Res* **2009**, *29*, 2933.

(212) Minko, T.; Paranjpe, P. V.; Qiu, B.; Lalloo, A.; Won, R.; Stein, S.; Sinko, P. J. *Cancer Chemother Pharmacol* **2002**, *50*, 143.

(213) Horn, M. A.; Heinstein, P. F.; Low, P. S. *Plant Physiol* **1990**, *93*, 1492.

(214) Green, N. M. *Method Enzymol* **1990**, *184*, 51.

(215) Lis, L. G.; Smart, M. A.; Luchniak, A.; Gupta, M. L., Jr.; Gurvich, V. J. *ACS Med Chem Lett* **2012**, *3*, 745.

(216) Sambaiah, T.; King, K. Y.; Tsay, S. C.; Mei, N. W.; Hakimclahi, S.; Lai, Y. K.; Lieu, C. H.; Hwu, J. R. *Eur J Med Chem* **2002**, *37*, 349.

(217) Byrd, C. A.; Bornmann, W.; Erdjument-Bromage, H.; Tempst, P.; Pavletich, N.; Rosen, N.; Nathan, C. F.; Ding, A. *Proc Natl Acad Sci U S A* **1999**, *96*, 5645.

(218) Dougherty, T. J.; Gomer, C. J.; Henderson, B. W.; Jori, G.; Kessel, D.; Korbelik, M.; Moan, J.; Peng, Q. *J Natl Cancer I* **1998**, *90*, 889.

(219) Vrouenraets, M. B.; Visser, G. W.; Stigter, M.; Oppelaar, H.; Snow, G. B.; van Dongen, G. A. *Cancer Res* **2001**, *61*, 1970.

(220) Vrouenraets, M. B.; Visser, G. W.; Stewart, F. A.; Stigter, M.; Oppelaar, H.; Postmus, P. E.; Snow, G. B.; van Dongen, G. A. *Cancer Res* **1999**, *59*, 1505.

(221) Mew, D.; Lum, V.; Wat, C. K.; Towers, G. H.; Sun, C. H.; Walter, R. J.; Wright, W.; Berns, M. W.; Levy, J. G. *Cancer Res* **1985**, *45*, 4380.

(222) Hamblin, M. R.; Miller, J. L.; Hasan, T. *Cancer Res* **1996**, *56*, 5205.

(223) Carcenac, M.; Dorvillius, M.; Garambois, V.; Glaussel, F.; Larroque, C.; Langlois, R.; Hynes, N. E.; van Lier, J. E.; Pelegrin, A. *Brit J cancer* **2001**, *85*, 1787.

(224) Shiah, J. G.; Sun, Y.; Peterson, C. M.; Straight, R. C.; Kopecek, J. *Clini Cancer Res : an official Jl Am Assoc for Cancer Res* **2000**, *6*, 1008.

(225) Hamblin, M. R.; Miller, J. L.; Rizvi, I.; Ortel, B.; Maytin, E. V.; Hasan, T. *Cancer Res* **2001**, *61*, 7155.

(226) Derycke, A. S. L.; de Witte, P. A. M. *Adv Drug Deliv Rev* **2004**, *56*, 17.

(227) Cinteza, L. O.; Ohulchanskyy, T. Y.; Sahoo, Y.; Bergey, E. J.; Pandey, R. K.; Prasad, P. N. *Mol Pharmaceut* **2006**, *3*, 415.

(228) Li, B. H.; Moriyama, E. H.; Li, F. G.; Jarvi, M. T.; Allen, C.; Wilson, B. C. *Photochem Photobiol* **2007**, *83*, 1505.

(229) Le Garrec, D.; Taillefer, J.; Van Lier, J. E.; Lenaerts, V.; Leroux, J. C. *J Drug Target* **2002**, *10*, 429.

(230) Zhang, G. D.; Harada, A.; Nishiyama, N.; Jiang, D. L.; Koyama, H.; Aida, T.; Kataoka, K. *J Control Release* **2003**, *93*, 141.

(231) Bae, B. C.; Na, K. *Int J Photoenergy* **2012**.

(232) Schneider, R.; Tirand, L.; Frochot, C.; Vanderesse, R.; Thomas, N.; Gravier, J.; Guillemin, F.; Barberi-Heyob, M. *Anti-cancer Agents in Med Chemistry* **2006**, *6*, 469.

(233) Gravier, J.; Schneider, R.; Frochot, C.; Bastogne, T.; Schmitt, F.; Didelon, J.; Guillemin, F.; Barberi-Heyob, M. *J Med Chem* **2008**, *51*, 3867.

(234) Schneider, R.; Schmitt, F.; Frochot, C.; Fort, Y.; Lourette, N.; Guillemin, F.; Muller, J. F.; Barberi-Heyob, M. *Bioorg & Med Chem* **2005**, *13*, 2799.

(235) Vlahov, I. R.; Santhapuram, H. K.; You, F.; Wang, Y.; Kleindl, P. J.; Hahn, S. J.; Vaughn, J. F.; Reno, D. S.; Leamon, C. P. *J Org Chem* **2010**, *75*, 3685.

(236) Vlahov, I. R.; You, F.; Santhapuram, H. K.; Wang, Y.; Vaughn, J. F.; Hahn, S. J.; Kleindl, P. J.; Fan, M.; Leamon, C. P. *Bioorg & Med ChemLett* **2011**, *21*, 1202.

(237) Reddy, J. A.; Dorton, R.; Westrick, E.; Dawson, A.; Smith, T.; Xu, L. C.; Vetzel, M.; Kleindl, P.; Vlahov, I. R.; Leamon, C. P. *Cancer Res* **2007**, *67*, 4434.

(238) Sausville, E. A.; Anthony, S. P.; Garbo, L. E.; Shkolny, D.; Yurkovetskiy, A. V.; Bethune, C.; Schwertschlag, U.; Fram, R. J. *Mol Cancer Ther* **2007**, *6*, 3383s.

(239) Vlahov, I. R.; Santhapuram, H. K.; Wang, Y.; Kleindl, P. J.; You, F.; Howard, S. J.; Westrick, E.; Reddy, J. A.; Leamon, C. P. *J Org Chem* **2007**, *72*, 5968.

(240) Vlahov, I. R.; Leamon, C. P. *Bioconjug Chem* **2012**, *23*, 1357.

(241) Kamen, B. A.; Smith, A. K.; Anderson, R. G. *J Clin Investig* **1991**, *87*, 1442.

(242) Leamon, C. P.; Reddy, J. A.; Klein, P. J.; Vlahov, I. R.; Dorton, R.; Bloomfield, A.; Nelson, M.; Westrick, E.; Parker, N.; Bruna, K.; Vetzel, M.; Gehrke, M.; Nicoson, J. S.; Messmann, R. A.; LoRusso, P. M.; Sausville, E. A. *J Pharmacol and Exper Therap***2011**, *336*, 336.

(243) Jiang, X. J.; Lo, P. C.; Tsang, Y. M.; Yeung, S. L.; Fong, W. P.; Ng, D. K. P. *Chem-Eur J* **2010**, *16*, 4777.

(244) Bio, M.; Nkepang, G.; You, Y. *Chem Commun (Camb)* **2012**, *48*, 6517.

(245) Guaragna, A.; Chiaviello, A.; Paolella, C.; D'Alonzo, D.; Palumbo, G. *Bioconjug Chem* **2012**, *23*, 84.

(246) Bae, J. W.; Pearson, R. M.; Patra, N.; Sunoqrot, S.; Vukovic, L.; Kral, P.; Hong, S. *Chem Commun* **2011**, *47*, 10302.

(247) Kano, K.; Minamizono, H.; Kitae, T.; Negi, S. *J Phys Chem A* **1997**, *101*, 6118.

(248) J. Moan, K. B. a. V. I. In Photodynamic tumour therapy 2nd and 3rd generation photosensitizers; Moser, J. G., Ed.; Harwood Academic Publishers: Amsterdam, 1998, p pp. 169.

(249) Akins, D. L.; Ozcelik, S.; Zhu, H. R.; Guo, C. *J Phys Chem-Us* **1996**, *100*, 14390.

(250) You, Y.; Gibson, S. L.; Hilf, R.; Ohulchanskyy, T. Y.; Detty, M. R. *Bioorg & Med Chem* **2005**, *13*, 2235.

(251) Zhang, F. L.; Huang, Q.; Zheng, K.; Li, J.; Liu, J. Y.; Xue, J. P. *Chem Commun* **2013**, *49*, 9570.

(252) Liu, F.; Deng, D. W.; Chen, X. Y.; Qian, Z. Y.; Achilefu, S.; Gu, Y. Q. *Mol Imaging Biol* **2010**, *12*, 595.

(253) Paulos, C. M.; Reddy, J. A.; Leamon, C. P.; Turk, M. J.; Low, P. S. *Mol Pharmacol* **2004**, *66*, 1406.

(254) Yoo, H. S.; Park, T. G. *J Control Release* **2004**, *96*, 273.

(255) Esmaeili, F.; Ghahremani, M. H.; Ostad, S. N.; Atyabi, F.; Seyedabadi, M.; Malekshahi, M. R.; Amini, M.; Dinarvand, R. *J Drug Target* **2008**, *16*, 415.

(256) Backus, H. H. J.; Pinedo, H. M.; Wouters, D.; Padron, J. M.; Molders, N.; Van der Wilt, C. L.; Van Groeningen, C. J.; Jansen, G.; Peters, G. J. *Int J Cancer* **2000**, *87*, 771.